

1987

Synthesis and characterization of zirconium chloride clusters stabilized by small interstitial atoms

Robin P. Ziebarth
Iowa State University

Follow this and additional works at: <https://lib.dr.iastate.edu/rtd>

 Part of the [Inorganic Chemistry Commons](#)

Recommended Citation

Ziebarth, Robin P., "Synthesis and characterization of zirconium chloride clusters stabilized by small interstitial atoms " (1987).
Retrospective Theses and Dissertations. 8603.
<https://lib.dr.iastate.edu/rtd/8603>

This Dissertation is brought to you for free and open access by the Iowa State University Capstones, Theses and Dissertations at Iowa State University Digital Repository. It has been accepted for inclusion in Retrospective Theses and Dissertations by an authorized administrator of Iowa State University Digital Repository. For more information, please contact digirep@iastate.edu.

INFORMATION TO USERS

While the most advanced technology has been used to photograph and reproduce this manuscript, the quality of the reproduction is heavily dependent upon the quality of the material submitted. For example:

- Manuscript pages may have indistinct print. In such cases, the best available copy has been filmed.
- Manuscripts may not always be complete. In such cases, a note will indicate that it is not possible to obtain missing pages.
- Copyrighted material may have been removed from the manuscript. In such cases, a note will indicate the deletion.

Oversize materials (e.g., maps, drawings, and charts) are photographed by sectioning the original, beginning at the upper left-hand corner and continuing from left to right in equal sections with small overlaps. Each oversize page is also filmed as one exposure and is available, for an additional charge, as a standard 35mm slide or as a 17"x 23" black and white photographic print.

Most photographs reproduce acceptably on positive microfilm or microfiche but lack the clarity on xerographic copies made from the microfilm. For an additional charge, 35mm slides of 6"x 9" black and white photographic prints are available for any photographs or illustrations that cannot be reproduced satisfactorily by xerography.

Order Number 8721944

**Synthesis and characterization of zirconium-chloride clusters
stabilized by small interstitial atoms**

Ziebarth, Robin P., Ph.D.

Iowa State University, 1987

U·M·I
300 N. Zeeb Rd.
Ann Arbor, MI 48106

PLEASE NOTE:

In all cases this material has been filmed in the best possible way from the available copy. Problems encountered with this document have been identified here with a check mark ✓.

1. Glossy photographs or pages _____
2. Colored illustrations, paper or print _____
3. Photographs with dark background _____
4. Illustrations are poor copy _____
5. Pages with black marks, not original copy _____
6. Print shows through as there is text on both sides of page _____
7. Indistinct, broken or small print on several pages ✓
8. Print exceeds margin requirements _____
9. Tightly bound copy with print lost in spine _____
10. Computer printout pages with indistinct print _____
11. Page(s) _____ lacking when material received, and not available from school or author.
12. Page(s) _____ seem to be missing in numbering only as text follows.
13. Two pages numbered _____. Text follows.
14. Curling and wrinkled pages _____
15. Dissertation contains pages with print at a slant, filmed as received _____
16. Other _____

University
Microfilms
International

Synthesis and characterization of zirconium chloride
clusters stabilized by small interstitial atoms

by

Robin P. Ziebarth

A Dissertation Submitted to the
Graduate Faculty in Partial Fulfillment of the
Requirements for the Degree of
DOCTOR OF PHILOSOPHY

Department: Chemistry
Major: Inorganic Chemistry

Approved:

Signature was redacted for privacy.

In Charge of Major Work

Signature was redacted for privacy.

For the Major Department

Signature was redacted for privacy.

For the Graduate College

Iowa State University
Ames, Iowa

1987

TABLE OF CONTENTS

	Page
INTRODUCTION	1
EXPERIMENTAL	13
Materials	13
Synthetic Techniques	15
Methods of Characterization	18
RESULTS AND DISCUSSION	23
M_6X_{12}	23
M_6X_{13}	42
M_6X_{14}	63
M_6X_{15}	78
M_6X_{16}	167
M_6X_{18}	195
Bonding	216
Additional Observations	224
FUTURE WORK	232
REFERENCES	237
ACKNOWLEDGEMENTS	247
APPENDIX A. ATOMIC ORBITAL PARAMETERS AND CLUSTER GEOMETRIES USED IN EXTENDED-HÜCKEL CALCULATIONS	248

	Page
APPENDIX B. OBSERVED AND CALCULATED STRUCTURE FACTOR AMPLITUDES FOR $\text{KZr}_6\text{Cl}_{13}\text{Be}$	250
APPENDIX C. OBSERVED AND CALCULATED STRUCTURE FACTOR AMPLITUDES FOR $\text{Zr}_6\text{Cl}_{14}\text{C}$	255
APPENDIX D. OBSERVED AND CALCULATED STRUCTURE FACTOR AMPLITUDES FOR $\text{Zr}_6\text{Cl}_{14}\text{B}$	259
APPENDIX E. OBSERVED AND CALCULATED STRUCTURE FACTOR AMPLITUDES FOR $\text{Zr}_6\text{Cl}_{15}\text{N}$	262
APPENDIX F. OBSERVED AND CALCULATED STRUCTURE FACTOR AMPLITUDES FOR $\text{Na}_{0.5}\text{Zr}_6\text{Cl}_{15}\text{C}$	265
APPENDIX G. OBSERVED AND CALCULATED STRUCTURE FACTOR AMPLITUDES FOR $\text{KZr}_6\text{Cl}_{15}\text{C}$	268
APPENDIX H. OBSERVED AND CALCULATED STRUCTURE FACTOR AMPLITUDES FOR $\text{CsKZr}_6\text{Cl}_{15}\text{B}$	275
APPENDIX I. SELECTED REFLECTIONS FROM CALCULATED AND OBSERVED POWDER DIFFRACTION PATTERNS OF $\text{CsZr}_6\text{Cl}_{15}\text{C}$	282
APPENDIX J. OBSERVED AND CALCULATED STRUCTURE FACTOR AMPLITUDES FOR $\text{K}_2\text{Zr}_6\text{Cl}_{15}\text{B}$	284
APPENDIX K. OBSERVED AND CALCULATED STRUCTURE FACTOR AMPLITUDES FOR $\text{K}_3\text{Zr}_6\text{Cl}_{15}\text{Be}$	289
APPENDIX L. OBSERVED AND CALCULATED STRUCTURE FACTOR AMPLITUDES FOR $\text{Na}_{3.9}\text{Zr}_6\text{Cl}_{16}\text{Be}$	299
APPENDIX M. OBSERVED AND CALCULATED STRUCTURE FACTOR AMPLITUDES FOR $\text{Cs}_{3.0}\text{Zr}_6\text{Cl}_{16}\text{C}$	306
APPENDIX N. OBSERVED AND CALCULATED STRUCTURE FACTOR AMPLITUDES FOR $\text{Rb}_5\text{Zr}_6\text{Cl}_{18}\text{B}$	313

INTRODUCTION

Over the past twenty-five years an extensive cluster chemistry has been developed for the rare earth and early transition metal halides based on six metal atom octahedra. The first compounds in this group, prepared and structurally characterized mainly in the mid- to late-1960s, were a series of what are now well-known niobium and tantalum halide clusters^{1,2} that included $K_4Nb_6Cl_{18}$,³ Ta_6Cl_{15} ,⁴ Nb_6F_{15} ⁵ and Nb_6Cl_{14} .⁶ In each of these compounds the principal building block was the M_6X_{12} cluster, a trigonal antiprismatic metal core surrounded by twelve halogen atoms that bridged each of the twelve edges of the metal core as shown in Figure 1. An additional feature characteristic of the M_6X_{12} clusters was the presence of a set of low energy bonding orbitals extending radially from the vertices of the M_6 core which were always occupied in some manner by another halogen atom.⁷ It was the presence of this set of orbitals and the various ways in which they were occupied that accounted for the variety of metal to halogen stoichiometries that were observed. A description of the various ways in which these terminal or outer positions can be occupied is provided later.

More recently, a number of phases containing M_6X_{12} clusters have been prepared with the electron-poorer transition elements Zr and Sc, and the rare earth metals in binary halide systems.^{8,9} In many cases, these M_6X_{12} metal halide clusters were condensed into extended metal-metal bonded arrays by the sharing of metal cluster edges,¹⁰⁻¹³ presumably because of an insufficient number of metal-metal bonding electrons for discrete cluster formation and the large metal to halogen ratios.

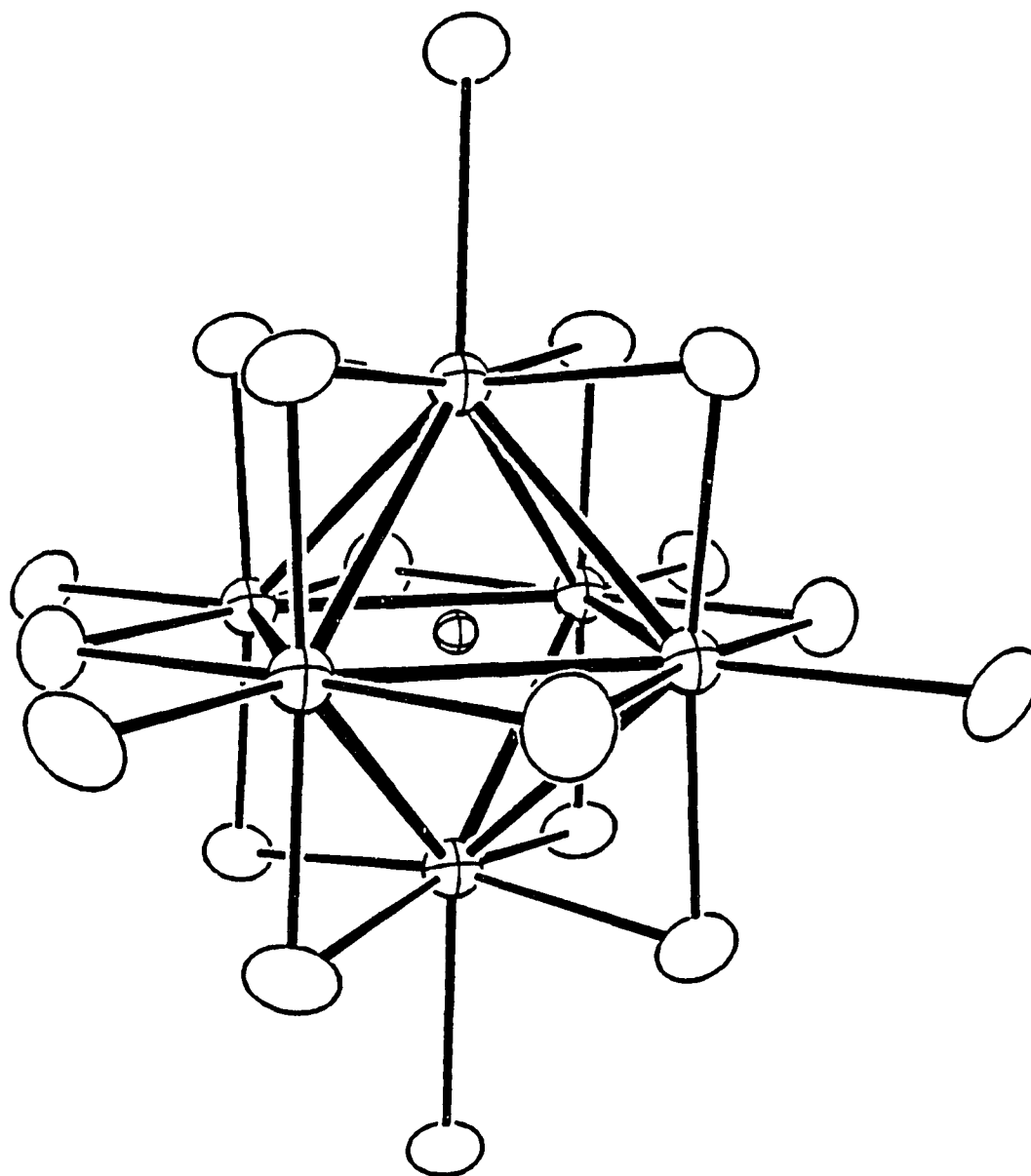


Figure 1. A centered M_6X_{12} -type cluster. Open ellipsoids are X atoms and large and small crossed ellipsoids are M and interstitial atoms, respectively. The 6 terminal X^a atoms have been included for completeness

Several discrete cluster phases, primarily for zirconium, were, however, also prepared.¹⁴⁻¹⁷ It should be noted, that cluster compounds for these electron-poor metals based on M_6X_8 clusters were also prepared.¹⁸⁻²¹ The M_6X_8 cluster, like the M_6X_{12} cluster, is made-up of a trigonal anti-prismatic metal core, but the eight halogen atoms cap faces of the M_6 core rather than bridge edges. The outwardly directed bonding orbitals seen in the M_6X_{12} cluster, are also present and occupied in the M_6X_8 cluster.⁷ Recognition of the two cluster types is important in later considerations.

The vast majority of these Sc, Zr and rare earth metal halide clusters were prepared from binary reactions of the metal with the fully oxidized metal halide. The yields in most cases were poor and often erratic, even after long equilibration periods ranging from weeks to months.^{11,14,22} In other cases, most notably Zr_6X_{12} ($X = Cl, Br$),²³ $M^I_2Zr_7Cl_{18}$ ($M^I = Na, K, Cs$)²³ and the rare earth metal monohalides,²⁴⁻²⁷ the compounds were prepared in good yields, but only under somewhat suspicious conditions, namely, under a H_2 atmosphere in the first two cases or with a large excess of powdered metal, but not strips, in the latter case. Interestingly, the poor yields from binary reactions were not universal. Several compounds, ZrX ($X = Cl, Br$),^{21,28,29} Sc_7Cl_{10} ²⁰ and Gd_2Cl_3 ^{18,19} for example, were prepared regularly and in excellent yields.

Three other common features besides the poor and irregular yields, provided additional clues to the real nature of these compounds. First, the compounds that were easily prepared in good yield were composed of

condensed M_6X_8 -type clusters while nearly all of the compounds prepared in poor and irregular yields were composed of either condensed or discrete M_6X_{12} -type clusters. Secondly, the poor yield compounds were all clearly electron deficient. The discrete M_6X_{12} -type clusters in Zr_6Cl_{15} and Zr_6Cl_{12} for example, appeared to have as few as 9- and 12-cluster electrons, respectively, in a set of metal-metal bonding orbitals capable of containing up to 16-cluster electrons³⁰⁻³² and that require 14 - 16 in the tantalum and niobium halide clusters.³³ Although the stability range and optimal electrons counts for condensed cluster phases are more difficult to ascertain, many of these appeared electron deficient as well. The structurally similar $M_{4/2}M_2X_6$ cluster chains in Sc_5Cl_8 ¹⁰ and $NaMo_4O_6$ ³⁴ contained 7- and 13-chain electrons per formula unit, respectively, a puzzling if not disconcerting difference. Finally, the vast majority of the crystal structures of the low yield compounds showed residual electron density in the interstices of the metal-metal bonded arrays. The residuals, often 5 - 8 electrons per \AA^3 , were usually attributed to an accumulation of diffraction errors which tend to be most prominent at high symmetry positions, or to stacking faults within the lattice.^{15,17} In several cases, the presence of a third, adventitious element which occupied the interstices was speculated on,^{14,17} but without substantiating evidence it proved to be no better an explanation than stacking faults or diffraction errors.

The discrete zirconium halide clusters as known five years ago, Zr_6X_{12} ($X = Cl, Br, I$),^{15,23} $CsZr_6I_{14}$,¹⁵ Zr_6Cl_{15} ^{14,17} and $M^I_2Zr_7Cl_{18}$ ($M^I = Na, K, Cs$),²³ were typical of the poor yield group described

above. Zr_6X_{12} ($X = Cl, Br$) and the related double salts $M^I_2Zr_7Cl_{18}$ were prepared in good yields only under hydrogen,²³ while the rest were only prepared erratically and in poor yields. The electron counts in these discrete M_6X_{12} -type clusters ranged from 9 in Zr_6Cl_{15} to 12 in Zr_6X_{12} and $M^I_2Zr_7Cl_{18}$, all less than the minimum value of 14 observed in the Group V metal halide clusters. Finally, $CsZr_6I_{14}$ and Zr_6Cl_{15} exhibited residual electron density inside the metal cluster in single crystal structural studies.

As a result of the work described in the succeeding sections and that of others,³⁵⁻⁴² it has become readily apparent over the past five years that the characteristic features of the poor yield group of compounds are actually symptomatic of metal clusters that are stabilized by, and indeed require, the presence of a third element. Obtained from adventitious sources in binary reactions, the third element (Z), typically a light nonmetal element, stabilized the structure by the formation of strong M - Z bonds and by the addition of its valence electrons to the cluster bonding orbitals. Occupying the nominal octahedral interstices in the metal lattice, the third element is frequently referred to as an interstitial atom or element. The parallel between this third interstitial element and the light nonmetal atoms in metals and alloys is obvious. In contrast to the rather inconsequential nature normally associated with an interstitial, the interstitial atom in a cluster phase has a pronounced effect on the metal-metal bonding orbitals in terms of their energies, characters and occupations. The effects of the interstitial atom are described in more detail in the section on Bonding.

Adventitiously stabilized compounds are by no means new. Classic examples from the literature include β -W,⁴³ CaCl⁴⁴ and τ -Ti₂S⁴⁵ which were later shown to be W₃O,⁴⁶ CaHCl⁴⁷ and TiSC,^{48,49} respectively. The first well-characterized example of a centered octahedral cluster was Nb₆I₁₁H,⁵⁰ an M₆X₈-type cluster with a hydrogen atom in the center. It also happens to be the only centered M₆X₈-type cluster known other than the related CsNb₆I₁₁H.⁵¹ Later, Seaverson and Corbett⁵² reported the first well-established example of a second period element bound within the metal-metal bonded array of a metal halide with ZrClO_x (0 ≤ x ≤ 0.4), a compound with oxygen atoms occupying tetrahedral holes between double-metal layers. Neither Nb₆I₁₁H nor ZrClO_x, however, can be rigorously classified as an interstitially stabilized cluster compound because the actual binary metal halides Nb₆I₁₁^{53,54} and ZrCl₂^{21,28} can both be prepared. The first well-characterized examples of interstitially stabilized early transition and rare earth metal halide compounds were a number of condensed and discrete rare earth metal halide clusters centered with isolated carbon atoms or dicarbide units.^{35,55-58} The field has grown rapidly over the past several years and has answered many of the questions concerning the previously prepared 'binary' metal halides.^{36,39-41,59} In addition, an entire class of new interstitially stabilized cluster compounds has developed by the purposeful addition of potential interstitial elements to cluster forming reactions. These new compounds include a host of new structure types which exhibit extended chains and sheets of condensed metal clusters, as well as discrete clusters.^{39,40,59,60} A large variety of interstitial atoms

have been incorporated into these structures and include H, second period elements from Be to O,^{52,59} larger main group elements^{37,61} such as Al, Si, P and Ge, some third period transition metals (Mn, Fe, Co, Ni),^{62,63} and even alkali metals.^{64,65} Also, noteworthy is a large body of related organometallic clusters containing interstitial atoms.⁶⁶⁻⁷¹

The research presented in the remaining sections details a portion of this development of interstitially stabilized cluster compounds, in particular, the preparation and characterization of discrete, centered, zirconium chloride clusters. The study of a variety $M^I\text{-Zr-Cl}$ -interstitial (Z) systems has led not only to a more complete understanding of the previously prepared clusters, Zr_6X_{12} ($X = \text{Cl}, \text{Br}$),²³ the related $M^I_2Zr_7Cl_{18}$ double salts²³ and Zr_6Cl_{15} ^{14,17} which are now known to be $Zr_6X_{12}H$, $M^I_2Zr_7Cl_{18}H$ and $Zr_6Cl_{15}N$, respectively, but also to an entire family of new centered zirconium chloride clusters based on discrete M_6X_{12} -type cluster units. A summary of the structure types and connectivities of the compounds prepared is given in Table 1. The diversity of this family of compounds which spans thirteen structure types, eleven of which are described in succeeding sections, is accessible through the use of various combinations of small interstitial atoms, alkali metal cation sizes and numbers, and zirconium to chlorine stoichiometries. Six of the structure types observed are new and two previously unknown stoichiometries for M_6X_{12} -type clusters, M_6X_{13} and M_6X_{16} are represented. It has also been shown that all of the discrete

Table 1. Structure types and connectivities of the known $[\text{Zr}_6\text{Cl}_{12}\text{Z}]\text{Cl}_n$, $n = 0-6$, compounds

Structure type	Connectivity	Reference
$\text{Zr}_6\text{I}_{12}\text{C}$	$[\text{Zr}_6\text{Cl}_6^i\text{Cl}_6^{i-a}]_{6/2}\text{Cl}_{6/2}^{a-i}$	15, 36
$\text{K}_2\text{ZrCl}_6 \cdot \text{Zr}_6\text{Cl}_{12}\text{H}$	$[\text{Zr}_6\text{Cl}_{12}^i]\text{Cl}_6^a$	23
$\text{KZr}_6\text{Cl}_{13}\text{Be}$	$[\text{Zr}_6\text{Cl}_{10}^i\text{Cl}_{2/2}^{i-i}]_{2/2}\text{Cl}_{6/3}^{a-a}$	this work
$\text{Nb}_6\text{Cl}_{14}$	$[\text{Nb}_6\text{Cl}_{10}^i\text{Cl}_{2/2}^{i-a}]_{2/2}\text{Cl}_{2/2}^{a-i}\text{Cl}_{4/2}^{a-a}$	6
$\text{Ta}_6\text{Cl}_{15}$	$[\text{Ta}_6\text{Cl}_{12}^i]\text{Cl}_{6/2}^{a-a}$	4
$\text{CsNb}_6\text{Cl}_{15}$	$[\text{Nb}_6\text{Cl}_{12}^i]\text{Cl}_{6/2}^{a-a}$	72
$\text{K}_2\text{Zr}_6\text{Cl}_{15}\text{B}$	$[\text{Zr}_6\text{Cl}_{12}^i]\text{Cl}_{6/2}^{a-a}$	this work
$\text{K}_3\text{Zr}_6\text{Cl}_{15}\text{Be}$	$[\text{Zr}_6\text{Cl}_{12}^i]\text{Cl}_{6/2}^{a-a}$	this work
Nb_6F_{15}	$[\text{Nb}_6\text{F}_{12}^i]\text{F}_{6/2}^{a-a}$	5
$\text{Cs}_3\text{Zr}_6\text{Cl}_{16}\text{C}$	$[\text{Zr}_6\text{Cl}_{12}^i]\text{Cl}_{4/2}^{a-a}\text{Cl}_2^a$	this work
$\text{Na}_4\text{Zr}_6\text{Cl}_{16}\text{Be}$	$[\text{Zr}_6\text{Cl}_{12}^i]\text{Cl}_{4/2}^{a-a}\text{Cl}_2^a$	this work
$\text{Rb}_5\text{Zr}_6\text{Cl}_{18}\text{B}$	$[\text{Zr}_6\text{Cl}_{12}^i]\text{Cl}_6^a$	this work
$\text{Li}_6\text{Zr}_6\text{Cl}_{18}\text{H}$	$[\text{Zr}_6\text{Cl}_{12}^i]\text{Cl}_6^a$	73

zirconium chloride clusters known contain, and in fact require, an interstitial atom in the cluster center.

A basic understanding of cluster structure types, particularly the manner in which chlorine atoms are shared between clusters, is necessary to appreciate the breadth of the systematic chemistry developed. As previously noted, all discrete clusters evidently have a low energy bonding orbital radially directed from each metal vertex of the cluster which is invariably occupied in some fashion by another chlorine atom. The chlorine atom that occupies this outer or terminal site may be: 1) an edge-bridging (inner) chlorine atom on another $Zr_6Cl_{12}Z$ cluster, 2) an additional chlorine atom that serves only to bridge between two adjacent clusters, or 3) an extra chlorine atom that is bound only to a single metal vertex. These modes of connectivity which can be seen in the structures in Figures 2, 11, and 40, respectively, are symbolically denoted in order by Cl^{a-i} , Cl^{a-a} and Cl^a ($i = \text{inner}$, $a = \text{ausser}$).¹ Unshared edge-bridging chlorine atoms are denoted by Cl^i . Barring additional connectivities, the stoichiometries obtained with various logical combinations of these connectivities fall in the family of compounds $(Zr_6Cl_{12}Z)Cl_n$, where n ranges from 0 to 6. The connectivities and respective stoichiometries are delineated in Table 2. In Table 2, the numerator of each fraction indicates the number of atoms per cluster involved in that particular type of connectivity and the denominator indicates the number of clusters each atom is shared between. The sum of the numerators on the 'inner' side must equal twelve as there are twelve edges to bridge, and the sum on the 'outer' side must equal six because

Table 2. Stoichiometry and connectivity of $(M_6 X_{12}^i) X_n^a$ clusters
 $0 \leq n \leq 6$

Stoichiometry	Inner X (12)		Outer X (6)		
	i	Connectivity Type		a-a	a
		i-a	a-i		
$M_6 X_{18}$	12				6
$M_6 X_{17}$	(12) ^a			(2/2)	(4)
$M_6 X_{16}$	12			4/2	2
$M_6 X_{15}$	12			6/2	
$M_6 X_{14}$	10	2/2		2/2	4/2
$M_6 X_{13}$	(8) ^a	(4/2)		(4/2)	(2/2)
$M_6 X_{12}$	6	6/2		6/2	
$M_6 (X^i)_{6+2n} (X^{i-a})_{6-2n} (X^{a-a})_{2n/2} (X^a)_0 \quad n = 0, 1, 2, 3$					
$M_6 (X^i)_{12} (X^{i-a})_0 (X^{a-a})_{(12-2n)/2} (X^a)_{2n-6} \quad n = 3, 4, 5, 6$					

^aConnectivity has not been observed.

there are six metal vertices. All of the zirconium chloride clusters prepared fall into this family of compounds except those with the $\text{KZr}_6\text{Cl}_{13}\text{Be}$ structure which show a more complex connectivity exhibiting shared edge-bridging chlorine atoms, Cl^{i-i} , as denoted in Table 1.

The M_6X_{17} member has not been identified.

Means to achieve these different stoichiometries, as well as to further enhance the structural variability, are evident from a consideration of the electronic factors involved. The bonding picture for these clusters (see Bonding section) clearly shows the valence electrons of the interstitial atom can be considered as 'donated' to the cluster bonding orbitals. The implication is that a change in the zirconium to chlorine ratio or stoichiometry can be compensated for electronically by a corresponding change in the interstitial atom. Hence, $\text{Zr}_6\text{Cl}_{12}\text{Be}$, $\text{Zr}_6\text{Cl}_{13}\text{B}$, $\text{Zr}_6\text{Cl}_{14}\text{C}$ and $\text{Zr}_6\text{Cl}_{15}\text{N}$ have different stoichiometries, combinations of connectivities, and structures and yet all have the same cluster electronic configuration. Combinations of alkali metal cations and interstitial atoms can also be used to compensate for changes in stoichiometry as in the series $\text{Zr}_6\text{Cl}_{13}\text{B}$, $\text{CsZr}_6\text{Cl}_{14}\text{B}$, $\text{K}_2\text{Zr}_6\text{Cl}_{15}\text{B}$, $\text{Cs}_3\text{Zr}_6\text{Cl}_{16}\text{B}$ and $\text{Rb}_5\text{Zr}_6\text{Cl}_{18}\text{B}$. Variations in the number of cations and the interstitial atom identity while maintaining a single zirconium to chlorine stoichiometry gives yet another example of the diversity possible, as seen in $\text{Zr}_6\text{Cl}_{15}\text{N}$, $\text{KZr}_6\text{Cl}_{15}\text{C}$, $\text{K}_2\text{Zr}_6\text{Cl}_{15}\text{B}$ and $\text{K}_3\text{Zr}_6\text{Cl}_{15}\text{Be}$. This last series, although having a single zirconium to chlorine stoichiometry and local connectivity, $[\text{Zr}_6\text{Cl}_{12}\text{Z}]\text{Cl}_{6/2}$, contains three distinct structural

arrangements of $Zr_6Cl_{12}Z$ clusters and one variation thereon. Additional variations can often be obtained by changes in cation size.

The remainder of the text is broken down into a series of sections based on zirconium to chlorine stoichiometries. Additional sections on bonding, observations, and potential areas for future work are found at the end. An interesting body of related work on interstitial derivatives of zirconium monochlorides, their synthesis, structure and bonding is found elsewhere.^{60,74}

EXPERIMENTAL

Materials

Reactor-grade crystal bar zirconium (<500 ppm Hf) was used to prepare zirconium powder via the thermal decomposition of ZrH_{2-x} . Typically 10 g of cleaned Zr strips were placed in a Mo boat and heated to 650°C under an atmosphere of hydrogen. After cooling to room temperature under hydrogen, the hydrogenated strips were pulverized with a diamond mortar and pestle in a dry box and passed through a 100-mesh sieve. Dehydrogenation was carried out by slowly heating the finely ground hydride in a Mo boat under dynamic vacuum from 350-700°C until the vacuum system remained below discharge. The slightly sintered metal powder was reground in the dry box and sealed under vacuum in Pyrex ampules. The lattice parameters of the powdered metal obtained by Guinier powder diffraction were within 3σ of the reported values for Zr metal,⁷⁵ indicating fairly low levels of impurities were present.

$ZrCl_4$ was prepared by the direct reaction of the elements in a sealed, two-arm fused silica reaction vessel. One arm, which contained high purity liquid chlorine (>99.5%, Matheson), was maintained at -30 to -40°C by immersion in a saturated aqueous $CaCl_2$ /ice bath, while the other arm, which contained a slight excess of reactor grade Zr strips, was heated with a torch to initiate the reaction. Once ignited, the reaction proceeded spontaneously, however, periodic heating with a torch, particularly near the completion of the reaction, was necessary to maintain a reasonable rate and prevent blockage of the reaction arm with crude $ZrCl_4$. The crude product was purified by three successive vacuum

sublimations over Zr metal and through a coarse-grade Pyrex frit at 250°C. Samples were stored in sealed glass ampules.

ZrBr₄ was prepared in a similar fashion using reactor-grade Zr strips and high purity Br₂ (<0.02% Cl₂, A. D. Mackay). The Br₂ was maintained slightly above room temperature during the reaction by placing the arm in a warm water bath. Multiple sublimations over Zr metal and through a frit were used to purify the material.

Reagent grade alkali metal chlorides, ammonium chloride and CsBr were slowly dried and then purified by vacuum sublimation. Most were stored in tightly capped vials in the dry box.

Spectroscopic grade graphite (National Brand, Union Carbide) and amorphous boron powder (95%, 325 mesh, Alfa), the latter complements of M. Ziebarth, University of Wisconsin, were degassed at 850°C under dynamic vacuum prior to use. Higher purity crystalline boron (99.9+%, Research Organic/Inorganic) obtained from R. N. Shelton of Ames Laboratory was used as received. The crystalline and amorphous boron gave products with equivalent lattice parameters, but use of the former resulted in significantly lower yields, presumably because of the smaller surface area and greater inertness of the crystalline lattice.

ZrNCl was prepared by passing anhydrous NH₃ (99.99%, Matheson) over recently sublimed ZrCl₄ contained in a Mo boat at 600°C.⁷⁶ NaN₃ (99%, Aldrich Chemical Co.) and NH₄Cl were also used as nitrogen sources.

Be flakes (Pechiney, France) were used as received. Special care should be taken when working with Be metal and its compounds as they are highly toxic.⁷⁷

$ZrH_{1.8}$ was prepared by the reaction of reactor-grade Zr strips in a Mo boat with hydrogen (99.999%, Matheson) at 650°C, followed by cooling under hydrogen to room temperature over a 6-8 hour period. The final hydride composition was calculated from the initial weight of the Zr metal and the change in pressure of the known volume of hydrogen used in the reaction.

$AlCl_3$ (Fischer Scientific Co.) was multiply sublimed, generally 4-5 times, over Al chunks and through a coarse-grade Pyrex frit under static vacuum until white and no residue remained behind. The $M^I AlCl_4$ salts were prepared by fusing stoichiometric amounts of recently sublimed $AlCl_3$ and the appropriate $M^I Cl$ in evacuated and sealed Pyrex ampules at 250-400°C.

Synthetic Techniques

The preparation of interstitially stabilized cluster compounds is dominated by one overriding concern, namely, the synthesis of cluster containing phases with identifiable interstitial elements. Although this concern seems rather basic and more a statement related to characterization, its importance in the synthetic process cannot be overestimated. Identification of the interstitial atom, particularly in cases where it is a light nonmetal element such as B, C, N or O, is based largely on the knowledge of what went into a reaction and the relative yield of the product rather than on an analysis of the product. Extensive experience has shown that nearly all interstitially stabilized cluster compounds can be prepared in 90-95% yields when the appropriate interstitial element is included in the reaction. It is enlightening to note, that as little as

0.1 mg of carbon in a typical reaction can produce an approximately 5% yield of what is often a highly crystalline and easily separable cluster phase. Almost ten years of zirconium, scandium and rare earth metal halide cluster chemistry shows what a little adventitious impurity can produce. The importance of minimizing adventitious elements during reactions in these systems is obvious.

The minimization of adventitious impurities in rare earth and early transition metal halide reactions is complicated by two factors. First, many of the reactants and products are air- and moisture-sensitive making the introduction of unknown quantities of hydrogen and oxygen quite easy. Secondly, the reduced halides of these metals, as well as the metals themselves, readily attack both Pyrex and fused silica at the elevated temperatures necessary for cluster formation ($>600^{\circ}\text{C}$), thus rendering these materials unsuitable as reaction containers. The former problem has been overcome by the use of a variety of inert atmosphere and vacuum techniques,⁷⁸ while the latter has been overcome by the use of welded tantalum tubing as a reaction container. A review on the use of tantalum reaction containers has recently appeared.⁷⁹

Reactions were run in 4 to 5 cm lengths of 3/8" tantalum tubing which had been etched in tantalum cleaning solution (55% conc. H_2SO_4 , 25% conc. HNO_3 and 20% conc. HF , by volume), rinsed with water and acetone and dried prior to the crimping and welding of one end. A second cleaning of the tube after the first weld is not recommended. Complete removal of the cleaning solution from the crimped end requires an extended period of rinsing and soaking in water, and failure to do so

results in the formation of a white or black residue, probably containing carbon, oxygen and several other elements, on the inside of the tube following rinsing with acetone and drying. This residue may account for some of the original synthesis of early transition and rare earth metal halide clusters containing unknown impurities.

In a typical reaction, 200 mg of reactants were weighed out in a dry box and placed in a tantalum tube which was then crimped and welded shut. All transfers and manipulations were carried out under an inert atmosphere except for a short transfer of the crimped reaction tube through air to the heli-arc welder⁸⁰ after which the welding chamber was immediately evacuated. Details of the proportions of reactants used to prepare a particular compound are included in the appropriate section in Results. Following the final weld, the reaction tube was encased in a fused silica jacket and the inside washed with tantalum cleaning solution, thoroughly rinsed and dried. Prior to sealing under a hard vacuum ($<10^{-4}$ torr) the jacket was 'flamed out' with a hot gas/oxygen flame to remove traces of adsorbed water from the surface of the fused silica.^{81,82} The thermal conditions and reaction periods used are included in Results. Reactions were generally air quenched following the reaction period.

All reaction tubes were opened in a dry box designed for crystal mounting²¹ which was equipped with a nearly horizontal window and a binocular microscope for careful visual examination of the reaction products. Single crystals large enough for X-ray diffraction studies were mounted with Vaseline jelly in 0.3 - 0.5 mm thin-walled glass capillaries inside the dry box. Powder diffraction samples were

routinely mounted of all reaction products. Most reaction products were sealed in evacuated Pyrex ampules and saved.

Methods of Characterization

X-ray powder diffraction

Guinier powder diffraction was used extensively in the identification of reaction products, estimation of their relative yields, and precise determination of their lattice parameters. Diffraction patterns of all reaction products were photographically recorded using an evacuable Hagg-Guinier camera equipped with a bent quartz crystal monochromator which was adjusted to give nearly clean Cu $K\alpha_1$ radiation, ($\lambda = 1.54056$ Å). Samples were mounted between layers of Scotch tape⁸³ with a small amount of NBS-Si powder (SRM-640) which was used as an internal standard. Patterns were read to within ± 0.005 mm on an Enraf-Nonius Guinier viewer and 2θ values calculated using the quadratic equation obtained from a least-squares fit of the first six Si line positions with the known diffraction angles by the program GUIN.⁸⁴ Intensities, when necessary, were visually estimated. Known patterns were manually indexed and lattice parameters calculated using the least-squares program LATT.⁸⁵ Calculated patterns of known and proposed structure types were obtained with the program POWDER⁸⁶ and plotted on the appropriate scale for direct comparison with film data with the program PPLOT.⁸⁷ Other patterns were obtained from the standard powder diffraction files.⁸⁸

Single crystal X-ray diffraction

Single crystal X-ray diffraction played an essential role in the identification and elucidation of the structural nature and composition of many of the cluster compounds prepared. Six new structure types for M_6X_{12} -type compounds were determined and several structural variations of known structure types were investigated. Without the structural data obtained by this method, research would have been limited to the three or four known structure types which could be identified by powder diffraction and then only in a much more qualitative manner.

All structural studies were carried out using data secured on a commercial SYNTEX P2₁ or DATEX⁸⁹ automated four-circle diffractometer. Both diffractometers were equipped with graphite single crystal monochromators to provide clean Mo K α radiation. The DATEX instrument employed the interactive software package ALICE,⁹⁰ while the SYNTEX diffractometer used the commercially available software.

Prior to data collection, all single crystals were examined by oscillation photographs taken on a Weissenberg camera with Cu K α radiation to verify their singularity and diffraction strength. In cases where it was clear how to align the crystal, Weissenberg photographs were also taken to obtain information on the lattice symmetry and axial lengths. In several cases, Weissenberg photographs were taken after completion of the structural determination to verify the absence of a superstructure or a lower crystallographic symmetry.

Details of the individual data collections are contained in each section of Results. A standard reflection, monitored every 50-100

reflections, showed no signs of decay or instrument instability in any of the reported data collections.

Following data collection, a ψ -scan at intervals of 10° in ϕ was collected on one or more moderately intense reflections near $\chi = \pm 90^\circ$ for use in the empirical absorption correction program ABSN.⁹¹ The absorption corrections in most cases were minimal because of the small absorption coefficients and nearly uniform crystal dimensions. The data were corrected for Lorentz-polarization effects and reduced with the program DATRD.⁹² Reflections were considered observed when $I_0 \geq 3\sigma_I$ and $F_0 > 3\sigma_F$. Data were averaged in the appropriate space group using the program FDATA.⁹³ All calculations were carried out on a VAX 11/780 computer.

The majority of compounds studied by single crystal X-ray diffraction were of unknown structure and composition. The phase problem was solved in each of these cases by either Patterson superposition techniques⁹⁴ or by direct methods using the program MULTAN-80.⁹⁵ Patterson superposition maps were analyzed, in part, using the program ALCAMPS.⁹⁶ The details of the individual structural solutions are outlined in their respective sections.

Structure factor and least-squares calculations were carried out with the full matrix program ALLS⁹⁷ using neutral atomic scattering factors with corrections for both the real and imaginary parts of anomalous dispersion for elements heavier than neon.⁹⁸ Secondary extinction corrections were made using a previously described method.⁹⁹ Anisotropic thermal parameters (B_{ij}) were defined by the expression

$T = \exp\left[(-1/4 (B_{11}h^2a^{*2} + B_{22}k^2b^{*2} + B_{33}l^2c^{*2} + 2B_{12}hka^*b^* + 2B_{13}hla^*c^* + 2B_{23}k\ell b^*c^*))\right]$ and have units of \AA^{-2} . The residual values R and R_w were defined by $R = \sum ||F_o| - |F_c||/|F_o|$ and $R_w = [\sum w(|F_o| - |F_c|)^2/w|F_o|^2]^{1/2}$. Weights were initially assumed to be equal to σ_F^{-2} . A statistical reweighting of the data sorted on the basis of $|F_{obs}|$ in overlapping groups of more than 125 independent reflections was accomplished with the program OMEGA.¹⁰⁰ The reweighting minimizes the dependence of $\sum w(|F_o| - |F_c|)^2$ on F_{obs} . Fourier series calculations were done with the program FOUR.¹⁰¹

Distances, estimated standard deviations and angles were calculated in all cases using lattice parameters obtained from Guinier powder diffraction patterns of material from the same reaction as the data crystal and a standard distance program. Structural drawings were produced with the program ORTEP.¹⁰²

In all cases it was found possible to vary the isotropic B and the occupancy of the interstitial atom simultaneously. Refined occupancies and thermal parameters are given for the interstitial atoms in each section.

¹H solid state NMR

¹H NMR spectra were collected by P. J. Chu using a 5.2 T superconducting magnet or a 1.3 T iron core solenoid magnet and a home-built pulsed NMR spectrometer similar to that described earlier.¹⁰³ Details of the measurements are described elsewhere.¹⁰⁴ The NMR data are presented in units of ppm with larger values corresponding to higher fields and

more negative values in kHz. All spectra are plotted with field increasing to the right.

Extended-Hückel calculations

Extended-Hückel calculations were carried out using programs that have previously been described.¹⁰⁵ Atomic orbital energies for zirconium were obtained by a linear interpolation of the values for yttrium¹⁰⁶ and molybdenum.¹⁰⁷ Other atomic energies were contained within the program package. A double-zeta expansion was used to describe the radial distribution of the zirconium 4d orbitals, while a single zeta function was used for all other atoms. Values used were as tabulated.¹⁰⁸ Atomic orbital parameters and molecular geometries used in the calculations are summarized in Appendix A.

RESULTS AND DISCUSSION



Although the metal cluster phase Zr_6Cl_{12} has been known for some time,^{109,110} questions concerning its actual composition and stability as an empty cluster remain. The compound was initially discovered in small amounts following $ZrCl/ZrCl_4$ equilibrations near the composition $ZrCl_2$.¹⁰⁹ The structure deduced by X-ray powder diffraction was identical to that of ' Zr_6I_{12} ', which is now known to actually be $Zr_6I_{12}C$.³⁶ However, consistent preparation of Zr_6Cl_{12} was never achieved, and sufficient quantities for physical property measurements were not obtained.

More recently, Imoto et al.²³ serendipitously obtained Zr_6Cl_{12} , Zr_6Br_{12} and the related $M_2ZrCl_6 \cdot Zr_6Cl_{12}$ ($= M_2Zr_7Cl_{18}$, $M = Na, K, Cs$) double salts by the thermal decomposition of ZrX ($X = Cl, Br$) in the presence of H_2 and, where appropriate, MCl near $750^\circ C$. Good yields of the cluster phases were obtained, but these were contaminated by sizable amounts of inseparable ZrH_{2-x} , the other reaction product. Reactions with $Zr:Cl$ ratios more appropriate to the composition of the cluster phases were not attempted. The greatly improved yields of Zr_6Cl_{12} achieved in the presence of hydrogen and its 0.3% larger lattice parameters compared with those formed in the earlier $ZrCl/ZrCl_4$ equilibrations¹¹⁰ led to speculation that Zr_6Cl_{12} might exist both as an empty cluster and as a hydride, similar to Nb_6I_{11} and $Nb_6I_{11}H$.⁵⁰ Solid state 1H NMR spectra of small samples of the Zr_6Cl_{12} and $Na_2ZrCl_6 \cdot Zr_6Cl_{12}$ prepared earlier under hydrogen showed only broad Lorentzian-shaped resonances (36 – 41 kHz wide at $\nu_0 = 56$ MHz) which were attributed to

the ZrH_{2-x} contaminant in these.²³ The binary $ZrH_{1.9}$ showed a 55-kHz-wide resonance under similar conditions. The broad resonance was in contrast to the sharp singlet expected for noninteractive and immobile protons, i.e., in a hydrogen-centered cluster. For example, the proton NMR spectrum of $CsNb_6I_{11}H$, a hydrogen-centered niobium cluster, contains a single peak 0.6 kHz wide ($\nu_0' = 35$ MHz).⁵¹ Thus, it was concluded on the basis of the NMR evidence that neither Zr_6Cl_{12} nor the $M_2Zr_7Cl_{18}$ compounds contained interstitial hydrogen. The greatly improved yields in the presence of hydrogen were attributed to kinetic factors and to the fact that the disproportionation of $ZrCl$ appeared driven by the formation of ZrH_{2-x} . Potential causes for a broad 1H resonance in other than ZrH_{2-x} , such as from a possibly paramagnetic cluster, were dismissed as was the complex ESR spectrum observed for this ' Zr_6Cl_{12} ' sample at room temperature.²³

Recent NMR work¹¹¹ on ^{13}C nuclei in zirconium iodide carbide clusters suggests that the breadth of an NMR signal from Zr_6Cl_{12} could be associated with the particular structure type. Thus, the spectrum of ^{13}C in the diamagnetic $Zr_6I_{12}C$, isostructural with Zr_6Cl_{12} , contains only a very broad resonance that extends from about 28 to 480 ppm. The breadth of the resonance is in distinct contrast to the well-resolved, ~38-ppm-wide resonance seen for ^{13}C in the paramagnetic $CsZr_6I_{14}C$.^{36,111} The factors responsible for the broadening of the ^{13}C resonance in the former have not been elucidated.

The present lack of conclusive physical evidence for the presence of hydrogen in Zr_6Cl_{12} appears to have stemmed from the poor quality of the

samples, as well as the difficulties in detecting small amounts of hydrogen. The circumstantial evidence, however, clearly points towards the presence of interstitial hydrogen. This suspicion is augmented by a great deal of recent experience which indicates that a large number of other zirconium and scandium chloride cluster phases can be obtained only when an interstitial element Be, B, C... is bound in each cluster so as to contribute additional binding and to raise the cluster-based electron count into the range of 13 – 16, with 14 electrons being most favored.^{40,59} Three of the four signs associated with the discovery of these other interstitially stabilized clusters also point to interstitial hydrogen in the Zr_6Cl_{12} phases: low and irregular yields, an otherwise electron deficient Zr_6Cl_{12} cluster ($12 e^-$), and improved yields upon addition of the appropriate interstitial element. The fourth sign, a residual electron density in the cluster center in X-ray studies, would not be expected for hydrogen, of course. Preparation of good quality samples appeared to be the key to unraveling the role of hydrogen in the preparation and stability of Zr_6Cl_{12} .

Synthesis

$Zr_6Cl_{12}H$ was initially prepared as a black, microcrystalline material by heating the layered $ZrCl_2$ ¹¹⁰ (3R-MoS₂ structure) at 710°C in a sealed Ta tube under a large excess of hydrogen at one atmosphere. The reaction, which was air quenched after seven days, produced $Zr_6Cl_{12}H$ in an estimated yield of 60-70%. The remainder of the product, a mixture of $ZrCl_4$ and ZrH_{2-x} , attested to the large equilibrium $ZrCl_4$ pressure at reaction temperature generated by disproportionation of the product.

Improved yields and elimination of the initial $ZrCl_2$ preparation were obtained by reactions with stoichiometric amounts of Zr powder, $ZrCl_4$ and $ZrH_{1.8}$ at 700-750°C. The reactions, heated for a period of 10-14 days, produced $Zr_6Cl_{12}H$ in 70-80% yields. The additional 20-30% of the products was a mixture of $ZrCl_4$ and $ZrCl$ with slightly expanded lattice parameters. The controlled amounts of hydrogen used in the reactions were critical in the elimination of ZrH_{2-x} from the products.

The use of a $ZrCl_4$ excess equivalent to approximately five atmospheres at 700°C (assuming ideal gas behavior) and a two- to four-fold excess of hydrogen pushed yields of $Zr_6Cl_{12}H$ into the 80-90% range. Removal of the excess $ZrCl_4$ by sublimation in a static vacuum at 250°C left $Zr_6Cl_{12}H$ and a second phase which was tentatively identified as $ZrClO_xH_y$ ($0 < x < 0.43$, $x + y < 1$) in a $ZrCl$ -type structure. The identification of the latter phase was based on line positions, intensities and lattice parameters determined from X-ray powder diffraction patterns.

A $ZrClO_x$ phase is known to form via continuous, random insertion of oxygen into tetrahedral metal interstices in $3R-ZrCl$, a structure in which tightly bound slabs are formed from close-packed homoatomic layers sequenced $Cl-Zr-Zr-Cl$.⁵² The oxide derivative has subsequently been found to take up hydrogen to form $ZrClO_xH_y$ presumably by filling the remaining tetrahedral sites up to an experimentally determined limit of $x + y \cong 1$.¹¹² Different structure types are formed for $ZrClH$ under similar conditions in the absence of oxygen.¹¹³ The excess hydrogen used

in the $Zr_6Cl_{12}H$ synthesis is presumably partially taken up by both the Ta reaction tube and this second oxide phase.

Two samples of $Zr_6Cl_{12}H$ were initially prepared for NMR measurements by the method described above in reactions heated at 700° for a 2 – 3 week period. Sample A, used for the spectra shown, was obtained from a reaction with a Zr:Cl:H stoichiometry of 6:12:4 and a 5 atm equivalent of excess $ZrCl_4$. The yield of $Zr_6Cl_{12}H$ was estimated from relative intensities in the Guinier powder diffraction pattern to be on the order of 90%, although a microscopic examination of the product suggested it might be 5 – 10% lower. This assessment excludes the excess $ZrCl_4$ which was first sublimed off. The other phase present was identified as $ZrClO_xH_y$ (ZrCl-type structure, $a = 3.4854(5)$, $c = 27.04(2)$ Å).

Sample B was prepared similarly with a Zr:Cl:H ratio of 6:12:1.8 and an approximately equivalent amount of excess $ZrCl_4$. The yield of $Zr_6Cl_{12}H$ was marginally (~5%) lower than in reaction A, with a slightly hydrogen-poorer $ZrClO_xH_y$ (ZrCl-type structure) making up the difference.

The presence of an oxygen-containing phase in both samples is inconvenient but not particularly surprising considering the air- and moisture-sensitive nature of the reactants and their small particle sizes. A small oxygen contaminant in any or all of the reactants may be at fault. Separation of the two phases is considered nearly impossible at the present time. Of particular importance is the recognition that the measurements were performed on a two-phase mixture.

The assignment of $ZrClO_xH_y$ as the second phase was also consistent with the evidence obtained from a third reaction. Sample C,

prepared with a Zr:Cl:H ratio of 6:12:1.8 and an ~ 10 atm equivalent of excess ZrCl_4 , was further hydrogenated at 200°C in Mo boat with 1 atm H_2 . The small sample size and large hydrogen volume prevented an accurate measure of the hydrogen uptake. However, the observed conversion of the ZrClO_xH_y impurity from the ZrCl- to ZrBr-type structure was consistent with previous experimental experience which showed that the ZrBr structure type is adopted by ZrClO_xH_y when $x + y \cong 1$.¹¹² Unfortunately, insufficient data are available to estimate the amount of hydrogen in the ZrClO_xH_y in either sample A or B.

An attempt to remove the hydrogen from $\text{Zr}_6\text{Cl}_{12}\text{H}$ by heating the material in a sealed Ta tube at 500°C under a high dynamic vacuum for 5 hrs resulted in decomposition of the cluster.

The $\text{M}_2\text{ZrCl}_6 \cdot \text{Zr}_6\text{Cl}_{12}\text{H}$ ($\text{M} = \text{Na}, \text{K}$ and Cs) double salts²³ can be prepared in a fashion similar to $\text{Zr}_6\text{Cl}_{12}\text{H}$ by the inclusion of a stoichiometric amount of the appropriate alkali metal chloride in the reaction. Significantly lower autogenous ZrCl_4 pressures are encountered over the double salts and a two atmosphere equivalent of excess ZrCl_4 produces about 90% yields. A mixture of ZrClO_xH_y and $\text{M}_2^{\text{I}}\text{ZrCl}_6$ make up the remainder of the product. In contrast to $\text{Zr}_6\text{Cl}_{12}\text{H}$ where microcrystalline materials are obtained, $\text{M}_2^{\text{I}}\text{Zr}_7\text{Cl}_{18}\text{H}$ reactions often contain moderately sized, well-formed, dark red crystals.

Both $\text{Zr}_6\text{Cl}_{12}\text{H}$ and the related $\text{M}_2\text{Zr}_7\text{Cl}_{18}\text{H}$ compounds contain 13-electron clusters. The 14-electron analogues, $\text{Zr}_6\text{Cl}_{12}\text{Be}$ and $\text{Cs}_2\text{Zr}_7\text{Cl}_{18}\text{Be}$, were prepared in 95+% yields by the reaction of stoichiometric amounts of Zr powder, ZrCl_4 , Be flakes and, if appropriate, CsCl at 800°C for 14

days. Crystal growth of the red-brown compounds was negligible. $\text{Cs}_2\text{Zr}_7\text{Cl}_{18}\text{Be}$ was initially prepared in about 50% yield in a reaction stoichiometrically loaded to produce $\text{CsZr}_6\text{Cl}_{14}\text{Be}$. Interestingly, the potassium double salt $\text{K}_2\text{Zr}_7\text{Cl}_{18}\text{Be}$ was not obtained. Stoichiometrically loaded reactions yielded a mixture of $\text{KZr}_6\text{Cl}_{13}\text{Be}$, discussed in the next section, and K_2ZrCl_6 . Although it has not been attempted, the $\text{M}_2\text{Zr}_7\text{Cl}_{18}\text{Be}$ ($\text{M} = \text{Na}, \text{K}, \text{Rb}$ and Cs) compounds can probably be prepared at lower temperatures by the direct reaction of $\text{Zr}_6\text{Cl}_{12}\text{Be}$ with M_2ZrCl_6 in a ZrCl_4/MCl melt.

Structural description

All compounds were identified by Guinier powder diffraction. Lattice parameters are compiled in Table 3. The structure of $\text{Zr}_6\text{Cl}_{12}\text{H}$ has previously been shown by Guinier powder diffraction to be isostructural with $\text{Zr}_6\text{I}_{12}\text{C}$.^{23,36} The principal building block of the structure is the $\text{Zr}_6\text{Cl}_{12}$ cluster, a trigonal antiprismatic Zr_6 core surrounded by 12 chlorine atoms that bridge each of the 12 metal cluster edges. The structure, shown in Figure 2, is composed of a cubic close-packed array of these $\text{Zr}_6\text{Cl}_{12}$ clusters with the $\bar{3}$ axis of each cluster normal to the layer direction. An extensive sharing of the chlorine atoms between clusters is necessitated by the stoichiometry and the bonding requirements of the cluster. Specifically, the six chlorine atoms around the waist, i.e., those bridging metal cluster edges that have a component parallel to the $\bar{3}$ axis, serve as more distant terminal chlorine atoms to metal vertices on six adjacent clusters, three above and three below.

Table 3. Cell parameters (Å) and volumes (Å³) of Zr₆Cl₁₂Z and Cs₂Zr₇Cl₁₈Z compounds^a

Compound	a	c	V
Zr ₆ Cl ₁₂ H ^b	13.005(1)	8.808(1)	1290.2(3)
Zr ₆ Cl ₁₂ H ^c	13.0021(6)	8.805(2)	1289.1(3)
Zr ₆ Cl ₁₂ H ^d	13.0071(8)	8.808(1)	1290.5(2)
Zr ₆ Cl ₁₂ He	12.975(1)	8.794(2)	1282.1(4)
Zr ₆ Cl ₁₂ He	12.9854(7)	8.790(1)	1283.5(2)
Zr ₆ Cl ₁₂ H ^f	12.983(1)	8.792(2)	1283.4(4)
Zr ₆ Cl ₁₂ Be	13.1608(8)	8.840(1)	1324.6(2)
Zr ₆ Br ₁₂ B	13.633(1)	9.307(1)	1498.0(3)
Cs ₂ ZrCl ₆ ·Zr ₆ Cl ₁₂ H ^b	9.595(1)	26.186(8)	2089.0(1)
Cs ₂ ZrCl ₆ ·Zr ₆ Cl ₁₂ Be	9.6461(9)	26.404(3)	2125.4(5)

^aAll values were obtained from Guinier powder diffraction data.

^bRef. 4, ZrCl/H₂ preparation.

^cZrCl/H₂ preparation by Imoto, pattern read by R. Ziebarth.

^dZrCl₂/H₂ preparation.

^eZr, ZrCl₄, ZrH_{1.8} preparation.

^fZrCl/ZrCl₄ preparation by Cisar, pattern read by R. Ziebarth.

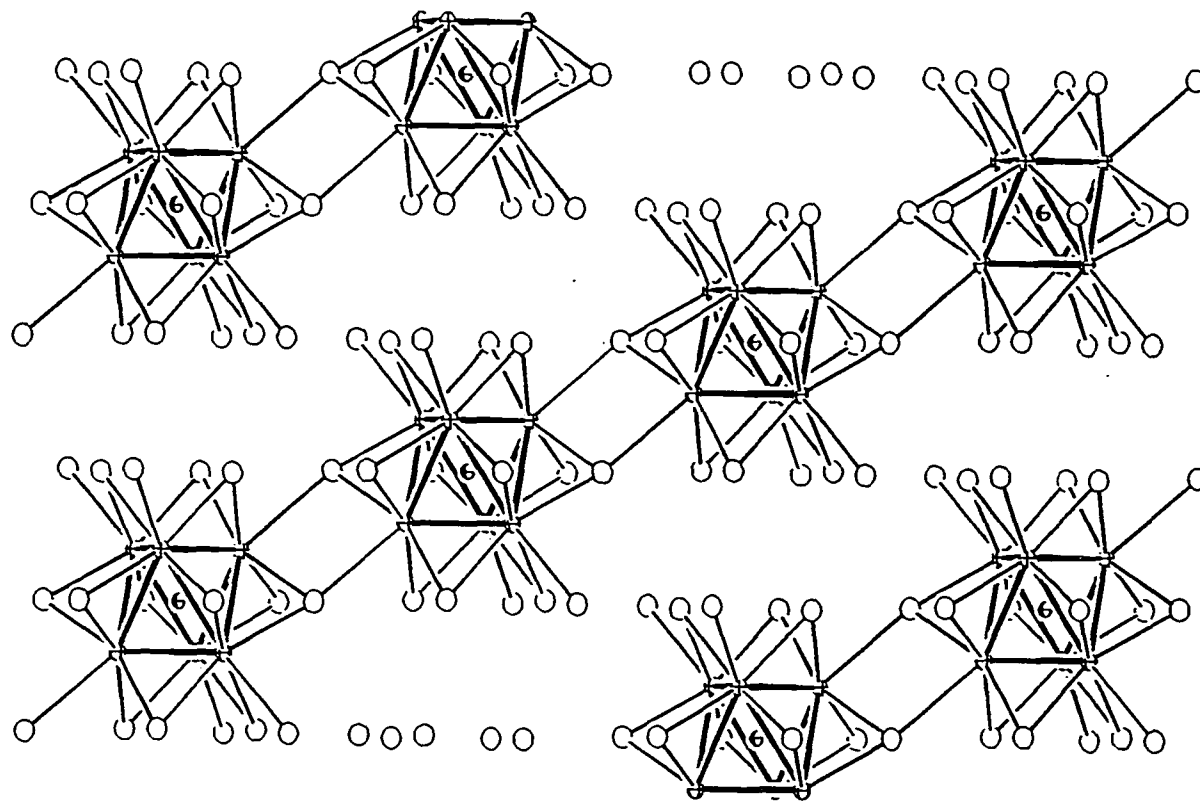


Figure 2. A $[1\bar{1}0]$ projection of the rhombohedral structure of $Zr_6Cl_{12}H$. The \vec{c} axis runs vertically in the plane of the figure, perpendicular to the close packed layers. A hydrogen atom occupies the center of each Zr_6Cl_{12} cluster

The connectivity is conveniently formulated as $[\text{Zr}_6\text{Cl}_6^i\text{Cl}_{6/2}^{i-a}]\text{Cl}_{6/2}^{a-i}$, where Cl^{i-a} and Cl^{a-i} reflect the connectivity just described while Cl^i is not shared. A hydrogen atom presumably is bonded within each $\text{Zr}_6\text{Cl}_{12}$ cluster just as a carbon atom is bound in each cluster in $\text{Zr}_6\text{I}_{12}\text{C}$. PES, dimensional and theoretical evidence indicate the hydrogen in such electron-rich environments should be considered hydridic in character.¹¹⁴

Alternatively, the structure may be viewed as a cubic close-packed arrangement of chlorine atoms, i.e., stacked ...ABC....²³ The zirconium atoms fill one-half of the octahedral sites between chlorine layers and congregate to form trigonal antiprismatic clusters around 'vacancies' in the chlorine layers. The 'vacancies' are the site of the interstitial atom. The packing of the structure creates an empty octahedral site surrounded by chlorine atoms above and below each cluster on the $\bar{3}$ axis. The site is completely occupied in the $\text{M}_7\text{X}_{12}\text{Z}$ compounds (M = Sc, R. E. metal; X = Cl, Br, I; Z = B, C, N) by M^{3+} cations,^{16,40,115} but no conclusive evidence for its occupation in any zirconium halide phases has been observed.

The M_6X_{12} cluster in $\text{Zr}_6\text{I}_{12}\text{C}$,³⁶ $\text{Sc}_7\text{X}_{12}\text{Z}$,^{40,115} and $\text{K}_2\text{Zr}_7\text{Cl}_{18}\text{H}^{23}$ all show a slight compression along the $\bar{3}$ axis which undoubtedly extends to $\text{Zr}_6\text{Cl}_{12}\text{H}$. The compression in the first two cases is probably a consequence of the additional bonding of the waist chlorine atoms to adjacent clusters, a situation which also occurs in $\text{Zr}_6\text{Cl}_{12}\text{H}$. The cluster dimensions in $\text{Zr}_6\text{Cl}_{12}\text{H}$ should be very similar to those in

$K_2Zr_7Cl_{18}H$. The Zr-Zr distances in $K_2Zr_7Cl_{18}H$ are 3.178(1) and 3.224(1) Å, while the Zr-cluster center distance is 2.264(1) Å. The latter distance is significantly longer than the Zr-H distances of 2.08 and 2.10 Å seen for four-coordinate hydrogen in ZrH_2 and Zr_2Br_2H , respectively.¹¹³

The structure of the related double salts, $M_2Zr_7Cl_{18}Z$,²³ is built-up of a cubic-close-packed array of $Zr_6Cl_{12}Z$ clusters similar to that in $Zr_6Cl_{12}H$. Hexachlorozirconate(2-) anions fill the octahedral sites between clusters while potassium cations reside in tetrahedral sites. The sharing of inner chlorine atoms as terminal atoms on adjacent cluster seen in $Zr_6Cl_{12}H$ has been replaced by a sharing of the chlorine atoms in the $ZrCl_6^{2-}$ anion with the clusters as terminal chlorine atoms.

A description of the structure from the viewpoint of a close-packed lattice of chlorine atoms is also appropriate.²³ The close-packed chlorine layers are sequenced ...ABABCBCAC... in the \vec{c} direction or $(chh)_3$ when described in terms of neighboring chlorine layers. Clusters from around 'vacancies' in the c layers. The potassium cations occupy one-seventh of the chlorine positions in the h layers while Zr^{4+} cations reside in one-seventh of the octahedral holes between h layers. Once again the nominal vacancy in the cluster center is occupied by the interstitial atom (Z).

¹H NMR results¹⁰⁴ and discussion

The presence of hydrogen in $Zr_6Cl_{12}(H)$ was conclusively established by solid state NMR. The spectrum of sample A, collected by P. J. Chu and obtained by Fourier transform techniques at two different magnetic fields ($\nu_0 = 220$ MHz and 56 MHz), is shown in Figure 3. Two peaks, one

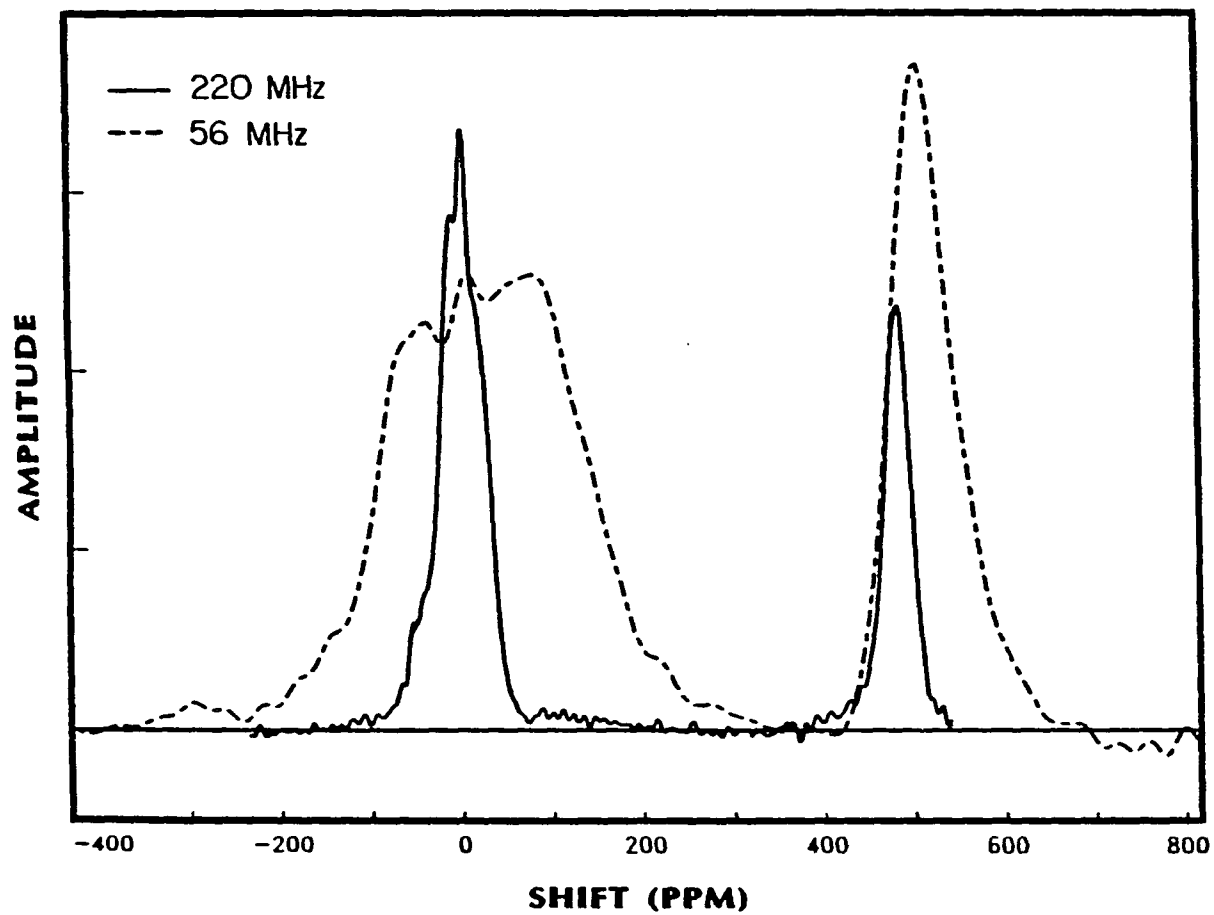


Figure 3. The room temperature ¹H NMR spectrum of Zr₆Cl₁₂H at 220 and 56 MHz. Only the upfield peak (~500 ppm) is associated with Zr₆Cl₁₂H (see text)

centered at -5.0 ppm and the other at about 500 ppm with respect to the proton resonance in $\text{H}_2\text{O}(\lambda)$, were resolved at both fields. The upfield (500 ppm) absorption is a Gaussian-shaped peak with a line width at 220 MHz of ~ 7.5 kHz. The low field absorption is a broader peak, about 11.5 kHz wide, which appears to be a poorly resolved multiplet. The ratio of the integrated intensities of the -5 ppm to 500 ppm peaks is approximately 2:1. The spectrum of sample B was identical to that of A except the peak area ratio (-5 ppm to 500 ppm) was slightly larger than 2:1.

The upfield peak, identified from its behavior under a variety of experimental conditions, results from a single hydrogen atom centered in the $\text{Zr}_6\text{Cl}_{12}$ cluster. Rapid spinning of the sample inclined at the magic angle with respect to the field (MAS) narrowed the upfield resonance slightly and did not result in a splitting of the resonance or the formation of any rotational side bands. The retention of the singlet under MAS conditions indicated the resonance was associated with protons having a single chemical shift, i.e., a single environment, and not an unresolved multiplet.¹¹⁶ The lack of rotational side bands indicated that any dipolar coupling between the protons was smaller than ~ 2 kHz, the sample rotational speed, which implied the hydrogen-hydrogen distances in the compound were in excess of 3.9 Å.^{116,117} The cluster-center to cluster-center distance in $\text{Zr}_6\text{Cl}_{12}\text{H}$ is about 8.0 Å. Application of an MREV-8 pulse sequence,¹¹⁸ a technique used to suppress homonuclear dipolar coupling, reduced the upfield peak to the noise level at room temperature. This behavior, also observed in YH_{2-x} ,¹¹⁹ is characteristic

of systems in which the nucleus of interest is undergoing rapid and isotropic motion on a time scale shorter than the sampling time of the pulse sequence,¹²⁰ 18 μ s in this case. The rapid motion prevents coherent averaging of the transient signal in the observation windows. The result for $Zr_6Cl_{12}H$ is consistent with the structural data for the $Zr_6Cl_{12}H$ cluster in $K_2Zr_7Cl_{18}H^{23}$ which shows the cluster cavity is too large for optimal Zr-H bonding. As noted earlier, the Zr to cluster-center distance is 2.264 Å, about 0.15 Å longer than the Zr-H distances observed for four-coordinate hydrogen in ZrH_{2-x} (2.08 Å) and Zr_2Br_2H (2.10 Å). Rapid motion of the hydrogen atom from one off-center position to another, i.e., rattling, within the cluster seem quite reasonable under the circumstances.

The exceptionally large chemical shift provided another strong indication that the 500 ppm resonance resulted from a hydrogen atom inside the Zr_6Cl_{12} cluster. Although a sizable upfield shift would be expected for a well-shielded, hydridic proton, the extreme nature of the shift suggested that other factors, particularly the paramagnetism of the cluster might be important. With a hydrogen atom in the center, the Zr_6Cl_{12} cluster would have 13 cluster-bonding electrons resulting in one unpaired spin (see Bonding section for M.O. diagram and electron counting scheme). The factor responsible for the large upfield shift was deduced from a variable temperature NMR study of the sample between 218 and 298 K. The study showed the chemical shift of the upfield resonance was strongly temperature dependent, moving to higher fields as the temperature decreased. The strong temperature dependence of the chemical

shift is characteristic of a coupling between the magnetic moments of a proton and an unpaired electron.^{121,122} If the shift had resulted solely from the hydridic character of the proton, no temperature dependence would have been observed because of the invariance of the electron cloud (or wave functions) responsible for the screening with respect to temperature.

By relating the change in the effective magnetic field to the bulk Curie law magnetic susceptibility,¹²² the magnitude of the chemical shift associated with the unpaired electron density can be calculated by:

$$\frac{\Delta H}{H} = \frac{g \mu_B}{\gamma \hbar} \frac{aS(S+1)}{3 kT}$$

where μ_B is the Bohr magneton, γ , the gyromagnetic ratio of the proton and a , the hyperfine coupling constant in units of energy. A plot of the chemical shift as a function of T^{-1} , shown in Figure 4, yields a line with a slope of 2.234×10^5 ppm-K and an intercept of -241 ppm. If one unpaired electron per cluster is assumed, the hyperfine coupling constant, after a conversion to frequency (divide by h), is calculated to be 28.3 MHz. This value corresponds to a hyperfine field of 10.1 G, a value typical of organic radicals and other cases where the unpaired spin density on the hydrogen atom is small.¹²³ The observed hyperfine field for a hydrogen atom, a situation where the spin is localized on the atom, is 506.8 G.¹²⁴ The value obtained for $Zr_6Cl_{12}H$, therefore, corresponds to an unpaired spin density at the hydrogen nucleus of $10.1/506.8 = 0.02$. The sign reflects an excess of electron density with spin $-1/2$ at the nucleus. The bulk magnetic susceptibility and the number of unpaired

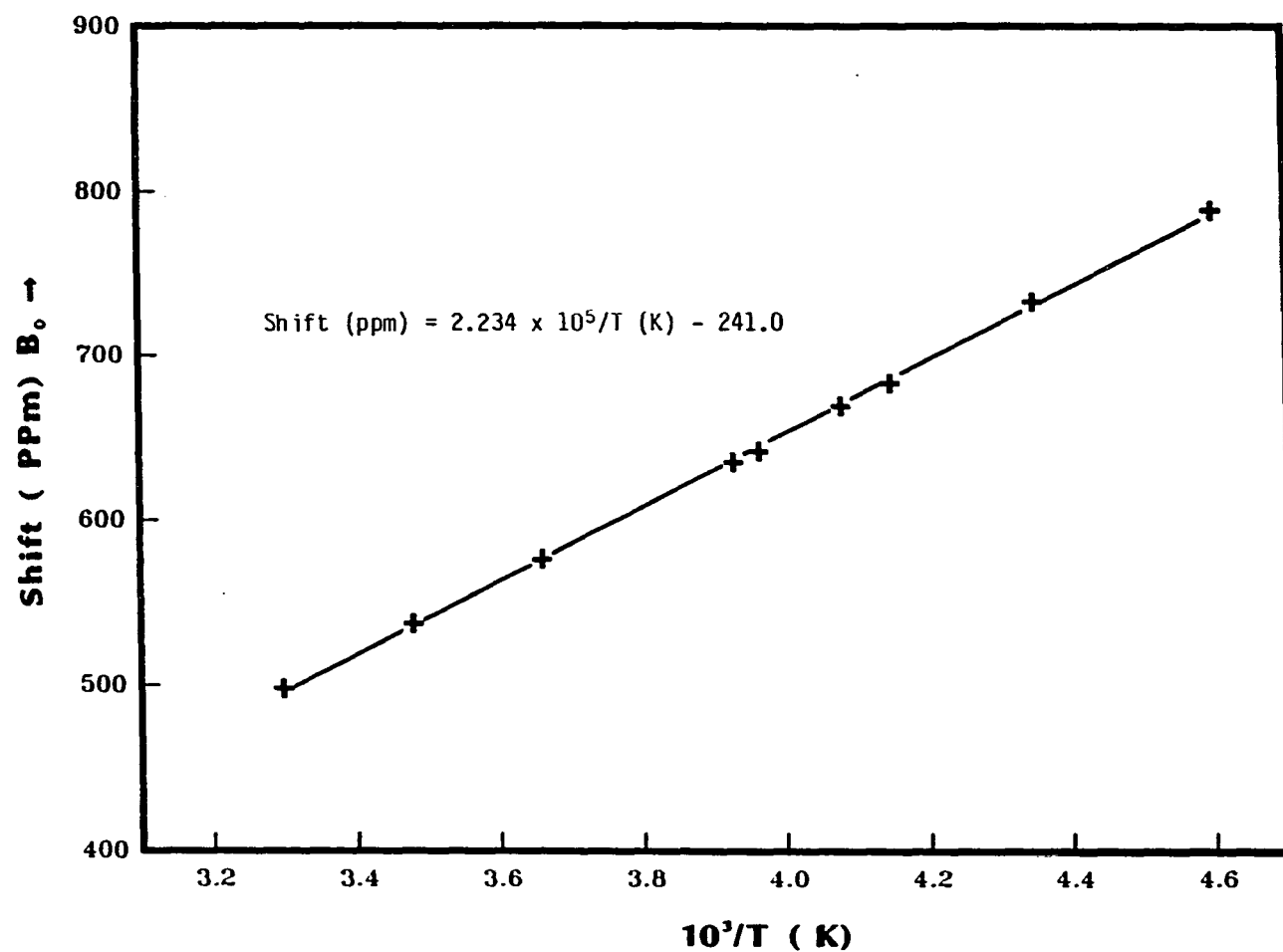


Figure 4. The variation of the chemical shift of the upfield peak between 218 and 298 K. The linear relationship of the shift with respect to T^{-1} is characteristic of a proton coupled to an unpaired electron

electrons per cluster cannot be calculated without an independent measure of the hyperfine coupling constant or the unpaired electron density at the hydrogen nucleus.

The NMR results indicate that the upfield peak is associated with a single hydrogen species which is highly mobile at room temperature, and situated near a paramagnetic center. When combined with the structure of $Zr_6Cl_{12}H$, the dimensions of the Zr_6Cl_{12} cluster (from $K_2Zr_7Cl_{18}H$), and the M.O. calculations which suggest a single unpaired electron would be present in a 13-electron cluster, the NMR results provide conclusive evidence for the presence of a hydrogen atom within each cluster of $Zr_6Cl_{12}H$.

The low field peak which has largely been neglected in the discussion until now, appears to arise from a small amount of $ZrClO_xH_y$ in the sample. $ZrClO_xH_y$ is a close-packed layered structure sequenced Cl-Zr-Zr-Cl with oxygen and hydrogen atoms randomly occupying tetrahedral sites between zirconium layers.¹¹² The assignment is based on several pieces of experimental evidence. First, the NMR samples were known to contain small amounts of a second phase. The second phase was identified as $ZrClO_xH_y$ by X-ray powder diffraction line positions and intensities, and by the behavior of the phase under further hydrogenation which showed a transformation from the ZrCl to ZrBr structure type. The structural change has previously been shown to occur for $ZrClO_xH_y$ as $x + y$ approaches unity.¹¹² Secondly, the relative amount of the impurity in the sample correlates nicely with the ratio of the integrated peak intensities. As the impurity content increases, the ratio of the -5 ppm

to 500 ppm areas increases. Finally, additional information extracted from the NMR experiments,¹⁰⁴ H-H distances of 2.5 ± 0.2 Å and quadrupolar coupling between the low field protons and neighboring chlorine nuclei at distances of roughly 2.7 Å, are consistent with the $ZrClO_xH_y$ structure and assignment.

An additional and unexpected result of this study of $Zr_6Cl_{12}H$, is the presence of two different sets of lattice parameters for the material differing by 7-8 Å³ per unit cell (Table 3). Samples prepared from $ZrCl/ZrCl_4$ mixtures with controlled amounts or adventitious hydrogen show the smaller cell, while $ZrCl$ or $ZrCl_2/H_2$ preparations always yield $Zr_6Cl_{12}H$ with the larger parameters. The NMR study on the material with the smaller cell and the need for hydrogen in the preparation of clusters with both cell sizes rules out hydrogen in one cluster and not the other as the cause. Rather, the difference appears to be closely linked to the degree of reduction of the starting mixture and, therefore, the presence or absence of ZrH_{2-x} in the product. The larger cell is found only in equilibrium with ZrH_{2-x} . A reasonable explanation which has previously been advanced,²³ is that a small fractional occupancy of the isolated cation site in $Zr_6Cl_{12}H$ by Zr^{4+} cations is responsible for the larger cell material. Complete occupation of the cation site by M^{3+} ions in numerous $M_7X_{12}Z$ compounds^{16,40,115} is well documented and easily recognized by powder diffraction intensities of certain reflections. The small fractional occupancy suggested for $Zr_{6+x}Cl_{12}H$ would, however, be virtually indistinguishable from the stoichiometric compound. The consistency of the two sets of lattice parameters within their respective

groups may indicate two discrete compositions or simply a failure thus far to produce intermediate compositions. Further synthetic work, as well as structural studies of both the large and small cell materials may be necessary to elucidate the factors responsible.

The presence of hydrogen in $Zr_6Cl_{12}H$ undoubtedly extends to the clusters in $M^I_2Zr_7Cl_{18}(H)$, $Zr_6Br_{12}(H)^{23}$ and the recently prepared $Li_6Zr_6Cl_{18}(H)^{73}$. The structural studies of both $K_2Zr_7Cl_{18}H$ and $Li_6Zr_6Cl_{18}H$ provide a valuable baseline for analyzing Zr-Zr distances in other clusters because the small size of the interstitial hydrogen atom does not limit the Zr-Zr interactions. Interestingly, the 3.201 Å average Zr-Zr distance in $K_2Zr_7Cl_{18}H$ is nearly identical the 3.205 Å average seen in the metal.¹²⁵ All of the other centered zirconium chloride clusters studied by single crystal X-ray diffraction show Zr-Zr distances at least 0.01 Å longer, except the 15-electron cluster in $Cs_{3.0}Zr_6Cl_{16}C$ which has an average Zr-Zr distance of 3.197 Å.

$Zr_6Cl_{12}Be$ and $Cs_2Zr_7Cl_{18}Be$ are the first two examples of transition metal clusters centered by beryllium atoms. Both are isostructural with the analogous hydrides. An increase of 13-14 Å³ per cluster is observed in both compounds over the corresponding hydrides, a reflection of the significantly larger interstitial atom (Table 3). Structural characterization by single crystal X-ray diffraction has not been carried out because of the lack of suitably sized crystals.



A variety of compounds containing M_6X_{12} -type clusters have been known for the niobium and tantalum halides for over twenty years.¹⁻⁶ The clusters in these compounds are found as isolated $M_6X_{12}^i X_6^a$ units as in $K_4Nb_6Cl_{18}$ ³ or as condensed versions of these M_6X_{18} units linked together by the sharing of chlorine atoms as in Nb_6Cl_{14} ⁶ and Ta_6Cl_{15} .⁴ About ten years ago a new structure type containing M_6X_{12} -type clusters, Zr_6I_{12} , now known to actually be $Zr_6I_{12}C$, was reported.^{14,15,36} As was the case with the niobium and tantalum halide cluster compounds, $Zr_6I_{12}C$ could also be viewed as a condensation product of M_6X_{18} clusters. A further examination of these early transition metal clusters shows that all of the structure types and their different stoichiometries are created using only two modes of intercluster connectivity or sharing of halogen atoms, namely, X^a-a and X^i-a . It also becomes quickly apparent that another combination of these two modes of connectivity, specifically $[M_6X_8^i X_{4/2}^{i-a}] X_{4/2}^{a-i} X_{2/2}^{a-a}$, would give the new composition M_6X_{13} (Table 2).

Recent work on centered zirconium halide clusters⁵⁹ has suggested that the metal to halogen ratio in these compounds can be controlled to a large extent by the choice of the interstitial atom and the number of cations present. The observed preference for 14 cluster-bonding electrons in these centered clusters indicated boron should be the element of choice as an interstitial atom in the preparation of $Zr_6Cl_{13}Z$. Indeed, $Zr_6Cl_{13}B$ had already been prepared while attempting the preparation of

$Zr_6Cl_{14}B$, but was obtained only as a powder and was unidentified. Identification of the compound had to wait for the preparation and single crystal diffraction study of $KZr_6Cl_{13}Be$. Interestingly, although the correct composition, M_6X_{13} , was obtained, the expected combination of χ^{i-a} and χ^{a-a} connectivities is not observed. Rather, two new modes of connectivity for isolated M_6X_{12} -type clusters are observed, namely, triply shared χ^{a-a} atoms and shared χ^{i-i} atoms.

Synthesis

$KZr_6Cl_{13}Be$ was initially prepared as a few dark red, intergrown parallelepipeds in a reaction at 800°C loaded with stoichiometric quantities of reactants to prepare the double salt $K_2ZrCl_6 \cdot Zr_6Cl_{12}Be$. Both the $Zr_6Cl_{12}Be$ cluster and the cesium double salt had previously been prepared under comparable conditions. The reaction of stoichiometric amounts of Zr powder, $ZrCl_4$, KCl and Be flakes to give $KZr_6Cl_{13}Be$ yields the desired material in 85-95% yield after two weeks at 800-850°C. The remainder of the product is a mixture of the 13-electron cluster, $K_2Zr_6Cl_{15}Be$, and the layered compound $ZrClO_x$.⁵² The oxygen is believed to come from a thin oxide layer on the beryllium metal. $K_2Zr_6Cl_{15}Be$ can be prepared in excellent yield (95%) by using stoichiometric amounts of reactants. Precise control of the ratios of reactants, particularly with respect to potassium, is important in obtaining formation of the desired product.

$RbZr_6Cl_{13}Be$ was prepared under conditions similar to those for $KZr_6Cl_{13}Be$ from stoichiometric amounts of Zr powder, $ZrCl_4$, RbCl and Be flakes. Yields in excess of 95% are obtained of the dark reddish-brown

material. $\text{Rb}_2\text{Zr}_6\text{Cl}_{15}\text{Be}$ has not been observed. $\text{RbZr}_6\text{Cl}_{13}\text{Be}$ was also prepared from $\text{KZr}_6\text{Cl}_{13}\text{Be}$ by ion exchange in molten RbAlCl_4 at 350°C . Cation exchange was complete after ten days as estimated by changes in Guinier powder diffraction patterns, both in terms of reflection positions and intensities. The reaction may be complete after shorter time periods, but these were not investigated.

Attempts to prepare the sodium analogue, $\text{NaZr}_6\text{Cl}_{13}\text{Be}$, using high temperature reactions and by the immersion of $\text{KZr}_6\text{Cl}_{13}\text{Be}$ in molten NaAlCl_4 at 350°C for nine days were unsuccessful.

$\text{Zr}_6\text{Cl}_{13}\text{B}$, isostructural with $\text{KZr}_6\text{Cl}_{13}\text{Be}$ neglecting the cation, was prepared as a brown microcrystalline material in 95% yield by the reaction of Zr powder, ZrCl_4 , and amorphous B powder in stoichiometric quantities at 850°C . Small amounts (<5%) of $\text{Zr}_6\text{Cl}_{14}\text{B}$ were often obtained also, usually in the form of highly reflective gem-like crystals.

$\text{Zr}_6\text{Br}_{13}\text{B}$ was prepared under identical conditions to those of the chloride in 80-85% yields using ZrBr_4 as the oxidizing reagent rather than ZrCl_4 . The remaining 15-20% of the product was $\text{Zr}_6\text{Br}_{12}\text{B}$ which is isostructural with $\text{Zr}_6\text{I}_{12}\text{C}^{36}$ and $\text{Zr}_6\text{Cl}_{12}\text{H}^{23}$. Formation of the 15-electron cluster, $\text{Zr}_6\text{Br}_{12}\text{B}$, can be at least partially suppressed by the addition of excess ZrBr_4 to the reaction. Lattice parameters for the known $\text{M}^{\text{I}}\text{Zr}_6\text{X}_{13}\text{Z}$ compounds are given in Table 4.

Intercalation reactions of $\text{Zr}_6\text{Cl}_{13}\text{B}$ and $\text{Zr}_6\text{Br}_{13}\text{B}$ were carried out in liquid NH_3 distilled from a K/NH_3 solution. Distillation of NH_3 onto a 1:1.1 mole ratio of $\text{Zr}_6\text{Cl}_{13}\text{B}$ and sodium or potassium metal resulted in

Table 4. Unit cell parameters for $M^I Zr_6 Cl_{13} Be$ and $Zr_6 X_{13} B$ compounds^a

Compound	a	b	c	V
$KZr_6 Cl_{13} Be$	11.627(2)	12.139(2)	7.472(1)	1054.6(3)
$RbZr_6 Cl_{13} Be$	11.694(1)	12.156(1)	7.4585(6)	1060.2(2)
$Rb_x K_{1-x} Zr_6 Cl_{13} Be^b$	11.685(1)	12.158(2)	7.4580(9)	1059.5(3)
$Zr_6 Cl_{13} B$	11.523(2)	12.142(2)	7.4221(9)	1038.4(3)
$Zr_6 Br_{13} B$	12.074(1)	12.6767(8)	7.7343(7)	1183.8(2)

^aGuinier powder diffraction data. Axial lengths are in Å, volumes in Å³.

^bPrepared by ion exchange, $x \approx 1$.

decomposition of the cluster compound. Reaction of the alkali metal with the host material as evidenced by the decolorization of the NH_3 solution occurred rapidly on melting of the NH_3 . Powder diffraction patterns of the product showed no changes in line positions or intensities from the starting material. $\text{M}^{\text{I}}\text{Cl}$ lines were seen in the diffraction patterns following annealing of the samples under vacuum at 150°C for several hours. Similarly unencouraging results were obtained with the bromide.

Cluster oxidation by cation removal from $\text{KZr}_6\text{Cl}_{13}\text{Be}$ was attempted with I_2 in tetrahydrofuran (THF) and acetonitrile. Although the yellow-brown color associated with I_2 in THF had decreased in intensity after 18 hours, the product showed no change in lattice parameters or relative reflection intensities from the starting material. Decomposition of the cluster phase is suspected. Decomposition also occurred in CH_3CN where $\text{KZr}_6\text{Cl}_{13}\text{Be}$ reacted with the solvent to form a dark blue solution plus undissolved material prior to I_2 addition. The stability of the cluster phase during ion exchange reactions suggests oxidation reactions in tetrachloroaluminate melts might be fruitful, but these have not been attempted.

Crystallography

Single crystal X-ray diffraction data were collected on a small, dark-red parallelepiped using monochromatic $\text{Mo K}\alpha$ radiation. The unit cell was chosen on the basis of 16 tuned reflections indexed with the program BLIND.¹²⁶ The predicted orthorhombic cell was confirmed both in axial lengths and symmetry by Polaroid axial photographs taken on the diffractometer. The axial photographs also revealed the presence of a

small satellite crystal with its \tilde{c} axis oriented colinearly with the \tilde{c} axis of the primary crystal. The other axes, of course, were not aligned. In spite of the potential difficulties associated with the data collection and the structural solution of such a crystal, two octants of data were collected. An inspection of a subset of symmetry equivalent reflections indicated the intensities averaged poorly. A third octant of data was subsequently collected to verify that the averaging problems did not result from a small monoclinic distortion of the lattice. The third octant also averaged poorly with both of the previously collected octants. The poor averaging of duplicate data appears to be a reflection of the multiple nature of the crystal rather than the consequence of a lower space group symmetry. Because of the averaging problems, the structure was solved and initially refined using only one octant of data ($hk\ell$). The structure was subsequently refined using a second octant of data with essentially the same results, but with slightly higher R values. No significant changes in atom positions were noted. Finally, the structure was refined using the entire data set, which was averaged with a 10σ cutoff. During averaging, 107 observed reflections, presumably those most affected by the presence of the satellite crystal, were eliminated. Pertinent crystallographic details of the data collection and the refinement of the $hk\ell$ octant and of the entire data set are listed in Table 5.

The observed systematic extinctions, $0k\ell: k + \ell = 2n$ and $h0\ell: h + \ell = 2n$, were consistent with the orthorhombic space groups $Pn\bar{m}$ and $Pnn2$. The former was chosen on the basis of a Wilson plot which suggested the

Table 5. Summary of crystallographic data for $\text{KZr}_6\text{Cl}_{13}\text{Be}$

Space Group	Pnm	
Z	2	
a, Å ^a	11.627(2)	
b	12.139(2)	
c	7.472(1)	
V, Å ³	1054.6(3)	
Crystal dimen., mm	0.20x0.18x0.12	
Radiation	Mo K α , graphite monochromator	
2 θ (max), deg.	55.0	
Scan Mode	ω	
Reflections		
octants	hk ℓ	hk ℓ , $\bar{h}\bar{k}\bar{\ell}$, $\bar{h}k\bar{\ell}$
measured refl.	1420	4557
observed refl.	984	2792
independent refl.	984	1006
R(ave), %	-	6.3
μ , cm ⁻¹	45.9	45.9
Transm. coeff. range	0.88 – 1.00	0.87 – 1.00
Secondary ext. coeff.	-	2.1(4) x 10 ⁻⁶
R, %	4.4	3.9
R(w), %	6.3	4.6

^aGuinier powder diffraction data.

structure was centric and later verified by the successful refinement of the structure in the space group. The structure was solved by Patterson superposition methods, and the program ALCAMPS⁹⁶ was used to facilitate map analysis. The similarity of the lattice parameters of $\text{KZr}_6\text{Cl}_{13}\text{Be}$ with those of $\text{Sc}_4\text{Cl}_6\text{Z}$ ($\text{Z} = \text{N}, \text{B}$)⁴⁰ prompted the choice of two zirconium positions from the list of 18 generated by ALCAMPS, which had coordinates similar to those for scandium in $\text{Sc}_4\text{Cl}_6\text{Z}$. The remaining atoms were located by successive cycles of least-squares refinements and Fourier map calculations. The potassium position was identified by its coordination environment which was made up entirely of chlorine atoms at distances slightly longer than 3.40 Å, the sum of the chlorine and ten-coordinate potassium crystal radii.¹²⁷ Following isotropic refinement of the structure, a Fourier map showed a 2-electron peak in the center of the zirconium cluster which was included in subsequent calculations as a beryllium atom. Anisotropic refinement of the structure converged at $R = 4.7\%$ and $R_w = 9.1\%$. A list of calculated structure factors for the $hk\ell$ octant showed the observed structure factors of four reflections deviated positively by more than 6σ from the calculated values. These deviations were attributed to the multiple nature of the crystal and the reflections removed from the data set. The data were reweighted on the basis of $|F_{\text{obs}}|$ in 15 overlapping divisions. Final residuals were $R = 4.4\%$ and $R_w = 6.3\%$. The refined potassium and beryllium occupancies, and the beryllium thermal parameter converged at 1.01(2), 1.36(12), and 1.5(5), respectively.

Refinement of the structure using the entire data set averaged with a 10σ cutoff, gave nearly identical results as the one octant refinement. Although the 10σ cutoff eliminated 107 observed reflections, most independent reflections were observed three times leaving at least two for averaging. The three octants of data averaged at 6.3%. The refinement converged to $R = 3.9\%$ and $R_w = 4.6\%$ after application of a secondary extinction correction, elimination of four reflections with F_{obs} deviating by more than 6σ from F_{calc} , and a reweighting of the data set in 10 overlapping divisions based on $|F_{\text{obs}}|$. Each of the four reflections eliminated was not observed in at least one of the octants measured. Positional parameters from the refinement are identical to those of the single octant refinement and have improved standard deviations. The thermal parameters in the B_{11} direction for all atoms are slightly larger than those in the single octant case and for Zr1 and Zr2 deviate by $\sim 5\sigma$.

The three octant refinement presumably provides the best approximation of the structure, having minimized the effects of the satellite crystal by the averaging of symmetry related reflections. Hence, positional and thermal parameters obtained using the entire data set are given in Table 6. Observed and calculated structure factor amplitudes for the refinement using the entire data set are given in Appendix B.

Structure and discussion

The structure of $\text{KZr}_6\text{Cl}_{13}\text{Be}$ is built-up of linear chains of $\text{Zr}_6\text{Cl}_{12}\text{Be}$ clusters sharing trans, inner chlorine atoms. The linear cluster chains are connected together into a three-dimensional network by

Table 6. Positional and thermal parameters for $\text{KZr}_6\text{Cl}_{13}\text{Be}$

Atom	x	y	z	B_{11}
Zr1	0.37475(8)	0.35010(7)	0	1.25(4)
Zr2	0.61259(5)	0.41346(5)	0.7828(1)	1.12(3)
C11	0	0	0	2.0(1)
C12	0.2312(2)	0.1736(2)	0	1.96(9)
C13	0.7430(2)	0.3167(2)	0	1.62(9)
C14	0.2399(1)	0.4306(1)	0.2403(3)	1.58(6)
C15	0.4846(1)	0.2434(1)	0.2429(3)	1.73(6)
κ^a	0	1/2	0	4.0(2)
Be ^b	1/2	1/2	0	1.7(4)

^aOccupancy refined to 1.00(2).^bOccupancy refined to 1.24(9).

B_{22}	B_{33}	B_{12}	B_{13}	B_{23}
0.99(4)	0.93(4)	-0.13(3)	0	0
1.06(3)	0.72(3)	0.09(2)	0.09(2)	-0.07(2)
2.1(1)	0.7(1)	-0.9(1)	0	0
1.6(1)	1.0(1)	-0.80(8)	0	0
1.6(1)	1.1(1)	0.62(8)	0	0
1.37(6)	1.50(8)	-0.28(5)	0.53(5)	-0.04(6)
1.26(6)	1.61(7)	-0.19(5)	-0.21(6)	0.46(6)
5.0(3)	5.0(3)	0.9(2)	0	0

additional triply-shared terminal chlorine atoms. A pair of cluster chains and their interconnectivity is shown in Figure 5. The connectivity around each cluster is formulated $[\text{Zr}_6\text{Cl}_{10}^i\text{Cl}_{2/2}^{i-i}\text{Be}]\text{Cl}_{6/3}^{a-a}$, where the superscripts describe the functionality of the chlorine atoms.

The three-dimensional connectivity of the structure packs the cluster chains in a pseudo-body-centered fashion, with the central cluster chain translated by $\tilde{c}/2$ with respect to the four surrounding chains. Within the space group Pnm, the central cluster chain is related to the four surrounding chains by n-glides with planes at $x = \pm 1/4$ and $y = \pm 1/4$. By virtue of the body-centered-type packing, each cluster chain is also surrounded by 4/4 channels which run parallel to the chains and contain the potassium (or rubidium) cations. In the cases of the borides, $\text{Zr}_6\text{Cl}_{13}\text{B}$ and $\text{Zr}_6\text{Br}_{13}\text{B}$, the channels are empty. The cation channels and the packing of the linear cluster chains are shown in a [001] view of the structure in Figure 6. The cation channels are composed of trans-edge shared trigonal antiprisms which have four additional chlorine atoms in the form of a rectangle around the waist, perpendicular to the pseudo- $\tilde{3}$ axis. Every other of these 3-4-3 chlorine polyhedra, shown in Figure 7, is occupied by a cation. The cation-cation distance within the channels is equal to the \tilde{c} dimension of the cell, 7.472 Å in $\text{KZr}_6\text{Cl}_{13}\text{Be}$.

The individual clusters in $\text{KZr}_6\text{Cl}_{13}\text{Be}$ have C_{2h} symmetry, the two-fold axis running down the center of the cluster chain. The Zr-Zr distances range from 3.246 - 3.356 Å and average 3.310 Å. The short Zr-Zr

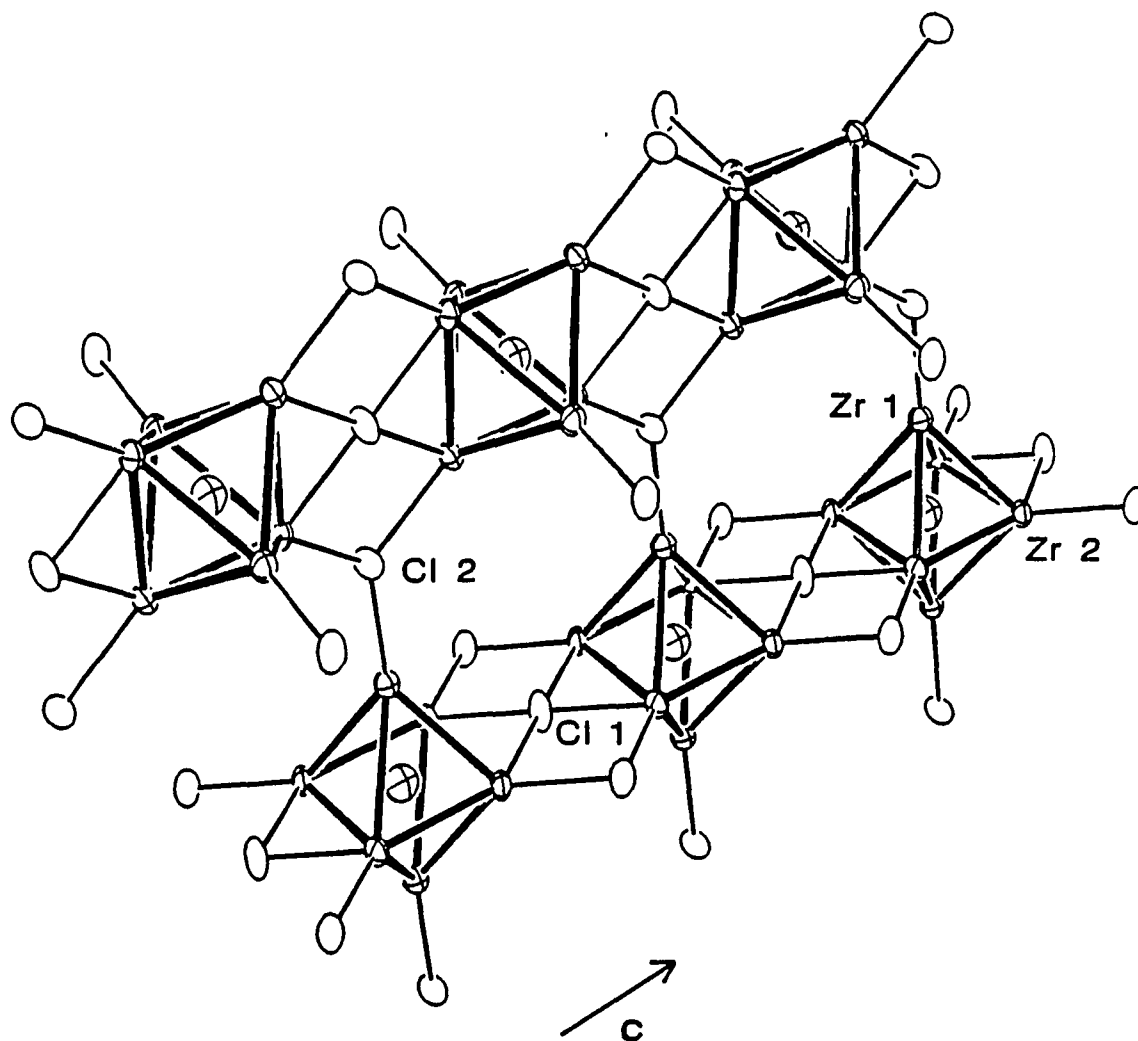


Figure 5. A pair of interconnected linear cluster chains in $\text{KZr}_6\text{Cl}_{13}\text{Be}$. Edge-bridging Cl^{I} atoms not involved in intercluster bonding are omitted for clarity. Particularly noteworthy are the triply shared $\text{Cl}^{\text{a-a}}$ atom between cluster chains and the $\text{Cl}^{\text{i-i}}$ atom between clusters within a chain. (90% ellipsoids.)

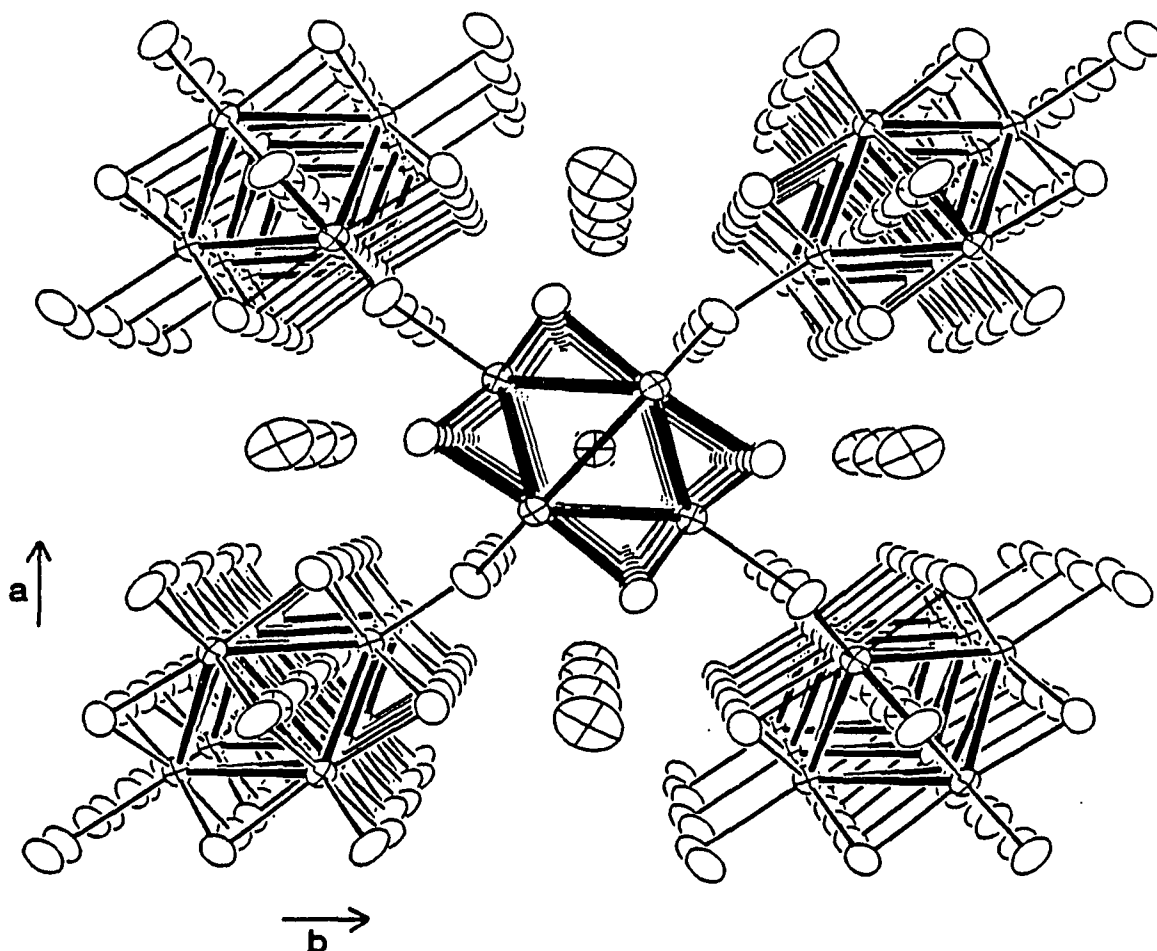


Figure 6. A [001] view of the structure of $\text{KZr}_6\text{Cl}_{13}\text{Be}$ emphasizing the cation channels between cluster chains, the pseudo-body-centered packing of the chains and the similarity of the chains to those in $\text{Sc}_4\text{Cl}_6\text{Z}$. Potassium cations are shown as large crossed ellipsoids between cluster chains. All atoms are drawn at 90% probability

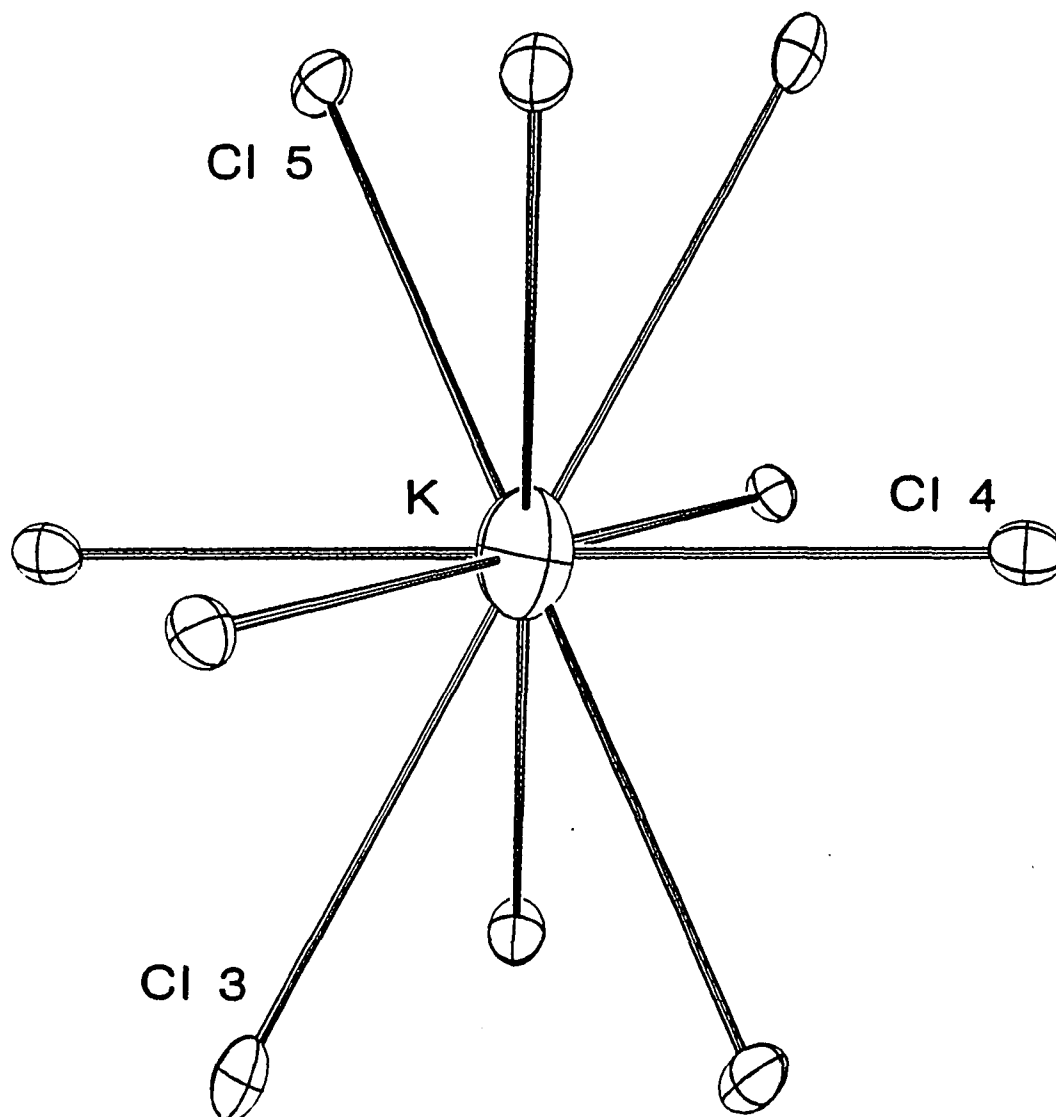


Figure 7. The potassium site in $\text{KZr}_6\text{Cl}_{13}\text{Be}$. The site has $2/m$ symmetry with the mirror plane approximately in the plane of the figure. All ellipsoids are drawn at 50% probability

distance is between atoms in the chain direction (\check{c}), while the long distances are perpendicular to the chain, between zirconium atoms bridged by the Cl^{i-i} atom. The Zr-Zr distance between clusters in the chain direction is 4.226 Å. The Zr-Be distances are 2.3306(9) and 2.3349(7) Å. The average value, 2.334 Å, gives an effective beryllium radius of 1.47 Å when the six-coordinate zirconium radius of 0.86 Å¹²⁷ is subtracted from it. The radius is similar to that obtained from other beryllium-centered zirconium clusters and is about 0.02 Å larger than the observed radius for boron. The Zr-Clⁱ distances are also typical of zirconium chloride clusters and average about the sum of the respective crystal radii.¹²⁷ The Zr-Clⁱ⁻ⁱ distances are considerably longer at 2.698(1) Å, presumably a reflection of the weaker Zr-Cl bonding associated with the unusual four-coordinate environment of the chlorine. The Zr-Cl^{a-a} distances are longer yet at 2.716(3) - 2.735(2) Å. Interatomic distances in $\text{KZr}_6\text{Cl}_{13}\text{Be}$ are given in Table 7.

The unusual Cl^{i-i} atom (Cl1) and its four zirconium neighbors are planar by symmetry, the site having C_{2h} point symmetry. The mirror plane lies perpendicular to the chain direction (\check{c}). The four zirconium atoms form a rectangle around the Cl^{i-i} atom with Zr-Zr distances of 4.226 Å parallel to the chain and 3.356 Å normal to it. The X^{i-i} connectivity observed in the $\text{M}^I\text{Zr}_6\text{Cl}_{13}\text{Z}$ compounds is very uncommon in the rare earth and early transition metal halide clusters and has previously been observed only in the condensed cluster structures of Er_4I_5 and Er_6I_7 .^{12,13} More recently, the highly distorted dicarbide cluster, $\text{Sc}_6\text{I}_{11}\text{C}_2$,¹²⁸ was observed to also have inner-inner halide connectivity.

Table 7. Interatomic distances in $\text{KZr}_6\text{Cl}_{13}\text{Be}$ (Å)

Zr-Zr		
Zr1-Zr2	(x4) ^a	3.297(1)
Zr1-Zr2	(x4)	3.301(1)
Zr2-Zr2	(x2)	3.246(2)
Zr2-Zr2	(x2)	3.357(1)
\bar{d}		3.300
Zr-Be		
Zr1-Be	(x2)	2.3306(9)
Zr2-Be	(x4)	2.3349(7)
\bar{d}		2.3335
Zr-Clⁱ		
Zr1-C15	(x4)	2.570(2)
Zr1-C14	(x4)	2.576(2)
Zr2-C13	(x4)	2.513(2)
Zr2-C15	(x4)	2.552(2)
Zr2-C14	(x4)	2.560(2)
Zr-Clⁱ⁻ⁱ		
Zr2-C11	(x4)	2.698(1)
Zr-Cl^{a-a}		
Zr1-C12	(x2)	2.716(3)
Zr2-C12	(x4)	2.735(2)
K-Cl		
K-C14	(x4)	3.423(2)
K-C15	(x4)	3.529(2)
K-C13	(x2)	3.725(3)
\bar{d}		3.526

^aNumber of times the distance occurs per cluster or cation.

The χ^i-i connectivity is also observed for oxygen in the extended chain structures of $\text{Sc}_{0.75}\text{Zn}_{1.25}\text{Mo}_4\text{O}_7$ and $\text{LiMo}_8\text{O}_{10}$.^{129,130}

The triply-shared Cl^{a-a} atom is unique to the $\text{KZr}_6\text{Cl}_{13}\text{Be}$ structure, although similar connectivity is observed for oxygen in several reduced ternary molybdenum oxide phases.¹³⁰

The structure of $\text{KZr}_6\text{Cl}_{13}\text{Be}$ from an alternate point of view, can be described in terms of close-packed layers of chlorine atoms in much the same way as the structures of $\text{Zr}_6\text{Cl}_{12}\text{C}$, $\text{Nb}_6\text{Cl}_{14}$ and $\text{K}_2\text{Zr}_7\text{Cl}_{18}\text{H}$ have been previously described.²³ The chlorine layers in $\text{KZr}_6\text{Cl}_{13}\text{Be}$ stack in the \tilde{a} direction in an ...ABAC... fashion or $(\text{ch})_2$ when described in terms of neighboring chlorine layers. The zirconium atoms cluster in octahedral sites above and below beryllium-filled voids in the A layer. Two additional chlorine vacancies per cell exist in the A layer and make-up the cation channels between cluster chains. As noted earlier, only every other vacancy is occupied by a cation. All told, the A chlorine layer is composed of five chlorine atoms, a beryllium atom, a potassium atom and a vacancy per unit cell. A projection of the layer at $x = 0$ with Zr_6 clusters superimposed is shown in Figure 8. The A layer at $x = 1/2$ is translated by $(\tilde{b}+\tilde{c})/2$ with respect to the A layer at $x = 0$. The B and C chlorine layers are complete, being composed of eight chlorine atoms per unit cell.

The close-packed description of $\text{KZr}_6\text{Cl}_{13}\text{Be}$ shows a remarkable similarity to that of the $\text{Nb}_6\text{Cl}_{14}$ structure.⁶ The chlorine layers in $\text{Nb}_6\text{Cl}_{14}$ stack ...ABAC... in the \tilde{c} direction with metal atoms clustering around vacancies in the A chlorine layers. A second vacancy also exists

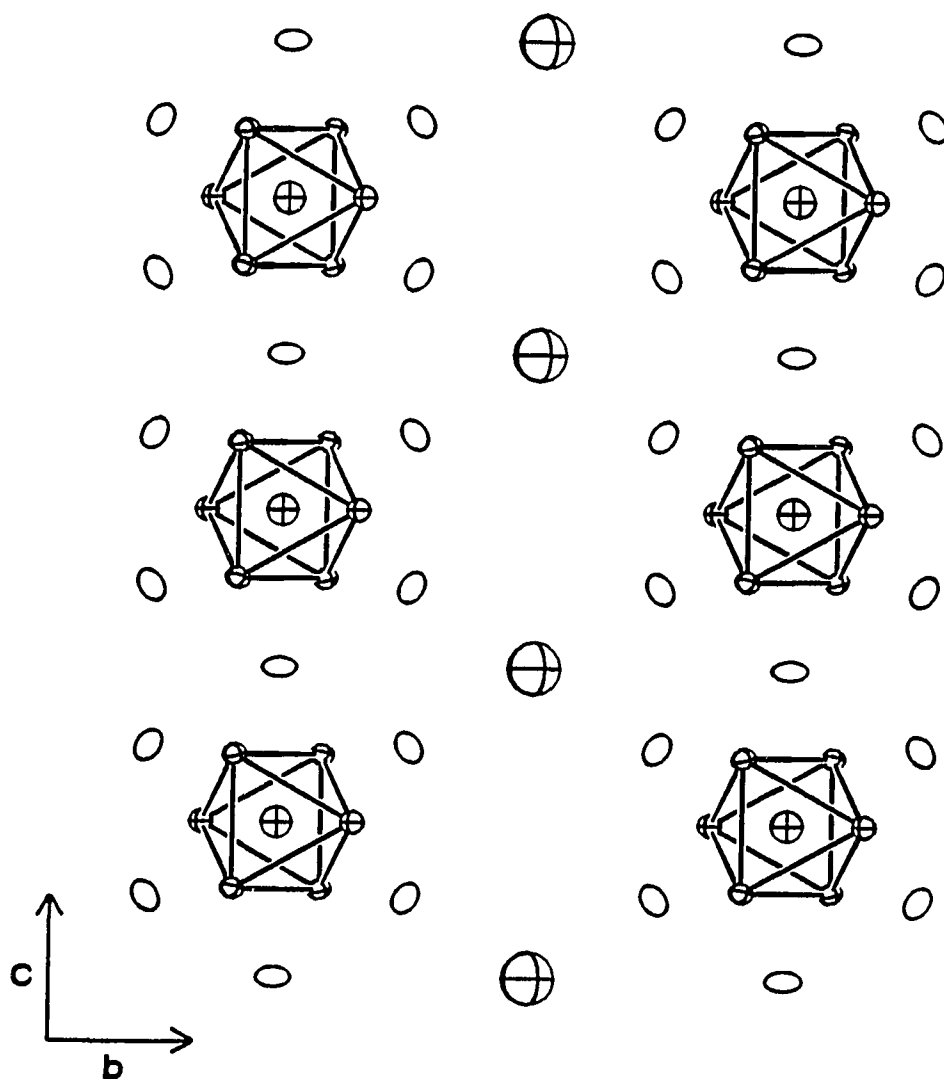


Figure 8. A $[100]$ projection on $x = 0$ of the A chlorine layer in $\text{KZr}_6\text{Cl}_{13}\text{Be}$ with Zr_6 clusters superimposed. The large and small crossed ellipses are K and Be atoms, respectively, and the open ellipses are chlorine atoms. Ellipses are drawn at 90% probability

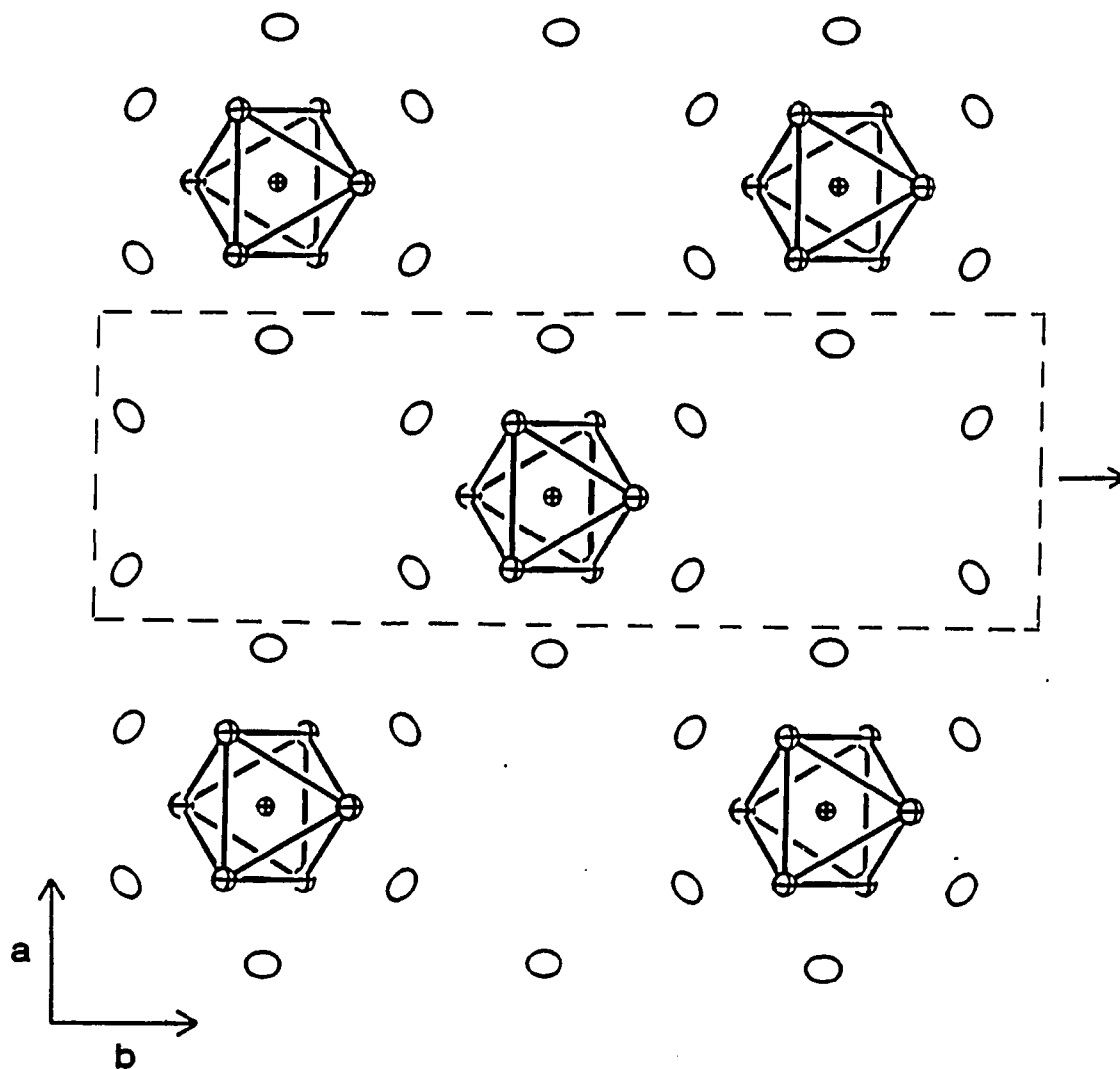


Figure 9. A [001] projection on $z = 1/2$ of the clusters in $Zr_6Cl_{14}B$. The open areas between clusters are the cation sites. Translation of every other row of clusters in \bar{a} , the section enclosed in the box, by $b/2$ gives the cluster arrangement seen in the $KZr_6Cl_{13}Be$ structure

in the A layer, apparently generated by the bridging requirements of the cluster and is the site of the alkali metal cation in the $M^I Zr_6 X_{14} Z$ compounds.^{36,37} As in $KZr_6 Cl_{13} Be$, the B and C chlorine layers in $Nb_6 Cl_{14}$ are complete.

The relationship between the two structure types is shown in the projections in Figures 8 and 9 of the A chlorine layers with metal clusters superimposed in $KZr_6 Cl_{13} Be$ and $Nb_6 Cl_{14}$, respectively. Transformation of the $Nb_6 Cl_{14}$ structure into the $KZr_6 Cl_{13} Be$ structure is accomplished by a translation of every other row of clusters in \vec{a} by $\vec{b}/2$. The fourteenth chlorine atom, lying in a channel between linear cluster chains following the translation, is replaced with a potassium atom. The vacant cation site in $Nb_6 Cl_{14}$ carries over into the $KZr_6 Cl_{13} Be$ structure and is the vacancy between potassium atoms in the cation channel. The quality of the above description is nicely illustrated by a comparison of the formula unit volumes of $Zr_6 Cl_{14} B$ and $Zr_6 Cl_{13} B$ in the $Nb_6 Cl_{14}$ and $KZr_6 Cl_{13} Be$ structures, respectively. $Zr_6 Cl_{14} B$ has a volume of 520 $\text{\AA}^3/\text{cluster}$, while $Zr_6 Cl_{13} B$, which has one additional cluster electron has a nearly equal volume of 519 $\text{\AA}^3/\text{cluster}$.

The unique structural framework of $KZr_6 Cl_{13} Be$ with its one-dimensional cation channels, offers a potentially rich chemistry of cation exchange, removal and insertion. The latter two areas also involve cluster oxidation or reduction, respectively. Although the cation removal and insertion reactions attempted were not particularly encouraging, as noted above, success of the cation exchange reaction in $RbAlCl_4$ clearly demonstrated that cation mobility and structure stability

can be achieved together in low temperature (350°C) tetrachloroaluminate melts. Additional work in either molten salts or other solvents may lead to routes for cation removal/cluster oxidation or cation insertion/cluster reduction. The preparation of further derivatives of $\text{KZr}_6\text{Cl}_{13}\text{Be}$ by ion-exchange possibly with multivalent cations, also appears promising.



A diverse interstitial chemistry has been developed over the past several years for the zirconium iodides in the $\text{Nb}_6\text{Cl}_{14}$ structure. Interstitial atoms ranging from small second period elements like boron and carbon^{36,37} to larger main group elements (P, Si, Al)^{37,61} and even metals (K, Fe, Co, Mn)^{62,64} have all been found to stabilize this otherwise electron-deficient zirconium cluster. The ability of the $\text{Nb}_6\text{Cl}_{14}$ structure to also accommodate a large cation in conjunction with the interstitial chemistry has allowed the metal-metal bonding levels within the cluster to be explored by the systematic variation of the cluster electron count.³⁶

The success of this chemistry for the zirconium iodides led to an exploration of analogous zirconium chloride systems. In many respects, the zirconium chloride systems fail to show the diversity of interstitial chemistry or the tolerance of various degrees of cluster oxidation which are characteristic of the iodides. The chloride systems, however, both by the successes and failures, provide further insight into the factors affecting cluster stability, particularly the effect of the anion matrix on the Zr-X^i antibonding contribution to the eighth metal-metal bonding

orbital (see Bonding section). In addition, work in the system, besides providing a number of new $M^I Zr_6 Cl_{14} Z$ compounds, has led to the preparation of compounds in several new structure types with stoichiometries other than $M_6 X_{14}$.

Synthesis

$Zr_6 Cl_{14} C$ was initially obtained as the major product (95+%) in a reaction designed to prepare ' $Zr_6 Cl_{15}$ '¹⁷ using stoichiometric amounts of Zr powder, $ZrCl_4$, and C in the form of graphite as the interstitial element at 850°C. The dark red-brown material was identified as $Zr_6 Cl_{14}$ by a comparison of the observed powder diffraction pattern with one calculated using the parameters from $Nb_6 Cl_{14}$.⁶ The excess $ZrCl_4$ in the reaction appeared to be approximately the amount necessary to generate the equilibrium $ZrCl_4$ pressure over the product at reaction temperature and could easily be removed by sublimation under static vacuum. A variety of temperatures from 700–950°C were used to prepare $Zr_6 Cl_{14} C$; however, crystal growth was negligible in all cases. Attempts to improve crystal growth by a variety of other techniques including $M^I Cl/ZrCl_4$ fluxes, temperature gradients, mobile carbon sources such as paraffin and slow cooling were also tried, but with minimal success. Crystals of $Zr_6 Cl_{14} C$ were obtained on two occasions, however, in reactions contaminated with oxygen. The data crystal came from a reaction designed to prepare ' $Na_4 Zr_6 Cl_{18}$ ' under H_2 at 700°C. A leak developed in the hydrogenation system during the reaction, surrounding the tantalum reaction tube with a hydrogen/air mixture. The carbon source in the reaction is unknown. Guinier powder diffraction patterns show the lattice parameters

to be slightly larger than those obtained for $Zr_6Cl_{14}C$ prepared with graphite (Table 8). A second reaction, loaded stoichiometrically to prepare $NaZr_6Cl_{15}^{13}C$, produced gem-like crystals of $Zr_6Cl_{14}C$, but the large amounts of $ZrClO_x$ also present indicated the reaction was contaminated with oxygen, presumably from an impure ^{13}C source. Lattice parameters in this case showed no significant deviation from those obtained from $Zr_6Cl_{14}C$ prepared with graphite. Reasons for the difficulties encountered growing crystals are not clear, particularly in light of the zirconium iodide results where crystal growth is exceptional.^{36,37} The experience with the reactions contaminated with oxygen, however, suggests chemical transport by CO may be useful for crystal preparation.^{81,131} Additional work will be required to verify the transport reaction and prepare single crystals.

$Zr_6Cl_{14}B$ was prepared in 5-10% yields in reactions at 950°C stoichiometrically loaded to prepare Zr_2Cl_2B . The highly reflective, black, gem-like crystals were easily separated from the dark-brown, microcrystalline Zr_2Cl_2B .¹³² The crystals were often twinned and mixed with similarly shaped crystals of $Zr_6Cl_{13}B$. Although prepared only in low yield, Guinier lattice parameters, given in Table 8, clearly support the identification of the material as a boride rather than a carbide formed from adventitious carbon. The identification is further supported by a single crystal X-ray diffraction study (below). The reaction of stoichiometric amounts of Zr powder, $ZrCl_4$, and amorphous B powder to prepare $Zr_6Cl_{14}B$ invariably produced $Zr_6Cl_{13}B$ in greater than 95% yield. Single

Table 8. Cell parameters (\AA) and volumes (\AA^3) of $\text{Zr}_6\text{Cl}_{14}\text{Z}$ ($\text{Z} = \text{C}, \text{B}$) and $\text{M}^1\text{Zr}_6\text{Cl}_{14}\text{B}$ compounds^a

Compound	a	b	c	V
$\text{Zr}_6\text{Cl}_{14}\text{C}$	14.021(2)	12.562(2)	11.480(3)	2022.0(8)
$\text{Zr}_6\text{Cl}_{14}\text{C}^{\text{b}}$	14.091(8)	12.595(5)	11.506(5)	2042(2)
$\text{Zr}_6\text{Cl}_{14}\text{B}$	14.243(1)	12.640(2)	11.546(1)	2078.6(5)
$\text{LiZr}_6\text{Cl}_{14}\text{B}$	14.267(3)	12.647(3)	11.536(2)	2081.4(8)
$\text{NaZr}_6\text{Cl}_{14}\text{B}$	14.110(2)	12.655(2)	11.535(2)	2059.6(5)
$\text{KZr}_6\text{Cl}_{14}\text{B}$	14.095(1)	12.640(1)	11.570(1)	2061.2(3)
$\text{RbZr}_6\text{Cl}_{14}\text{B}$	14.113(1)	12.647(2)	11.624(1)	2074.4(4)
$\text{CsZr}_6\text{Cl}_{14}\text{B}$	14.143(1)	12.678(2)	11.707(1)	2098.9(4)
$\text{TlZr}_6\text{Cl}_{14}\text{B}$	14.095(1)	12.621(1)	11.583(1)	2060.6(3)
$\text{Zr}_6\text{Br}_{14}\text{C}$	14.690(3)	13.229(3)	11.991(3)	2330(1)
$\text{CsZr}_6\text{Br}_{14}\text{C}$	14.737(1)	13.297(2)	12.108(1)	2372.7(5)
$\text{Zr}_6\text{Br}_{14}\text{Fe}$	14.988(3)	13.408(2)	12.232(2)	2458.1(7)

^aAll values were obtained from Guinier powder diffraction data.

^bAdventitious C, data crystal.

phase amounts of $Zr_6Cl_{14}B$ large enough for physical property measurements were not obtained.

The $M^I Zr_6Cl_{14}B$ phases (see Table 8) were obtained in 95+% yields by the reaction of stoichiometric amounts of Zr powder, $ZrCl_4$, amorphous B powder and $M^I Cl$, except for $TlZr_6Cl_{14}B$ where Tl metal was used, at 850°C for 10-21 days. Good crystal growth was obtained in the $M^I = Na, K, Rb, \text{ and } Cs$ cases. Lattice parameters obtained from Guinier powder diffraction patterns are compiled in Table 8. The case for $LiZr_6Cl_{14}B$ is not unambiguous and will require magnetic susceptibility results to verify Li incorporation.

A variety of other $M^I Zr_6Cl_{14}Z$ reactions with third period interstitial elements and cluster electron counts from 13 to 16 were attempted with limited success. Several new compounds were prepared, but with stoichiometries other than $M^I Zr_6Cl_{14}Z$. A compilation of attempted syntheses, reaction temperatures and major products is given in Table 9. Although the size of the interstitial atom appeared to be an important factor in the failure to prepare other $M^I Zr_6Cl_{14}Z$ compounds, the recent preparation of $CsZr_6Cl_{15}Fe$ and $Zr_6Cl_{15}Co$,⁶³ both with what are comparatively large interstitial atoms, suggests other factors are also important. The thermodynamic stability of adjacent phases is also clearly an overriding criterion.

Crystallography

Two octants of data were collected on a small, gem-like crystal of $Zr_6Cl_{14}Z$ using monochromatic $Mo K\alpha$ radiation. The crystal was obtained from the $Na_4Zr_6Cl_{18}$ reaction described above and, hence, the identity of

Table 9. Unsuccessful $M^I Zr_6 Cl_{14} Z$ reactions

Proposed compound	Electron count	Temperature °C	Major Products
$Zr_6 Cl_{14} Si$	14	800	$Zr_5 Si_3$, $ZrCl_4$ $ZrCl$, $ZrCl_{3-x}$
$CsZr_6 Cl_{14} Al$	14	800	unidentified multiphase product
$CsZr_6 Cl_{14} Be$	13	800	$Cs_2 Zr_7 Cl_{18} Be$
$BaZr_6 Cl_{14} Be$	14	800	unidentified
$Zr_6 Cl_{14} B$	13	850	$Zr_6 Cl_{13} B$
$HgZr_6 Cl_{14} B$	15	850	Hg, $Zr_6 Cl_{13} B$
$CsZr_6 Cl_{14} C$	15	850	$CsZr_6 Cl_{15} C$
$KZr_6 Cl_{14} C$	15	850	$KZr_6 Cl_{15} C$
$NaZr_6 Cl_{14} C$	15	850	$Na_{0.5} Zr_6 Cl_{15} C$
$Zr_6 Cl_{14} N^a$	15	850	1T- $Zr_2 Cl_2 N$, 3R- $ZrClN_x$, ZrN , $ZrCl_4$
$Zr_6 Cl_{14} O^b$	16	850	$ZrClO_x$, $ZrCl_{3-x}$

^a $ZrNCl$ was the nitrogen source.

^b ZrO_2 was the oxygen source.

the interstitial atom is not certain. Details of the data collection are given in Table 10.

Refinement of the known structure-type was begun with the niobium and chlorine positional parameters from $\text{Nb}_6\text{Cl}_{14}$ ⁶ after the appropriate transformation from the nonstandard space group Bbam to Cmca. The zirconium and chlorine positions and isotropic thermal parameters refined uneventfully to $R = 7.3\%$ at which point a Fourier map showed an approximately 7-electron residual in the cluster center. Because of the unknown nature of the interstitial atom, several refinements with different elements in the interstitial site were carried out. Carbon was finally chosen as the interstitial atom because of the similarity of the crystal's lattice constants to those of $\text{Zr}_6\text{Cl}_{14}\text{C}$ prepared from graphite, and the consistency of the refined Zr-Zr and Zr-C distances with those in other structurally characterized carbon-centered clusters. In addition, boron and nitrogen were systematically eliminated because $\text{NaZr}_6\text{Cl}_{14}\text{B}$ and $\text{Zr}_6\text{Cl}_{15}\text{N}$, respectively, would be expected to form under the given conditions with purposeful addition of these interstitial elements. $\text{Zr}_6\text{Cl}_{14}\text{B}$ also shows significantly different lattice parameters from those obtained (Table 8). Sodium and oxygen interstitial atoms were ruled out because the compounds could not be independently prepared with the appropriate elements present. The structural refinement with carbon converged to $R = 4.5\%$ and $R_w = 7.9\%$. The slightly expanded lattice parameters over $\text{Zr}_6\text{Cl}_{14}\text{C}$ and the refined carbon occupancy larger than unity, suggest that a 'mixed interstitial', primarily carbon in character, may be present. The possible combinations of interstitial atoms and the stabilities of

Table 10. Summary of crystallographic data for $Zr_6Cl_{14}C$ and $Zr_6Cl_{14}B$

	<u>$Zr_6Cl_{14}C$</u>	<u>$Zr_6Cl_{14}B$</u>
Space Group	Cmca	Cmca
Z	4	4
a, Å ^a	14.091(8)	14.243(1)
b	12.595(5)	12.640(2)
c	11.506(5)	11.546(1)
V, Å ³	2042(2)	2078.6(5)
Crystal dimen., mm	0.15x0.15x0.20	0.15x0.15x0.15
Radiation	Mo K α , graphite monochromator	Mo K α , Zr β -filter
2 θ (max), deg.	55.0	55.0
Scan mode	ω	2 θ/θ
Reflections		
octants	h,k, $\pm l$	hkl
measured refl.	2391	1252
observed refl.	1653	652
independent refl.	894	652
R(ave), %	1.8	-
μ , cm ⁻¹	46.7	45.9
Transm. coeff. range	0.76 — 1.00	0.82 — 1.00
Secondary ext. coeff.	-	-
R, %	4.5	6.1
R(w), %	7.9	7.9

^aGuinier lattice parameters.

the compounds formed are presently unknown. Evidence for mixed interstitials in the zirconium iodide clusters is fairly conclusive, however.^{15,36,37}

The structure of $Zr_6Cl_{14}B$ was refined with one octant of data collected on a small, gem-like crystal using monochromatic Mo $K\alpha$ radiation. Details of the data collection are summarized in Table 10.

Refinement of the structure of $Zr_6Cl_{14}B$ was carried out using the atomic positions of zirconium and chlorine from the refinement of $Zr_6Cl_{14}C$. A Fourier map calculated following isotropic refinement of the zirconium and chlorine parameters showed a 5-electron residual in the cluster center which was included as a boron atom in subsequent calculations. The model converged to residuals of $R = 6.1\%$, and $R_w = 7.9\%$ after anisotropic refinement of the zirconium and chlorine thermal parameters and a reweighting of the data set. The final difference map showed several 0.5 - 1.0 electron features all associated with refined atom positions. The cation site at (0,0,0) was unoccupied. The anisotropic thermal parameters of all atoms showed a slight elongation in the \vec{b} direction, presumably a consequence of poor crystal quality and/or an inadequate absorption correction.

Positional and thermal parameters for $Zr_6Cl_{14}C$ and $Zr_6Cl_{14}B$ are given in Table 11. Observed and calculated structure factor amplitudes are listed in Appendices C and D for $Zr_6Cl_{14}C$ and $Zr_6Cl_{14}B$, respectively.

Table 11. Positional and thermal parameters for $Zr_6Cl_{14}C$ and $Zr_6Cl_{14}B$

Atom	x	y	z	B_{11}
<u>$Zr_6Cl_{14}C$</u>				
Zr1	0.38286(8)	0.07095(9)	0.8826(1)	0.89(4)
Zr2	0	0.3507(1)	0.8926(1)	0.92(6)
Cl1	0.1242(2)	0.0876(2)	0.2497(3)	1.7(1)
Cl2	0.1240(2)	0.2551(2)	0.0083(3)	1.5(1)
Cl3	1/4	0.3448(4)	1/4	1.3(2)
Cl4	0	0.1582(4)	0.7629(4)	1.5(2)
Cl5	0.2474(3)	0	0	1.0(1)
c^a	0	0	1/2	0.4(3)
<u>$Zr_6Cl_{14}B$</u>				
Zr1	0.3844(1)	0.0715(1)	0.8827(1)	0.51(5)
Zr2	0	0.3502(2)	0.8905(2)	0.66(8)
Cl1	0.1240(3)	0.0881(3)	0.2486(4)	1.2(2)
Cl2	0.1252(3)	0.2547(3)	0.0069(4)	0.9(1)
Cl3	1/4	0.3431(5)	1/4	0.7(2)
Cl4	0	0.1592(4)	0.7623(5)	1.0(2)
Cl5	0.2491(4)	0	0	0.5(2)
b^b	0	0	1/2	2(1)

^aOccupancy refined to 1.4(1).

^bOccupancy refined to 1.0(1).

B_{22}	B_{33}	B_{12}	B_{13}	B_{23}
0.85(4)	0.98(4)	0.00(3)	0.01(4)	0.06(3)
0.96(6)	0.91(6)	0	0	-0.05(5)
1.5(1)	1.2(1)	0.18(9)	0.5(1)	0.34(9)
1.2(1)	1.1(1)	0.48(9)	-0.23(9)	-0.22(8)
1.7(2)	1.3(1)	0	-0.7(1)	0
1.6(2)	1.1(1)	0	0	-0.6(1)
1.8(2)	1.2(1)	0	0	0.1(1)
1.43(6)	0.54(5)	-0.06(5)	-0.11(5)	0.11(5)
1.28(9)	0.55(7)	0	0	-0.01(8)
1.5(2)	1.0(1)	0.0(1)	0.6(1)	0.3(1)
1.4(1)	1.3(1)	0.4(1)	-0.3(1)	-0.2(1)
2.3(3)	1.2(2)	0	-0.7(2)	0
1.2(2)	1.1(2)	0	0	-0.3(2)
2.7(3)	1.0(2)	0	0	0.5(2)

Structure and Discussion

The $\text{Nb}_6\text{Cl}_{14}$ structure, parent type of $\text{Zr}_6\text{Cl}_{14}\text{C}$, $\text{Zr}_6\text{Cl}_{14}\text{B}$ and the $\text{M}^{\text{I}}\text{Zr}_6\text{Cl}_{14}\text{B}$ compounds, has previously been described.^{6,15} From a simplistic point of view, the structure may be viewed as an array of randomly oriented M_6X_{12} clusters packed in layers normal to the [111] direction. Octahedral holes formed by the close-packed clusters are occupied by the cations in the $\text{M}^{\text{I}}\text{Zr}_6\text{Cl}_{14}\text{B}$ compounds.

A more comprehensive description recognizes that the stoichiometry of the compound and the cluster bonding requirements necessitate a complicated sharing of chlorine atoms between clusters. Ten of the twelve edge-bridging Cl^{i} atoms on each cluster are unshared, while the remaining two, serve in a dual capacity as Cl^{i} atoms on one cluster and Cl^{a} atoms on adjacent clusters. The six terminal positions on each cluster are filled by four additional chlorine atoms which are shared with adjacent clusters and by two more distant Cl^{i} atoms from adjacent clusters as described above (see Figure 10). The connectivity in $\text{Zr}_6\text{Cl}_{14}\text{C}$ is, therefore, formulated $[\text{Zr}_6\text{Cl}_{10}^{\text{i}}\text{Cl}_{2/2}^{\text{i-a}}]\text{Cl}_{2/2}^{\text{a-i}}\text{Cl}_{4/2}^{\text{a-a}}$.

An alternative and somewhat enlightening description of the structure is as a close-packed array of chlorine atoms.^{15,23} The chlorine layers, which can easily be visualized between the layers of metal atoms in Figure 10, pack in an ...ABAC... fashion parallel to \vec{c} or as $(\text{ch})_2$ when described in terms of neighboring chlorine layers. Two-eighths of the chlorine positions in the A layer ($z = 0$ and $1/2$) are vacant in $\text{Nb}_6\text{Cl}_{14}$. In the $\text{M}^{\text{I}}\text{Zr}_6\text{Cl}_{14}\text{Z}$ compounds one-half of the

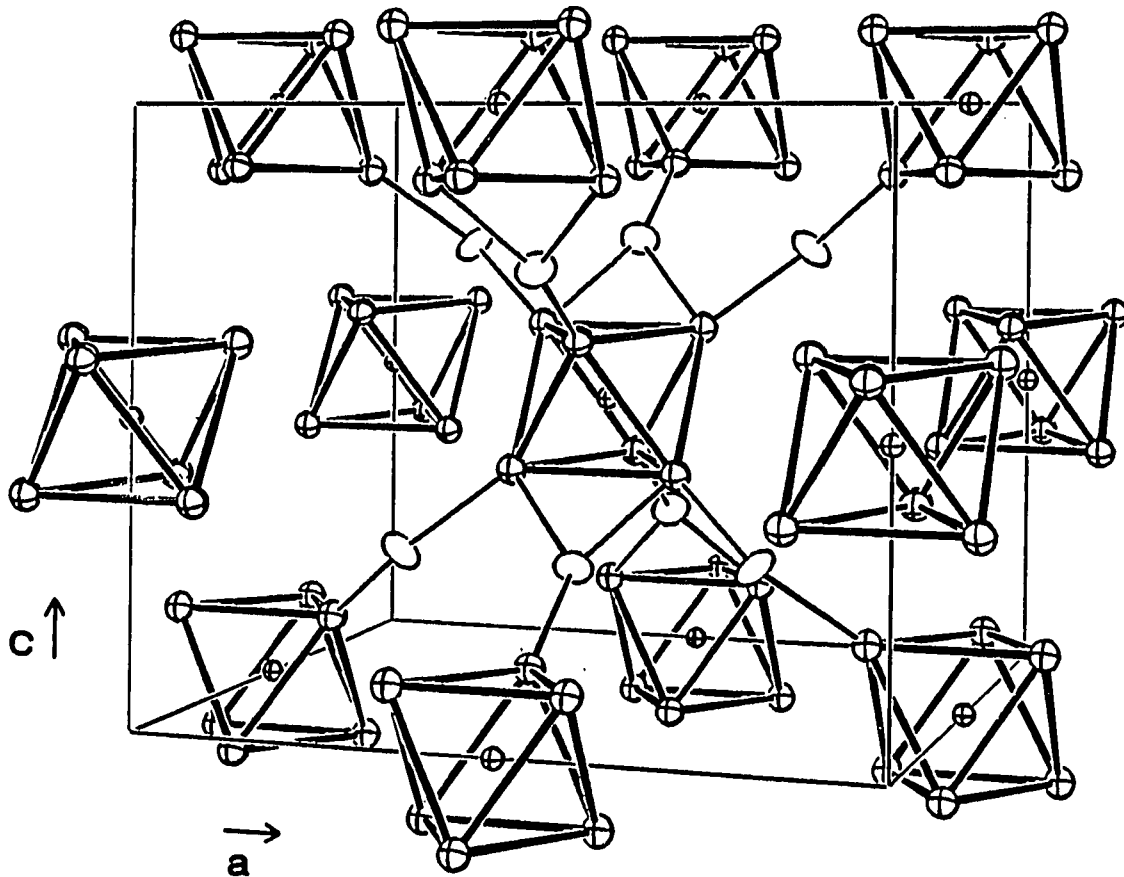


Figure 10. The structure of $Zr_6Cl_{14}C$ emphasizing the intercluster connectivity. Mirror planes lie at $x = 0$ and $1/2$. Although the Cl^I atoms not involved in intercluster connectivity have been omitted for clarity, the close-packed anion layers stacked parallel to \bar{c} can easily be imagined between layers of metal atom. (90% ellipsoids)

vacancies, those in the center of the clusters, are occupied by Z atoms and the other half, apparently generated by the bridging requirements of the clusters, contain the M^I cations if present. Metal atoms occupy 37.5% of the octahedral holes above and below the A layer, clustering around either one-half of the vacant sites in Nb_6Cl_{14} or the Z atom sites in $M^IZr_6Cl_{14}Z$. The B and C chlorine layers are complete.

The crystal structures of $Zr_6Cl_{14}C$ and $Zr_6Cl_{14}B$, while not the best M_6X_{14} structural refinements available, are important in that they are the only structurally refined $Zr_6Cl_{12}Z$ -type clusters that are directly comparable with the interstitially stabilized zirconium iodide clusters, i.e., they are of the same structure type. In addition, the $Zr_6Cl_{14}B$ structure verified the presence of the boron interstitial atom when the cluster could only be prepared in the 5-10% yields typically associated with adventitiously stabilized phases. Interatomic distances for $Zr_6Cl_{14}C$ and $Zr_6Cl_{14}B$ are given in Table 12.

The structural trends established by the $M^IZr_6I_{14}Z$ work^{36,37} are seen to carry over to the chloride clusters in virtually all respects. The $Zr_6Cl_{12}Z$ clusters in both $Zr_6Cl_{14}C$ and $Zr_6Cl_{14}B$ exhibit the slight tetragonal distortion expected on the basis of the effects of the asymmetric bonding of the terminal chlorine atoms.³⁶ The Zr-Zr and Zr-Z distances lengthen, as expected, when going from the carbide to the boride. Both types of distances for their respective interstitial atoms are consistent with distances calculated from tabulated¹²⁷ or derived (from NaCl-type transition metal carbides and borides) crystal radii and with distances from other structurally characterized zirconium chloride

Table 12. Interatomic distances in $Zr_6Cl_{14}C$ and $Zr_6Cl_{14}B$ (Å)

	$Zr_6Cl_{14}C$	$Zr_6Cl_{14}B$
Zr-Zr		
Zr1-Zr1	(x2) ^a 3.235(2)	3.256(3)
Zr1-Zr1	(x2) 3.290(2)	3.294(3)
Zr1-Zr2	(x4) 3.217(2)	3.247(2)
Zr1-Zr2	(x4) 3.218(2)	3.248(2)
\bar{d}	3.232	3.257
Zr-Z		
Zr1-Z	(x4) 2.307(1)	2.316(1)
Zr2-Z	(x2) 2.243(2)	2.277(2)
\bar{d}	2.286	2.303
Zr-Clⁱ		
Zr1-Cl5	(x2) 2.497(3)	2.523(4)
Zr1-Cl2	(x2) 2.522(3)	2.544(4)
Zr1-Cl1	(x2) 2.512(3)	2.546(4)
Zr2-Cl1	(x2) 2.518(3)	2.532(4)
Zr2-Cl2	(x2) 2.503(3)	2.538(4)
Zr-Clⁱ-a		
Zr1-Cl4	(x2) 2.591(3)	2.597(4)
Zr-Cl^a-i		
Zr2-Cl4	(x2) 2.836(4)	2.832(6)
Zr-Cl^a-a		
Zr1-Cl3	(x4) 2.630(2)	2.679(3)

^aNumber of times the distance occurs per cluster or cation.

clusters. Distances in the zirconium iodide clusters tend to be slightly larger because of the matrix effect associated with the larger, tightly packed iodine atoms. The most significant difference observed between the chloride and iodide clusters, also a consequence of the matrix effect, is the degree to which the zirconium atoms have been pulled in from the square faces of the cuboctahedron formed by the X^i atoms. In $Zr_6I_{14}C$ each zirconium atom is pulled in from the square face of the I^i atoms surrounding it by nearly 0.5 Å compared with the approximately 0.25 Å distance in $Zr_6Cl_{14}C$. The difference plays a significant role in the character of the eighth metal-metal bonding orbital which affects the stability of 15- and 16-electron clusters. The character of the eighth M-M bonding orbital is discussed in the section on Bonding.

Structural relationships between $Zr_6Cl_{14}Z$ and $KZr_6Cl_{13}Be$ and $K_2Zr_6Cl_{15}B$ are discussed in the latter two sections, respectively.

M_6X_{15}

The M_6X_{15} compounds offer a wide variety of structure types all exhibiting $[M_6X_{12}^i]X_{6/2}^{a-a}$ connectivity, but which have distinctly different local geometries around the M_6X_{12} clusters and are also structurally unrelated in their larger three-dimensional connectivity. Four distinct structural frameworks and several variations thereon are presently known for the M_6X_{15} compounds.^{4,5,59} The preparation of a series of interstitially stabilized zirconium chloride clusters in all of the known frameworks has allowed the elucidation of some of the specific factors involved in the differentiation and formation of the various structure types. Three of the four primary structural frameworks, i.e.,

those found in the Ta_6Cl_{15} ,⁴ $CsNb_6Cl_{15}$ ⁷² and $K_2Zr_6Cl_{15}B^{59}$ structures, and their variations will be discussed in detail in connection with specific zirconium chloride cluster compounds with those structure types. The fourth structural framework, that found in Nb_6F_{15} ⁵ and the recently identified $Zr_6Cl_{15}Co$,⁶³ will be included in the discussion of the structural details which differentiate the four M_6X_{15} structure types and the factors which are responsible for the formation of the different cluster frameworks.

Compounds with the Ta_6Cl_{15} structural framework

Zr_6Cl_{15} has been known since 1978.¹⁴ It was initially prepared in very low yield as black transported gem-like crystals in a $ZrCl/ZrCl_4$ equilibration with a Cl:Zr ratio less than 2:1 carried out under a 750/600°C temperature gradient.^{14,17} Attempts to reproduce the synthesis using more appropriate Zr:Cl ratios were unsuccessful. A single crystal structural analysis of a crystal from the initial preparation had identified the compound as Zr_6Cl_{15} and showed it to be isostructural with Ta_6Cl_{15} .^{4,17} An approximately 5-6 electron residual was observed in the cluster center. Zr_6Cl_{15} was later identified as a red-brown, microcrystalline coating on a zirconium strip from an attempt to prepare single crystals of $ZrClH_{0.5}$ from Zr strips and $ZrCl_4$ under a hydrogen atmosphere in a 610-700°C gradient.¹³³ Once again, however, synthesis of the apparently 9-electron cluster could not be replicated.

By now the signs of an interstitially stabilized cluster have become fairly apparent. The low and irregular yield of an apparently electron deficient M_6X_{12} cluster and a crystal structure with residual electron

density in the cluster center, clearly identify Zr_6Cl_{15} as an interstitially stabilized cluster. In this case, the interstitial atom has been identified as nitrogen.⁵⁹

Synthesis $Zr_6Cl_{15}N$ was prepared in virtually quantitative yield as dark-red, gem-like crystals from the reaction of stoichiometric quantities of Zr powder, $ZrCl_4$ and $ZrNCl$ at 700°C for two weeks. The lattice parameters of the material obtained were marginally larger than those reported for ' Zr_6Cl_{15} '¹⁷ (0.15%). The discrepancy is typical of those found between lattice constants obtained by Guinier powder diffraction using an internal Si standard and those obtained by tuning reflections on a diffractometer without a calibrant. Small changes in the effective wavelength occur in the latter method as a result of adjustments in the graphite monochromator setting. The observed deviation in lattice constants could result from an error in the wavelength used in the calculation of less than 0.15%. The exceptional improvement in yields with the introduction of nitrogen into the reaction and the good agreement between the crystal structures, particularly in the Zr-Zr distances of ' Zr_6Cl_{15} ' and $Zr_6Cl_{15}N$, leave little doubt as to the identity of the interstitial atom in ' Zr_6Cl_{15} '. Similar reactions in the 800-900°C range give ZrN as the primary nitrogen containing compound with small amounts of $1T-Zr_2Cl_2N$ and $3R-ZrClN_x$ ($x \ll 1$).⁶⁰ No $Zr_6Cl_{15}N$ was observed in any of the higher temperature reactions.

$Zr_6Cl_{15}N$ may also be prepared in 95+% yields using NaN_3 or NH_4Cl as a nitrogen source under the 700°C conditions given above. The lattice parameters of the materials obtained using these alternate nitrogen

sources are within 3σ of those obtained with $ZrNCl$, indicative of no Na or H incorporation into the compound. Lines associated with a $NaCl/ZrCl_4$ double salt are observed in the powder diffraction patterns of the products from reactions containing NaN_3 . The excess hydrogen in NH_4Cl reactions is apparently taken up by the Ta reaction container. No $Zr_6Cl_{12}H$ was observed.

The exceptional crystal growth observed in all reactions suggests a chemical transport reaction is at work, although the mechanism has not been established. Attempts to prepare $Zr_6Cl_{15}C$ invariably yielded $Zr_6Cl_{14}C$.

The approximately isovalent compound $Na_xZr_6Cl_{15}C$ ($x < 1$) was prepared by the reaction of stoichiometric amounts of Zr powder, $ZrCl_4$, NaCl and graphite over a two week period at $850^\circ C$. The compound, produced as dark-red, gem-like crystals, ground to a reddish-brown powder and gave a powder diffraction pattern which clearly identified it as being isostructural with $Zr_6Cl_{15}N$. The cubic unit cell parameters were slightly larger than those of the nitride, consistent with the incorporation of sodium cations in the lattice and the replacement of the nitrogen interstitial atom with a carbon atom. The substitution of the Na-C pair for N leaves the cluster electron count unchanged. Attempts to incorporate or substitute larger cations into the carbide structure, i.e., K, Rb, and Cs, resulted in other M_6X_{15} structure types.¹³⁴ Reactions to prepare $LiZr_6Cl_{15}C$ resulted in yet another compound whose structure and composition are presently unknown. Several reactions were run with excess NaCl under reducing conditions after the crystal structure of

$\text{Na}_{0.5}\text{Zr}_6\text{Cl}_{15}\text{C}$ showed the structure was capable of accommodating up to three cations per cluster. All reactions failed to produce the more reduced compound $\text{Na}_x\text{Zr}_6\text{Cl}_{15}\text{C}$ ($1 < x < 3$), but yielded instead an unidentified product which by powder diffraction appears to be similar in structure to $\text{K}_4\text{Nb}_6\text{Cl}_{18}$.³

Further sodium incorporation was accomplished, however, by the substitution of B for C in the reaction. $\text{Na}_2\text{Zr}_6\text{Cl}_{15}\text{B}$ was prepared from the reaction of stoichiometric amounts of Zr powder, ZrCl_4 , NaCl and amorphous B powder at 850°C. The powder pattern clearly shows a $\text{Ta}_6\text{Cl}_{15}$ -type structure with lattice parameters slightly larger than those of $\text{Na}_x\text{Zr}_6\text{Cl}_{15}\text{C}$. A small splitting of all the lines in the powder diffraction pattern except those associated with the Si standard is also evident and suggests a distortion of the lattice from cubic symmetry.

Further incorporation of Na into the lattice by the substitution of Be for B was not successful. Stoichiometrically loaded reactions for $\text{Na}_3\text{Zr}_6\text{Cl}_{15}\text{Be}$ at 800°C yielded mixtures of $\text{Na}_4\text{Zr}_6\text{Cl}_{16}\text{Be}$ and $\text{Zr}_6\text{Cl}_{12}\text{Be}$. The distortion of the lattice noted for $\text{Na}_2\text{Zr}_6\text{Cl}_{15}\text{B}$ may signify the stability limits of Na inclusion in the $\text{Ta}_6\text{Cl}_{15}$ structure.

Crystallography Single crystal X-ray diffraction studies of nicely shaped, gem-like crystals of $\text{Zr}_6\text{Cl}_{15}\text{N}$ and $\text{Na}_{0.5}\text{Zr}_6\text{Cl}_{15}\text{C}$ were carried out on the SYNTEX and DATEX diffractometers, respectively, using monochromatic Mo $K\alpha$ radiation. Axial photographs on the diffractometer verified the axial lengths obtained from powder diffraction patterns and showed the expected mirror symmetry. Neither crystal showed any

indication of decay during data collection. Pertinent details of the data collections are given in Table 13.

The structure of $Zr_6Cl_{15}N$ was refined starting with the refined positions from Zr_6Cl_{15} .¹⁷ Isotropic refinement of the Zr and Cl atoms followed by a Fourier map, clearly revealed the presence of the interstitial nitrogen atom by an approximately 7-electron residual at the cluster center. A nitrogen atom was included at the cluster center in subsequent calculations. Anisotropic refinement of the heavy atoms (Zr and Cl), application of a secondary extinction correction and a reweighting of the data set resulted in final residual factors of $R = 6.1\%$ and $R_w = 4.9\%$. Simultaneous refinement of the N occupancy and isotropic thermal parameter (B) gave values of 0.96(7) and 0.5(7), respectively. The final difference map was flat to less than $\pm 0.5 e^-/\text{\AA}^3$.

The structural refinement of $Na_{0.5}Zr_6Cl_{15}C$ was approached in a similar manner. Isotropic and positional refinement of the Zr and Cl parameters from Zr_6Cl_{15} followed by the calculation of an electron density map, clearly showed the carbon atom at the cluster center. A subsequent map, after inclusion of the carbon atom and anisotropic refinement of the Zr and Cl thermal parameters, located the Na atoms randomly occupying $\sim 1/6$ of the 48g positions. The approximately 2-electron Na peaks stood out prominently against what was otherwise a very flat electron density difference map. The Na occupancy refined to 0.53(3) atoms randomly distributed over three symmetry equivalent sites per cluster (8.5(5) Na atoms over 48 sites per unit cell). An earlier

Table 13. Summary of crystallographic data for $Zr_6Cl_{15}N$ and $Na_{0.5}Zr_6Cl_{15}C$

Space Group	Ia3d	Ia3d
Z	16	16
a, Å ^a	21.1712(9)	21.4660(9)
V, Å ³	9489(1)	9891(1)
Crystal dimen., mm	0.30x0.10x0.10	0.25x0.20x0.20
Radiation	Mo K α , graphite monochromator	Mo K α , graphite monochromator
2 θ (max), deg.	55.0	55.0
Scan Mode	ω	ω
Reflections		
octants	hk ℓ ($h \leq k$)	hk ℓ ($h \leq k$)
measured refl.	2872	3080
observed refl.	1095	2065
independent refl.	451	689
R(ave), %	3.3	1.7
μ , cm ⁻¹	41.4	39.7
Transm. coeff. range	0.91 – 1.00	0.88 – 1.00
Secondary ext. coeff.	7(2) x 10 ⁻⁴	4(1) x 10 ⁻⁴
R, %	6.1	3.2
R(w), %	4.9	3.4

^aGuinier powder diffraction data.

diffraction study of a smaller crystal of $\text{Na}_x\text{Zr}_6\text{Cl}_{15}\text{C}$ under poorer diffraction conditions,¹³² i.e., with a less intense beam and no monochromator, had failed to separate the Na position from the background, apparently because of the low occupancy and poor quality of the data set. Final residuals for the present structure of $R = 3.2\%$ and $R_w = 2.5\%$ were obtained after application of a secondary extinction correction and a reweighting of the data set sorted on $|F_{\text{obs}}|$. The carbon interstitial atom refined to an occupancy of 1.17(5) with an isotropic B of 2.5(3). The final difference map was flat to less than $\pm 1/3 \text{ e}^-/\text{\AA}^3$.

Final positional and thermal parameters for $\text{Zr}_6\text{Cl}_{15}\text{N}$ and $\text{Na}_{0.5}\text{Zr}_6\text{Cl}_{15}\text{C}$ are given in Table 14 and relevant interatomic distances are compiled in Table 15. Calculated and observed structure factor amplitudes are contained in Appendices E and F for $\text{Zr}_6\text{Cl}_{15}\text{N}$ and $\text{Na}_{0.5}\text{Zr}_6\text{Cl}_{15}\text{C}$, respectively.

Although data were not collected for $\text{Na}_2\text{Zr}_6\text{Cl}_{15}\text{B}$, several single crystals were examined by X-ray diffraction to verify and, if possible, elucidate the nature of the distortion responsible for the splitting of the lines in the powder diffraction pattern. The most informative and conclusive results were obtained from the largest crystal and only those will be discussed. Data obtained with the smaller crystals were also consistent with the conclusions drawn here. Polaroid axial photographs taken on the diffractometer showed the cell to have mmm Laue symmetry, limiting the distortion to either a tetragonal or an orthorhombic modification of the cubic cell. Unconstrained least-squares refinement of 27 reflections tuned on the diffractometer showed a small tetragonal

Table 14. Positional and thermal parameters for $Zr_6Cl_{15}N$ and $Na_{0.5}Zr_6Cl_{15}C$

$Zr_6Cl_{15}N$	x		y		z	
Zr	0.06143(6)		0.96547(6)		0.08099(6)	
Cl1	0.1569(1)		0.0291(2)		0.0511(2)	
Cl2	0.1097(2)		0.8764(2)		0.0195(1)	
Cl3	0.5707(2)		1/4-x		1/8	
N	0		0		0	
$Na_{0.5}Zr_6Cl_{15}C$						
Zr	0.06091(2)		0.96545(2)		0.07960(2)	
Cl1	0.15554(6)		0.02940(7)		0.05022(7)	
Cl2	0.10871(7)		0.87695(7)		0.01884(6)	
Cl3	0.57195(8)		1/4-x		1/8	
Na	0.253(1)		1/4-x		1/8	
C	0		0		0	
$Zr_6Cl_{15}N$	B_{11}	B_{22}	B_{33}	B_{12}	B_{13}	B_{23}
Zr	1.40(6)	1.40(6)	1.34(6)	0.18(4)	-0.02(4)	0.27(4)
Cl1	0.7(1)	2.1(1)	1.3(1)	-0.3(1)	-0.2(1)	0.5(1)
Cl2	1.6(1)	1.2(1)	1.1(1)	0.8(1)	-0.2(1)	0.1(1)
Cl3	1.2(2)	B_{11}	1.8(2)	0.0(2)	-0.4(1)	0
N ^a	0.5(7)					
$Na_{0.5}Zr_6Cl_{15}C$						
Zr	2.12(2)	2.31(2)	2.21(2)	0.38(1)	0.09(1)	0.51(2)
Cl1	2.28(5)	4.11(7)	3.64(6)	-0.47(4)	-0.53(4)	0.90(5)
Cl2	3.41(6)	3.10(6)	3.01(6)	1.66(5)	0.13(4)	0.49(4)
Cl3	3.68(6)	B_{11}	5.4(1)	-0.39(7)	-1.85(6)	0
Na ^b	4.0(5)					
C ^c	2.5(3)					

^aOccupancy refined to 0.96(7).^bOccupancy refined to 0.18(1).^cOccupancy refined to 1.17(5).

Table 15. Interatomic distances in $Zr_6Cl_{15}N$ and $Na_{0.5}Zr_6Cl_{15}C$ (Å)

	$Zr_6Cl_{15}N$	$Na_{0.5}Zr_6Cl_{15}C$
Zr-Zr		
Zr-Zr	(x6) ^a 3.206(2)	3.2194(9)
Zr-Zr	(x6) 3.222(2)	3.2175(9)
\bar{d}	3.214	3.218
Zr-Z		
Zr-Z	(x6) 2.273(1)	2.2758(5)
Zr-Clⁱ		
Zr-Cl1	(x6) 2.510(3)	2.532(2)
Zr-Cl1	(x6) 2.517(3)	2.535(1)
Zr-Cl2	(x6) 2.506(3)	2.517(1)
Zr-Cl2	(x6) 2.510(4)	2.522(2)
Zr-Cl^{a-a}		
Zr-Cl3	(x6) 2.594(3)	2.646(1)
Na-Cl		
Na-Cl2	(x2)	2.71(3)
Na-Cl1	(x2)	2.73(2)
Na-Cl3	(x2)	3.32(3)

^aNumber of times the distance occurs per cluster or cation.

distortion of the cell, with one axis about 0.15 Å longer than the other two. The angles, as expected, refined to within 3σ of 90.0° . The unconstrained cell parameters, as well as those with orthorhombic and tetragonal constraints are given in Table 16. No significant changes in relative intensities for formerly equivalent reflections in Ia3d were observed in the single crystal diffraction data. The admittedly small set was consistent, however, with a rough visual estimate of 2:1 for the relative intensities of the members of each pair of reflections in the powder diffraction pattern. The minor changes in reflection intensities suggest that the positions of the heavy atoms in the distorted structure are essentially unchanged from the undistorted form. It is believed that the distortion is associated with the increased sodium content of the cell and probably reflects an ordering of the cations and/or a slight deformation of the chloride lattice to create a more favorable 5- or 6-coordinate sodium position. A single crystal diffraction study will be necessary to verify the suspected ordering and the nature of the distortion.

Structure and discussion The $\text{Ta}_6\text{Cl}_{15}$ structure type has previously been described.^{4,17} The structure, composed of 16 symmetry related clusters, is contained within a body-centered-cubic unit cell with Ia3d symmetry. Each cluster is interconnected with six neighboring clusters through shared Cl^{a-a} atoms to give the connectivity typically ascribed to M_6X_{15} compounds, $[\text{M}_6\text{X}_{12}]^{a-a}_{6/2}$. The sheer size of the cell, combined with the extraordinarily high symmetry of the space group Ia3d, makes a complete description of the structure within

Table 16. Constrained and triclinic lattice parameters for $\text{Na}_2\text{Zr}_6\text{Cl}_{15}\text{B}^{\text{a}}$

Triclinic	Orthorhombic	Tetragonal
a = 21.64(1)	21.611(9)	21.603(5)
b = 21.63(1)	21.600(9)	21.603(5)
c = 21.79(1)	21.763(9)	21.763(9)
α = 90.14(7)	(90.0)	(90.0)
β = 90.06(7)	(90.0)	(90.0)
γ = 90.14(7)	(90.0)	(90.0)

^aDiffractometer data.

the guidelines of the unit cell somewhat cumbersome and unwieldy. A simplification of the structural description, with little loss of generality, is obtained by focusing on a single octant (1/8) of the unit cell. Positioned at each of the corners and the body center of the subcell is an $M_6X_{12}^i$ cluster. A $\bar{3}$ axis runs down one body diagonal of the subcell ([111] for example), intersecting clusters at two of the corners and the body center. No direct linkage of the clusters on the $\bar{3}$ axis through Cl^{a-a} atoms exists. The body-centered cluster is connected through shared Cl^{a-a} atoms to the six clusters on the remaining corners. The connectivity of the central cluster within the subcell is shown in Figure 11. The two clusters on the corners intersected by the $\bar{3}$ axis and all of the Cl^i atoms have been omitted for clarity. The difference between octants and the reason necessitating the larger unit cell is the orientation of the $\bar{3}$ axis within each octant. When combined, the eight subcells create a unit cell with seven nonintersecting $\bar{3}$ axes. In the full unit cell, a single $\bar{3}$ axis runs along the [111] body diagonal, while the six other $\bar{3}$ axes which are all related by the body diagonal $\bar{3}$, extend from the center of each face to the center of a neighboring edge. The connectivity of clusters within the entire unit cell is pictured schematically in Figure 12. The $\bar{3}$ axes can be identified by recalling that no direct connectivity between clusters on a $\bar{3}$ axis occurs.

An alternate description that is conceptually simple, but fails to adequately describe the symmetry or the connectivity between clusters, is to view the structure as a cubic close-packed array of randomly oriented

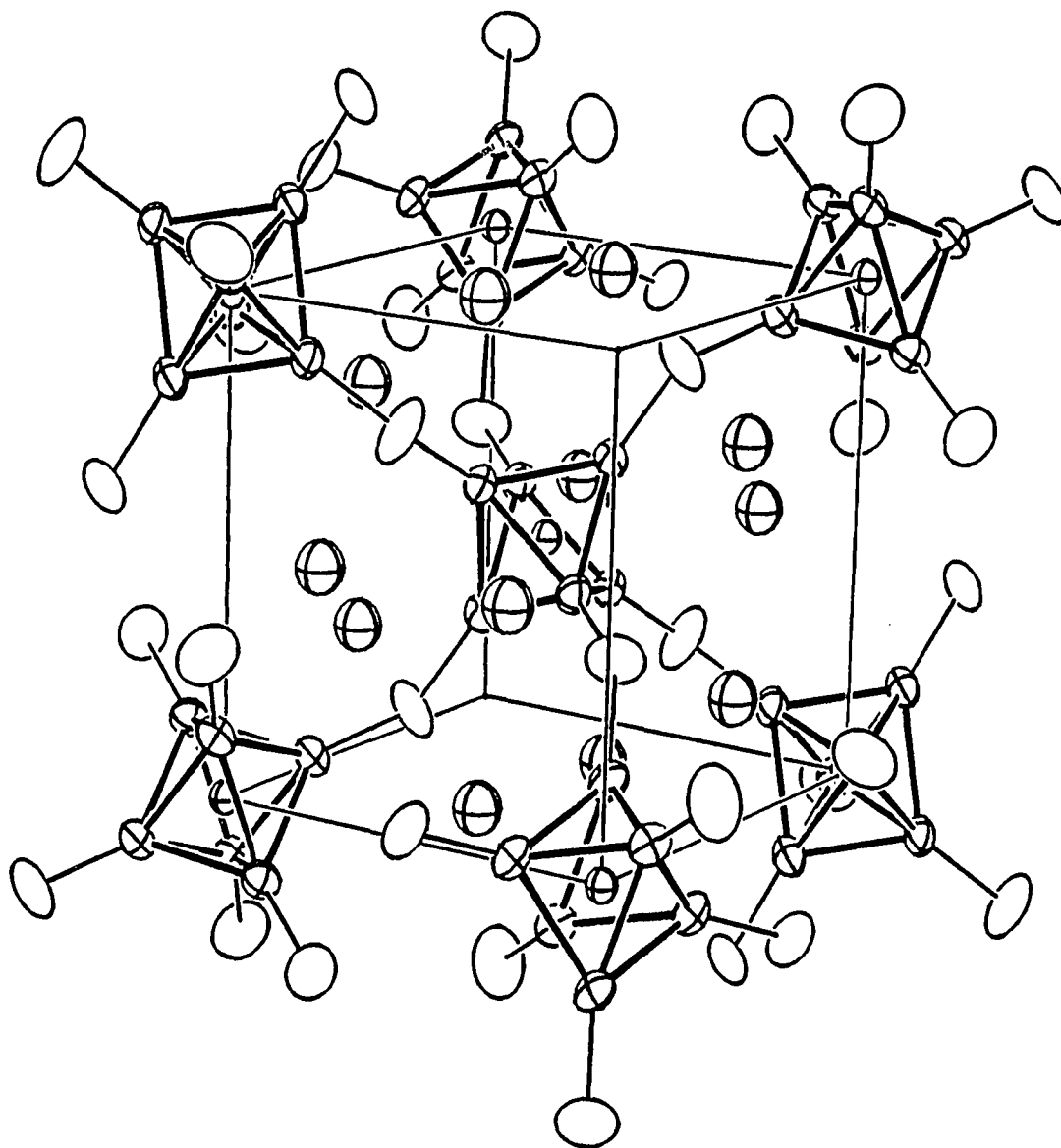


Figure 11. One octant of the unit cell in $\text{Na}_{0.5}\text{Zr}_6\text{Cl}_{15}\text{C}$ showing the intercluster connectivity. The clusters on the two corners intersected by the $\bar{3}$ axis and all of the Cl^i atoms have been omitted for clarity. Sodium cations are the crossed ellipsoids lying in pairs on each face. (90% ellipsoids)

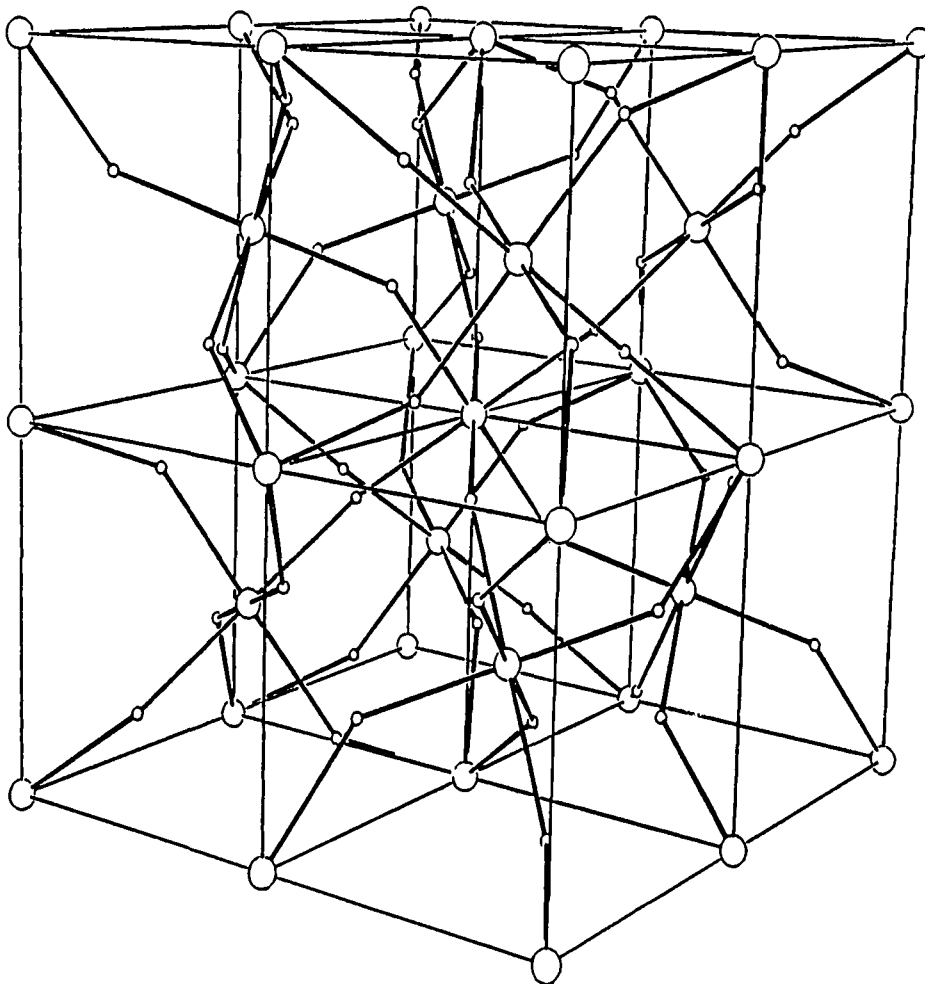


Figure 12. A schematic drawing depicting the cluster connectivity in the complete unit cell of $Zr_6Cl_{15}N$. Octant boundaries have been included. Large spheres represent $[Zr_6Cl_{12}N]$ clusters and small spheres are intercluster bridging Cl^{2-} atoms. The $[111]$ body diagonal runs through the top front and bottom rear corners

clusters. Treating each M_6X_{12} cluster as a sphere, the structure is seen to pack in an $\dots(ABC)_4\dots$ fashion down the [111] body diagonal. The packing is not ideal, but rather is compressed in the [111] direction, i.e., normal to the cluster layers.

The cation site, partially occupied in $Na_{0.5}Zr_6Cl_{15}C$ and $Na_2Zr_6Cl_{15}B$, is a 48-fold position which is coordinated by 4 Cl^i atoms in an approximately tetrahedral arrangement at distances of 2.72(3) Å. The next-nearest neighbors are two Cl^a atoms at a distant 3.32(2) Å. The entire coordination environment around Na is shown in Figure 13. The location of the Na site within the unit cell is once again more easily visualized by focusing on a single octant of the unit cell. From this viewpoint, the Na positions are seen to lie in approximately linear chains which run across the center of each face of the subcell (see Figure 11). Two sites lie on each face, positioned at 1/4 and 3/4 of the way across the face. The chains of Na positions are oriented relative to one another in perpendicular directions on adjacent faces, reminiscent of the chains of A atoms in A_3B compounds with the A15 structure (β -W).¹³⁵ The analogy, of course, is no more than a convenient method of describing the structural arrangement of sodium sites and in no way implies a bonded sodium chain. Sodium sites in the chains are slightly over 5 Å apart. In the close-packed description, the Na atoms lie in irregularly shaped sites between the cluster layers. In $Na_{0.5}Zr_6Cl_{15}C$, one-sixth of the sodium sites are randomly occupied. No evidence of ordering (in the form of superstructure reflections) was observed in either powder diffraction patterns or axial photographs taken on the diffractometer. In

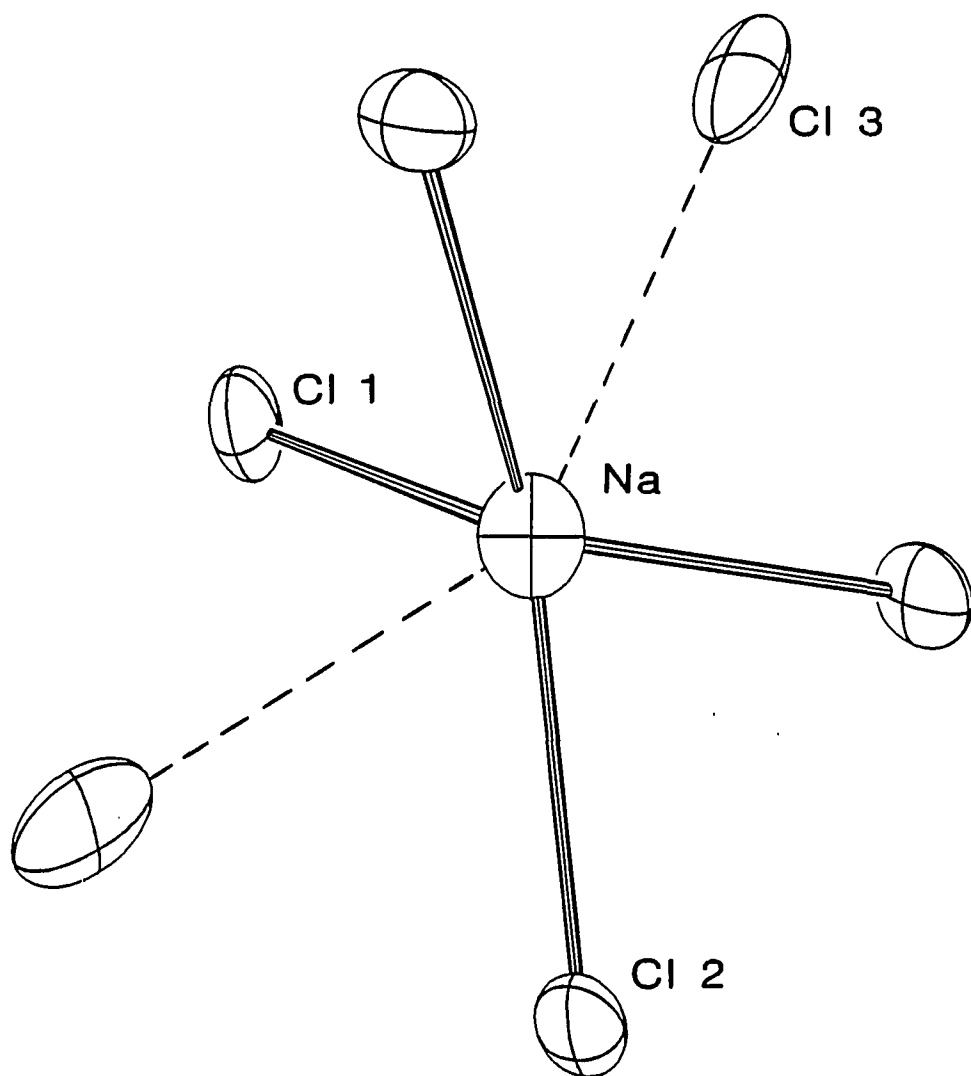


Figure 13. The local environment of the Na atom in $\text{Na}_{0.5}\text{Zr}_6\text{Cl}_{15}\text{C}$. The Cl3 atoms are 3.32 Å from the Na atom. A two-fold axis runs diagonally across the page from the lower right- to upper left-hand corner. (50% ellipsoids)

$\text{Na}_2\text{Zr}_6\text{Cl}_{15}\text{B}$, the tetragonal distortion is believed to be associated with an ordering of the sodium atoms and/or a small deformation of the structural framework.

The $\text{M}_6\text{X}_{12}^{\text{i}}$ cluster in all compounds in the $\text{Ta}_6\text{Cl}_{15}$ structure has crystallographically imposed $\bar{3}$ symmetry. In $\text{Zr}_6\text{Cl}_{15}\text{N}$, the cluster shows a slight elongation along the $\bar{3}$ axis which makes the Zr-Zr distances around the waist 0.016 Å longer than those perpendicular to it. In contrast, the $\text{Zr}_6\text{Cl}_{12}^{\text{i}}$ cluster in $\text{Na}_{0.5}\text{Zr}_6\text{Cl}_{15}\text{C}$ is octahedral within the tolerances of the measurement, as is the $\text{Ta}_6\text{Cl}_{12}^{\text{i}}$ cluster in $\text{Ta}_6\text{Cl}_{15}$.⁴ The reason for the cluster distortion in $\text{Zr}_6\text{Cl}_{15}\text{N}$ is not entirely clear. The distortion does not appear to be a consequence of the electronic configuration as both zirconium clusters have 14-cluster electrons, an electrostatic effect caused by the lack of a cation since $\text{Ta}_6\text{Cl}_{15}$ shows no elongation, or an inequivalent Zr orbital contribution caused by different Zr-Cl^{a-a} distances as seen in $\text{Zr}_6\text{I}_{14}\text{C}^{36}$ because all the Zr-Cl^{a-a} distances are equivalent by symmetry. The effect may, however, be related to the packing of the clusters. To efficiently pack the larger zirconium clusters, a reduction of the M-Cl^{a-a}-M angle from 142° in $\text{Ta}_6\text{Cl}_{15}$ to 138° in $\text{Zr}_6\text{Cl}_{15}\text{N}$ is required. The reduction in the angle pulls in the six zirconium clusters disposed around the waist of the central cluster, causing the cluster to elongate slightly along the $\bar{3}$ axis [see Figure 11]. In $\text{Na}_{0.5}\text{Zr}_6\text{Cl}_{15}\text{C}$, while the angle increases only slightly to 139°, the Zr-Cl^{a-a} bonds expand by 0.05 Å, increasing the distances between the central cluster and those disposed around its waist. The expansion of the intercluster distance

results primarily from a 'propping' open of the structure by the insertion of Na cations in the voids between clusters. The short Cl₂-Cl₂ distance between clusters noted in Ta₆Cl₁₅ and attributed to steric effects⁴ is seen in both Zr₆Cl₁₅N and Na_{0.5}Zr₆Cl₁₅C.

The Zr-C distances in Na_{0.5}Zr₆Cl₁₅C are all 2.276 Å and are typical of the distances observed in other carbon-centered clusters. The 2.273 Å Zr-N distance observed in Zr₆Cl₁₅N is slightly larger than that expected on the basis of the trend established from beryllium-, boron-, and carbon-centered clusters (see Figure 49). The smaller than expected change may indicate the Zr-N distance is limited by Zr-Zr interactions or simply that the change in the interstitial radius is not linear across the period. The observed nitrogen radius, calculated by subtracting the 0.86 Å radius of Zr⁴⁺¹²⁷ from the 2.273 Å interatomic distance is 1.41 Å. A similar calculation for ZrN gives a nitrogen radius of 1.43 Å.¹²⁵

Compounds with the CsNb₆Cl₁₅ structural framework¹³⁴

Over the past several years, an increasing number of octahedral metal clusters that require a heteroatom within the cluster for stability have been reported within rare-earth and early transition metal halides.^{36-41,59} As a result of these investigations, it is becoming increasingly evident that many, but not all, of the previously prepared clusters and condensed clusters of these elements that were implicitly presumed to be empty actually are interstitially stabilized by small nonmetals. Prime examples are Zr₆Cl₁₅,¹⁷ Sc₅Cl₈¹⁰ and the rare-earth metal monohalides²⁴⁻²⁷ which are now recognized to be the halide mononitride,⁶⁰ -carbide⁴¹ and -hydrides,^{39,42} respectively.

These results also suggest that a vast and largely untapped potential exists for the preparation of new cluster compounds by the purposeful and systematic addition of potential interstitial elements to cluster-forming reactions. The potential lies not only in the ability to alter the number of cluster electrons and hence the electronic properties of a cluster by changing the interstitial element, but also in an ability to generate completely new structural arrangements of clusters and novel stoichiometries. The syntheses and structures of $\text{KZr}_6\text{Cl}_{15}\text{C}$ and $\text{CsKZr}_6\text{Cl}_{15}\text{B}$, as well as the preparation of the related compounds $\text{RbZr}_6\text{Cl}_{15}\text{C}$, $\text{CsZr}_6\text{Cl}_{15}\text{C}$, $\text{KZr}_6\text{Cl}_{15}\text{N}$, $\text{Rb}_2\text{Zr}_6\text{Cl}_{15}\text{B}$ and $\text{CsRbZr}_6\text{Cl}_{15}\text{B}$, are representative of this latter potential.¹³⁴ All of their structures are based on a common $(\text{Zr}_6\text{Cl}_{12})\text{Cl}_{6/2}$ framework, where the $\text{Zr}_6\text{Cl}_{12}$ cluster is centered by a boron, carbon or nitrogen atom. However, the availability and occupation of more than one set of cation sites within this matrix generates some interesting variations as well as complications.

Syntheses Preparations of the $\text{M}_x^{\text{I}}\text{Zr}_6\text{Cl}_{15}\text{Z}$ compounds typically utilized stoichiometric quantities of Zr powder and ZrCl_4 together with graphite, boron or ZrNCl and the appropriate $\text{M}^{\text{I}}\text{Cl}$. A small excess of ZrCl_4 was added to each reaction to allow for the autogenous ZrCl_4 pressure ($\sim 2 - 4$ atm) over the cluster product at temperature. The systems were usually heated to 850°C over a 24-hour period, equilibrated for two weeks, and then air quenched. The product distributions in these reactions are largely controlled by the initial ratio of the reactants. For example, $\text{RbZr}_6\text{Cl}_{14}\text{B}$, $\text{Rb}_2\text{Zr}_6\text{Cl}_{15}\text{B}$ and

$\text{Rb}_5\text{Zr}_6\text{Cl}_{18}\text{B}$ can all be prepared from $\text{Zr}/\text{ZrCl}_4/\text{B}$ mixtures simply by varying the amount of RbCl present.

The products obtained under the appropriate conditions were single phase as judged by careful examination of Guinier powder diffraction patterns and by microscopic inspection of the reaction products. The former means that powder data were consistent not only in position, but also in intensity with those in the pattern calculated using the indicated lattice constants and positional parameters for the known structure type. The high yields, estimated to be in excess of 95% when the correct stoichiometric proportions are used, are an important factor in establishing the identity of the interstitial element since X-ray diffraction cannot be counted on to distinguish reliably among light nonmetal atoms such as B, C, or N. All of the $\text{M}_x^{\text{I}}\text{Zr}_6\text{Cl}_{15}$ carbides ($x = 1$) and borides ($x = 2$) occur as black microcrystalline powders mixed with some larger well-faceted, very dark-red parallelepipeds. Several of the compounds have also been observed as very thin, dark-red rods or blades, apparently formed by slow chemical transport when reactions were run under a 20 – 30°C temperature gradient. Recognizable single crystals were not obtained for the nitride. Lattice parameters for all of the $\text{M}_x\text{Zr}_6\text{Cl}_{15}\text{Z}$ prepared compounds are given in Table 17.

Crystallography Two octants of diffraction data were initially measured for both $\text{KZr}_6\text{Cl}_{15}\text{C}$ and $\text{CsKZr}_6\text{Cl}_{15}\text{B}$ at room temperature using nicely shaped, dark-red rectangular prisms and monochromatic $\text{Mo K}\alpha$ radiation. Data were later recollected for $\text{CsKZr}_6\text{Cl}_{15}\text{B}$ over four

Table 17. Lattice Parameters (Å) and Cell Volumes (Å³) for the CsNb₆Cl₁₅-type Compounds Studied^a

Compound	a	b	c	V	cation site type ^b
KZr ₆ Cl ₁₅ C	18.489(5)	13.909(3)	9.690(3)	2492(1)	a
RbZr ₆ Cl ₁₅ C	18.468(5)	13.891(4)	9.648(3)	2475(1)	b
CsZr ₆ Cl ₁₅ C	18.509(4)	13.923(3)	9.646(2)	2485.6(9)	b
CsKZr ₆ Cl ₁₅ B	18.672(4)	14.026(4)	9.731(2)	2548(1)	a+b
Rb ₂ Zr ₆ Cl ₁₅ B	18.666(2)	14.033(2)	9.757(1)	2555.8(6)	a+b
CsRbZr ₆ Cl ₁₅ B	18.703(2)	14.087(2)	9.771(1)	2574.4(5)	a+b
KZr ₆ Cl ₁₅ N	18.292(2)	13.824(1)	9.590(1)	2425.1(5)	a
CsZr ₆ Br ₁₅ Fe	19.721(3)	14.863(3)	10.265(2)	3009(1)	b

^aGuinier powder diffraction data.

^bSee text.

octants. Pertinent details of the data collections are contained in Table 18.

For $\text{KZr}_6\text{Cl}_{15}\text{C}$, a primitive orthorhombic cell was chosen on the basis of 12 indexed reflections and was subsequently supported by the layer spacings and mirror symmetry seen in axial (Polaroid) photographs taken on the diffractometer. Axial photographs of $\text{CsKZr}_6\text{Cl}_{15}\text{B}$ taken on the diffractometer also confirmed the orthorhombic unit cell expected on the basis of Guinier powder diffraction patterns (below) and predicted by reflections indexed on the diffractometer. In addition, no evidence suggesting a higher or lower space group symmetry or a superlattice for the second compound was found on either oscillation or Weissenberg photographs.

The space group Pmma was established on the basis of the systematic extinctions apparently observed, an assumed centricity, and the successful refinement of the structure in this space group.

The structure was solved by Patterson superposition methods utilizing the program ALCAMPSS^{96} for map analysis. Twelve atom positions were identified and assigned to five zirconium and seven chlorine atoms, these being differentiated by interatomic distances and Patterson peak heights. The remaining atomic positions were identified by successive cycles of least-squares refinement and calculation of electron density maps. The potassium position was initially refined with a chlorine atom, but this was later replaced with the cation after it was observed that the atom had only chlorine nearest neighbors at distances of $\sim 3.4 \text{ \AA}$, about the sum of the K^+ and Cl^- radii.¹²⁷ Refinement of the atomic

Table 18. Summary of Crystal and Diffraction Data for $\text{KZr}_6\text{Cl}_{15}\text{C}$ and $\text{CsKZr}_6\text{Cl}_{15}\text{B}$

	$\text{KZr}_6\text{Cl}_{15}\text{C}$	$\text{CsKZr}_6\text{Cl}_{15}\text{B}$
Space Group	Pmma	Pmma
Z	4	4
a, Å ^a	18.489(5)	18.672(4)
b	13.909(3)	14.026(4)
c	9.690(3)	9.731(2)
V, Å ³	2492(1)	2548(1)
Crystal dimen, mm	0.35x0.25x0.15	0.45x0.20x0.15
Radiation	Mo K α , graphite monochromator	Mo K α , graphite monochromator
2 θ (max), deg.	55.0	55.0
Scan Mode	ω	ω
Reflections		
octants	h,k,l; -h,-k,l	h,k, \pm l; h,-k, \pm l
measured refl.	6613	12553
observed refl.	4725	7394
independent refl.	2404	2144
R(avg), %	4.3	3.3
μ , cm ⁻¹	40.9	54.4
Transm. coeff. range	0.70 – 1.00	0.83 – 1.00
Secondary ext. coeff.	1.0(2) x 10 ⁻⁴	1.3(3) x 10 ⁻⁵
R, %	3.1	3.9
R _w , %	3.2	3.6

^aGuinier powder diffraction data.

positions and anisotropic thermal parameters of all atoms, except carbon which was refined isotropically, proceeded smoothly and converged at $R = 0.031$, $R_w = 0.032$, after reweighting. Refinement of the K, Cl and C2 occupancies did not result in values significantly different from unity (0.976(8), 0.97(3) and 1.06(3), respectively), and these were hence fixed at full occupancy. A secondary extinction correction⁹⁹ was applied to the data after a comparison of $|F_{obs}|$ vs $|F_{calc}|$ showed that the former was smaller for a disproportionate number of intense reflections. The final difference map was flat to less than $\pm 0.25 \text{ e}^-/\text{Å}^3$.

The structure of $\text{CsKZr}_6\text{Cl}_{15}\text{B}$ was deduced by a comparison of its observed powder pattern with those calculated on the bases of the $\text{CsNb}_6\text{Cl}_{15}$ ⁷² and $\text{KZr}_6\text{Cl}_{15}\text{C}$ structures, these differing only in the cation sites that are occupied. Least-squares refinement of the zirconium and chlorine positional parameters obtained for $\text{KZr}_6\text{Cl}_{15}\text{C}$ followed by a calculation of a Fourier map clearly showed the occupation of three additional sites in the lattice, corresponding to both the potassium position in $\text{KZr}_6\text{Cl}_{15}\text{C}$ (type a) and the two cesium positions in $\text{CsNb}_6\text{Cl}_{15}$ (type b). Isotropic refinement proceeded smoothly to $R = 10.6\%$ with the inclusion of the indicated atoms. Boron atoms were included in the centers of the two independent clusters at this point and refined isotropically at unit occupancy, while the rest of the atoms in the structure were refined anisotropically. Simultaneous refinement of the occupancies of the three alkali metals, application of a secondary extinction correction, and a reweighting of the data set led to final values of $R = 0.039$ and $R_w = 0.036$. The potassium and cesium occupancies converged at somewhat more

(1.27(1)) and slightly less than unity (0.937(6) and 0.784(6)), respectively, indicating a small amount of cation mixing between sites (below). The final difference map was flat to less than $\pm 0.5 \text{ e}^-/\text{\AA}^3$. The largest peaks, 0.5 and 0.3 $\text{e}^-/\text{\AA}^3$, were associated with Cs1 and Cs2, respectively.

The refined thermal ellipsoids for certain atoms in the $\text{CsKZr}_6\text{Cl}_{15}\text{B}$ structure indicated further consideration of the structure and its refinement was necessary, particularly with respect to supercells or lower space group symmetries. In contrast to the $\text{KZr}_6\text{Cl}_{15}\text{C}$ structure, which shows normal thermal parameters except for the somewhat flattened ellipsoids for the interconnected $\text{Zr4-C12}^{a-a}\text{-C15}$ atoms along the linear cluster chain ($\text{mm}2$ symmetry), the $\text{CsKZr}_6\text{Cl}_{15}\text{B}$ refinement provides several examples of extreme thermal parameters. Most exceptional are the two newly added cesium atoms. The inclusion of the cesium atoms in two rather unsymmetrical cavities in the cluster framework (see Structural results and discussion) produces highly distorted thermal ellipsoids with principal axial ratios (and site symmetries) of 1.7:1:4.1 ($\text{mm}2$) and 1.3:1:16.1 ($2/m$) for Cs1 and Cs2, respectively. Attempts to refine Cs2 anisotropically in two inversion-related sites of equal occupancy failed to converge. Less remarkable disparities between principal axes of the ellipsoids also appear for other atoms that lie on symmetry elements in this space group, namely C13 ($\text{mm}2$), the bridging atom in the zig-zag cluster chain, C14 (2), C18 (m), and C19 (m), with one axis or another being 33-44% of the largest. It is noteworthy that the latter group of chlorine atoms are all neighbors of one or the other of the cesium atoms

that are new to the structure, and their thermal ellipsoids may therefore reflect more the character of the cation disposition than an intrinsic thermal property.

The geometric details of the cesium coordination polyhedra will be considered later. More important at the moment is the question as to whether the "thermal" parameters actually represent a crystallographic error in the choice of the unit cell or space group, since the troubled atoms all lie on symmetry elements in the space group utilized, Pmma.

First, a superstructure could not be found by film methods or diffractometer scans. Six apparently new h00 peaks for h odd were detected by ω -scans on the diffractometer when λ was doubled, but $\theta - 2\theta$ scans showed these all arose from streaking of the neighboring and strong h-even reflections. The raw data sets for both phases were also reconsidered. The two octants of data for $\text{CsKZr}_6\text{Cl}_{15}\text{B}$ contained ~10% of the "extinct" hk0, $h = 2n + 1$, as weak but observed reflections, in particular, five of a possible twelve in the h00 set. Re-examination of the potassium data, where averaging in Pmma had not been very good (4.3%), revealed that 9 of 78 possible hk0 reflections with h-odd were observed, all weakly, but in both octants. Six of these were h00.

The acentric space group Pmm2 is the only orthorhombic member that is consistent with these violations and the general features of the structure. It also removes the centers of symmetry otherwise present at both cesium positions. Refinement of the first $\text{CsKZr}_6\text{Cl}_{15}\text{B}$ data set in Pmm2 encountered substantial coupling problems between pairs of Zr, Cl and K atoms that were formerly identical by inversion, while coupling of the

'inversion-related' cesium atoms was significantly less. An R of ~6% was obtained by anisotropic refinement of the cesium atoms together with alternate sets of the coupled Zr, Cl, and K pairs. The Cs2 atom moved off the original (0,0,1/2) position by 0.3 Å in the (101) direction, but it continued to exhibit the problematic thermal ellipsoid seen in Pmma, as did the average of the pairs of Cs1 atoms that were clearly coupled. The final difference map in Pmma had shown two small peaks at $\pm x$ for Cs1, suggesting a displacement of the atom from the mirror plane perpendicular to \vec{a} . Further consideration of the apparent problem with Cs2, its movement from the inversion center in Pmm2, and the cluster matrix in general, also made the two-fold axis along \vec{b} and the accompanying inversion center suspect, if only a refinement in too high a symmetry space group was responsible for the observed thermal ellipsoid problems. Elimination of the suspect symmetry elements reduces the space group from Pmma to P2/m (loss of the \vec{a} glide and mirror perpendicular to \vec{a}) and finally to Pm (\vec{b} unique) (loss of two-fold along \vec{b} and $\bar{1}$). Refinements of the second (four-octant) data set were then attempted in Pmm2, P2/m (\vec{b} unique), and Pm (\vec{b}).

Averaging of equivalent reflections in the new data set gave marginally better results for a monoclinic cell with a unique \vec{b} axis (2.3%), as expected, relative to either of the other monoclinic settings (\vec{a} -unique (3.0%), \vec{c} -unique (3.0%)) or the original orthorhombic cell (3.3%). Unfortunately, refinement of the data in P2/m or Pm (\vec{b} -unique) failed to resolve the apparent ellipsoid problem or even to provide a significant improvement over the orthorhombic results.

A refinement in $P2_1/m$ (\vec{a} -unique) to check the validity of the mirror perpendicular to \vec{b} , showed no significant atomic displacements or improvement in ellipsoid behavior. A final effort in $P\bar{1}$ also failed to provide a solution. In all cases, the ellipsoids for Cs1 and Cs2 retained proportions close to those originally refined in Pmma and often became larger in magnitude. Atomic positions in all space groups tried converged to within 3σ of the originally refined positions, except for Cs2 in Pm and Pmm2 (above) and Zr4 and Cl2 in Pm which moved 6 and 8σ , respectively, off the mirror plane formerly perpendicular to \vec{a} .

The results of these considerations leave one with the conclusion that particularly the cesium ellipsoids are reflections, in the harmonic description, of a real atom disorder in the crystal studied and not an error in space group symmetry. The thermal parameters in the potassium structure are much more well-behaved and, in fact, give a valuable baseline from which to better judge the CsKZr₆Cl₁₅B results. Whatever atom displacements are responsible for the weak violations of the \vec{a} glide in Pmma are too small in either structure to be refined by the least-squares method.

Structural results and discussion Final positional and thermal parameters for KZr₆Cl₁₅C and CsKZr₆Cl₁₅B are compiled in Tables 19 and 20, respectively, and relevant interatomic distances are given in Tables 21 and 22. Observed and calculated structure factor amplitudes are available in Appendices G and H for KZr₆Cl₁₅C and CsKZr₆Cl₁₅B, respectively.

Table 19. Positional and thermal parameters for $\text{KZr}_6\text{Cl}_{15}\text{C}$

Atom	x	y	z	B_{11}
Zr1	0.47012(2)	0.38378(2)	0.34235(3)	1.37(1)
Zr2	0.61430(2)	1/2	0.41815(5)	1.25(2)
Zr3	0.33785(2)	0.11656(2)	0.15743(3)	1.62(1)
Zr4	1/4	0	0.38799(6)	1.70(3)
Zr5	1/4	0	0.92519(6)	1.80(3)
C11	0.43822(5)	0.25078(7)	0.15795(9)	2.41(4)
C12	1/4	0	0.6571(2)	4.1(1)
C13	1/4	1/2	0.6837(2)	1.30(6)
C14	0	0.24508(9)	1/2	2.22(5)
C15	0.43405(7)	1/2	0.1549(1)	2.71(5)
C16	0.59583(5)	0.37143(6)	0.23619(9)	1.70(3)
C17	0.33952(4)	0.37381(6)	0.41802(9)	1.43(3)
C18	1/4	0.25565(9)	0.1505(1)	2.23(5)
C19	0.44244(7)	0	0.1573(1)	1.62(4)
C110	0.34551(5)	0.12701(7)	0.41792(8)	2.33(3)
C111	0.15284(5)	0.12775(7)	0.89612(9)	2.48(4)
K	1/4	0.2529(1)	0.6691(2)	4.06(8)
C1	1/2	1/2	1/2	1.6(1)
C2	1/4	0	0.1562(6)	0.7(1)

B_{22}	B_{33}	B_{12}	B_{13}	B_{23}
1.48(1)	1.52(1)	-0.06(1)	-0.08(1)	-0.14(1)
1.48(2)	1.58(2)	0	-0.01(1)	0
1.49(1)	1.12(1)	0.18(1)	0.02(1)	0.05(1)
1.53(3)	0.80(2)	0	0	0
1.59(3)	0.80(2)	0	0	0
2.17(3)	1.99(3)	-0.81(3)	0.31(3)	-0.55(3)
4.0(1)	0.70(6)	0	0	0
2.82(8)	2.07(7)	0	0	0
1.47(4)	2.44(5)	0	-0.49(4)	0
2.27(5)	1.61(4)	0	-0.52(4)	0
2.37(3)	2.26(3)	-0.11(3)	0.26(3)	-0.75(3)
2.07(3)	2.22(3)	-0.31(3)	0.01(2)	-0.45(3)
1.44(4)	2.43(5)	0	0	-0.05(4)
2.09(5)	2.57(5)	0	0.10(4)	0
2.13(3)	1.33(3)	-0.61(3)	-0.15(3)	-0.22(3)
2.32(4)	1.28(3)	-0.57(3)	-0.19(3)	-0.15(3)
3.35(7)	4.02(8)	0	0	-1.06(6)

Table 20. Positional and thermal parameters for CsKZr₆Cl₁₅B

Atom	x	y	z	B ₁₁
Zr1	0.47097(3)	0.38355(4)	0.34042(6)	1.06 (2)
Zr2	0.61493(4)	1/2	0.4191(1)	0.81 (3)
Zr3	0.33804(3)	0.11672(4)	0.14675(6)	1.28 (2)
Zr4	1/4	0	0.3790(1)	1.39 (4)
Zr5	1/4	0	0.9130(1)	1.69 (5)
Cl1	0.4379(1)	0.2509(1)	0.1551(2)	2.34 (7)
Cl2	1/4	0	0.6465(4)	5.0 (2)
Cl3	1/4	1/2	0.6869(4)	1.1 (1)
Cl4	0	0.2453(1)	1/2	2.06 (9)
Cl5	0.4365(1)	1/2	0.1503(3)	2.15 (9)
Cl6	0.59714(8)	0.3711(1)	0.2378(2)	1.36 (5)
Cl7	0.33966(8)	0.3747(1)	0.4130(2)	1.07 (5)
Cl8	1/4	0.2556(1)	0.1407(3)	1.80 (8)
Cl9	0.4427(1)	0	0.1501(3)	1.19 (8)
Cl10	0.34515 (8)	0.1274(1)	0.4093(2)	1.89 (5)
Cl11	0.15269(9)	0.1274(1)	0.8856(2)	2.39 (6)
K	1/4	0.2515(1)	0.6588(2)	3.01 (9)
Cs1	1/4	1/2	0.0911(2)	3.68 (6)
Cs2	0	0	1/2	9.8 (1)
B1	1/2	1/2	1/2	1.5 (3)
B2	1/4	0	0.145(1)	0.6 (3)

B_{22}	B_{33}	B_{12}	B_{13}	B_{23}
0.94 (2)	1.48 (2)	-0.10 (2)	-0.08 (2)	-0.17 (2)
0.99 (3)	1.49 (3)	0	-0.02 (2)	0
0.99 (2)	1.05 (2)	0.19 (2)	0.04 (2)	0.01 (2)
1.04 (4)	0.63 (5)	0	0	0
1.17 (4)	0.64 (4)	0	0	0
1.96 (6)	2.05 (7)	-1.06 (5)	0.47 (6)	-0.75 (5)
3.8 (2)	0.6 (1)	0	0	0
2.6 (1)	2.0 (1)	0	0	0
1.03 (7)	2.33 (9)	0	-0.53 (8)	0
1.72 (8)	1.62 (9)	0	-0.45 (8)	0
1.94 (6)	2.28 (7)	-0.14 (5)	0.23 (5)	-0.74 (5)
1.48 (5)	2.24 (6)	-0.26 (4)	0.08 (5)	-0.43 (6)
0.86 (7)	2.5 (1)	0	0	0.08 (7)
1.80 (9)	3.0 (1)	0	0.30 (8)	0
1.62 (5)	1.30 (5)	-0.56 (5)	-0.19 (5)	-0.20 (5)
2.11 (6)	1.16 (6)	-0.65 (6)	-0.30 (5)	-0.22 (5)
2.03 (7)	2.83 (9)	0	0	-0.58 (6)
2.14 (5)	8.7 (1)	0	0	0
2.19 (7)	19.6 (3)	0	-11.9 (2)	0

The structures of $\text{KZr}_6\text{Cl}_{15}\text{C}$ and $\text{CsKZr}_6\text{Cl}_{15}\text{B}$ are, like those of all other known M_6X_{15} compounds, composed of M_6X_{12} -type clusters with unshared, edge-bridging inner halogen atoms (X^i), and these are linked together through additional, shared terminal halogens atoms (X^{a-a}) at every metal vertex. The general arrangement is more succinctly described as $[\text{M}_6\text{X}_{12}^i]\text{X}^{a-a}_{6/2}$. The primary structural framework for these zirconium chlorides is identical to that of $\text{CsNb}_6\text{Cl}_{15}$ ⁷² if the cations and interstitial atoms are neglected.

The structure of $\text{KZr}_6\text{Cl}_{15}\text{C}$ can be viewed in terms of the two crystallographically independent chains of $\text{Zr}_6\text{Cl}_{12}\text{C}$ clusters that run in perpendicular directions and are interlinked by Cl atoms. The illustration in Figure 14 of the two chains in $\text{KZr}_6\text{Cl}_{15}\text{C}$ will also serve as a description for $\text{CsKZr}_6\text{Cl}_{15}\text{B}$. One chain, parallel to the \bar{a} axis, is split by the mirror plane at $y = 1/2$ and exhibits bent Cl^{a-a} linkages similar to those in $\text{Ta}_6\text{Cl}_{15}$.⁴ It therefore has a zig-zag appearance, with $\text{Zr}-\text{Cl}^{a-a}-\text{Zr}$ angles of $\sim 140^\circ$. Each cluster in this chain has C_{2h} point symmetry and Zr-Zr distances that average 3.228 Å. The Zr-C distances in the compound average 2.280 Å which, when considered with the 0.86 Å crystal radius for Zr,¹²⁷ gives an effective carbon crystal radius of 1.42 Å. This value is slightly smaller than the 1.46 Å radius similarly derived from a number of rock-salt-type transition metal monocarbides,³⁶ but is the same as that from $\text{Sc}_7\text{X}_{12}\text{C}$ ($\text{X} = \text{Br}, \text{I}$),¹¹⁵ and slightly larger than the 1.40 Å value for the more electron-rich $\text{Zr}_6\text{I}_{12}\text{C}$.³⁶

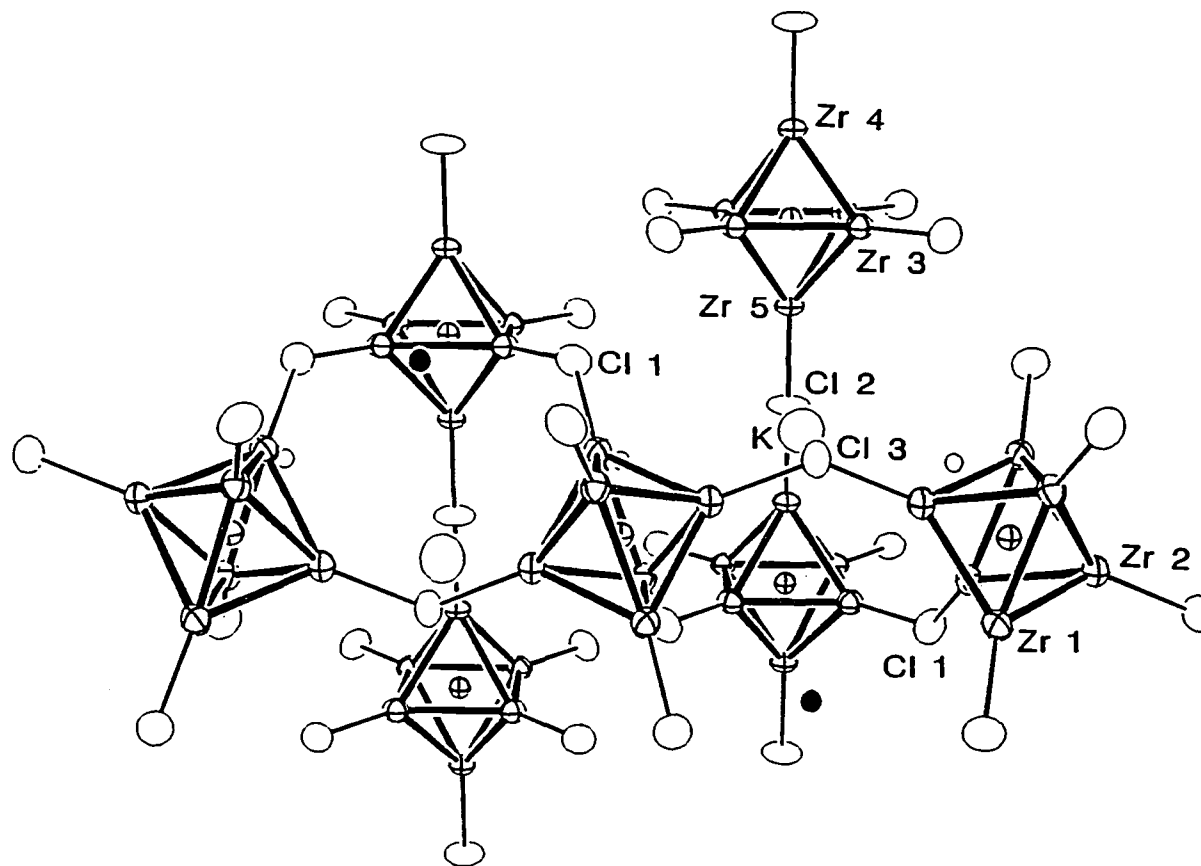


Figure 14. An approximately $[00\bar{1}]$ view of the structure of $K[Zr_6Cl^{i}_{12}C]Cl^{a-a}_{6/2}$ with the \bar{c} axis vertical. The zirconium atoms are connected by heavy lines while the Cl^i atoms have been omitted for clarity. One mirror plane parallel to the paper lies in the zig-zag $-(Zr_6C - Cl3)-$ chain, and a second one normal to the figure contains the linear $-(Zr_6C - Cl2)-$ chain and K. (90% probability thermal ellipsoids.) The small solid and open circles mark the Cs1 and Cs2 (b type) positions, respectively, in $CsZr_6Cl_{15}B$

Table 21. Interatomic distances in $\text{KZr}_6\text{Cl}_{15}\text{C}$ (Å)

	Cluster 1 (zig-zag chain)		Cluster 2 (linear chain)	
Zr-Zr				
Zr1-Zr1	(x4) ^a	3.2329(9)	Zr3-Zr3	(x2) 3.2424(9)
Zr1-Zr1	(x4)	3.249(1)	Zr3-Zr3	(x2) 3.248(1)
Zr1-Zr2	(x4)	3.2028(8)	Zr3-Zr4	(x4) 3.2028(8)
Zr1-Zr2	(x4)	3.2303(8)	Zr3-Zr5	(x4) 3.2141(8)
\bar{d}		3.225	\bar{d}	3.221
Zr-C				
Zr1-C1	(x4)	2.2916(5)	Zr3-C2	(x4) 2.2949(5)
Zr2-C1	(x2)	2.2571(7)	Zr4-C2	(x1) 2.247(6)
\bar{d}		2.2801	Zr5-C2	(x1) 2.238(6)
			\bar{d}	2.277
Zr-C1ⁱ				
Zr1-C15	(x4)	2.521(1)	Zr3-C19	(x4) 2.524(1)
Zr1-C14	(x4)	2.522(1)	Zr3-C18	(x4) 2.527(1)
Zr1-C17	(x4)	2.527(1)	Zr3-C110	(x4) 2.532(1)
Zr1-C16	(x4)	2.547(1)	Zr3-C111	(x4) 2.543(1)
Zr2-C17	(x4)	2.516(1)	Zr4-C110	(x4) 2.515(1)
Zr2-C16	(x4)	2.534(1)	Zr5-C111	(x4) 2.542(1)
Zr-C1^{a-a}				
Zr1-C11	(x4)	2.639(1)	Zr3-C11	(x4) 2.632(1)
Zr2-C13	(x2)	2.696(1)	Zr4-C12	(x1) 2.608(2)
			Zr5-C12	(x1) 2.598(2)
K-C1				
K-C11	(x2)	3.331(2)		
K-C17	(x2)	3.389(2)		
K-C16	(x2)	3.418(2)		
K-C13	(x2)	3.440(2)		
K-C110	(x1)	3.479(2)		
K-C12	(x1)	3.519(2)		
\bar{d}		3.419		

^aNumber of times the distance occurs per cluster or cation.

A perpendicular chain runs parallel to the \bar{c} axis and contains highly unusual $\text{Zr4-Cl2}^{\text{a-a}}\text{-Zr5}$ linkages between clusters that are constrained to linearity by symmetry, the three atoms lying on the intersection of two mirror planes. This $\text{Cl}^{\text{a-a}}$ atom shows a plate-like thermal ellipsoid perpendicular to the chain axis, consistent with either a greater thermal motion in what is presumably the most facile direction of vibration, or some disordering around or small displacement of the chlorine atom from the axial site. The cluster in the linear chain shows a 0.05 – 0.06 Å compression along the pseudo-four-fold axis of the chain. The crystallographically imposed symmetry is C_{2v} . The range and average of the Zr-Zr distances in this chain are very similar to those in the zig-zag member, and the same is true of the Zr-C distances.

The four remaining terminal Cl1 atoms form bent bridges ($\sim 132^\circ$) in interlinking the two types of cluster chains and creating the relatively open framework shown in Figure 14. These bridges appear equally strong so that the network could also be described, with some loss of simplicity, in terms of chains of mixed cluster types connected by Cl1.

The Zr-Cl^{i} distances in both clusters are typical and about the sum of the six-coordinate crystal radii¹²⁷ for Zr^{4+} and Cl^- , 2.53 Å. The $\text{Zr-Cl}^{\text{a-a}}$ distances are somewhat longer, as is usual, 2.70 Å in the zig-zag chain, 2.60 Å in the linear chain, and an intermediate 2.64 Å for those interconnecting the two chains.

The potassium atom is situated in a ten-coordinate position of mirror symmetry (type a) that is centered between a pair bridging $\text{Cl}^{\text{a-a}}$ atoms from the linear and zig-zag chains and also contains

eight Cl^{i} atoms from four clusters, two in each chain. As shown in Figure 15, the coordination sphere around the potassium is a distorted bicapped cube, the capping $\text{Cl}^{\text{a-a}}$ atoms lying over opposite faces. The K-Cl distances tabulated in Table 21 average 3.42 Å, nearly equal to the sum of the appropriate crystal radii, 3.40 Å.¹²⁷

In addition to the site occupied by the potassium atom, two other potential cation sites exist within the interlinked cluster framework. These each have half the multiplicity and are used exclusively when a larger cation is present. Such is the case in the parent structure $\text{CsNb}_6\text{Cl}_{15}$, where these two sites are fully occupied and the smaller potassium site is completely empty.⁷² It is evident from a comparison of calculated and observed Guinier powder diffraction patterns that both $\text{RbZr}_6\text{Cl}_{15}\text{C}$ and $\text{CsZr}_6\text{Cl}_{15}\text{C}$ also adopt this alternate placement of cations (Appendix I). The observed decrease in the unit cell volume between $\text{KZr}_6\text{Cl}_{15}\text{C}$ and these two heavier analogues (Table 17) is also consistent with the occupation of the larger, alternate set of cation sites. The nature of the larger cation sites will be examined in detail in connection with the structure of $\text{CsKZr}_6\text{Cl}_{15}\text{B}$.

$\text{CsKZr}_6\text{Cl}_{15}\text{B}$ has been studied by single crystal X-ray diffraction in order to confirm the occupation of and the ordering between the cation sites. Structurally, $\text{CsKZr}_6\text{Cl}_{15}\text{B}$ exhibits the same orthorhombic symmetry and metal-halogen skeleton as do $\text{KZr}_6\text{Cl}_{15}\text{C}$ and $\text{CsNb}_6\text{Cl}_{15}$, Figure 14. The difference lies, as expected, in the identity of the interstitial atom with the resulting changes in distances and in the simultaneous occupation of all three cation sites. The Zr-Zr and Zr- Cl^{i} distances are all

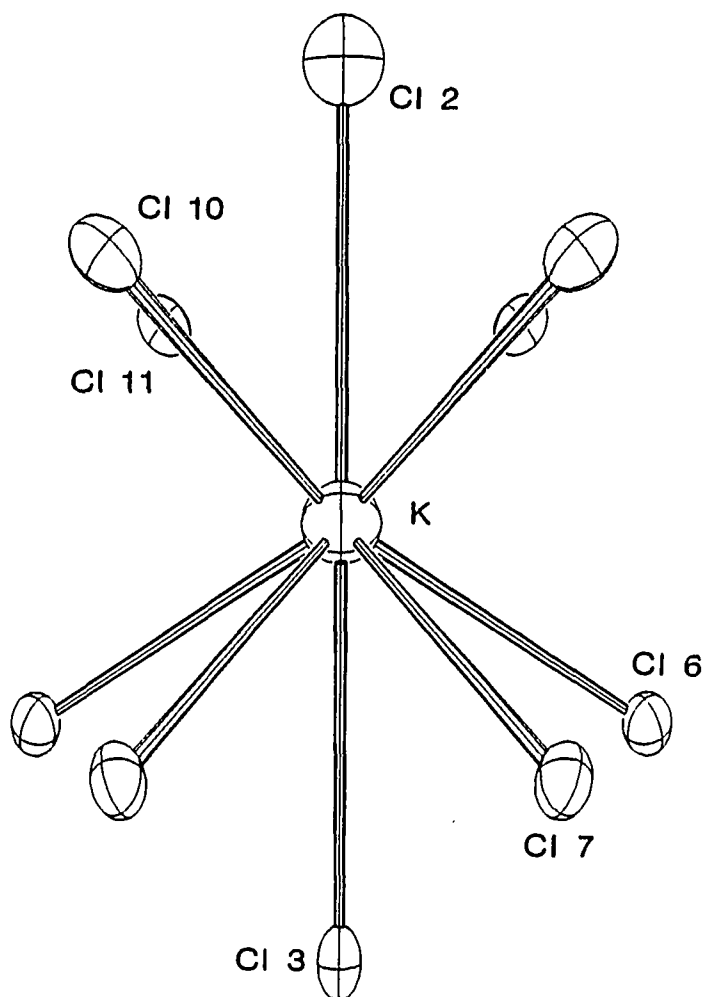


Figure 15. The potassium surroundings in $\text{KZr}_6\text{Cl}_{15}\text{C}$ (and $\text{CsKZr}_6\text{Cl}_{15}\text{B}$), with chain-bridging Cl2 and Cl3 at top and bottom, respectively. A vertical mirror plane lies normal to the drawing (50% ellipsoids)

Table 22. Interatomic distances in CsKZr₆C1₁₅B (Å)

		Cluster 1 (zig-zag chain)	Cluster 2 (linear chain)	
Zr-Zr				
Zr1-Zr1	(x4) ^a	3.267(1)	Zr3-Zr3	(x2) 3.274(1)
Zr1-Zr1	(x4)	3.289(1)	Zr3-Zr3	(x2) 3.288(1)
Zr1-Zr2	(x4)	3.2370(9)	Zr3-Zr4	(x4) 3.239(1)
Zr1-Zr2	(x4)	3.274(1)	Zr3-Zr5	(x4) 3.249(1)
\bar{d}		3.263	\bar{d}	3.256
Zr-B				
Zr1-B1	(x4)	2.3179(6)	Zr3-B2	(x4) 2.3201(6)
Zr2-B1	(x2)	2.2860(8)	Zr4-B2	(x1) 2.227(1)
\bar{d}		2.3073	Zr5-B2	(x1) 2.26(1)
			\bar{d}	2.302
Zr-C1ⁱ				
Zr1-C15	(x4)	2.550(2)	Zr3-C19	(x4) 2.549(2)
Zr1-C14	(x4)	2.543(2)	Zr3-C18	(x4) 2.549(2)
Zr1-C17	(x4)	2.555(2)	Zr3-C110	(x4) 2.563(2)
Zr1-C16	(x4)	2.565(2)	Zr3-C111	(x4) 2.552(2)
Zr2-C17	(x4)	2.545(2)	Zr4-C110	(x4) 2.537(2)
Zr2-C16	(x4)	2.548(2)	Zr5-C111	(x4) 2.562(2)
Zr-C1^{a-a}				
Zr1-B1	(x4)	2.663(2)	Zr3-C11	(x4) 2.651(2)
Zr2-B1	(x2)	2.725(2)	Zr4-C12	(x1) 2.603(4)
\bar{d}		2.3073	Zr5-C12	(x1) 2.593(4)
			\bar{d}	2.302
K-C1				
K-C11	(x2)	3.347(2)	Cs-C1	
K-C17	(x2)	3.393(2)	Cs1-C18	(x2) 3.462(2)
K-C16	(x2)	3.460(2)	Cs1-C15	(x2) 3.530(2)
K-C13	(x2)	3.476(2)	Cs1-C13	(x1) 3.933(4)
K-C110	(x1)	3.496(2)	Cs1-C17	(x4) 3.963(2)
K-C12	(x1)	3.529(2)	\bar{d}	3.752
\bar{d}		3.438	Cs2-C14	(x2) 3.440(2)
			Cs2-C110	(x4) 3.511(2)
			Cs2-C19	(x2) 3.569(3)
			\bar{d}	3.508

^aNumber of times the distance occurs per cluster or cation.

slightly longer than in the carbide, a result of the cluster expansion necessary to accommodate the larger boron interstitial. The Zr-B distances average ~ 2.31 Å, giving as before, an effective crystal radius of 1.45 Å for boron, slightly larger than that seen for carbon. Relatively few simple borides exist without B-B bonding, making a meaningful comparison of the observed Zr-B distance with other structures difficult. A small sample of NaCl-type zirconium and hafnium borides, mixed boride nitrides and boride carbides¹²⁵ yields an effective boron radius of 1.46 Å, which compares nicely with the observed boron radius in these and other zirconium chloride cluster phases like $Zr_6Cl_{14}B$, $K_2Zr_6Cl_{15}B$ and $Rb_5Zr_6Cl_{18}B$.

The crystallographic results for $CsKZr_6Cl_{15}B$ clearly show that all three cation sites in the structure are occupied. The refined nominal occupancies, 1.27(1), 0.937(6), and 0.784(6) for neutral atoms in the smaller potassium site (a) and the two larger cesium sites (b), respectively, are indicative of a small amount of cation mixing, primarily between the K and Cs2 positions. Consideration of the atomic numbers, multiplicities and refined occupancies indicates that, as a whole, the present structure contains 71.5 e⁻/formula unit for the cations compared with the expected value of 74 e⁻ for the indicated composition. These occupancies allow estimates of the cation distribution among sites, namely, $\sim 14\%$ cesium on the potassium site and $\sim 10\%$ potassium on the Cs1 site and $\sim 33\%$ on the Cs2 site.

Dimensionally, the smaller site occupied by potassium in the boride is nearly identical to the corresponding position in $KZr_6Cl_{15}C$, the 0.02

A increase in the average K-Cl distance probably reflects the expansion of the anion matrix associated with the larger boron interstitial.

The pair of contrasting type (b) cation positions are quite interesting because of the very unusual coordination environment each provides for the larger cesium cations. Their locations are marked in Figure 14 by small solid and open circles for Cs1 and Cs2, respectively. The Cs1 site is approximately square pyramidal in shape, as shown in more detail in Figure 16. It lies on the intersection of two mirror planes at $1/4, 1/4, z$ and is approximately centered between Cl8 atoms on clusters in adjacent linear chains. The atom sits ~ 0.5 Å above the least-squares plane of Cl5 and Cl8 atoms that form the base of a square pyramid (planar within ± 0.05 Å) with Zr-Cl distances of 3.463(3) and 3.531(3) Å. The sum of six-coordinate radii is 3.48 Å.¹²⁷ The fifth atom at the apex of the pyramid, Cl3, lies directly over the cesium atom at a distance 3.935(5) Å, leaving the cation essentially four-coordinate. Four additional Cl7 atoms lie in a plane below the pyramid base at comparable distances of 3.960(3) Å from the cesium atom. The B_{33} value for cesium along the pseudo-four-fold axis of the pyramid is about three times the average perpendicular value, a plausible result.

In $\text{CsNb}_6\text{Cl}_{15}$,⁷² the cesium atom sits nearly 0.5 Å higher above the pyramidal base, correspondingly shortening the distance to the apex chlorine and giving five more nearly equal Cs-Cl distances. This striking difference between the two compounds appears to be largely a consequence of the change in the size of the interlinked cluster matrix, the dimensions of the average $\text{Zr}_6\text{Cl}_{12}\text{B}$ cluster being 10 – 15% greater

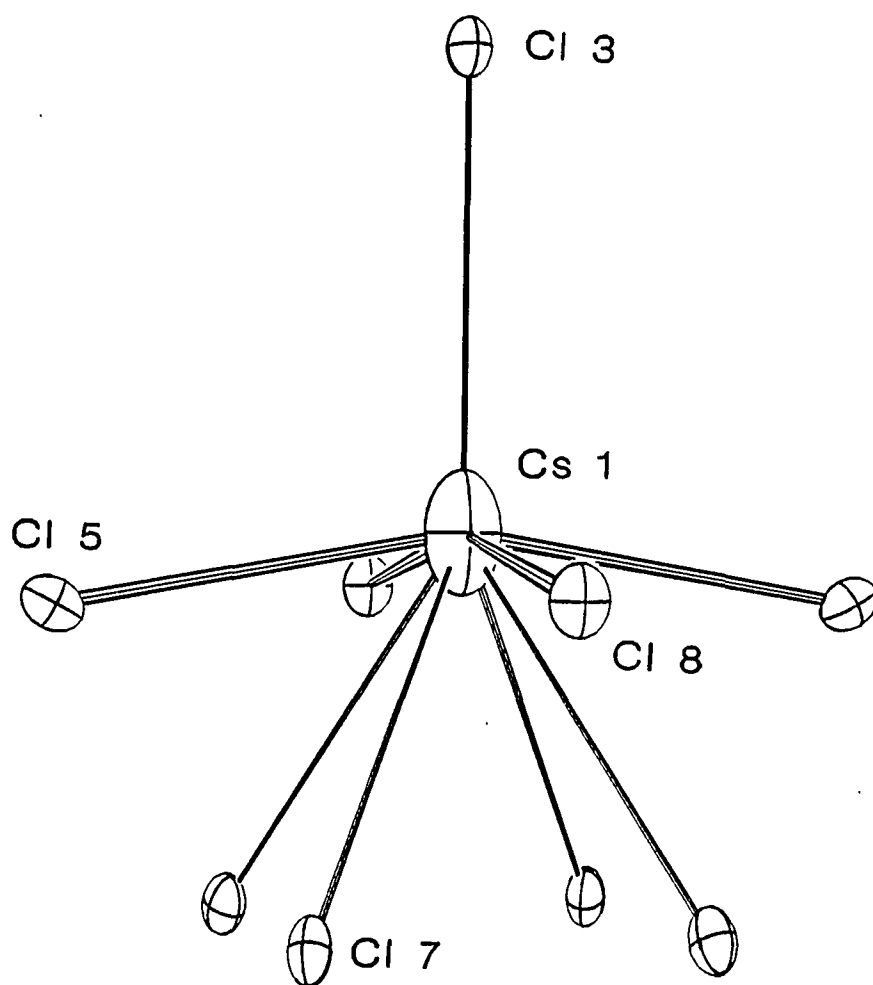


Figure 16. The Cs1 site in $\text{CsKZr}_6\text{Cl}_{15}\text{B}$. The \bar{c} axis is vertical, the Cl5 and Cl8 atoms lie on perpendicular mirror planes, and Cl3 at the top bridges between clusters in the zig-zag chain (50% ellipsoids)

than those of the niobium analog. The increased cluster size creates increased nonbonded Cl-Cl distances and larger voids, particularly between chlorine atoms on different clusters such as the basal C15 and C18 atoms in the pyramid. This requires that the cesium atom in the zirconium phase move closer to the pyramid base in order to retain four comparable Cs-Cl distances, but at the expense of the one coulombic interaction with the apex chlorine atom.

The second cesium atom is even more unusual in its coordination geometry. As shown in Figure 17, it resides in or near an eight-coordinate position of $2/m$ symmetry along \bar{a} and midway between linear cluster chains. Four C19 and two C110 atoms from clusters within those chains form a very elongated trigonal antiprism with Cs-Cl distances of 3.514(2) Å [x4] and 3.566(3) Å [x2]. The two remaining C14 atoms that also bridge cluster edges within the zig-zag chain lie on a two-fold axis normal to the long axis of the antiprism and give the shortest Cs-Cl distances, 3.440(2) Å. There are no other neighbors within 4.8 Å. The Cs2 atom in such an asymmetric environment refines with the extremely elongated ellipsoid shown that protrudes out opposite faces of the trigonal antiprism perpendicular to the (pseudo) $\bar{3}$ axis. An alternate description, which better illustrates the unusual coordination about the cesium atom, starts with the note that the cesium atom lies in a rigorous plane of six chlorine atoms. The remaining C19 atoms lie on a line through the cesium atom that intersects the plane of the six chlorine atoms at an angle of $\sim 55^\circ$. The cesium ellipsoid is elongated essentially

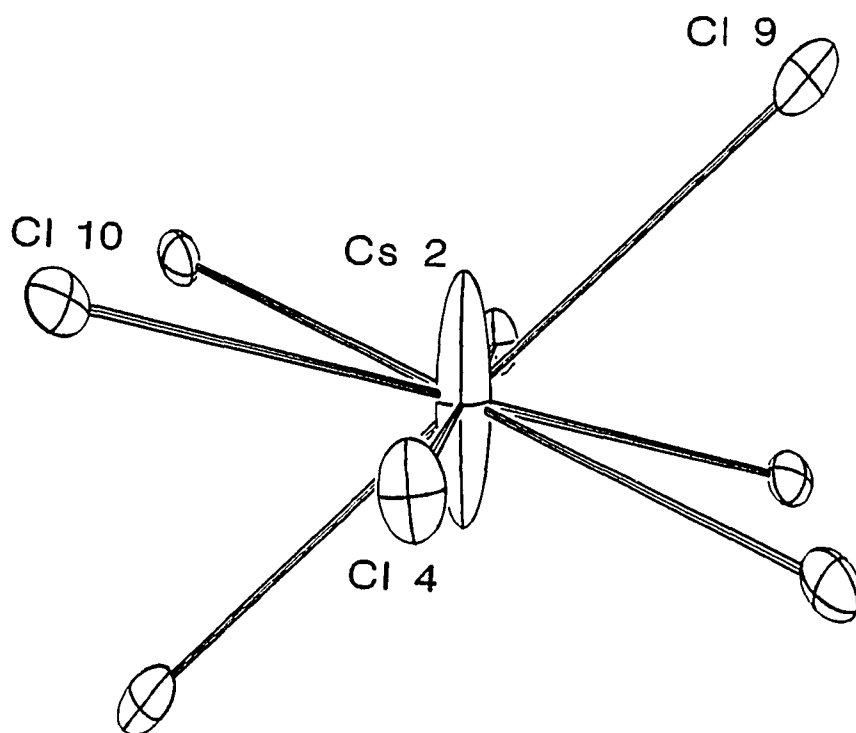


Figure 17. The cesium(2) site in $\text{CsKZr}_6\text{Cl}_{15}\text{B}$ as refined in space group Pmma . A mirror plane through $\text{Cs}2$ and $\text{Cl}9$ lies approximately in the plane of the paper with a two-fold axis through $\text{Cl}4$ and $\text{Cs}2$ (50% ellipsoids)

perpendicular to the plane, but slightly canted away from the C19 atoms lying above and below it.

A larger view of the surroundings about the Cs2 site is shown in Figure 18 in terms of just the chlorine atoms in neighboring clusters. The Figure emphasizes that the structural framework defining the Cs2 cavity leaves the site tightly girded around the waist, but relatively open in the [101] direction. Some twisting (torsion) of the host matrix can also be imagined, particularly if the problem cation were to order, and a harmonic description of the cation distribution may not be suitable. The apparent disorder of a cation at this site is thus a logical consequence of the structure, a problem that should extend to other compounds that utilize this site, i.e., $\text{RbZr}_6\text{Cl}_{15}\text{C}$, $\text{CsZr}_6\text{Cl}_{15}\text{C}$, $\text{Rb}_2\text{Zr}_6\text{Cl}_{15}\text{B}$ and $\text{CsRbZr}_6\text{Cl}_{15}\text{B}$. The same disorder occurs in $\text{CsZr}_6\text{Cl}_{15}\text{Fe}^{63}$ where there are even larger clusters, and should also occur in $\text{CsZr}_6\text{Br}_{15}\text{Fe}$ unless the present potassium site becomes sufficiently large to accommodate cesium.

The most simplistic view of the refinement results for the two cesium sites, particularly the second, is that a number of positions are occupied in the asymmetric array produced by a somewhat flexible anion matrix. The collection of problem thermal ellipsoids found at first suggested that the structure had been refined with too high an imposed symmetry, but no solution could be found in any of the lower symmetry space groups that were consistent with the general character of the structure (see Crystallography). A plausible but presently unprovable explanation of these difficulties is that all of the crystals available are twinned via alternative displacements of cations, Cs2 in particular,

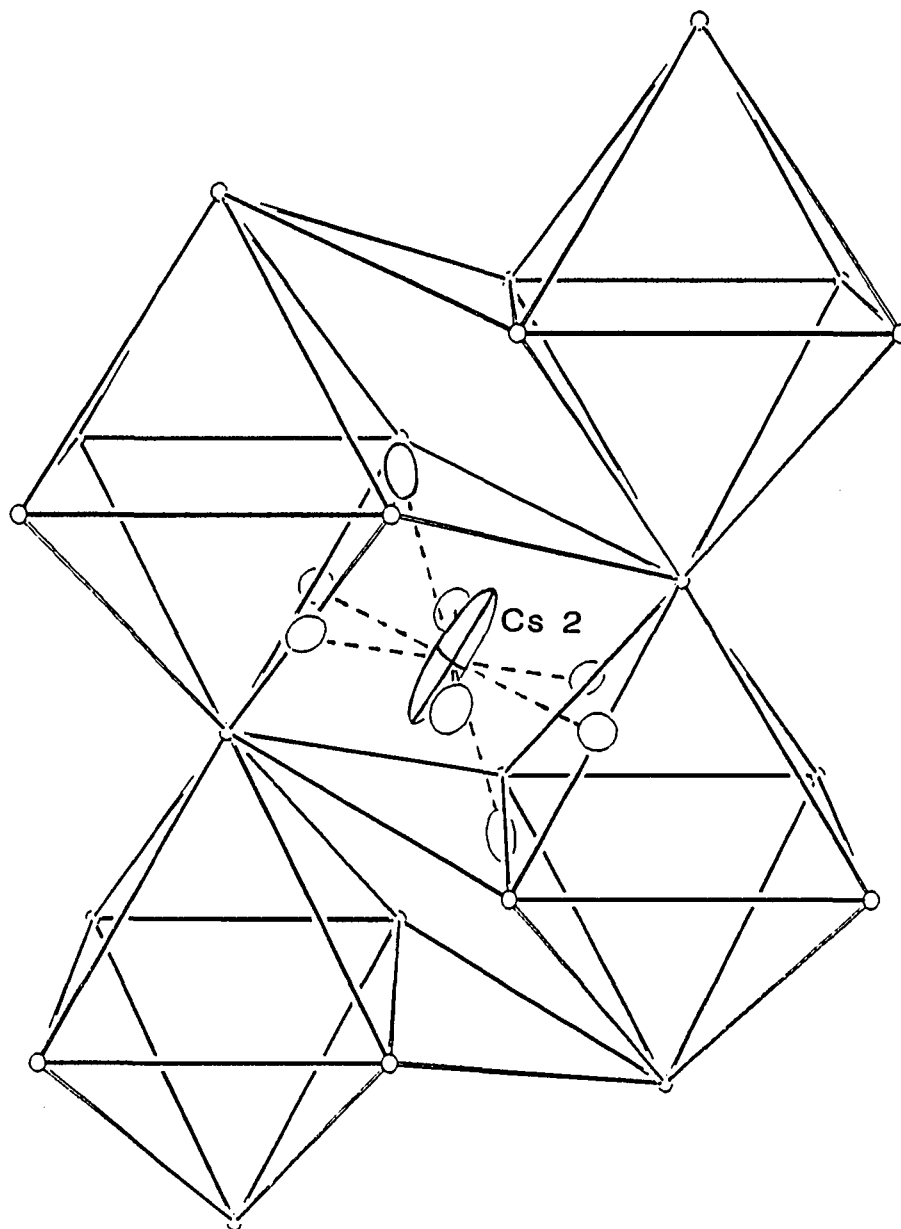


Figure 18. A larger, approximately $[0\bar{1}0]$ view of the Cs2 site between polyhedra defined by chlorine atoms on neighboring clusters. Small circles are cluster-bridging $\text{Cl}^{\text{a-a}}$; larger ellipsoids are the nearest neighbor Cl^1 atoms in Figure 17. The solid lines define chlorine polyhedra and their contacts, not bonds

and this is accompanied by small shifts of the neighboring chlorine environment and possibly some small twisting of the cluster matrix as well. Some probable potassium occupancy of the Cs2 site is an additional complication. Fortunately the $\text{KZr}_6\text{Cl}_{15}\text{C}$ example is well-behaved so as to better define the structural arrangement.

The structure described here represents first a new arrangement for some old examples, namely M_6X_{12} clusters interconnected at all vertex positions by bridging halides to give an $(\text{M}_6\text{X}_{12})\text{X}_{6/2}$ stoichiometry. The present arrangement is evidently generated so that alkali metal cations can also be accommodated, but the sites available within this cluster anion framework do not always provide ideal environments for that purpose, as first shown for $\text{CsNb}_6\text{Cl}_{15}$.⁷² This particular structure is also unusual because it furnishes one of the few examples of linearly bridged clusters $-(\text{Zr}_6\text{Cl}_{12}\text{Z})-\text{Cl}-$ in the metal halide systems. Equally important, the necessity of an interstitial atom within the cluster introduces a new variability to the chemistry possible.

The presence of two sets of cation sites that are separately and completely occupied in $\text{KZr}_6\text{Cl}_{15}\text{C}$ and $\text{CsNb}_6\text{Cl}_{15}$ depending on the cation size, first provided the impetus to prepare compounds containing two different cations, one on each set. The addition of another cation within the framework might be achieved by either a one-electron reduction of each cluster or by a compensating increase in nonmetal charge. The addition of another electron to the cluster bonding orbitals seemed unlikely based on our experience with numerous zirconium chloride clusters as these show a marked proclivity for 14 cluster-bonding electrons.⁶⁰

Attempts to add additional electrons often produced a compensating increase in the Cl:Zr ratio in the phase even under mildly reducing conditions, although a few 15-electron clusters have been recently obtained, the present $\text{KZr}_6\text{Cl}_{15}\text{N}$ among them. Although an increase in nonmetal charge without a change in electron count could potentially be accomplished by substitution of chalcogenide for chloride, the replacement of the interstitial carbon atom with boron is operationally much more facile. Indeed, reactions with halides of the cation pairs CsRb, CsK, and Rb_2 all proceed readily in the presence of boron and give essentially quantitative yields of $\text{MM}'\text{Zr}_6\text{Cl}_{15}\text{B}$ in the desired structure.

$\text{K}_2\text{Zr}_6\text{Cl}_{15}\text{B}$ and $\text{K}_3\text{Zr}_6\text{Cl}_{15}\text{Be}$: two new interrelated M_6X_{15} structures

The $\text{Ta}_6\text{Cl}_{15}$ and Nb_6F_{15} structure types with $[\text{M}_6\text{X}_{12}^i]\text{X}^{a-a}_{6/2}$ connectivity have been known for some time.^{4,5} More recently, a series of compounds with the structural framework of a third M_6X_{15} structure, $\text{CsNb}_6\text{Cl}_{15}$, but with a much more diverse cation and interstitial chemistry have been prepared.^{72,134} The known M_6X_{15} structure types, although related by their common local connectivity, show a diversity in their structural chemistry in virtually every other aspect; from the local geometry around the intercluster bridging X^{a-a} atoms which can be all bent, all linear, or a combination thereof, to the accommodation of a variety of cations, to the larger three-dimensional connectivity of the structure. The diversity of this group is further enhanced by two new compounds, $\text{K}_2\text{Zr}_6\text{Cl}_{15}\text{B}$ and $\text{K}_3\text{Zr}_6\text{Cl}_{15}\text{Be}$, which represent new structure types in the M_6X_{15} family. Both structures show a combination of structural features found in the other three cluster frameworks and yet are

unrelated to any of them in a larger three-dimensional sense. Interestingly, however, $K_2Zr_6Cl_{15}B$ and $K_3Zr_6Cl_{15}Be$ are related to one another in this three-dimensional connectivity, such that the latter can be viewed as a monoclinic distortion of the former.

Synthesis $K_2Zr_6Cl_{15}B$ was initially prepared as the major product in a reaction designed to explore the limits of stability of the $CsNb_6Cl_{15}$ structure with different pairs of cations. The reaction, run at 850°C for 29 days before being air quenched, was loaded with stoichiometric amounts of Zr powder, $ZrCl_4$, KCl and amorphous boron powder. The yield of the dark red, crystalline material was estimated to be greater than 95%. The slightly reducing conditions created by the $ZrCl_4$ used to maintain the autogenous pressure over the product appears to facilitate the preferential formation of $K_2Zr_6Cl_{15}B$ over $KZr_6Cl_{14}B$ and K_2ZrCl_6 .

The isostructural 13-electron cluster $K_2Zr_6Cl_{15}Be$ was prepared from stoichiometric amounts of Zr powder, $ZrCl_4$, KCl and Be flakes at 800-850°C over a 2-3 week period. Yields near 95% were often obtained. As with other 13-electron zirconium chloride clusters, the autogenous $ZrCl_4$ pressure over $K_2Zr_6Cl_{15}Be$ at reaction temperature was somewhat larger than that for comparable 14-electron cluster compounds. $K_2Zr_6Cl_{15}Be$ is often found as a minor product in preparations of $KZr_6Cl_{13}Be$.

$K_3Zr_6Cl_{15}Be$ was prepared while attempting the synthesis of ' $K_4Zr_6Cl_{16}Be$ ' by the direct reaction of stoichiometric quantities of Zr powder, $ZrCl_4$, KCl and Be flakes at 800°C. The reaction, which was

quenched after 21 days, contained a mixture of $K_3Zr_6Cl_{15}Be$ and K_2ZrCl_6 . $Rb_3Zr_6Cl_{15}Be$ forms under similar conditions. Both compounds were obtained in ~95% yields. Crystals from reactions to prepare $K_3Zr_6Cl_{15}Be$ or $Rb_3Zr_6Cl_{15}Be$ were often severely intergrown, although single crystals large enough for X-ray diffraction work could be found or chipped from the intergrown masses.

Partial occupancy of the cation sites, at least in the case of $K_3Zr_6Cl_{15}Be$, does not appear to occur. A reaction to prepare $K_{2.5}Zr_6Cl_{15}Be$ yielded an approximately 50:50 mixture of $K_2Zr_6Cl_{15}Be$ and $K_3Zr_6Cl_{15}Be$. Lattice parameters of the $K_3Zr_6Cl_{15}Be$ obtained were not significantly different from those measured for material prepared with excess KCl.

Lattice parameters of the compounds prepared in the $K_2Zr_6Cl_{15}B$ and $K_3Zr_6Cl_{15}Be$ structure types are given in Table 23.

Crystallography Single crystal X-ray diffraction data for $K_2Zr_6Cl_{15}B$ and $K_3Zr_6Cl_{15}Be$ were collected on small, dark red, rectangular prisms of the compounds using monochromatic Mo $K\alpha$ radiation and variable rate ω -scans. The orthorhombic and monoclinic cells chosen, respectively, for $K_2Zr_6Cl_{15}B$ and $K_3Zr_6Cl_{15}Be$, were derived from sets of tuned low angle reflections using the program BLIND.¹²⁶ Axial photographs taken on the diffractometer were consistent with the calculated cells both in terms of layer spacings and Laue symmetry. Pertinent details of the data collections are given in Table 24.

For $K_2Zr_6Cl_{15}B$ the space group symmetry of Cccm was chosen on the basis of the observed systematic extinctions and an assumed centricity

Table 23. Lattice parameters of compounds in the $K_2Zr_6Cl_{15}B$ and $K_3Zr_6Cl_{15}Be$ structure types^a

Compound	a	b	c	β	V
$K_2Zr_6Cl_{15}B^b$	11.386(1)	15.980(1)	14.008(1)	90.0	2548.6(4)
$K_2Zr_6Cl_{15}Be^b$	11.446(1)	16.108(3)	14.097(1)	90.0	2599.1(6)
$K_3Zr_6Cl_{15}Be^c$	16.372(2)	11.396(2)	14.071(1)	92.74(1)	2622.2(6)
$Rb_3Zr_6Cl_{15}Be^c$	16.473(2)	11.555(1)	14.083(2)	93.14(1)	2676.6(6)

^aGuinier powder diffraction data, axial lengths are in Å, and cell volumes in Å³.

^b $K_2Zr_6Cl_{15}B$ structure, orthorhombic.

^c $K_3Zr_6Cl_{15}Be$ structure, monoclinic.

Table 24. Summary of crystallographic data for $K_2Zr_6Cl_{15}B$ and $K_3Zr_6Cl_{15}Be$

	$K_2Zr_6Cl_{15}B$	$K_3Zr_6Cl_{15}Be$
Space Group	Cccm	C2/c
Z	4	4
a, Å ^a	11.386(1)	16.372(2)
b	15.980(1)	11.396(2)
c	14.008(1)	14.071(1)
β, deg.	90.0	92.74(1)
V, Å ³	2548.6(4)	2622.2(6)
Crystal dimen., mm	0.20x0.13x0.35	0.15x0.20x0.20
Radiation	Mo Kα, graphite monochromator	Mo Kα, graphite monochromator
2θ(max), deg.	55.0	55.0
Scan Mode	ω	ω
Reflections		
octants	hk±l	h,±k,±l
measured refl.	2925	12192
observed refl.	1772	5232
independent refl.	977	2651
R(ave), %	1.9	2.6
μ, cm ⁻¹	41.7	42.1
Transm. coeff. range	0.73 — 1.00	0.78 — 1.00
Secondary ext. coeff.	1.4(2)x10 ⁻⁴	7(6)x10 ⁻⁷
R, %	3.3	4.8
R(w), %	4.1	3.2

^aGuinier powder diffraction data.

which was supported by a Wilson plot and later confirmed by the structural refinement. The initial atomic coordinates were determined by direct methods using the program MULTAN-80.⁹⁵ Four randomly oriented octahedral zirconium clusters were included as input into MULTAN-80 to aid in the normalization process. An earlier attempt to solve the structure by direct methods without 'molecular fragments' had given a partial solution (Zr_4 butterflies), but had incorrectly assigned the origin which prevented a complete solution. The correct solution, obtained using 'molecular fragments', translated the origin by $(1/4, 1/4, 0)$ and gave octahedral Zr_6 clusters.

The structure was initially calculated by Fourier synthesis using only the two 'heaviest' atoms obtained from MULTAN-80 which were assumed to be Zr atoms. Successive cycles of least-squares refinement and electron density map calculations located the remaining atoms in the structure and identified the composition as $K_2Zr_6Cl_{15}B$. The expected boron interstitial atom was included in the refinement after an approximately 5-electron residual was observed at the cluster center following isotropic refinement of all atoms in the structure. The refinement converged to $R = 0.033$ and $R_w = 0.041$ after application of a secondary extinction correction and a statistical reweighting of the data set. The occupancies of B, K1, and K2 refined to 0.99(7), 0.99(1) and 0.92(2), respectively.

The K2 atom, which occupies a site of $2/m$ symmetry, shows a somewhat elongated thermal ellipsoid in the \vec{b} direction. The elongation is apparently a consequence of the local chlorine environment which creates

a long cylindrical cavity similar, in many respects, to the Cs2 site in $\text{CsKZr}_6\text{Cl}_{15}\text{B}$.¹³⁴ A reduction in symmetry to a monoclinic space group seems unwarranted on the basis of the mirror symmetry seen in the axial photographs, the excellent R of data averaging and the quality of the refinement. A refinement of the structure was attempted in the monoclinic space group $C2/c$, however, to look for signs of the type of distortion seen in $\text{K}_3\text{Zr}_6\text{Cl}_{15}\text{Be}$ (the \vec{a} and \vec{b} axes of the orthorhombic cell have to be interchanged in $C2/c$). Although the K2 atom was not allowed to move from the inversion center, refinement of the remaining atoms under the reduced symmetry conditions showed no deviation from the orthorhombic symmetry of $Cccm$. The final difference map was flat to less than $\pm 0.4 \text{ e}^-/\text{\AA}^3$. The K2 portion showed positive 0.3 e^- peaks at each end in the \vec{b} direction.

For $\text{K}_3\text{Zr}_6\text{Cl}_{15}\text{Be}$, the monoclinic space group $C2/c$ was chosen on the basis of the observed systematic extinctions and later confirmed by the successful refinement of the structure in the space group.

Three zirconium positions were found by direct methods,⁹⁵ while the remainder of the atoms in the structure were located in subsequent Fourier maps. The Be atom, an approximately 3-electron residual in the cluster center, was included in the model following isotropic refinement of the Zr, Cl and K atoms. Simultaneous refinement of the occupancy of the Be site and the corresponding thermal parameter (B) gave values of 1.08(5) and 1.5(3), respectively. The occupancy of K1 refined to 0.999(7) and that of K2 to 1.00(1). The final residual factors for the

structural refinement following a correction for secondary extinction and a reweighting of the data set were $R = 0.048$ and $R_w = 0.032$.

Atomic coordinates and thermal parameters are given for $K_2Zr_6Cl_{15}B$ and $K_3Zr_6Cl_{15}Be$ in Tables 25 and 26, respectively. Structure factor amplitudes are tabulated in Appendix J for $K_2Zr_6Cl_{15}B$ and Appendix K for $K_3Zr_6Cl_{15}Be$.

Structure and Discussion The structures of $K_2Zr_6Cl_{15}B$ and $K_3Zr_6Cl_{15}Be$, like that of $KZr_6Cl_{15}C$,¹³⁴ show a combination of bent and linear Cl^{a-a} bridges between cluster units. Unlike $KZr_6Cl_{15}C$, however, both $K_2Zr_6Cl_{15}B$ and $K_3Zr_6Cl_{15}Be$ are built-up of only linear cluster chains which are interconnected into a three-dimensional array by additional bent Cl^{a-a} bridges. One-third of the intercluster Cl^{a-a} bridges are linear compared with one-sixth in $KZr_6Cl_{15}C$. Important differences also exist between $K_2Zr_6Cl_{15}B$ and $K_3Zr_6Cl_{15}Be$. Bonding distances in $K_2Zr_6Cl_{15}B$ and $K_3Zr_6Cl_{15}Be$ are tabulated in Tables 27 and 28, respectively.

The linear cluster chains in $K_2Zr_6Cl_{15}B$ are packed to give a criss-crossing pattern of chains when viewed down the \tilde{c} axis as shown in Figure 19. The criss-crossing linear chains intersect in projection at an angle of $\sim 109^\circ$. The $Zr-Cl^{a-a}-Zr$ bridge in the linear cluster chain is constrained to linearity by the crystallographically imposed $2/m$ symmetry of the Cl^{a-a} site. Interestingly, the linear chain is very slightly puckered, however, because the $Zr-Cl^{a-a}$ bond in the linear bridge comes into the cluster pointed 2.6° off center, i.e., the $Cl^{a-a}-Zr-B$ angle is 177.4° . Similar deviations from linearity of

Table 25. Positional and thermal parameters for $K_2Zr_6Cl_{15}B$

Atom	x	y	z	B_{11}
Zr1	0.86207(9)	0.13199(6)	1/2	1.27(4)
Zr2	0.36805(5)	0.19108(4)	0.11677(4)	1.21(2)
Cl1	0.5078(2)	0.3173(1)	0.1261(1)	0.86(6)
Cl2	0.2517(2)	0.0545(1)	0.1290(1)	1.38(6)
Cl3	1/4	1/4	0.2557(2)	1.11(8)
Cl4	0.5121(2)	0.1232(2)	0	1.0(1)
Cl5	0	0	0	2.3(2)
Cl6	1/2	0.1217(2)	1/4	2.2(1)
K1 ^a	1/2	1/2	1/4	3.9(2)
K2 ^b	1/4	3/4	0	2.1(2)
B ^c	1/4	1/4	0	1.0(4)

^aOccupancy refined to 0.99(1).

^bOccupancy refined to 0.92(2).

^cOccupancy refined to 0.99(7).

B_{22}	B_{33}	B_{12}	B_{13}	B_{23}
1.33(4)	1.17(3)	0.38(3)	0	0
1.53(3)	1.14(2)	-0.15(2)	-0.22(2)	0.13(2)
1.54(7)	1.27(6)	-0.42(6)	-0.55(6)	0.13(6)
1.26(6)	1.58(7)	-0.52(6)	-0.46(6)	0.57(5)
2.5(1)	0.57(8)	-0.04(9)	0	0
1.9(1)	1.5(1)	0.55(9)	0	0
1.6(2)	3.2(2)	-1.4(2)	0	0
1.2(1)	1.7(1)	0	-1.3(1)	0
2.6(2)	2.6(2)	0	0	0
11.2(6)	3.5(3)	-0.2(3)	0	0

Table 26. Positional and thermal parameters for $K_3Zr_6Cl_{15}Be$

Atom	x	y	z	B_{11}
Zr1	0.13369(3)	0.13509(4)	0.49888(3)	1.05(2)
Zr2	0.30275(3)	0.14997(4)	0.63509(3)	1.21(2)
Zr3	0.68798(3)	0.11323(4)	0.09790(4)	1.29(2)
C11	0.81105(9)	0.0324(1)	0.6017(1)	2.15(6)
C12	0.55011(8)	0.2270(1)	0.1027(1)	1.39(5)
C13	0.26559(9)	0.2165(1)	0.24632(9)	2.44(6)
C14	0.37599(9)	0.0091(1)	0.0409(1)	2.68(6)
C15	0	0	0	1.73(8)
C16	0.37684(9)	0.9534(1)	0.2891(1)	1.86(5)
C17	0.32483(8)	0.4843(1)	0.3530(1)	1.75(5)
C18	0.06513(9)	0.2234(1)	0.3478(1)	1.66(5)
K1 ^a	0	0.0615(3)	3/4	6.0(2)
K2 ^b	0.1140(1)	0.2448(1)	0.0674(1)	3.83(9)
Be ^c	3/4	1/4	0	1.5(3)

^aOccupancy refined to 0.999(7).

^bOccupancy refined to 1.00(1).

^cOccupancy refined to 1.08(5).

B_{22}	B_{33}	B_{12}	B_{13}	B_{23}
1.02(2)	0.98(2)	-0.30(1)	-0.02(1)	0.04(1)
1.03(2)	0.79(2)	-0.10(2)	-0.08(1)	0.14(1)
0.95(2)	0.90(2)	0.02(1)	0.09(1)	0.12(1)
1.53(5)	1.83(6)	-0.56(4)	0.45(4)	-0.68(4)
1.73(5)	2.08(6)	0.11(4)	0.45(4)	0.32(4)
1.46(5)	0.90(5)	0.10(4)	0.06(4)	-0.10(4)
1.60(5)	1.44(5)	-0.86(5)	-0.10(4)	-0.04(4)
2.40(9)	3.6(1)	1.30(7)	-0.03(7)	-0.23(8)
1.83(5)	1.41(5)	0.21(4)	-0.11(4)	-0.74(4)
1.41(5)	1.42(5)	-0.37(4)	-0.20(4)	0.48(4)
2.25(6)	1.62(5)	-0.64(4)	-0.59(4)	0.68(4)
5.0(2)	4.0(1)	0	2.7(2)	0
2.44(7)	4.39(9)	-0.36(6)	0.13(7)	0.04(6)

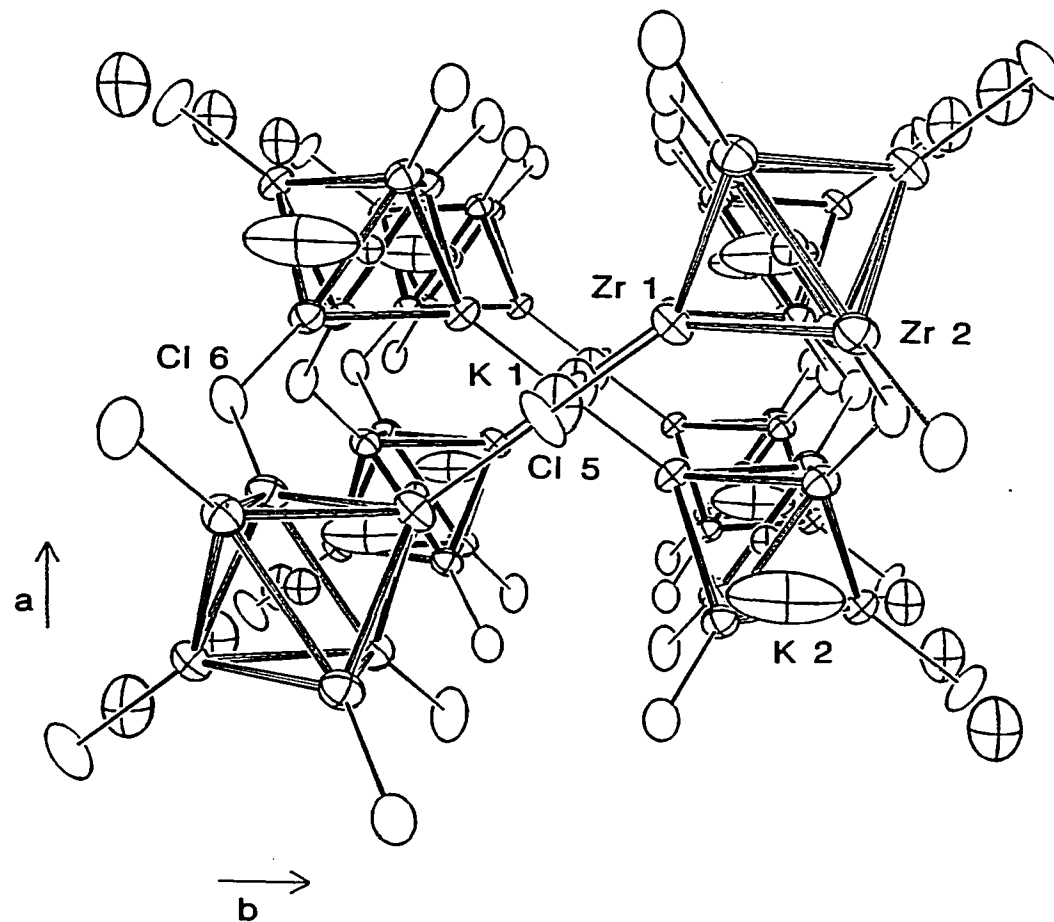


Figure 19. An approximately $[00\bar{1}]$ view of the structure of $K_2Zr_6Cl_{15}B$ with Cl^i atoms omitted for clarity. The Zr_6B clusters are outlined. Cl^{a-a} atoms are drawn as open ellipsoids and K atoms as crossed-ellipsoids. Thermal ellipsoids are 90% probability

Table 27. Bond distances in $K_2Zr_6Cl_{15}B$ (Å)

Zr-Zr		
Zr1-Zr2	(x4) ^a	3.230(1)
Zr1-Zr2	(x4)	3.267(1)
Zr2-Zr2	(x2)	3.271(1)
Zr2-Zr2	(x2)	3.282(1)
\bar{d}		3.253
Zr-B		
Zr1-B	(x2)	2.277(1)
Zr2-B	(x4)	2.3170(6)
\bar{d}		2.304
Zr-Clⁱ		
Zr1-Cl1	(x4)	2.555(2)
Zr1-Cl2	(x4)	2.546(2)
Zr2-Cl1	(x4)	2.573(2)
Zr2-Cl2	(x4)	2.559(2)
Zr2-Cl3	(x4)	2.546(2)
Zr2-Cl4	(x4)	2.558(2)
Zr-Cl^{a-a}		
Zr1-Cl5	(x2)	2.630(1)
Zr2-Cl6	(x4)	2.640(1)
K-Cl		
K1-Cl1	(x4)	3.397(2)
K1-Cl2	(x4)	3.441(2)
K1-Cl5	(x2)	3.5020(3)
\bar{d}		3.436
K2-Cl4	(x2)	3.383(3)
K2-Cl3	(x2)	3.422(2)
K2-Cl1	(x4)	3.447(2)
\bar{d}		3.425

^aNumber of times the distance occurs per cluster or cation.

the $\text{Cl}^{\text{a-a}}\text{-Zr}$ -interstitial angle are observed in practically all other cluster compounds. In this case, the deviation may play a role in relieving what appears to be a compression down the linear chain. In $\text{KZr}_6\text{Cl}_{15}\text{C}$ and $\text{CsKZr}_6\text{Cl}_{15}\text{B}$ where no mechanism exists for a tilting of the cluster because of the imposed crystallographic symmetry, a more severe flattening of the thermal ellipsoids of the atoms in the chain, particularly for the intercluster bridging $\text{Cl}^{\text{a-a}}$ atom, is seen.¹³⁴

In $\text{K}_2\text{Zr}_6\text{Cl}_{15}\text{B}$, the potassium atoms reside in two crystallographically distinct sites. K1 lies between adjacent linearly bridging $\text{Cl}^{\text{a-a}}$ atoms on 2-fold axes parallel to \vec{c} . The atoms are arranged to give infinite strings of $\dots\text{Cl}^{\text{a-a}}\text{-K1-Cl}^{\text{a-a}}\text{-K1}\dots$ down the edges and center of the cell in the \vec{a} direction (Figure 19). The local environment of K1, shown in Figure 20, is composed of ten chlorine atoms in a polyhedron with 222 symmetry (D_{2d}) which can be visualized as a distorted bicapped square antiprism. The K-Cl distances are typical, about the sum of the ten-coordinate K and Cl crystal radii.¹²⁷

The K2 site is more unusual and lies midway between $[\text{Zr}_6\text{Cl}_{12}^{\text{I}}\text{B}]$ clusters in \vec{c} . The site, with 2/m symmetry, is bounded by eight inner chlorine atoms in the form of a highly elongated trigonal antiprism. Two of the long edges of the antiprism are bridged in a trans-fashion by Cl3 atoms at intermediate distances of 3.422(2) Å. The local chlorine geometry around the K2 atom, shown in Figure 21, is very similar to the Cs2 site in $\text{CsKZr}_6\text{Cl}_{15}\text{B}$.¹³⁴ The nearest chlorine neighbors of K2 out opposite faces of the trigonal antiprism in the \vec{b} direction are over 5 Å away. Just as with Cs2 in $\text{CsKZr}_6\text{Cl}_{15}\text{B}$, the K2 atom is elongated

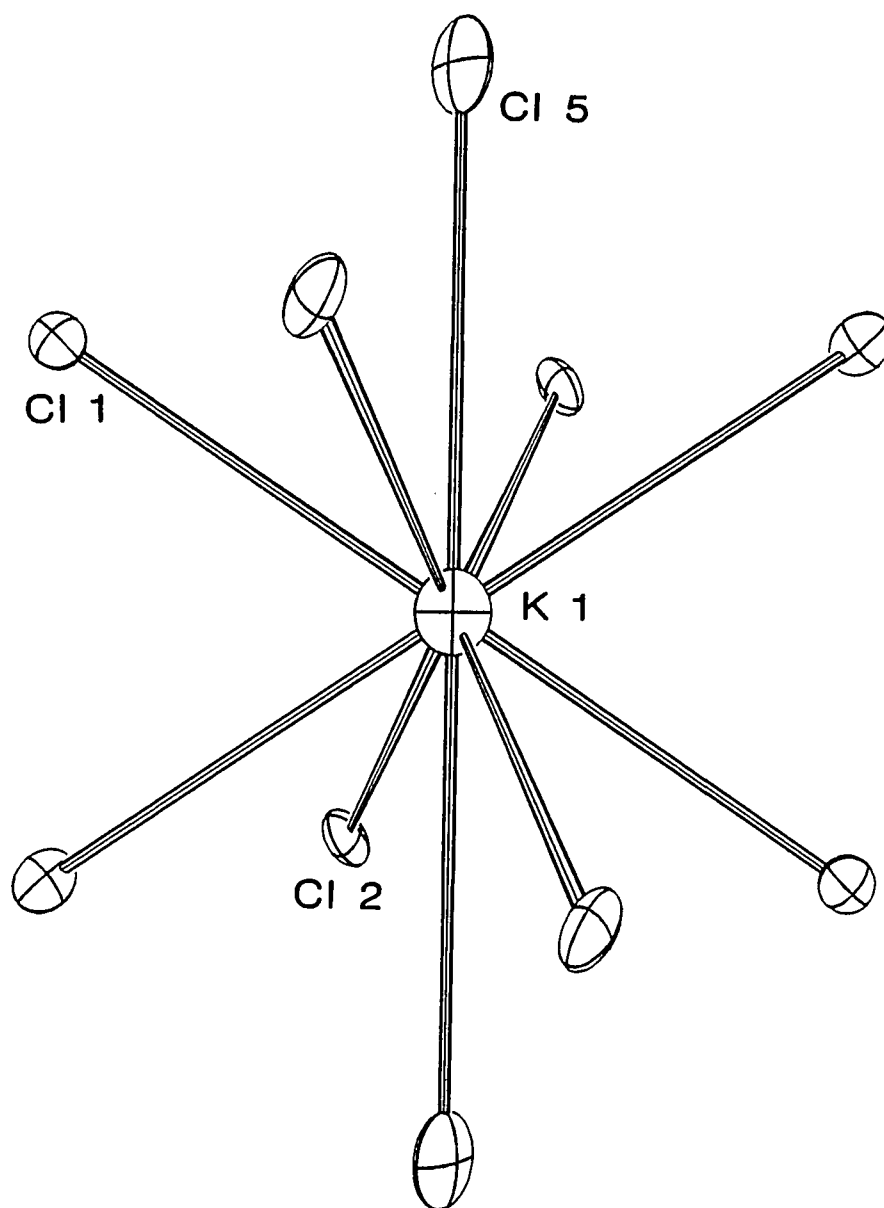


Figure 20. The local chlorine environment around K1 in $K_2Zr_6Cl_{15}B$. The site has 222 symmetry with two-fold axes running vertically and horizontally in the figure and perpendicular to the page. Thermal ellipsoids are drawn at 50% probability

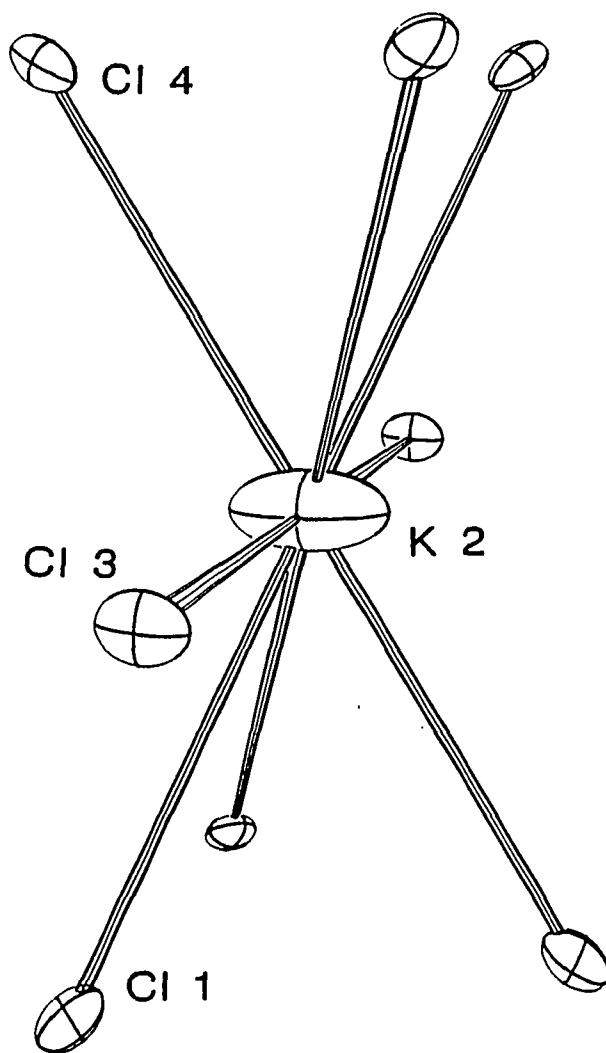


Figure 21. The chlorine environment around K2 in $K_2Zr_6Cl_{15}B$. The site has $2/m$ symmetry with Cl3 and K2 on the axis, and the mirror plane containing Cl4 approximately in the plane of the paper. The site is very similar to the Cs2 site in $CsKZr_6Cl_{15}B$. Thermal ellipsoids are drawn at 50% probability

out opposite faces of the antiprism in the \vec{b} direction, apparently a consequence of the structural framework. The ratios of the principal axes for K2 are 1:5.3:1.7.

The $Zr_6Cl_{12}B$ cluster has crystallographically imposed $2/m (C_{2h})$ symmetry. The two metal triangular faces perpendicular to \vec{a} are nearly equilateral, but have been displaced with respect to one another to give four shorter (3.230 Å) and two longer (3.282 Å) interlayer Zr-Zr distances per cluster. The average Zr-Zr distance of 3.253 Å is typical of boron-centered metal chloride clusters.^{40,134} The calculated effective boride crystal radius, obtained by subtracting the tabulated 0.86 Å value for six-coordinate Zr^{127} from the average Zr-B distance of 2.304 Å, is 1.44 Å.

An alternative approach to the structure of $K_2Zr_6Cl_{15}B$ is to view it as a close-packed array of chlorine layers with an ordered occupancy of octahedral sites between layers by zirconium. The chlorine layers which are clearly visible in Figure 19 stack in the \vec{a} direction. Unlike other structures which have been previously described in terms of the close-packed anion layers,^{15,23,56} the individual layers in $K_2Zr_6Cl_{15}B$ are not close-packed. Rather, two distinct 'modified' close-packed nets are seen in $K_2Zr_6Cl_{15}B$. One net, designated A' and A'', contains all of the K1 and Cl^{a-a} atoms (C15 and C16) and some of the Cl^i atoms and is located at $x = 0$ and $1/2$. The layer is composed of strips of close-packed atoms which come together to form seams of square packing. The arrangement of atoms in A' is projected on $x = 0$ in Figure 22. The A'' layer, at $x = 1/2$, has the same square net seam translated by $\vec{b}/2$.

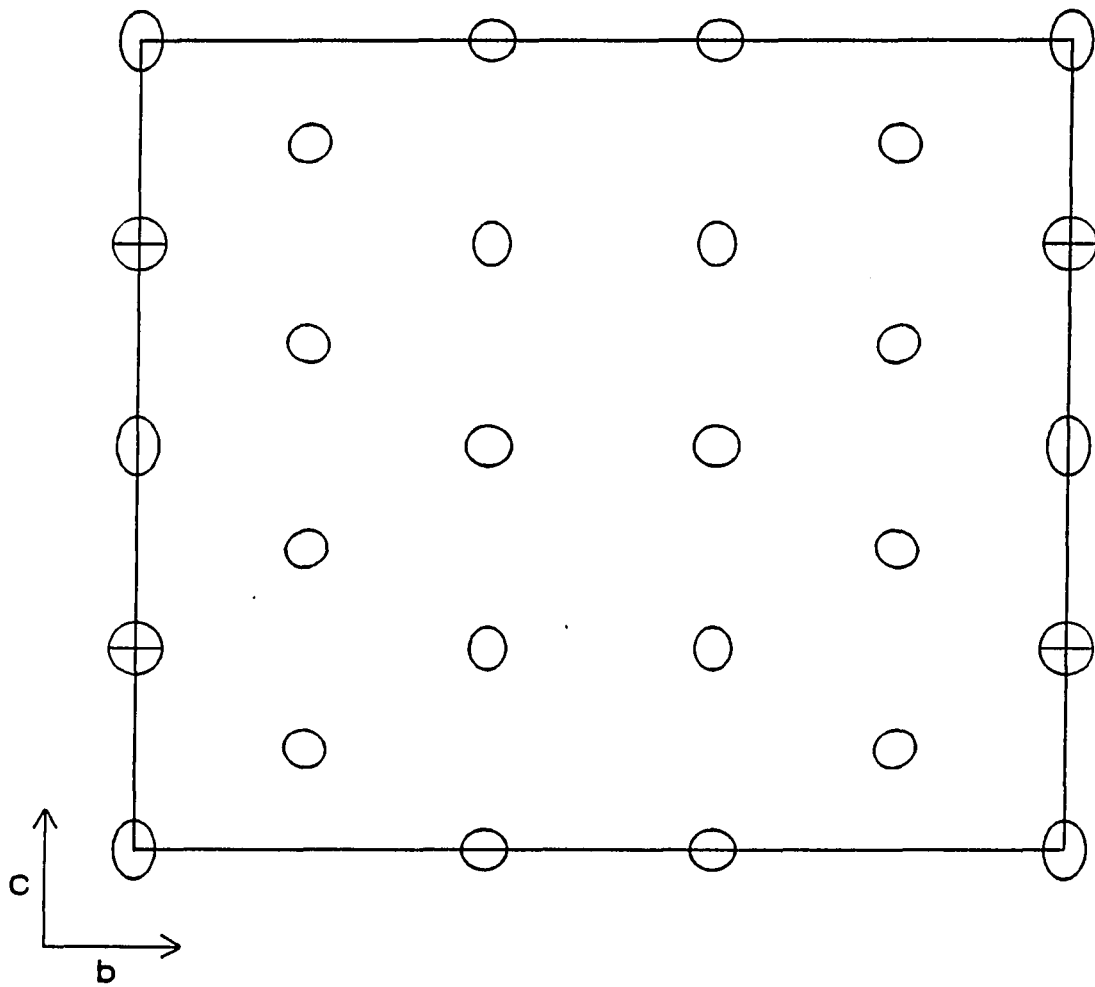


Figure 22. A [100] projection on $x = 0$ of the modified close-packed layer of atoms designated A'. The square net formed where the strips of close-packed atoms come together runs down the center of the projection. The open ellipses are chlorine atoms and the crossed ellipses K1 atoms

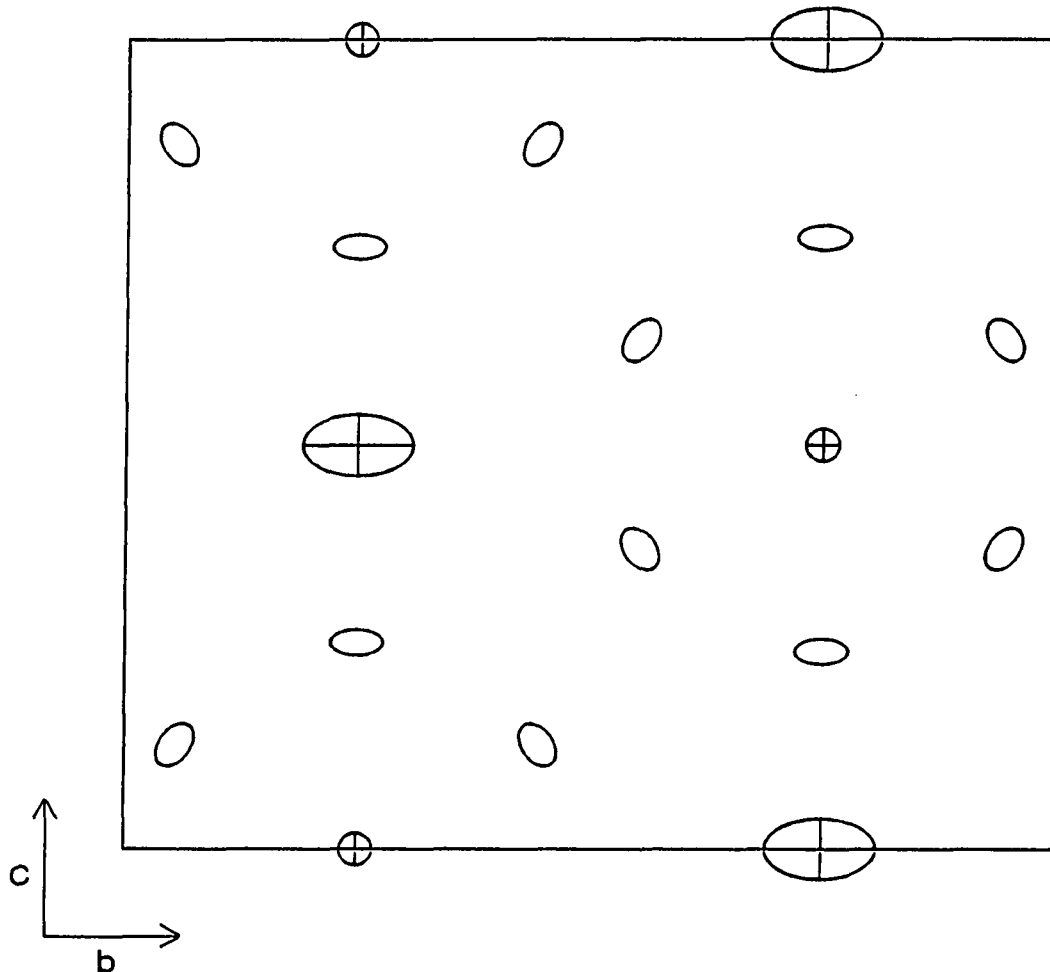


Figure 23. A $[100]$ projection on $x = 1/4$ of the expanded close-packed layer of atoms designated B' . The small and large crossed ellipses are B and K_2 , respectively, and the open ellipses, Cl^I atoms. The expansion of the layer in the b direction is obvious from the four chlorine atoms down the center of the cell ($y = 0.5$) which would lie on a line in a close-packed array

The second modified net designated B' and B'', is positioned at $x = 1/4$ and $3/4$, respectively. The B' net at $x = 1/4$ is projected in Figure 23. The net is a formerly close-packed array of atoms that has been expanded ~25% in the \vec{b} direction to form zig-zag rifts parallel to \vec{c} between the rows of clusters. Formation of the rifts is necessary for the layer to mesh with zones of square packing in the layers above and below. The expansion of the layer in the \vec{b} direction is also responsible for the extended K2 cavity between clusters. As with A' and A'', B' and B'' are related by a translation of $\vec{b}/2$. The stacking of the modified layers in $K_2Zr_6Cl_{15}B$ is ...A'B'A''B''....

The expansion of the individual layers, either by the insertion of square-packed zones or the formation of rifts between rows of clusters, is a compromise between the need to accommodate linear intercluster Cl^{a-a} bridges and to maintain reasonable Zr- Cl^{a-a} distances. As will be seen, room for the second cation is also created in the expansion and appears to be the primary driving force for the formation of the linear intercluster Cl^{a-a} bridges. The connection between linear Cl^{a-a} bridges and cation site formation is described in more detail in the M_6X_{15} Discussion section.

The description of $K_2Zr_6Cl_{15}B$ as a close-packed layering of chlorine atoms provides a convenient way of visualizing the structure and packing, and also allows its relationship to $KZr_6Cl_{14}B$ to be seen more easily. The projection of a layer of clusters in $K_2Zr_6Cl_{15}B$ onto $z = 1/4$, Figure 24, shows a striking resemblance to an analogous projection in $KZr_6Cl_{14}B$ onto $z = 1/2$, Figure 25. The basic arrangement of clusters within the

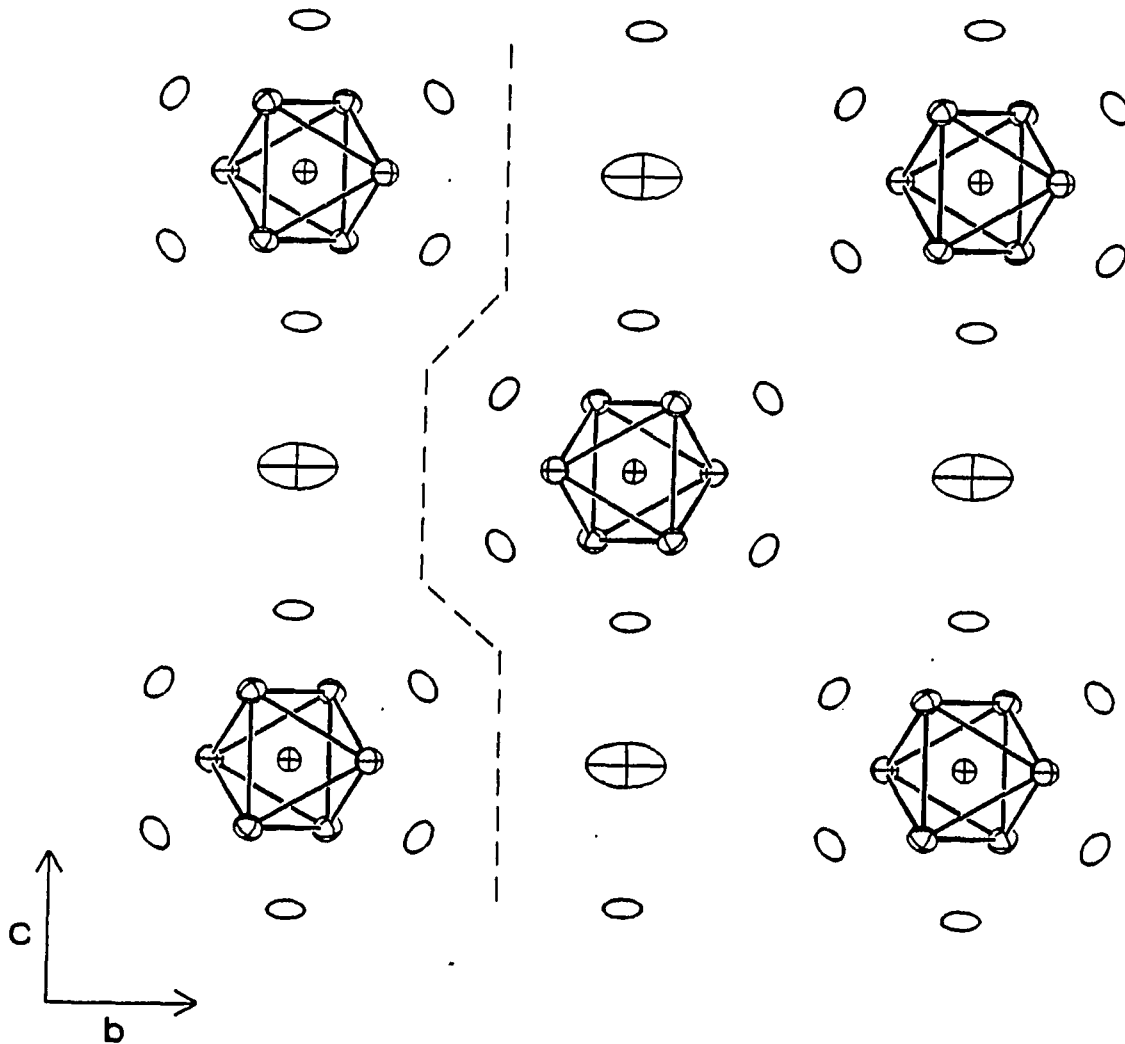


Figure 24. A [100] projection of the cluster layer centered at $x = 1/4$ in $K_2Zr_6Cl_{15}B$. One of the rifts in the close-packed layer caused by the expansion in \vec{b} is marked by the dashed line. Particular attention should be paid to the orientation of the clusters with respect to one another and the elongation of the K2 site in the \vec{b} direction

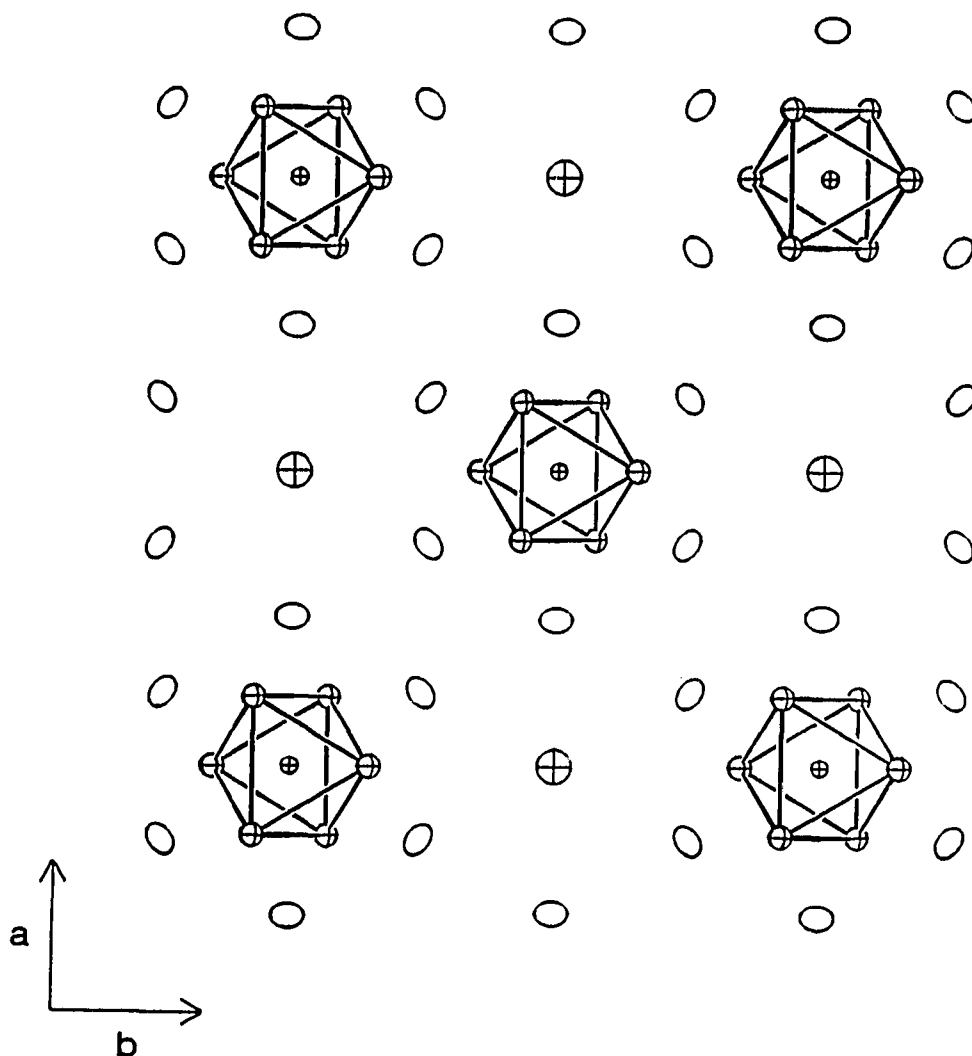


Figure 25. A [001] projection of the clusters and a close-packed layer in $\text{KZr}_6\text{Cl}_{14}\text{B}$ centered at $z = 1/2$. The crossed ellipsoids from largest to smallest mark K, Zr and B, respectively. Note that, unlike $\text{K}_2\text{Zr}_6\text{Cl}_{15}\text{B}$, all clusters are oriented in the same manner

layer in the two compounds is identical, except the clusters in every other row in $K_2Zr_6Cl_{15}B$ have been rotated 180° around an axis perpendicular to the layer. The stacking of the cluster layers is the same in both compounds with the next layer translated by $\vec{b}/2$. The cation position in $KZr_6Cl_{14}B$ also clearly carries over into the K2 site in the $K_2Zr_6Cl_{15}B$ structure. The rifts in the $K_2Zr_6Cl_{15}B$ cluster layer can easily be visualized as a result of an expansion of the $KZr_6Cl_{14}B$ cluster layer. The reorientation of every other row of clusters and the expansion of the cluster layer are both consequences of the replacement of Cl^{a-i} connectivity with linear Cl^{a-a} intercluster connectivity.

The entire process can be understood in terms of the need to create a second cation site on conversion of the $KZr_6Cl_{14}B$ structure to the $K_2Zr_6Cl_{15}B$ structure.

The $K_2Zr_6Cl_{15}B$ structure is also more distantly related to $CsKZr_6Cl_{15}B$.¹³⁴ The transformation of $CsKZr_6Cl_{15}B$ to $K_2Zr_6Cl_{15}B$ involves the linearization of the zig-zag cluster chain (which requires an extensive breaking and reformation of $Zr-Cl^{a-a}$ bonds) and translations of the linear cluster chains in the chain direction. The details of the transformation are somewhat tedious and not particularly educational. Of interest, however, is the transformation of the cation sites from one structure to the other. The Cs1 and Cs2 sites in $CsKZr_6Cl_{15}B$ transform to one equivalent site with Cs2 character that accommodates K2. The K site in $CsKZr_6Cl_{15}B$ carries over largely unchanged. The similarities in the sites can be seen by a comparison of Figures 17 with 21 (Cs2 in

CsKZr₆Cl₁₅B and K2 in K₂Zr₆Cl₁₅B) and Figure 15 with 20 (K in CsKZr₆Cl₁₅B and K1 in K₂Zr₆Cl₁₅B).

The monoclinic structure of K₃Zr₆Cl₁₅Be, shown in Figure 26 looking down the \vec{c} axis, is seen to be directly related to the orthorhombic structure of K₂Zr₆Cl₁₅B. Like K₂Zr₆Cl₁₅B, the structure is composed of a criss-crossing network of linear cluster chains connected into a three-dimensional array by additional bent Cl^{a-a} bridges. Room for a third cation has been created by a small monoclinic distortion of the lattice which splits the former K2 site in K₂Zr₆Cl₁₅B, into two inversion-related sites with no crystallographically imposed symmetry. The details of the monoclinic distortion include a slight displacement of the linear cluster chains with respect to one another in the \vec{b} direction (K₂Zr₆Cl₁₅B axes), a result of the 2.7° increase in the monoclinic angle (α in K₂Zr₆Cl₁₅B), and an approximately 7° rotation of each linear cluster chain around its axis. The chains at $z = 0$ and $z = 1/2$ rotate forward and backwards, respectively, when viewed down \vec{c} . The K1 atoms have been displaced 0.7 Å from what were formerly two-fold axes parallel to \vec{c} in K₂Zr₆Cl₁₅B. The crystallographic \vec{a} and \vec{b} axes in K₂Zr₆Cl₁₅B have been interchanged in K₃Zr₆Cl₁₅Be to be consistent with crystallographic convention (unique monoclinic \vec{b} axis).

Rotation of the cluster chains, while important in the formation of the third cation site, significantly disrupts the pseudo-close-packed anion layers seen in K₂Zr₆Cl₁₅B. The 'layers' in K₃Zr₆Cl₁₅Be, now packed in the \vec{b} direction, are extremely puckered with a peak to valley height of over 1.0 Å. In other words, atoms within a layer deviate from

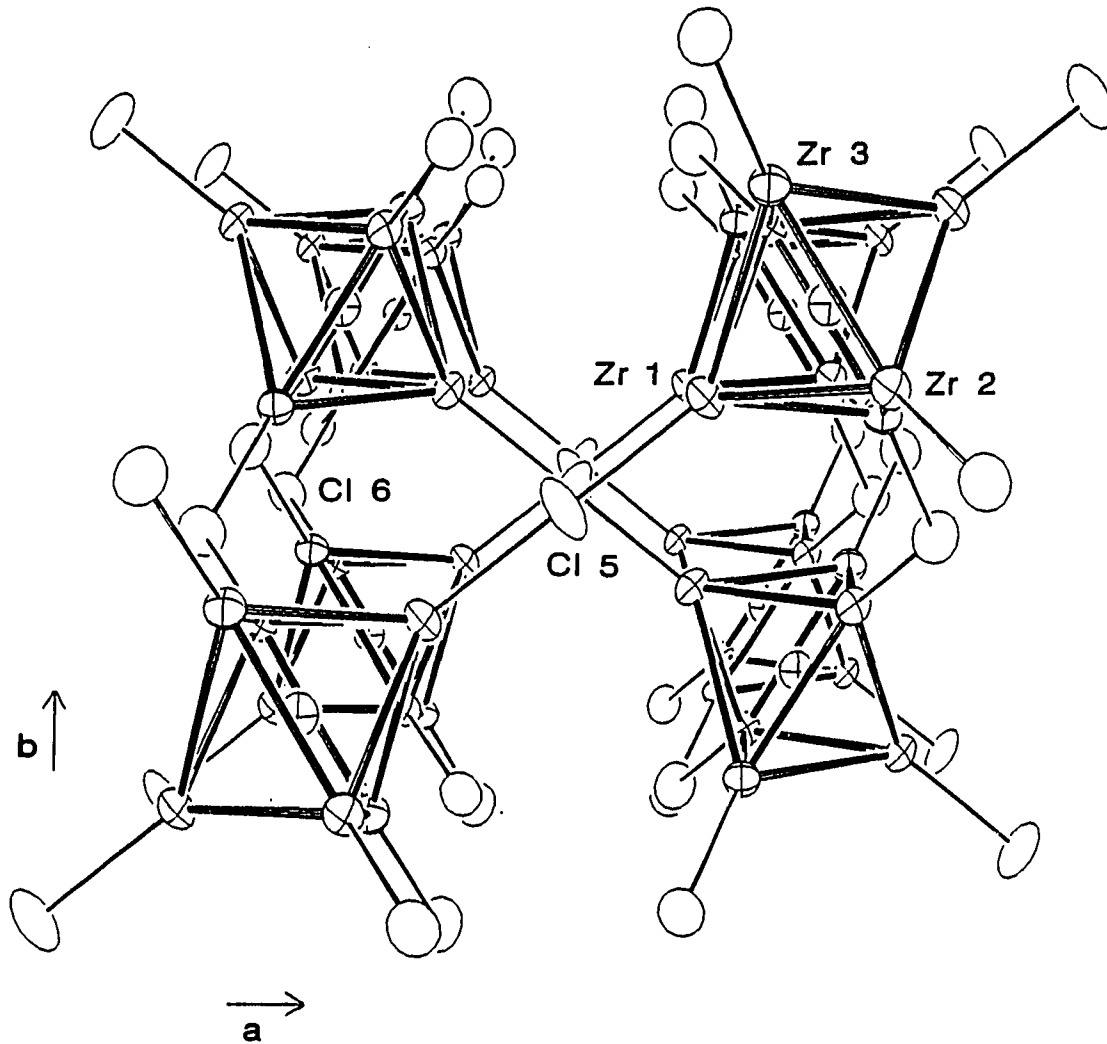


Figure 26. An approximately $[00\bar{1}]$ view of the three-dimensional cluster framework in $K_3Zr_6Cl_{15}Be$. (90% thermal ellipsoids.) The Cl^i and K atoms have been omitted for clarity. The Zr_6 clusters are drawn in heavy lines and are centered by beryllium atoms. Rotation of the cluster chains is particularly evident from the up-down row of $Cl^{a-\bar{a}}$ atoms on the left side of the drawing

Table 28. Bond distances in $K_3Zr_6Cl_{15}Be$ (Å)

Zr-Zr			Zr-Cl^{a-a}		
Zr1-Zr2	(x2) ^a	3.2900(8)	Zr1-Cl5	(x2)	2.6767(6)
Zr1-Zr2	(x2)	3.2948(8)	Zr2-Cl6	(x2)	2.703(1)
Zr1-Zr3	(x2)	3.2895(8)	Zr3-Cl6	(x2)	2.670(2)
Zr1-Zr3	(x2)	3.2923(8)			
Zr2-Zr3	(x2)	3.3155(8)	K-Cl		
Zr2-Zr3	(x2)	3.3158(7)	K1-Cl2	(x2)	3.307(3)
\bar{d}		3.2997	K1-Cl7	(x2)	3.316(2)
Zr-Be			K1-Cl5	(x2)	3.5869(7)
Zr1-Be	(x2)	2.3104(5)	K1-Cl1	(x2)	3.663(2)
Zr2-Be	(x2)	3.3456(5)	K1-Cl8	(x2)	3.665(3)
Zr3-Be	(x2)	3.3435(5)	\bar{d}		3.508
\bar{d}		2.3332	K2-Cl6	(x1)	3.118(2)
Zr-Clⁱ			K2-Cl4	(x1)	3.200(2)
Zr1-Cl7	(x2)	2.554(1)	K2-Cl8	(x1)	3.227(2)
Zr1-Cl8	(x2)	2.562(2)	K2-Cl7	(x1)	3.311(2)
Zr1-Cl1	(x2)	2.566(2)	K2-Cl5	(x1)	3.463(2)
Zr1-Cl2	(x2)	2.582(2)	K2-Cl3	(x1)	3.465(2)
Zr2-Cl3	(x2)	2.555(1)	K2-Cl2	(x1)	3.526(2)
Zr2-Cl4	(x2)	2.575(2)	K2-Cl1	(x1)	3.647(2)
Zr2-Cl7	(x2)	2.601(1)	\bar{d}		3.370
Zr2-Cl8	(x2)	2.602(2)			
Zr3-Cl3	(x2)	2.571(1)			
Zr3-Cl4	(x2)	2.581(2)			
Zr3-Cl2	(x2)	2.607(1)			
Zr3-Cl1	(x2)	2.609(2)			

^aNumber of times the distance occurs per cluster or cation.

the calculated least-squares plane of the layer by over ± 0.5 Å. Interestingly, the monoclinic distortion and cation addition appear to have improved the packing efficiency of the cell. A direct comparison of the cell volumes of $K_2Zr_6Cl_{15}Be$ and $K_3Zr_6Cl_{15}Be$ shows a volume change of only $5.8 \text{ \AA}^3/\text{K atom}$, a value nearly 40% less than that expected based on the molar volume increment of $16 \text{ cm}^3\text{mol}^{-1}$ ($9.6 \text{ \AA}^3/\text{atom}$) derived by Biltz.¹³⁶ The simple comparison is not entirely valid however, because the change from $K_2Zr_6Cl_{15}Be$ to $K_3Zr_6Cl_{15}Be$ involves not only the addition of a third cation, but also a one-electron reduction of the cluster and a concomitant decrease in cluster volume. A rough estimate of the volume change associated with a 13- to 14-electron cluster reduction is 4.4 \AA^3 . (Calculated from a comparison of the volumes of $Zr_6Cl_{14}B$ and $KZr_6Cl_{14}B$, a case where the occupied cation site is nearly the same size as the unoccupied site.) The compensated volume change of $10.2 \text{ \AA}^3/\text{K atom}$ is thus nearly equal to the value predicted and suggests little change in packing efficiency has occurred.

The $Zr_6Cl_{12}Be$ cluster in $K_3Zr_6Cl_{15}Be$ has increased in size over the cluster in $K_2Zr_6Cl_{15}B$ as expected simply on the basis of the encapsulation of the larger beryllide interstitial. The Zr-Zr distances average 3.300 \AA and are comparable with those in other clusters containing beryllium. The average Zr-Be distance is 2.333 \AA . The cluster distortion seen in $K_2Zr_6Cl_{15}B$ has largely disappeared, although a very slight compression of the $Zr_6Cl_{12}Be$ cluster down the linear chain is observed. The slight puckering of the linear cluster chains associated with the

nonlinearity of the Cl^{a-a}-Zr-Interstitial bond angle is also nearly gone. The Cl^{a-a}-Zr1-Be angle is 179.07(2)°.

The K1 site in K₃Zr₆Cl₁₅Be is not significantly different from that found in K₂Zr₆Cl₁₅B. The displacement from the former two-fold axis and the cluster chain rotation has reduced the site symmetry from 222 to 2 (D_{2d} to C₂) and allowed a slight lengthening of six K1-Cl distances and a shortening of four. The local geometry, shown in Figure 27, has changed little from that in K₂Zr₆Cl₁₅B and also shows a strong similarity to the K site in KZr₆Cl₁₅C.¹³⁴

The K2 site, in contrast, is significantly different from the site observed in K₂Zr₆Cl₁₅B. As shown in Figure 28, it is a somewhat irregularly shaped eight-coordinate site with a large open face directed towards the former K2 site. The new site is displaced by ~2.2 Å from the site in K₂Zr₆Cl₁₅B. Pairs of the K2 sites are located between each cluster pair in \vec{c} .

The creation of the new pairs of K2 sites from the K2 site in K₂Zr₆Cl₁₅B is fundamentally linked to the rotation of the cluster chains. The K2 site in K₂Zr₆Cl₁₅B is, as one will recall, an elongated trigonal antiprism with two long trans-edges bridged by additional chlorine atoms (Figure 21). The K2 thermal ellipsoid is elongated in the \vec{b} direction toward the distant Cl2 atoms which form the outer boundaries of the cavity. Rotation of the cluster chains causes a pair of Cl1 atoms in the trigonal antiprism to collapse towards the center of the K2 site. Simultaneously, both ends of the cavity expand outward to form the new K2 sites. The transformation is schematically diagrammed in projection in

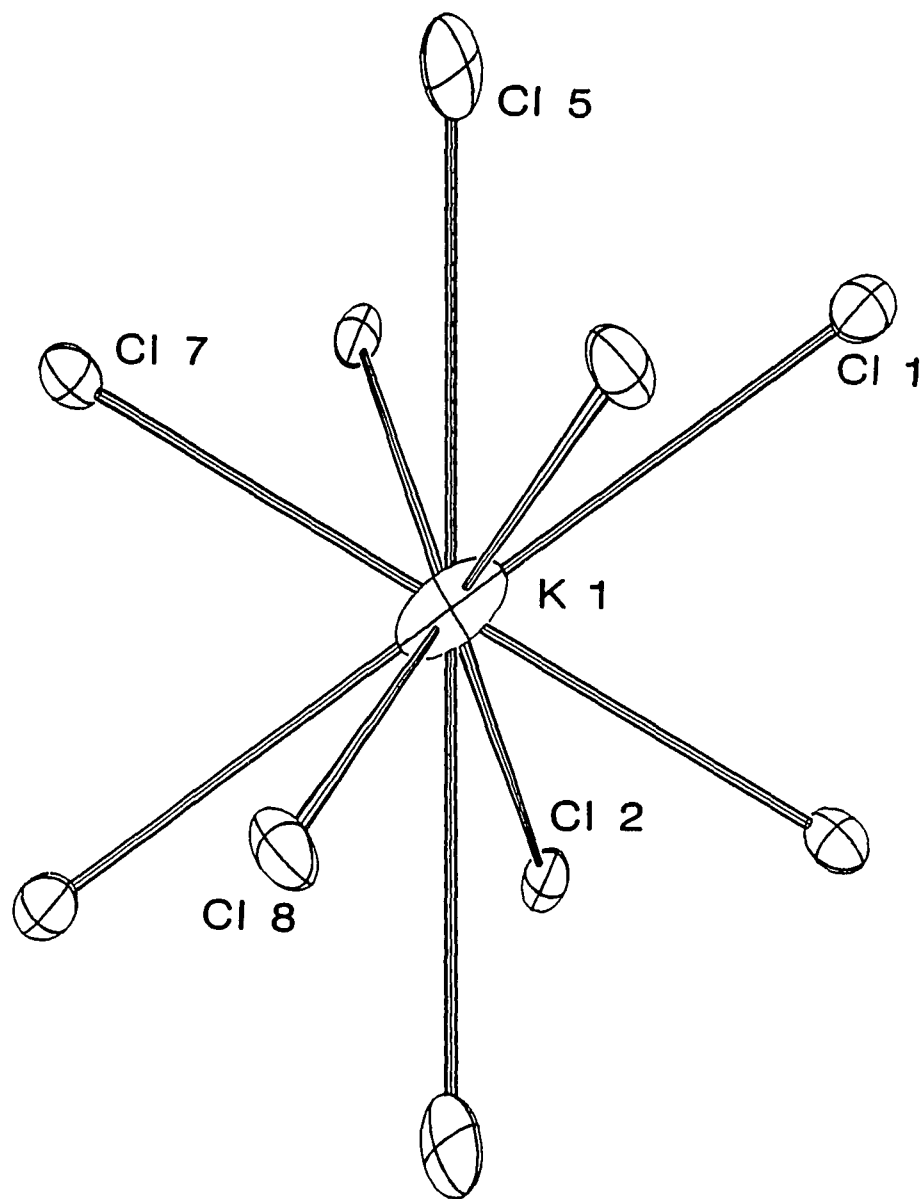


Figure 27. The local chlorine environment around K1 in $K_3Zr_6Cl_{15}Be$ viewed along the two-fold axis. Thermal ellipsoids are drawn at 50% probability

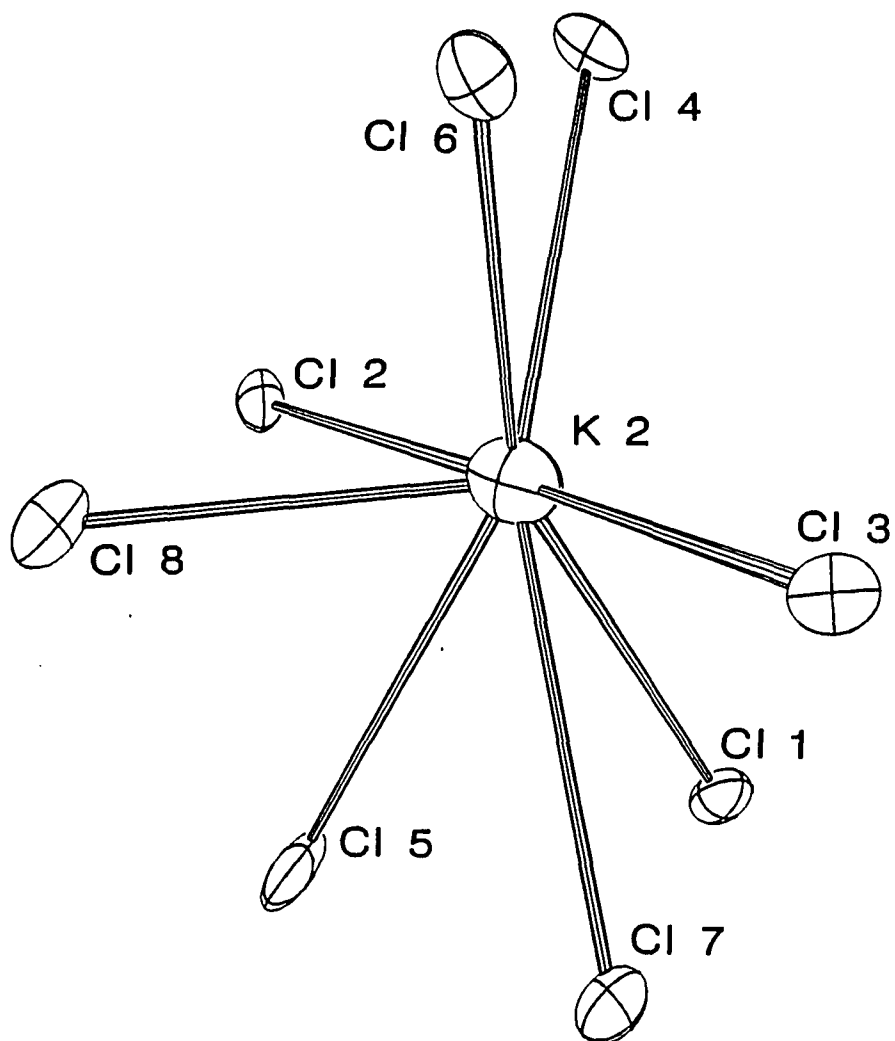


Figure 28. The eight-coordinate K2 site in $K_3Zr_6Cl_{15}Be$. The large open face defined by chlorine atoms 1, 3 and 4 is directed towards the former K2 site in $K_2Zr_6Cl_{15}B$ and, beyond, an inversion-related K2 site. Thermal ellipsoids are drawn at 50% probability

Figure 29. Interestingly, the diagram appears to show a second energy equivalent distortion, a mirror image of the first with chain rotations in the opposite directions. The new K2 sites from the second distortion are shown as the set of small circles in Figure 29. The space group symmetry, however, is inconsistent with the formation of $K_3Zr_6Cl_{15}Be$ enantiomers, and a closer examination shows the second distortion is identical to the first by a two-fold rotation.

M_6X_{15} Discussion

The interrelationships among the four distinct and structurally characterized M_6X_{15} frameworks, i.e., the Ta_6Cl_{15} ,⁴ $CsNb_6Cl_{15}$,^{72,134} $K_2Zr_6Cl_{15}B$ and Nb_6F_{15} ⁵ structure types, and the factors which govern their formation are not always readily apparent. The ability to prepare all four structure types and variations thereon in a single system, namely the zirconium chlorides, has however, helped to elucidate some of these interrelationships and formation factors. Although all of the known M_6X_{15} compounds have the same style of local connectivity, $[M_6X_{12}^i]X_{6/2}^{a-a}$, major structural differences appear in the larger three-dimensional cluster connectivity, the local Cl^{a-a} geometry and, of course, the lattice symmetry. These details are summarized later in Table 29.

When viewed as a continuum, the M_6X_{15} structure types create a nicely defined series whose members are differentiated by their local Cl^{a-a} geometry. The Ta_6Cl_{15} structure,⁴ which includes the relevant $Zr_6Cl_{15}N$, $Na_{0.5}Zr_6Cl_{15}C$ and the slightly distorted $Na_2Zr_6Cl_{15}B$ examples,⁶⁰ occurs at one end of the series and has only bent X^{a-a}

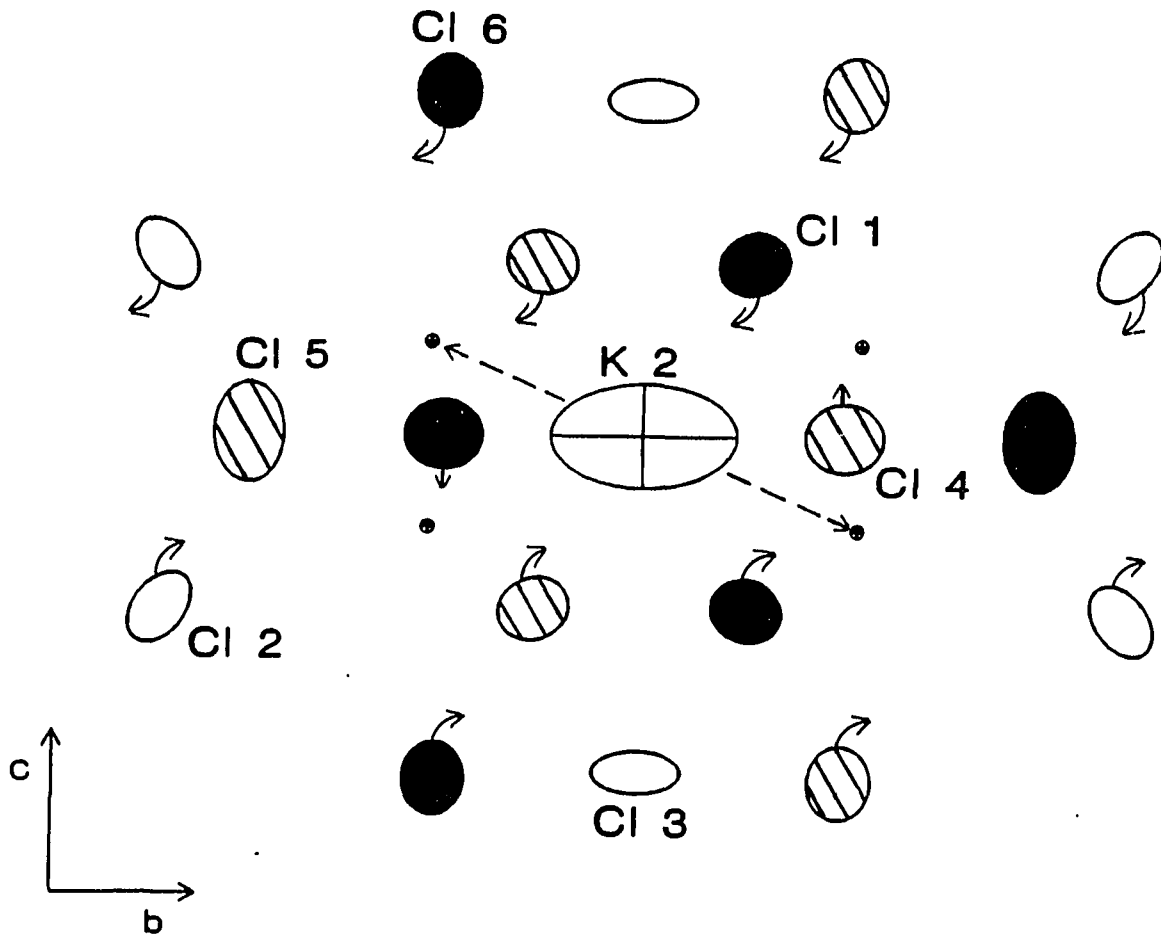


Figure 29. A [100] projection of the K2 site in $K_2Zr_6Cl_{15}B$ and the atomic displacements associated with the distortion of the site that occur during the conversion to $K_3Zr_6Cl_{15}Be$. The dotted line indicates the directions of K2 motion and the small circles, the final site. \odot $y \approx 1/2$, \circ $y \approx 1/4$, \bullet $y \approx 0$. Arrows curved to the right indicate movement up and arrows curved to the left, movement down. A two-fold axis lies parallel to c

bridges joining clusters, while Nb_6F_{15} ⁵ and the recently prepared isostructural $\text{Zr}_6\text{Cl}_{15}\text{Co}^{63}$ are at the opposite end and contain only linear $\text{X}^{\text{a-a}}$ bridges. The other M_6X_{15} structure types exhibit intermediate combinations of bent and linear $\text{X}^{\text{a-a}}$ bridges; $\text{CsNb}_6\text{Cl}_{15}$, $\text{KZr}_6\text{Cl}_{15}\text{C}$, $\text{CsKZr}_6\text{Cl}_{15}\text{B}$ and the like (Table 17) have one-sixth linear $\text{X}^{\text{a-a}}$ bridges, the remainder bent,^{72,134} and the other two $\text{M}_6\text{X}_{12}\text{X}^{\text{a-a}}_{6/2}$ type structures, $\text{K}_2\text{Zr}_6\text{Cl}_{15}\text{B}$ and $\text{K}_3\text{Zr}_6\text{Cl}_{15}\text{Be}$, both show one-third linear bridges. Compounds with larger percentages of linear $\text{X}^{\text{a-a}}$ bridges have probably not been observed because of the packing inefficiencies associated with the linear bridges. The presence of more and larger cations may be able to circumvent this problem.

The need to accommodate a specific number of cations to obtain a preferred electronic state of the cluster and the sizes of the cations are both important factors in differentiating the formation of the various structure types. In general, the introduction of linear $\text{X}^{\text{a-a}}$ bridges tends to create larger voids within the structure and consequently room for more or larger cations.¹³⁴ The trend is nicely illustrated going from $\text{Ta}_6\text{Cl}_{15}$ with no linear bridges, to $\text{CsKZr}_6\text{Cl}_{15}\text{B}$ with one-sixth linear bridges, to $\text{K}_3\text{Zr}_6\text{Cl}_{15}\text{Be}$ with one-third linear bridges, and finally to Nb_6F_{15} with all linear bridges. The $\text{Ta}_6\text{Cl}_{15}$ structure presently appears to be limited either to compounds with no cations, such as $\text{Ta}_6\text{Cl}_{15}$ ⁴ and $\text{Zr}_6\text{Cl}_{15}\text{N}$,⁶⁰ or to those compounds that contain small cations, $\text{Na}_{0.5}\text{Zr}_6\text{Cl}_{15}$ ⁶⁰ and $\text{Na}_x\text{Nb}_6\text{Cl}_{15}$ ($x < 1$)⁷² being examples. In contrast, the $\text{CsNb}_6\text{Cl}_{15}$ structure has been obtained only in compounds

containing one cation as large as potassium or, if with two cations, one at least as large as rubidium.^{72,134} The $K_3Zr_6Cl_{15}Be$ structure with one-third linear χ^{a-a} bridges has been found only for compounds that contained three potassium or rubidium cations. Finally, in Nb_6F_{15} the voids created by the linear χ^{a-a} bridges have become so large that it is possible/necessary to fill these with a second interpenetrating lattice of Nb_6F_{15} clusters.

The factors that differentiate the formation of the Ta_6Cl_{15} and Nb_6F_{15} structures are more subtle. The only important difference between $Zr_6Cl_{15}N$ and $Zr_6Cl_{15}Co^{63}$ in the Ta_6Cl_{15} and Nb_6F_{15} structures, respectively, is the size of the interstitial atom, and hence, the proximity of the zirconium atoms to the square faces of the cuboctahedron formed by the twelve edge-bridging Cl^i atoms. The change in the metal atom position suggests the formation of the two structures is probably determined by small differences in bonding and packing efficiencies, with the more ideal clusters, i.e., those with the M atoms nearest the faces formed by the Cl^i atoms, adopting the Nb_6F_{15} structure. The importance of having the M atom near the face is that it allows a reasonable $M-Cl^{a-a}$ bond distance to be maintained while leaving adequate room for the second interpenetrating lattice.

Although exhibiting the same local connectivity around each cluster, the structural frameworks of Ta_6Cl_{15} , $CsNb_6Cl_{15}$, $K_2Zr_6Cl_{15}B$ and Nb_6F_{15} , are not related to one another in a larger three-dimensional sense. In other words, none of the four structural frameworks can be interconverted simply by rotation of clusters and bending at bridging chlorine atoms,

i.e., without breaking $M-X^{a-a}$ bonds. The inequivalence of the structures can be seen by examining them in light of two criteria, namely: 1) whether or not any of the six clusters connected to a central cluster are directly interconnected through an X^{a-a} atom, and 2) after choosing one of the six clusters connected to a central cluster, how many of the other five are indirectly linked to it through one additional cluster excluding of course, the central cluster which indirectly interconnects all six. The first criterion conveniently separates the $CsNb_6Cl_{15}$ structure which has directly connected clusters linked to a common central cluster from the rest of the structure types. Described somewhat differently, but none the less equivalently, the shortest bonding path through the $CsNb_6Cl_{15}$ structure back to a starting point without retracing, is $(M-M-Cl^{a-a})_3$.¹³⁴ Such a path is easily seen for $KZr_6Cl_{15}C$ in Figure 14. In all of the other M_6X_{15} structure types the shortest path is $(M-M-Cl^{a-a})_4$, i.e., none of the clusters linked to a common central cluster is directly connected to one-another. The Nb_6F_{15} structure can be separated from the rest by recognizing its structural framework is actually two interpenetrating lattices. The inequivalence of the remaining two structures, Ta_6Cl_{15} and $K_2Zr_6Cl_{15}B$, requires the use of the second, more complicated criterion which is concerned with the indirect interconnectivity of the six clusters joined to a common central cluster. Starting with one of the six first bonding sphere (FBS) clusters, the distinguishing feature is the number of the other FBS clusters that are connected to the first through one additional external cluster. Because all of the clusters in these structures are equivalent

by symmetry, the cluster chosen as the central cluster is immaterial. The concept is illustrated in Figure 30 which shows a schematic representation of the connectivity in one of the interpenetrating lattices in Nb_6F_{15} . The common central cluster is the solid black ellipsoid and the first bonding sphere of clusters are the ellipsoids labeled one through six. Choosing cluster 1, it is quickly evident it can be indirectly connected through one cross-hatched cluster to clusters 2, 3, 4 and 5 which are all directly connected to the black central cluster. In other words, each FBS cluster is indirectly connected through one additional cluster to four other FBS clusters. The idea can also be expressed in terms of circular bonding paths through the structure, specifically; starting at a FBS cluster, how many of the other five FBS clusters can be included in $(\text{M}-\text{M}-\text{X}^{\text{a-a}})_4$ rings which include the central cluster. Using the schematic of the connectivity in the $\text{Ta}_6\text{Cl}_{15}$ structure in Figure 31, one finds that each cluster in the first bonding sphere is indirectly connected through one other cluster to two other FBS clusters. The situation in $\text{K}_2\text{Zr}_6\text{Cl}_{15}\text{B}$ is slightly different. Here one finds the number of clusters indirectly connected is dependent on whether the chosen cluster is connected to the central cluster through a linear $\text{Cl}^{\text{a-a}}$ bridge or a bent bridge. The schematic of the connectivity in $\text{K}_2\text{Zr}_6\text{Cl}_{15}\text{B}$ is illustrated in Figure 32. Clusters linearly bridged to the central cluster are indirectly connected to two other FBS clusters, while clusters connected through a bent $\text{Cl}^{\text{a-a}}$ bridge are indirectly joined to three others. Results are summarized in Table 29. The second criterion not only shows the inequivalence of the $\text{Ta}_6\text{Cl}_{15}$ and $\text{K}_2\text{Zr}_6\text{Cl}_{15}\text{B}$

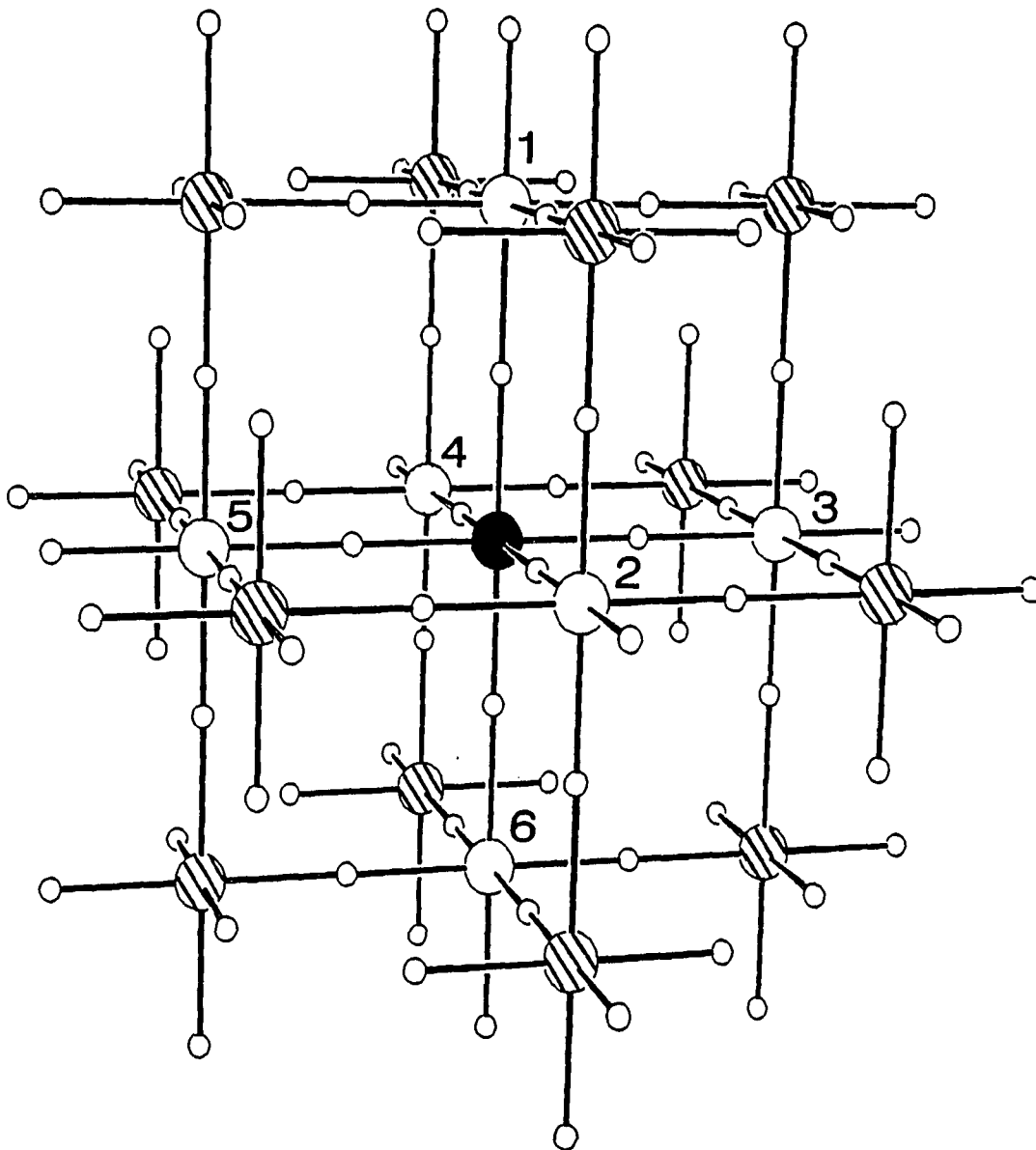


Figure 30. A schematic representation of the cluster connectivity in one of the interpenetrating lattices in Nb_6F_{15} . The large filled ellipsoid represents the central Nb_6F_{15} cluster, and small spheres, bridging $\text{F}^{\text{a-a}}$ atoms. First bonding sphere (FBS) clusters are represented by the large open spheres labeled 1-6, and the cross-hatched spheres indirectly connect FBS clusters

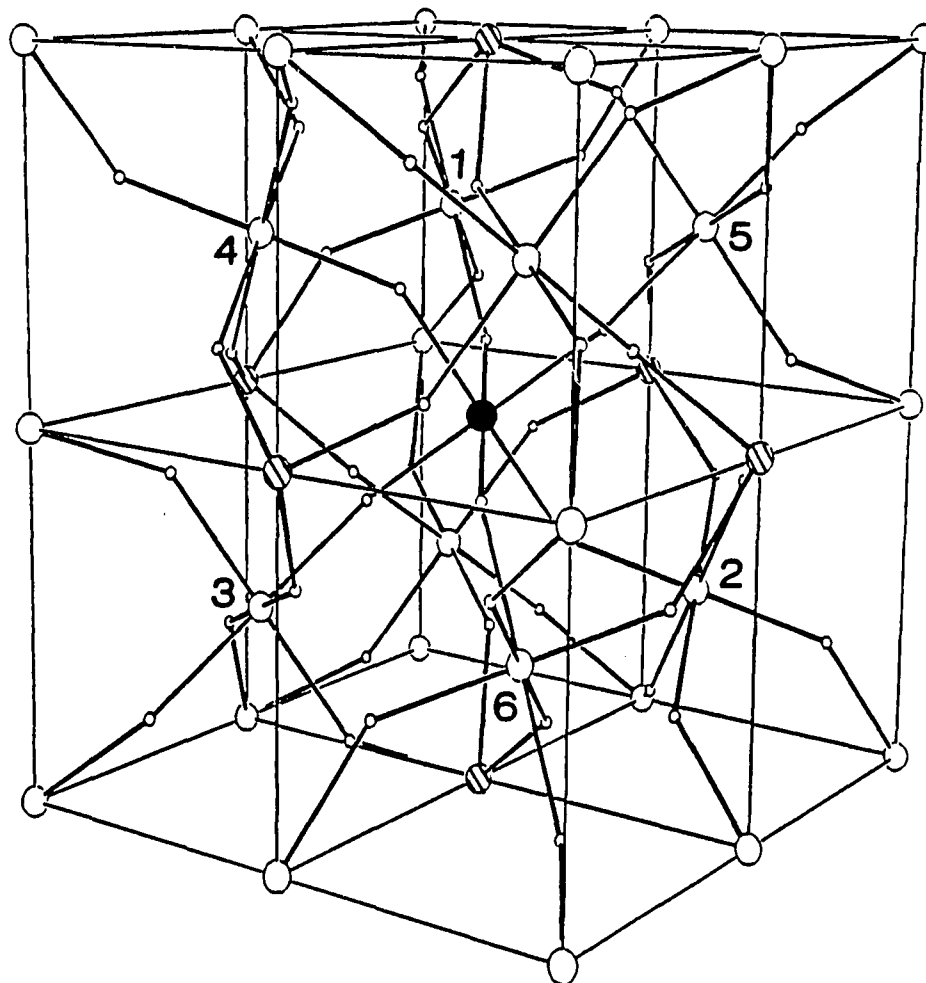


Figure 31. A schematic representation of the three-dimensional cluster connectivity in the Ta_6Cl_{15} structure. Large and small spheres represent M_6X_{12} clusters and Cl^{a-a} atoms, respectively. The numbered open spheres are first bonding sphere clusters about the central black sphere. Cross-hatched spheres are involved in indirect coupling of the FBS clusters

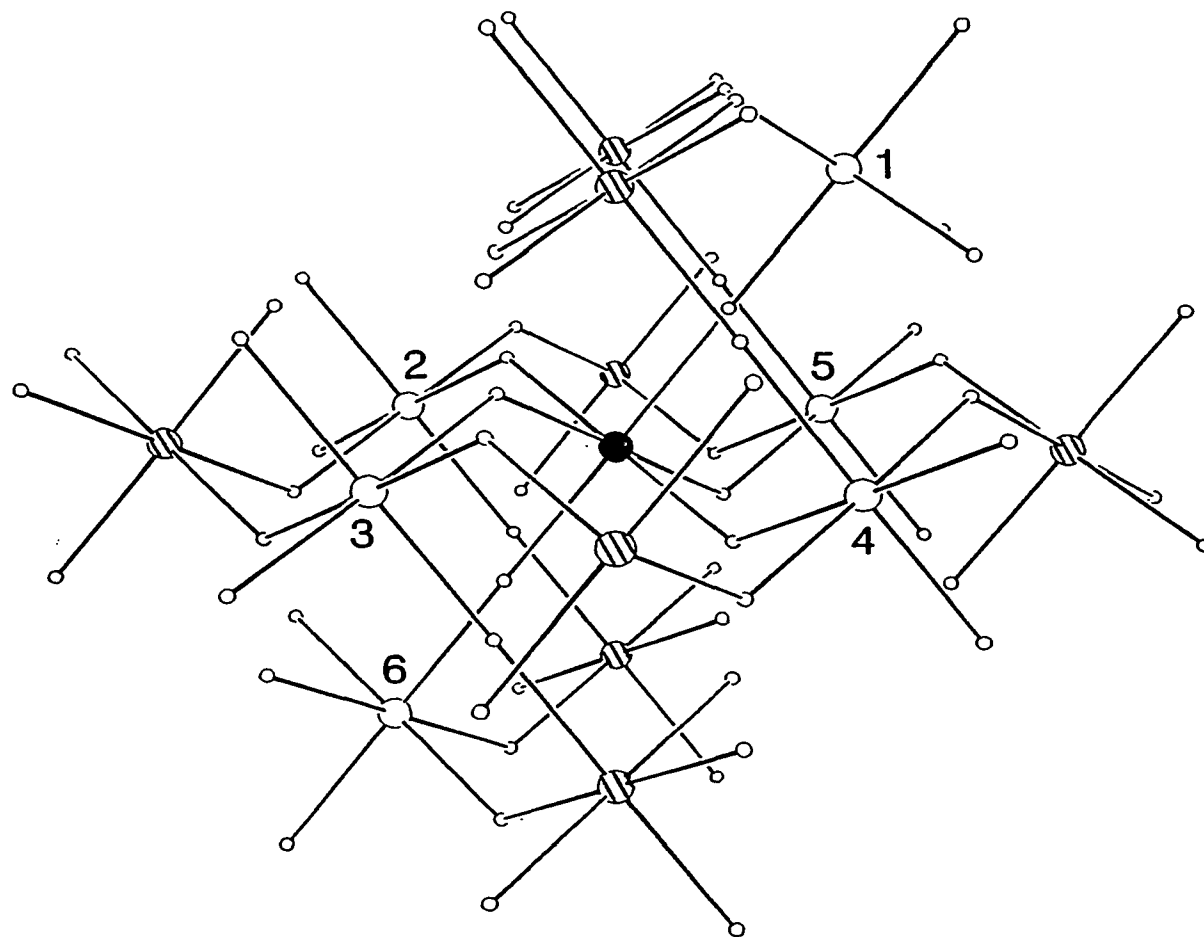


Figure 32. A schematic representation of the cluster connectivity in $K_2Zr_6Cl_{15}B$. Large spheres represent $Zr_6Cl_{12}B$ clusters while small spheres are bridging Cl^{a-a} atoms. Open ellipsoids are first bonding sphere clusters about the solid central cluster. Cross-hatched ellipsoids indirectly connect FBS clusters

Table 29. Distribution of X^{a-a} bridges in M₆X₁₂X_{6/2}-type structures

Structure type	Space group	X ^{a-a} bridge type, %		FBS ^a clusters directly linked ^b	Number of FBS ^a clusters indirectly linked ^c
		linear	bent		
Ta ₆ Cl ₁₅	Ia3d	0	100	no	2
CsNb ₆ Cl ₁₅	Pmma	17	83	yes	-
K ₂ Zr ₆ Cl ₁₅ B	Cccm	33	67	no	2,3
K ₃ Zr ₆ Cl ₁₅ Be	C2/c	33	67	no	2,3
Nb ₆ F ₁₅	Im3m	100	0	no	4

^aFirst bonding sphere (FBS) - see text.

^bCriterion 1 - see text.

^cCriterion 2 - see text.

structures, but also shows their inequivalence to the interpenetrating networks in Nb_6F_{15} . The fifth structure type, $\text{K}_3\text{Zr}_6\text{Cl}_{15}\text{Be}$, has already been described as equivalent to the $\text{K}_2\text{Zr}_6\text{Cl}_{15}\text{B}$ structure through cluster rotations without bond breakage. The results clearly illustrate the inadequacy of both a simple $[\text{M}_6\text{X}_{12}^i]\text{X}_{6/2}^{a-a}$ structural description and the view that all M_6X_{15} compounds are simply another folding of the same three-dimensional cluster net around an array of cations. The findings also serve to illuminate the richness and elegance of the structural chemistry of the M_6X_{15} compounds.

M_6X_{16}

A variety of M_6X_{12} cluster compounds have been prepared over the past twenty years with M_6X_{12} to M_6X_{15} stoichiometries.^{4-6,14} All of the cluster compounds, other than those with the unusual $\text{KZr}_6\text{Cl}_{13}\text{Be}$ structure,⁶⁰ are built upon various combination of X^{a-i} and X^{a-a} connectivities between clusters. M_6X_{15} terminated the series with all X^{a-a} intercluster connectivity. Extension of the series to larger X:M ratios by the incorporation of unshared terminal X^a atoms has been realized only in the $[\text{M}_6\text{X}_{12}^i]\text{X}_6^a$ case, where a number of niobium chloride and bromide clusters have been prepared.^{2,3,137} Intermediate compositions, i.e., $[\text{M}_6\text{X}_{12}]\text{X}_4$ and $[\text{M}_6\text{X}_{12}]\text{X}_5$, with combinations of X^{a-a} connectivity and X^a atoms have not been previously observed. The analogous compounds composed of M_6X_8 clusters, namely $[\text{M}_6\text{X}_8]\text{X}_4$ and $[\text{M}_6\text{X}_8]\text{X}_5$, have been prepared. $[\text{Mo}_6\text{X}_8]\text{X}_4$ ($\text{X} = \text{Cl}, \text{Br}, \text{I}$),¹³⁸ has been known since the late 1960s, and more recently, a variety of molybdenum

and rhenium M_6X_8 clusters have been prepared with the $[M_6X_8]X_4$ and $[M_6X_8]X_5$ stoichiometries.^{139,140}

The apparent stability of $Zr_6Cl_{12}Z$ clusters with 14 cluster-bonding electrons and the relative ease with which many second period elements can be incorporated into the Zr_6Cl_{12} cluster, suggested that compounds within the M_6X_{15} to M_6X_{18} sequence might be prepared by appropriate choices of interstitial atoms in concert with the number of cations. Although the oxide, $Zr_6Cl_{16}O$, appears to be an obvious target, the stability of $ZrClO_x$ ($0 \leq x \leq 0.43$)⁵² even under oxidizing conditions seems to preclude cluster formation. As is often the case in synthetic chemistry, the first $[M_6X_{12}]X_4$ compound, $Na_{3.9}Zr_6Cl_{16}Be$, was prepared by accident. The second, $Cs_{3.0}Zr_6Cl_{16}C$, was more by design, while $Cs_3Zr_6Cl_{16}B$ and $Cs_4Zr_6Cl_{16}Be$ were prepared as planned.

Synthesis

$Na_{3.9}Zr_6Cl_{16}Be$ was initially prepared in a reaction designed for the preparation of $Na_3Zr_6Cl_{15}Be$. The recently completed crystal structure of $Na_{0.5}Zr_6Cl_{15}C$ had located the sodium cations in a partially occupied 48-fold site in the chlorine lattice. Complete occupation of the site (3 cations per cluster) coupled with an interstitial atom to give 14 cluster-bonding electrons suggested $Na_3Zr_6Cl_{15}Be$ might be prepared in the Ta_6Cl_{15} structure⁴ or a distorted version thereof (see $Na_2Zr_6Cl_{15}B$). The initial reactions, loaded with stoichiometric amounts of Zr powder, $ZrCl_4$, NaCl and Be flakes plus a 40% excess of NaCl, produced a nearly quantitative yield of the new compound $Na_{3.9}Zr_6Cl_{16}Be$ after two weeks at 800°C. Incidentally, the 40% excess of NaCl gave a

stoichiometry of $\text{Na}_{4.2}\text{Zr}_6\text{Cl}_{16.2}\text{Be}$. Reactions loaded for the composition $\text{Na}_4\text{Zr}_6\text{Cl}_{16}\text{Be}$ produce the desired compound at 800°C in 95% yield as dark red, rectangular parallelepipeds. The original compound sought, $\text{Na}_3\text{Zr}_6\text{Cl}_{15}\text{Be}$, has not been prepared. Reactions with stoichiometric compositions of Zr powder, ZrCl_4 , NaCl and Be yield mixtures of $\text{Zr}_6\text{Cl}_{12}\text{Be}$ and $\text{Na}_{3.9}\text{Zr}_6\text{Cl}_{16}\text{Be}$ at $800\text{--}850^\circ\text{C}$.

The ion exchange product of $\text{Na}_{3.9}\text{Zr}_6\text{Cl}_{16}\text{Be}$ with KAlCl_4 at 300°C is believed to be a $\text{K}_x\text{Zr}_6\text{Cl}_{16}\text{Be}$ compound with a more puckered cluster sheet than $\text{Na}_{3.9}\text{Zr}_6\text{Cl}_{16}\text{Be}$, but it has not been characterized.

$\text{Cs}_{3.0}\text{Zr}_6\text{Cl}_{16}\text{C}$ was obtained as a dark brown, highly crystalline material from a reaction to prepare $\text{Cs}_3\text{Zr}_6\text{Cl}_{15}\text{C}$ using stoichiometric quantities of Zr powder, ZrCl_4 , CsCl and graphite at 850°C . The reaction stoichiometry was prompted by similar reactions with other alkali metal halides ($\text{M}^{\text{I}} = \text{Na}, \text{K}, \text{Rb}$) which had yielded compounds of unknown composition and structure. Unfortunately, crystal intergrowth and twinning problems had prevented a satisfactory structural solution for these new compounds. It was hoped that a larger cation might reduce the problems associated with single crystal growth. The cesium containing compound prepared, although not isostructural with the products from the other $\text{M}^{\text{I}}\text{Cl}$ ($\text{M}^{\text{I}} = \text{Na}, \text{K}, \text{Rb}$) reactions, was also new from a structural and compositional viewpoint. The reducing conditions produced by the chlorine-poor stoichiometry appear to be important in preparing the 15-electron cluster $\text{Cs}_{3.0}\text{Zr}_6\text{Cl}_{16}\text{C}$. A reaction with approximately 5% more ZrCl_4 produced a mixture of the 14-electron cluster $\text{CsZr}_6\text{Cl}_{15}\text{C}$ and Cs_2ZrCl_6 . Indeed, two more attempts were required to prepare a second

sample of $\text{Cs}_{3.0}\text{Zr}_6\text{Cl}_{16}\text{C}$. The second 'failure', which contained small excesses (<5%) of CsCl and ZrCl_4 over the $\text{Cs}_3\text{Zr}_6\text{Cl}_{15}\text{C}$ stoichiometry, produced an unidentified compound with a cell volume slightly less than twice that of $\text{Cs}_{3.0}\text{Zr}_6\text{Cl}_{16}\text{C}$ in more than 90% yield. Several nice single crystals were obtained. The structure, which presumably contains eight cluster units per cell, has not been solved, although data have been collected.¹⁴¹ $\text{Cs}_{3.0}\text{Zr}_6\text{Cl}_{16}\text{C}$ was finally prepared again from a reaction utilizing stoichiometric amounts of reactants for the composition $\text{Cs}_3\text{Zr}_6\text{Cl}_{15}\text{C}$. The other more reduced product was not identified.

Two additional compounds, identified by Guinier powder diffraction as being isostructural with $\text{Cs}_{3.0}\text{Zr}_6\text{Cl}_{16}\text{C}$, have also been prepared. $\text{Cs}_3\text{Zr}_6\text{Cl}_{16}\text{B}$ was prepared in greater than 90% yield from a reaction with appropriate amounts of Zr powder, ZrCl_4 , CsCl and amorphous boron powder to give the composition $\text{Cs}_3\text{Zr}_6\text{Cl}_{15}\text{B}$. As was observed for the carbide $\text{Cs}_{3.0}\text{Zr}_6\text{Cl}_{16}\text{C}$, more oxidizing reaction conditions yield a different compound which, in this case, is also unknown and different from the unknown carbide. $\text{Cs}_4\text{Zr}_6\text{Cl}_{16}\text{Be}$ was obtained in about 90% yield from a stoichiometrically loaded reaction heated at 850°C for 2 weeks. A small amount of Cs_2ZrCl_6 was also observed in the powder diffraction pattern of the product. The exact cesium content of the boride and beryllide compounds is not known, but is crystallographically limited to four cesium atoms per cluster. The preferred electronic configuration containing 14 cluster-bonding electrons suggested the given compositions of $\text{Cs}_3\text{Zr}_6\text{Cl}_{16}\text{B}$ and $\text{Cs}_4\text{Zr}_6\text{Cl}_{16}\text{Be}$. Additional work in these systems will be necessary to

determine the actual compositions of the boride and beryllide and the nature of the unknown compounds prepared.

Crystallography

Two octants of data were collected on a small, dark red, rectangular prism of $\text{Na}_{3.9}\text{Zr}_6\text{Cl}_{16}\text{Be}$ using monochromatic Mo $K\alpha$ radiation. The orthorhombic unit cell, chosen on the basis of a small set of reflections indexed with the program BLIND,¹²⁶ was verified by axial photographs taken on the diffractometer which showed the expected layer spacings and mirror symmetry. The minimal absorption effects were correct for using a ψ -scan method. Details of the data collection and refinement are given in Table 30.

The space group Pccn was chosen for $\text{Na}_{3.9}\text{Zr}_6\text{Cl}_{16}\text{Be}$ on the basis of the observed systematic extinctions and verified by the subsequently successful refinement of the structure in it. The structure was solved by direct methods using the program MULTAN-80.⁹⁵ Four randomly oriented, octahedral zirconium clusters were included as 'molecular fragments' in the normalization routine. Three zirconium positions identified with the aid of MULTAN-80, were used to phase a subsequent Fourier map from which the majority of the chlorine atoms in the structure were identified. Successive cycles of least-squares refinement and Fourier map synthesis were used to locate the remaining atoms. The interstitial beryllium atom was observed as an approximately 3-electron residual in the cluster center following isotropic refinement of the zirconium and chlorine atoms in the structure. The data were reweighted in ten overlapping groups sorted on $|F_{\text{obs}}|$ and a secondary extinction correction was applied

Table 30. Selected crystallographic data for $\text{Na}_{3.9}\text{Zr}_6\text{Cl}_{16}\text{Be}$ and $\text{Cs}_{3.0}\text{Zr}_6\text{Cl}_{16}\text{C}$

	<u>$\text{Na}_{3.9}\text{Zr}_6\text{Cl}_{16}\text{Be}$</u>	<u>$\text{Cs}_{3.0}\text{Zr}_6\text{Cl}_{16}\text{C}$</u>
Space Group	Pccn	$P2_1/n$
Z	4	4
a, Å ^a	13.251(1)	11.032(2)
b	14.319(1)	11.851(3)
c	14.092(2)	12.473(3)
β, deg.	(90)	108.01(2)
V, Å ³	2674.0(5)	1550.8(6)
Crystal dimen., mm	0.10x0.15x0.15	0.12x0.13x0.05
Radiation	Mo Kα, graphite monochromator	Mo Kα, graphite monochromator
2θ(max), deg.	55.0	55.0
Scan Mode	ω	ω
Reflections		
octants	h,k,±l	h,±k,±l
measured refl.	5912	7023
observed refl.	2933	3073
independent refl.	1646	1596
R(ave), %	2.7	3.1
μ, cm ⁻¹	39.6	67.4
Transm. coeff. range	0.89 – 1.00	0.74 – 1.00
Secondary ext. coeff.	5.6(9) x 10 ⁻⁵	-
R, %	4.3	6.2
R(w), %	3.8	6.8

^aGuinier lattice parameters.

to give final residuals of $R = 4.3\%$ and $R_w = 3.8\%$. The refined occupancies of Na1, Na2, Na3 and Be were, respectively, 0.97(2), 0.60(2), 0.79(2) and 1.06(2). Taking into account the different multiplicities of the sodium sites, the refined composition is $\text{Na}_{3.9(1)}\text{Zr}_6\text{Cl}_{16}\text{Be}$. The final difference map was flat to less than $0.5 \text{ e}^-/\text{\AA}^3$.

Four octants of single crystal diffraction data were collected on a dark brown, rectangular prism of $\text{Cs}_{3.0}\text{Zr}_6\text{Cl}_{16}\text{C}$ using monochromatic $\text{Mo K}\alpha$ radiation and ω -scans. A monoclinic cell was deduced from a set of low angle reflections indexed using the program BLIND.¹²⁶ Axial photographs taken on the diffractometer were consistent in terms of symmetry and axial lengths with the chosen monoclinic cell. Pertinent crystallographic data are compiled in Table 30.

The systematic extinctions observed in the data set and an assumed centricity uniquely identified the space group as $P2_1/n$. The phase problem was solved by direct methods using MULTAN-80.⁹⁵ Two randomly oriented Zr_6 clusters were included as 'molecular fragments' in the normalization process. The three most intense peaks in the Fourier synthesis calculated from the phase set were assigned to zirconium atoms and used as a starting point for subsequent calculations. All calculations were carried out in $P2_1/n$. The remaining atoms in the structure were located by successive cycles of least-squares refinement and Fourier map calculations. The carbon atom was found as a 6-electron residual situated in the cluster center at (0,0,0). The carbon atom was added to the model following isotropic refinement of the zirconium, chlorine and cesium atoms. Anisotropic refinement of the structure followed by a

reweighting of the data set gave final residuals of $R = 6.2$ and $R_w = 6.8\%$. The Cs1 and Cs2 positions refined to occupancies of 0.983(7) and 0.535(6), respectively, or a total of 3.04(3) cesium atoms per $Zr_6Cl_{16}Be$ cluster. The carbon atom converged to an occupancy of 1.2(1) and a $B = 2.6(8)$.

The final difference map was littered with a sizable number of ~ 0.5 -electron residuals. In addition, an approximately 3-electron residual was observed between cluster layers about midway between Cs2 atoms in \vec{b} . When included in the model as a fraction of a Cs atom, the residual refined to an occupancy of 0.126(5), an isotropic B of 6.3(4) and a final position of (0.333(1), 0.494(1), -0.001(1)). R and R_w improved to 5.1 and 5.3%, respectively. The position was surrounded by 5 chlorine atoms at distances of 3.40 – 3.55 Å, but also had two Cs neighbors at unreasonably short distances of ~ 3.05 Å. Although the residual could be interpreted as a small amount of Cs disorder between the cluster layers (with the residual site occupied by Cs only when the 2 nearest neighbor Cs sites are unoccupied), it is not presently believed to be an inherent feature of the structure. It is more likely that the residual is associated with the (poor) quality and small size of the data crystal. This latter interpretation is supported by a second crystal structure determination of $Cs_3Zr_6Cl_{16}Z$.¹⁴² The crystal used in the determination was of unknown origin (found in the crystal mounting box), and hence, the identity of the interstitial atom is uncertain, but limited to C, B or Be. More importantly, the structural refinement, which converged to $R = 5.2$ and $R_w = 4.8\%$ with a carbon atom in the cluster center, showed a

residual of less than $1 e^-/A^3$ at the position of the 3-electron residual in the study under consideration. In light of the results of this second crystal structure, the 3-electron residual was not included in the final stages of the present study. It should be noted that the higher R values in this structure compared to those of other zirconium chloride clusters are largely associated with the ignored residual.

Final positional and thermal parameters for $Na_{3.9}Zr_6Cl_{16}Be$ and $Cs_{3.0}Zr_6Cl_{16}C$ are listed in Tables 31 and 32, respectively. Observed and calculated structure factor amplitudes are contained in Appendices L and M.

Structures and discussion

The $Zr_6Cl_{16}Z$ structures, $Na_{3.9}Zr_6Cl_{16}Be$ and $Cs_{3.0}Zr_6Cl_{16}C$, like the analogous Mo_6Cl_{12} structure composed of M_6X_8 clusters,¹³⁸ are built-up of two-dimensional networks of interconnected $Zr_6Cl_{12}Z$ clusters. Four Cl^{a-a} atoms serve to link adjacent clusters into a two-dimensional, four-connected net, while unshared Cl^a atoms fill the two remaining terminal positions above and below the cluster sheet. The two-dimensional intercluster connectivity is symbolically formulated $2[Zr_6Cl_{12}^iBe]Cl^{a-a}_{4/2}Cl^a_2$. Beyond the presence of the two-dimensional cluster sheets, however, significant differences exist between $Na_{3.9}Zr_6Cl_{16}Be$ and $Cs_{3.0}Zr_6Cl_{16}C$, particularly with respect to cell symmetries, cation sites and relative cluster orientations.

The two-dimensional cluster sheets in $Na_{3.9}Zr_6Cl_{16}Be$ pack in a staggered fashion, such that Cl^a atoms from clusters in one layer lie in voids in the cluster layers above and below. The stacking of the

Table 31. Positional and thermal parameters for $\text{Na}_{3.9}\text{Zr}_6\text{Cl}_{16}\text{Be}$

Atom	x	y	z	B_{11}
Zr1	0.97817(8)	0.40092(6)	0.37087(6)	1.28(4)
Zr2	0.52704(8)	0.37501(6)	0.10262(6)	1.27(4)
Zr3	0.17340(7)	0.46780(6)	0.50062(8)	0.97(3)
C11	0.3420(2)	0.3299(2)	0.1153(2)	1.8(1)
C12	0.7200(2)	0.3954(2)	0.1125(2)	1.6(1)
C13	0.2873(2)	0.5743(2)	0.1433(2)	1.4(1)
C14	0.6656(2)	0.6438(2)	0.1440(2)	1.7(1)
C15	0.5081(2)	0.4725(2)	0.2569(2)	2.7(1)
C16	0.8712(2)	0.5662(2)	0.0050(2)	1.33(9)
C17	0.4481(2)	0.7236(2)	0.2769(2)	2.4(1)
C18	0.4423(2)	0.7466(2)	0.0301(2)	3.0(1)
Na1 ^a	0.5520(4)	0.0890(3)	0.0830(3)	2.5(1)
Na2 ^b	0.6264(7)	0.8295(6)	0.1742(6)	3.0(2)
Na3 ^c	1/4	3/4	0.2248(7)	3.7(3)
Be ^d	1/2	1/2	0	1.4(4)

^aOccupancy refined to 0.97(2).

^bOccupancy refined to 0.60(2).

^cOccupancy refined to 0.79(2).

^dOccupancy refined to 1.06(6).

B_{22}	B_{33}	B_{12}	B_{13}	B_{23}
1.09(3)	0.99(3)	0.03(3)	-0.00(3)	-0.13(3)
0.98(3)	1.09(3)	0.03(3)	0.01(3)	0.14(3)
1.21(3)	1.25(3)	0.15(4)	0.02(3)	-0.01(3)
1.9(1)	2.1(1)	-0.59(8)	0.08(9)	0.64(9)
2.2(1)	1.7(1)	0.15(8)	-0.33(8)	0.48(9)
2.3(1)	1.8(1)	-0.01(9)	0.37(8)	-0.52(9)
2.1(1)	2.0(1)	-0.29(9)	-0.07(9)	-0.84(9)
1.7(1)	1.10(8)	0.4(1)	0.16(8)	0.11(8)
2.7(1)	3.2(1)	-0.11(9)	0.0(1)	0.4(1)
1.6(1)	1.48(9)	0.03(9)	0.05(9)	-0.57(8)
1.13(9)	1.52(9)	0.3(1)	0.13(9)	0.02(8)

Table 32. Positional and thermal parameters for $\text{Cs}_{3.0}\text{Zr}_6\text{Cl}_{16}\text{C}$

Atom	x	y	z	B_{11}
Zr1	0.1151(2)	0.0928(2)	0.9049(1)	1.07(7)
Zr2	0.8233(2)	0.0965(2)	0.9032(1)	0.69(7)
Zr3	0.0488(2)	0.1359(2)	0.1323(2)	0.98(7)
Cl1	0.6053(5)	0.2044(4)	0.7925(4)	1.4(2)
Cl2	0.8557(5)	0.2619(5)	0.0391(4)	1.9(2)
Cl3	0.1781(5)	0.2588(5)	0.0402(4)	1.8(2)
Cl4	0.0712(5)	0.7909(5)	0.2154(4)	1.4(2)
Cl5	0.7425(5)	0.3002(5)	0.2930(5)	2.1(2)
Cl6	0.1695(4)	0.4955(5)	0.4970(4)	0.8(2)
Cl7	0.2472(5)	0.5427(4)	0.2401(4)	1.2(2)
Cl8	0.5752(5)	0.5509(4)	0.2469(4)	1.7(2)
Cs1 ^a	0.6045(2)	0.0285(2)	0.2878(2)	2.45(8)
Cs2 ^b	0.5100(3)	0.2969(3)	0.0218(3)	2.8(1)
C ^c	0	0	0	2.6(8)

^aOccupancy refined to 0.983(7).

^bOccupancy refined to 0.535(6).

^cOccupancy refined to 1.2(1).

B_{22}	B_{33}	B_{12}	B_{13}	B_{23}
1.21(8)	0.72(8)	-0.07(7)	0.17(6)	0.15(6)
1.27(8)	0.99(8)	0.06(6)	0.06(6)	0.12(7)
1.18(8)	0.90(7)	-0.10(6)	0.13(6)	-0.12(6)
2.0(2)	1.7(2)	0.3(2)	0.4(2)	0.7(2)
1.6(2)	1.6(2)	0.2(2)	0.0(2)	-0.5(2)
1.9(2)	1.7(2)	-0.5(2)	0.5(2)	-0.4(2)
1.9(2)	1.4(2)	0.2(2)	0.3(2)	0.7(2)
2.2(3)	2.5(3)	0.0(2)	1.1(2)	-0.4(2)
2.3(2)	1.8(2)	-0.2(2)	0.4(2)	-0.7(2)
1.9(2)	1.3(2)	-0.2(2)	-0.4(2)	0.2(2)
1.7(2)	1.5(2)	0.4(2)	0.8(2)	0.4(2)
2.89(9)	5.9(1)	-0.17(6)	1.09(7)	-0.81(8)
4.9(2)	2.5(2)	-0.0(1)	0.6(1)	-0.2(1)

cluster layers occurs in the \vec{a} direction and is illustrated in Figure 33. The relative orientation of the cluster layers with respect to one another is described by the pair of two-fold axes situated between cluster layers at $y = 1/4$ and $3/4$. The interlayer distance, $\vec{a}/2$, is 6.626 Å. The slightly puckered appearance of the layers is caused by a small tilting of the clusters within each layer. Each cluster is canted approximately 11° , primarily in the \vec{b} direction, from the direction normal to the cluster sheet. Every other row of clusters within the sheet is canted in the opposite direction, such that clusters at $y = 1/2$ are canted to the right, while those at $y = 0$ and 1 are canted to the left. Four sodium cations per cluster, distributed above, below and within the cluster layers, electrostatically bind the anionic layers together. $[\text{Mo}_6\text{Cl}^{\text{i}}_8]\text{Cl}_4$, the $\text{M}_6\text{X}^{\text{i}}_8$ cluster structural analogue of $[\text{M}_6\text{X}^{\text{i}}_{12}]\text{X}_4$, packs in a similar fashion, however, canting of the clusters within the layers is not observed.

The principal component of the layers, the $\text{Zr}_6\text{Cl}^{\text{i}}_{12}\text{Be}$ cluster, has crystallographically imposed $\bar{1}$ symmetry. The cluster is slightly elongated normal to the cluster sheet and toward Cl^{a} . The Zr-Zr distances within the layer average 3.291 Å, while those roughly perpendicular to the layer average 3.303 Å. The Zr-Be distances of 2.32-2.34 Å are consistent with the analogous distances in other beryllium-centered zirconium chloride clusters. The Zr- Cl^{i} distances are all about 2.57(2) Å. The Zr- Cl^{a} distances are slightly longer at 2.667(3) Å, and the Zr- $\text{Cl}^{\text{a-a}}$ distances are longer yet at 2.772(3) Å. Interestingly, the $\text{Zr1-Cl}^{\text{a-a}}\text{-Zr2}$ intercluster bridge, as well as having the longest

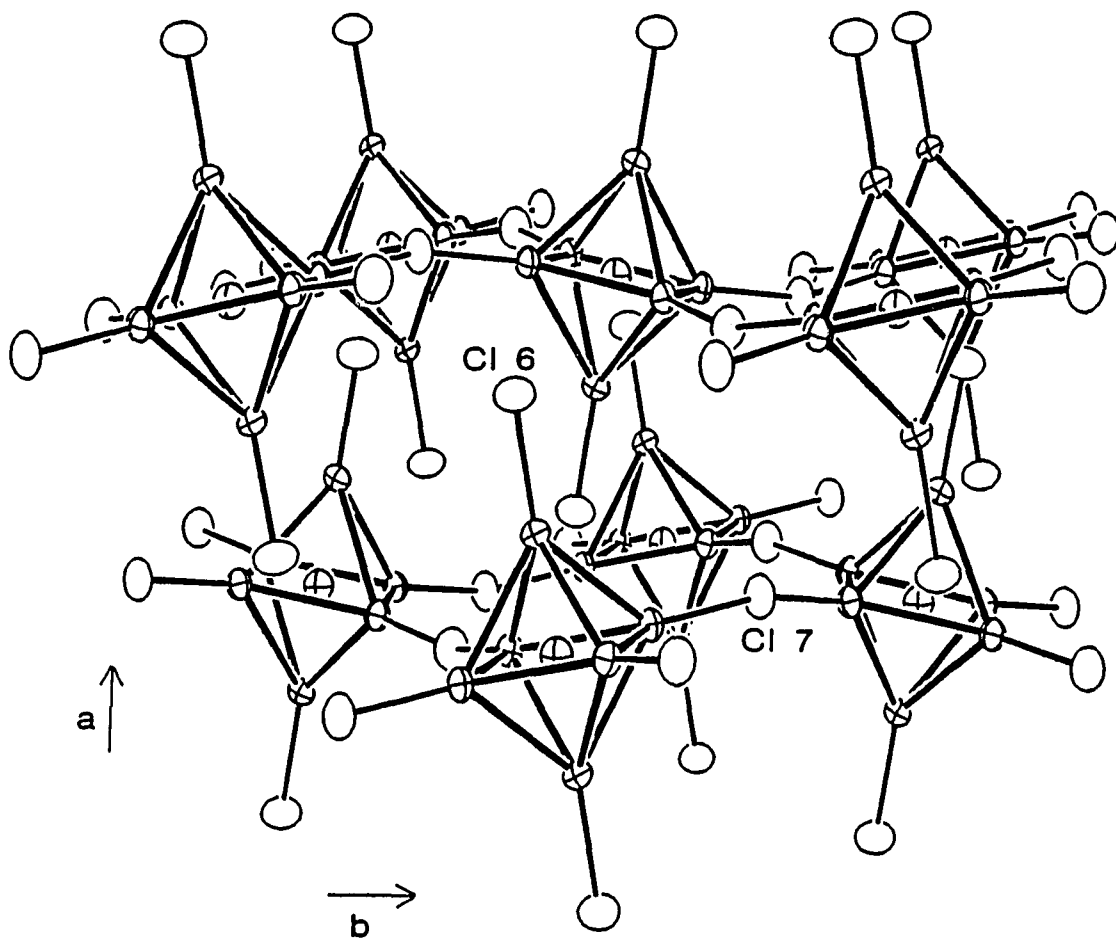


Figure 33. An approximately [001] view of the structure of $\text{Na}_{3.9}\text{Zr}_6\text{Cl}_{16}\text{Be}$. All Cl^{I} and Na atoms have been omitted for clarity. Two-fold axes parallel to \tilde{c} in the tunnel-like structures between layers relate the top layer at $x = 1/2$ with the bottom layer at $x = 0$. (90% ellipsoids)

Zr-Cl^{a-a} distances observed in any of the zirconium chloride clusters studied, is bent at the atypical angle of 161°, about midway between the more commonly observed angles of ~140 and 180°. Relevant interatomic distances are given in Table 33.

The sodium atoms occupy three distinct crystallographic sites within the lattice. Partial occupancy of two of the sodium sites coupled with the complete occupation of the third site gives a refined composition of Na_{3.9}Zr₆Cl₁₆Be. Complete occupation of all of the sodium sites would give a total of five cations per cluster.

Na1 occupies a six-coordinate site situated between clusters within the cluster layer. The site deviates ±0.7 Å from the [100] plane and is about the same level as the Cl^{a-a} atoms within the layer. The chlorine polyhedron, shown in Figure 34, can be viewed as a highly distorted octahedron with Na1-Cl distances ranging from 2.68 to 3.06 Å. The site refined to full occupancy in Na_{3.9}Zr₆Cl₁₆Be.

The Na2 site, only 60% occupied in Na_{3.9}Zr₆Cl₁₆Be, lies ~1.7 Å above and below the cluster plane, about the same level as the Cl^a atoms from the cluster layers above and below (see Figure 33). Five chlorine atoms surround the site, shown in Figure 35, at distances of less than 3.00 Å, while a sixth chlorine atom, Cl7, is at 3.16 Å.

The third sodium site, illustrated in Figure 36, lies on the two-fold axis in the tunnel-like structure between layers. The tunnel-like structure between layers is readily seen in Figure 33. The site, which is 80% occupied, is surrounded by six chlorine atoms in a distorted trigonal antiprism at distances from 2.75 to 3.15 Å.

Table 33. Interatomic distances in $\text{Na}_{3.9}\text{Zr}_6\text{Cl}_{16}\text{Be}$ (Å)

Zr-Zr			Zr-Cl^a-a		
Zr1-Zr2	(x2) ^a	3.288(1)	Zr1-Cl7	(x2)	2.771(3)
Zr1-Zr2	(x2)	3.294(1)	Zr2-Cl7	(x2)	2.773(3)
Zr1-Zr3	(x2)	3.294(1)			
Zr1-Zr3	(x2)	3.310(1)			
Zr2-Zr3	(x2)	3.299(1)	Zr-Cl^a		
Zr2-Zr3	(x2)	3.308(1)	Zr3-Cl6	(x2)	2.667(3)
\bar{d}		3.299			
Zr-Be			Na-Cl		
Zr1-Be	(x2)	2.3255(9)	Na1-Cl6	(x1)	2.681(5)
Zr2-Be	(x2)	2.3286(9)	Na1-Cl6	(x1)	2.717(6)
Zr3-Be	(x2)	2.3436(9)	Na1-Cl7	(x1)	2.759(5)
\bar{d}		2.333	Na1-Cl8	(x1)	2.844(5)
			Na1-Cl5	(x1)	2.916(5)
			Na1-Cl2	(x1)	3.058(6)
			Na1-Na1	(x1)	3.724(9)
			Na1-Zr1	(x1)	4.078(4)
Zr-Clⁱ					
Zr1-Cl3	(x2)	2.561(3)	Na2-Cl4	(x1)	2.743(9)
Zr1-Cl4	(x2)	2.574(3)	Na2-Cl6	(x1)	2.813(9)
Zr1-Cl8	(x2)	2.576(3)	Na2-Cl4	(x1)	2.814(9)
Zr1-Cl5	(x2)	2.585(3)	Na2-Cl5	(x1)	2.883(9)
Zr2-Cl11	(x2)	2.542(3)	Na2-Cl11	(x1)	2.997(9)
Zr2-Cl12	(x2)	2.578(3)	Na2-Cl7	(x1)	3.159(9)
Zr2-Cl8	(x2)	2.588(3)	Na2-Cl8	(x1)	3.389(9)
Zr2-Cl5	(x2)	2.596(3)	Na2-Zr2	(x1)	3.802(9)
Zr3-Cl11	(x2)	2.559(3)	Na2-Zr1	(x1)	3.893(8)
Zr3-Cl13	(x2)	2.576(3)	Na2-Na2	(x1)	3.99(2)
Zr3-Cl4	(x2)	2.592(3)			
Zr3-Cl2	(x2)	2.600(3)	Na3-Cl7	(x2)	2.752(4)
			Na3-Cl3	(x2)	2.810(5)
			Na3-Cl2	(x2)	3.122(8)
			Na3-Zr1	(x2)	3.953(3)

^aNumber of times the distance occurs per cluster or cation.

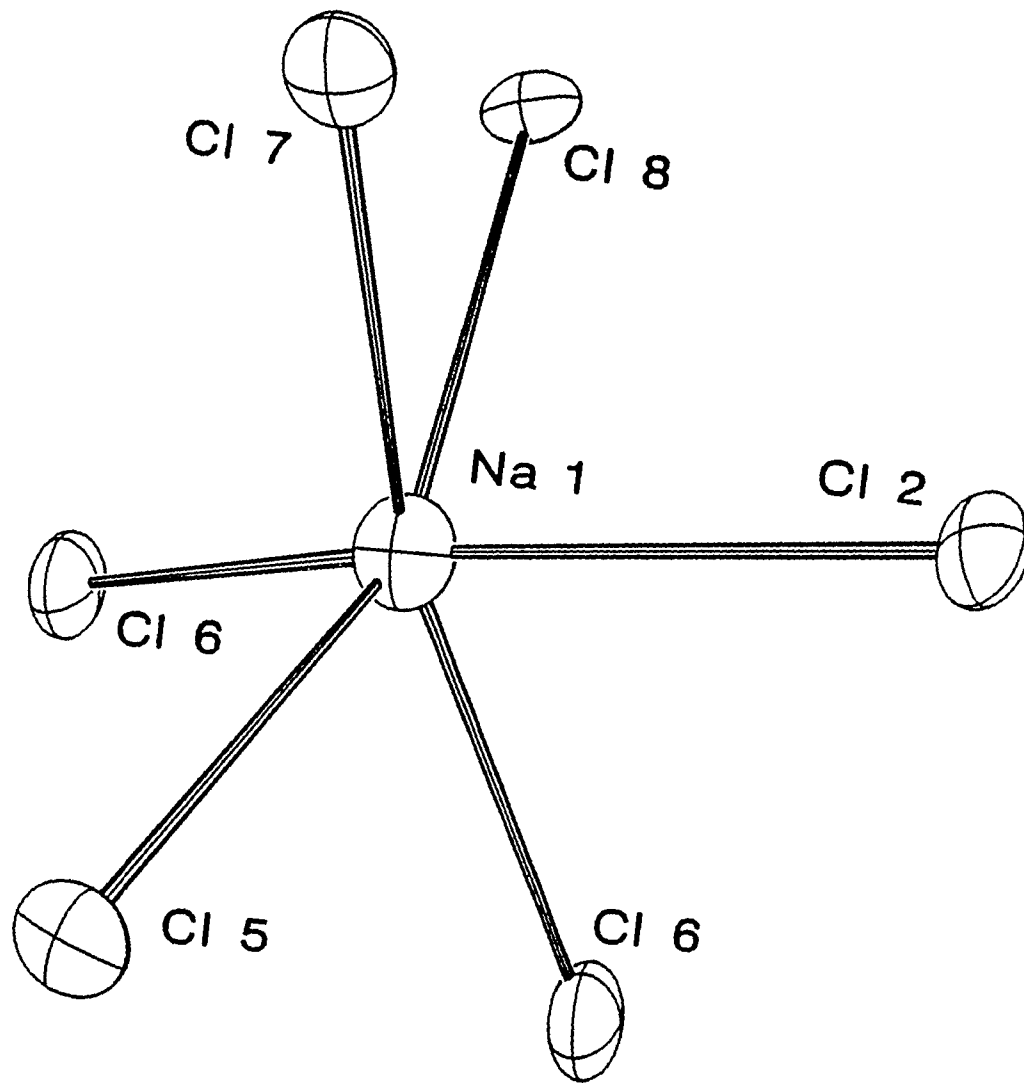


Figure 34. The chlorine environment around the Na1 site in $\text{Na}_{3.9}\text{Zr}_6\text{Cl}_{16}\text{Be}$. The two shortest Na1-Cl distances are to the unshared terminal Cl6 atoms. All ellipsoids are drawn at 50% probability

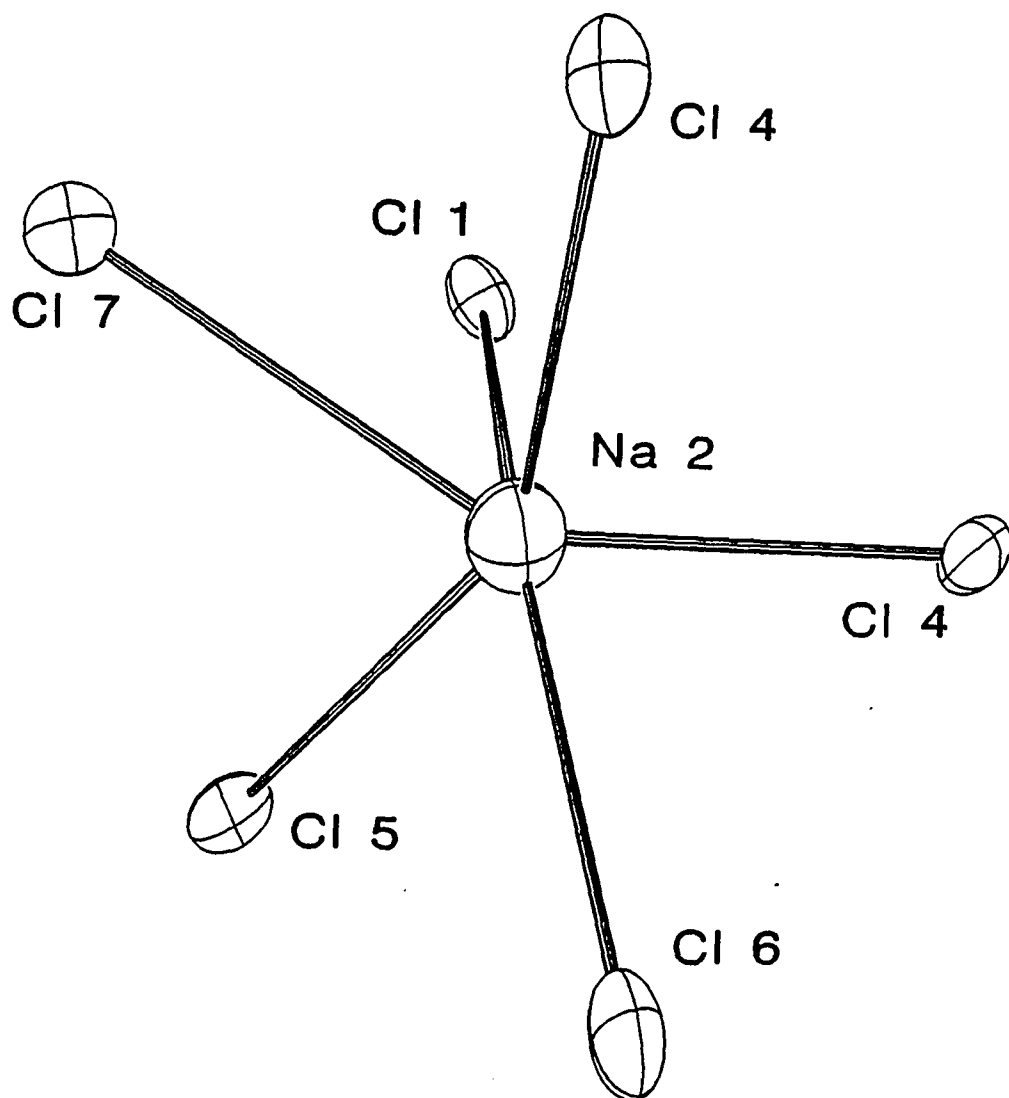


Figure 35. The six-coordinate Na2 site in $\text{Na}_{3.9}\text{Zr}_6\text{Cl}_{16}\text{Be}$. The site has no crystallographically imposed symmetry. Cl6 is the unshared terminal chlorine atom. (50% ellipsoids)

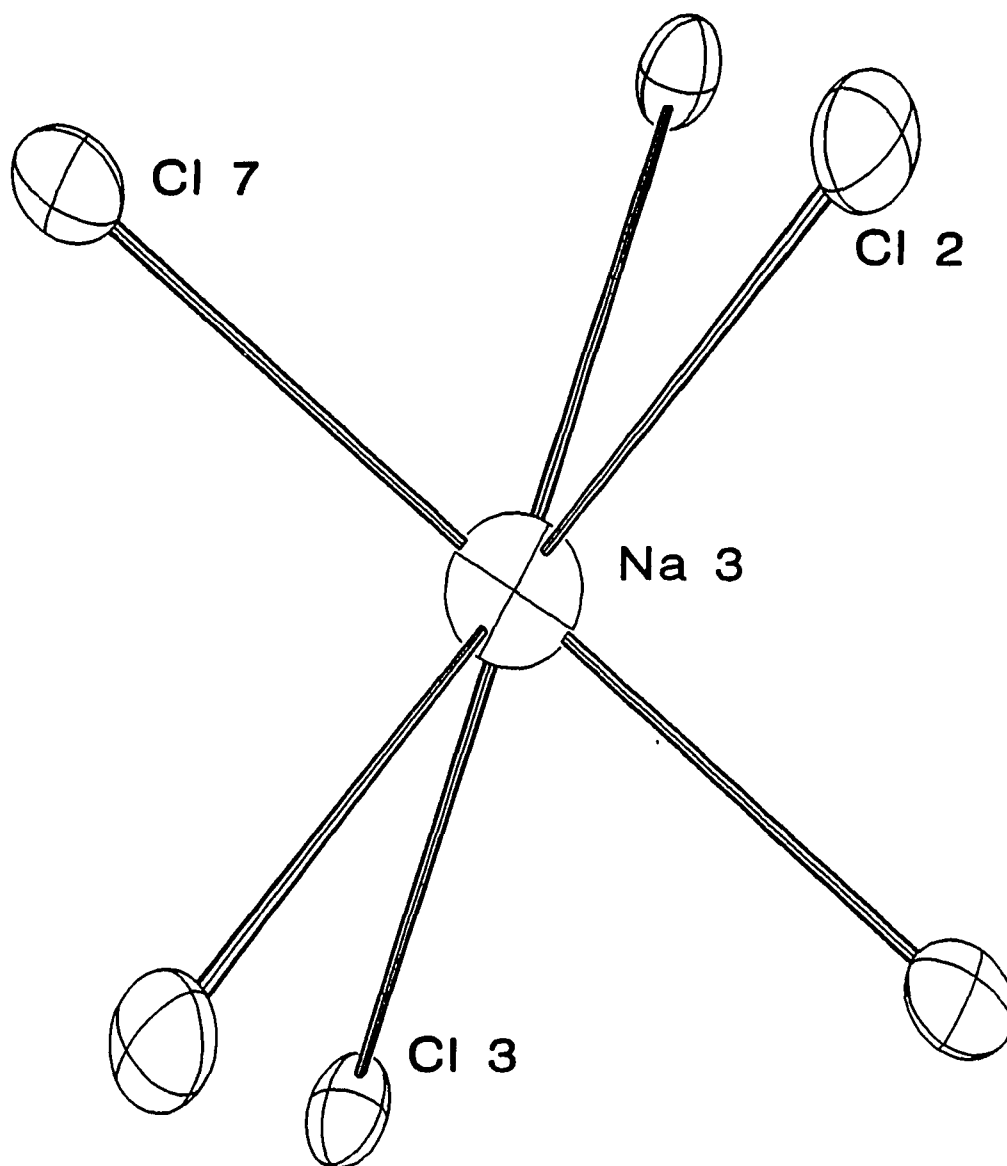


Figure 36. The Na3 site in $\text{Na}_{3.9}\text{Zr}_6\text{Cl}_{16}\text{Be}$. The six-coordinate site has $\bar{1}$ symmetry, and no terminal Cl6^a atoms lie within 4.0 Å. The shortest Na3-Cl distances are to Cl7^{a-a} at 2.752(4) Å. (50% ellipsoids)

Occupation of the three cation sites appears to be controlled largely by electrostatic factors. The Na2 site at 60% occupancy, has two next-nearest zirconium neighbors at 3.8–3.9 Å. The Na3 site, 80% occupied, has two zirconium neighbors at 3.95 Å and the fully occupied Na2 site has only one zirconium neighbor at 4.08 Å. A second sodium cation site lies 3.72 Å from the Na1 site, but this should be electrostatically less important than the distances to the presumably more positively charged zirconium atoms. In addition, two short contacts with the more negative chlorine atoms in the structure, the unshared terminal Cl6 atoms, make the Na1 site the preferred cation position.

The structure of $\text{Cs}_{3.0}\text{Zr}_6\text{Cl}_{16}\text{C}$ is clearly related to that of $\text{Na}_{3.9}\text{Zr}_6\text{Cl}_{16}\text{Be}$, being made up of stacked, two-dimensional sheets of $\text{Zr}_6\text{Cl}_{12}^{\text{i}}\text{C}$ clusters. The connectivity is analogously formulated $\frac{2}{\infty}[\text{Zr}_6\text{Cl}_{12}^{\text{i}}\text{C}]\text{Cl}_{4/2}^{\text{a-a}}\text{C}_2^{\text{a}}$. Accommodation of the larger cesium cations however, results in some interesting modifications of the cluster layers and their stacking.

The cluster layers, which run in the $10\bar{1}$ direction in $\text{P}2_1/n$, have a significantly more buckled appearance than those in $\text{Na}_{3.9}\text{Zr}_6\text{Cl}_{16}\text{Be}$, with the clusters now canted nearly 30° from the direction normal to the cluster layers. The buckling has also reduced the $\text{Zr-Cl}^{\text{a-a}}\text{-Zr}$ intercluster bridging angle to a more typical value of 133° . Transformation of the structure from $\text{P}2_1/n$ to $\text{P}2_1/c$, which moves the cluster sheet from the $[10\bar{1}]$ plane to the $[100]$ plane, shows that although the repeat distance in the stacking direction is only one layer thick, the layers are stacked such that clusters in one layer lie over

voids in the layers above and below. The translation of the cluster layers is described by the $\sim 130^\circ$ monoclinic angle. The cluster layers are related by a series of screw axes between them. Conversion of the cell to one with pseudo-orthorhombic symmetry with $\text{Na}_{3.9}\text{Zr}_6\text{Cl}_{16}\text{Be}$ -type geometry, Figure 37, shows the angle between the cluster layers and the stacking direction (γ in $\text{Na}_{3.9}\text{Zr}_6\text{Cl}_{16}\text{Be}$) has opened-up to 97.4° . The interlayer distance has increased 43% over that in $\text{Na}_{3.9}\text{Zr}_6\text{Cl}_{16}\text{Be}$ to 9.44 Å in order to accommodate the larger cesium cations. The small tunnel-like structures between layers in $\text{Na}_{3.9}\text{Zr}_6\text{Cl}_{16}\text{Be}$ have also collapsed as a consequence of the increased tilt of the clusters.

The $\text{Zr}_6\text{Cl}_{12}\text{C}$ cluster in $\text{Cs}_{3.0}\text{Zr}_6\text{Cl}_{16}\text{C}$ is the first 15-electron cluster prepared in the zirconium chloride system and exhibits Zr-C and Zr-Zr distances which are consistently shorter than those in the corresponding 14-electron, carbon-centered clusters. The Zr-C distances average 2.261 Å which gives an effective carbon crystal radius of 1.40 Å, a value identified to that seen in the 16-electron cluster $\text{Zr}_6\text{I}_{12}\text{C}$. The Zr-Zr distances average 3.197 Å, about 0.025 Å shorter than the average Zr-Zr distances in the 14-electron clusters $\text{KZr}_6\text{Cl}_{15}\text{C}$ and $\text{Na}_{0.5}\text{Zr}_6\text{Cl}_{15}\text{C}$. The Zr-Cl distances are slightly shorter than those in $\text{Na}_{3.9}\text{Zr}_6\text{Cl}_{16}\text{Be}$, but follow the same trend. The Zr-Cl^a distance is 2.596(6) Å and the Zr-Cl^{a-a} distances average 2.689 Å. Interatomic distances in $\text{Cs}_{3.0}\text{Zr}_6\text{Cl}_{16}\text{C}$ are compiled in Table 34.

The $\text{Cs}_{3.0}\text{Zr}_6\text{Cl}_{16}\text{C}$ structure has two distinct crystallographic cation sites which are virtually identical in geometry and together are capable of accommodating up to four cations per cluster.

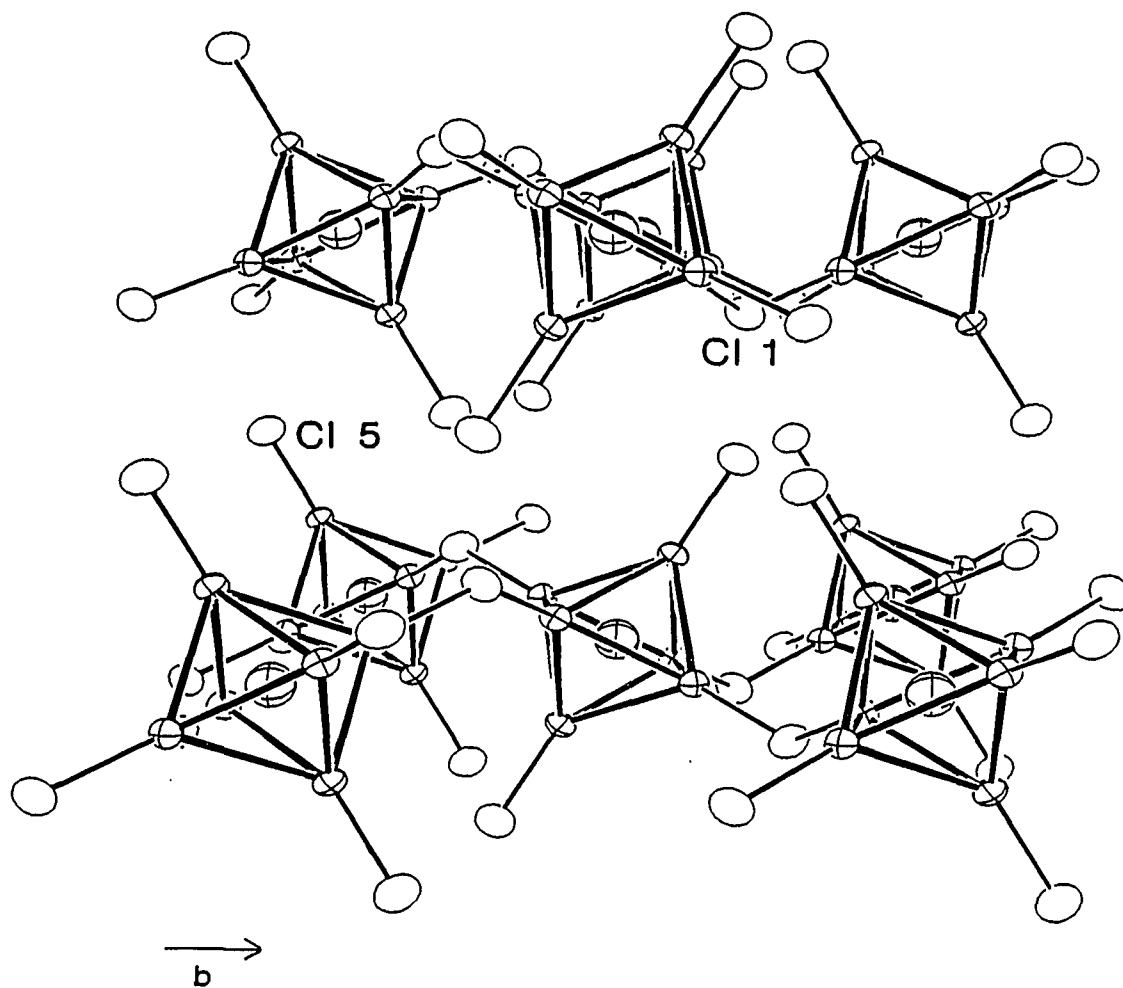


Figure 37. An approximately [001] view of the structure of $\text{Cs}_{3.0}\text{Zr}_6\text{Cl}_{16}\text{C}$ in $P2_1/c$. The \tilde{a} axis runs from the front lower left cluster to the upper left cluster. All $\text{Cl}^{\tilde{1}}$ and Cs atoms have been omitted for clarity. (90% ellipsoids)

Table 34. Interatomic distances in $\text{Cs}_{3.0}\text{Zr}_6\text{Cl}_{16}\text{C}$ (Å)

Zr-Zr			Zr-Cl^{a-a}		
Zr1-Zr2	(x2) ^a	3.197(3)	Zr2-Cl1	(x2)	2.697(5)
Zr1-Zr2	(x2)	3.214(3)	Zr3-Cl1	(x2)	2.682(6)
Zr1-Zr3	(x2)	3.182(3)			
Zr1-Zr3	(x2)	3.212(3)			
Zr2-Zr3	(x2)	3.188(3)	Zr-Cl^a		
Zr2-Zr3	(x2)	3.190(3)	Zr1-Cl5	(x2)	2.596(6)
\bar{d}		3.197			
Zr-C			Cs-Cl		
Zr1-C	(x2)	2.272(2)	Cs1-Cl5	(x1)	3.498(6)
Zr2-C	(x2)	2.261(2)	Cs1-Cl1	(x1)	3.542(6)
Zr3-C	(x2)	2.249(2)	Cs1-Cl5	(x1)	3.554(6)
\bar{d}		2.261	Cs1-Cl4	(x1)	3.658(6)
			Cs1-Cl8	(x1)	3.700(5)
			Cs1-Cl2	(x1)	3.775(6)
			Cs1-Cl7	(x1)	3.791(5)
Zr-Clⁱ			Cs1-Cl6	(x1)	3.908(6)
Zr1-Cl8	(x2)	2.537(5)	Cs1-Cl3	(x1)	3.917(6)
Zr1-Cl4	(x2)	2.544(5)	Cs1-Cl6	(x1)	3.919(6)
Zr1-Cl3	(x2)	2.545(6)	\bar{d}		3.726
Zr1-Cl6	(x2)	2.583(5)	Cs2-Cl1	(x1)	3.514(6)
Zr2-Cl4	(x2)	2.528(5)	Cs2-Cl5	(x1)	3.558(6)
Zr2-Cl2	(x2)	2.543(6)	Cs2-Cl5	(x1)	3.602(6)
Zr2-Cl7	(x2)	2.552(5)	Cs2-Cl4	(x1)	3.656(6)
Zr2-Cl6	(x2)	2.582(5)	Cs2-Cl8	(x1)	3.664(6)
Zr3-Cl8	(x2)	2.536(5)	Cs2-Cl3	(x1)	3.766(6)
Zr3-Cl3	(x2)	2.547(6)	Cs2-Cl2	(x1)	3.776(6)
Zr3-Cl2	(x2)	2.566(6)	Cs2-Cl6	(x1)	3.942(6)
Zr3-Cl7	(x2)	2.570(5)	Cs2-Cl8	(x1)	4.027(6)
			Cs2-Cl6	(x1)	4.055(6)
			\bar{d}		3.756

^aNumber of times the distance occurs per cluster or cation.

The Cs1 site, fully occupied in $\text{Cs}_{3.0}\text{Zr}_6\text{Cl}_{16}\text{C}$, lies approximately one-third and two-thirds of the way between cluster layers, associated with a void in the cluster layer closest to it. The site, shown in Figure 38, has no crystallographically imposed symmetry and is surrounded by seven chlorine atoms at an average distance of 3.645 Å. Six of the chlorine atoms form a ring slightly below the cation, while the seventh chlorine atom lies above and over an edge of the ring. Three additional chlorine atoms between 3.90 and 3.92 Å from the Cs position fill out the coordination sphere above and below the ring. Dashed lines have been drawn between these three latter chlorine atoms and the cesium atom in Figure 38 to indicate the somewhat longer distances.

The second cesium site, pictured in Figure 39, is nearly identical in size and shape to the Cs1 site just described. Topologically, the site is composed of ten chlorine atoms, two above a six-membered ring and two below. The cesium atom sits slightly above the six-membered ring. As was done in Figure 38, the three longest Cl-Cs2 distances have been drawn in dashed lines in Figure 39 and are approximately 0.2 Å longer than any of the other Cs2-Cl distances. The Cs2 site is situated approximately midway between cluster layers and has a refined occupancy of 0.535(6) Å in $\text{Cs}_{3.0}\text{Zr}_6\text{Cl}_{16}\text{C}$. The site is just slightly larger than the Cs1 site (a 0.03 Å difference in the average Cs-Cl distance) which appears to account for its partial occupancy compared to the full occupancy of the Cs1 site.

Although the rather unusual chlorine environment around both the cesium atoms has not significantly affected their thermal parameters,

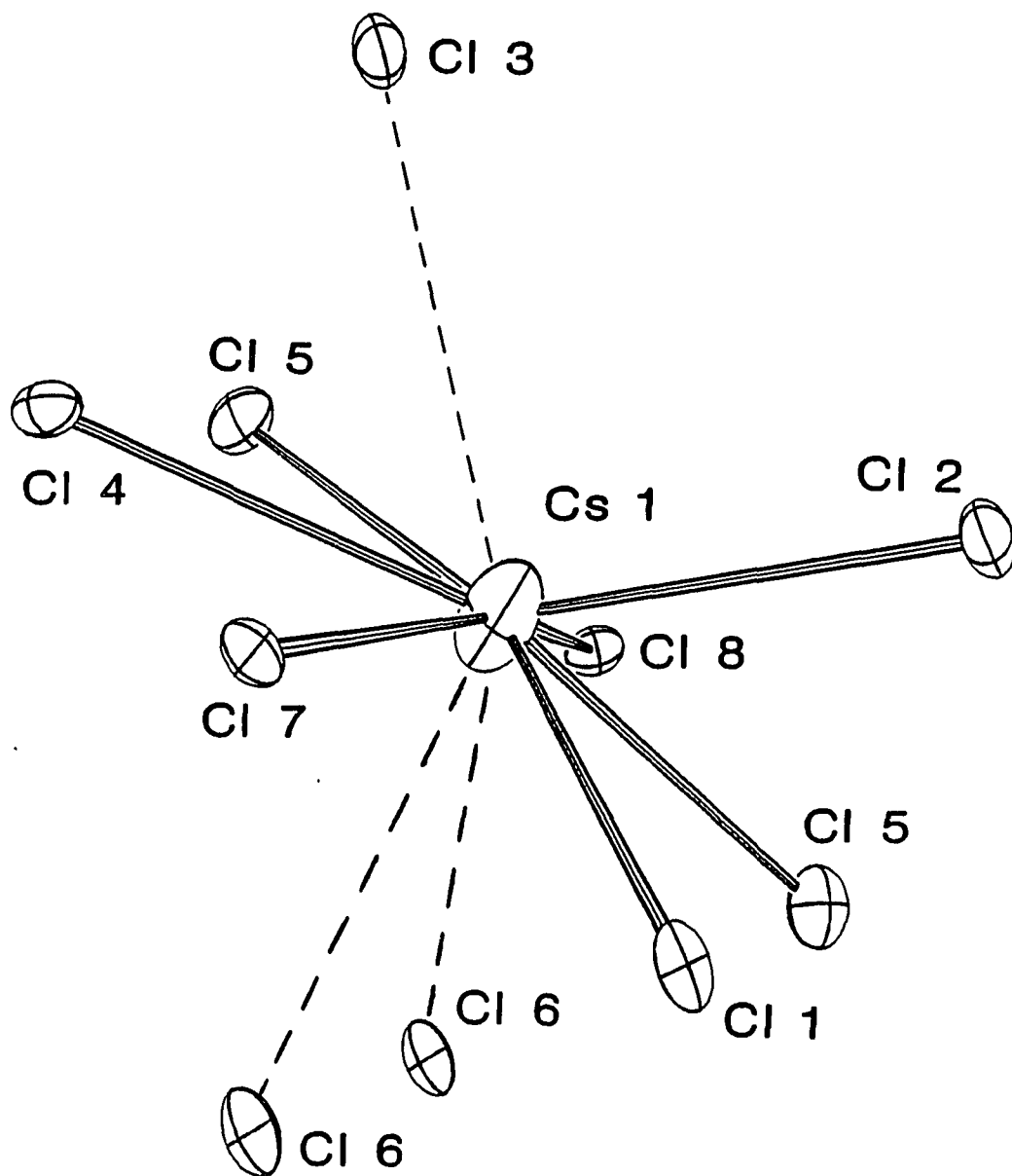


Figure 38. The chlorine environment around Cs1 in $\text{Cs}_{3.0}\text{Zr}_6\text{Cl}_{16}\text{C}$. The site has no crystallographically imposed symmetry. The Cl5 atoms are unshared terminal chlorine atoms. The dashed lines are distances over 3.90 Å. (50% ellipsoids)

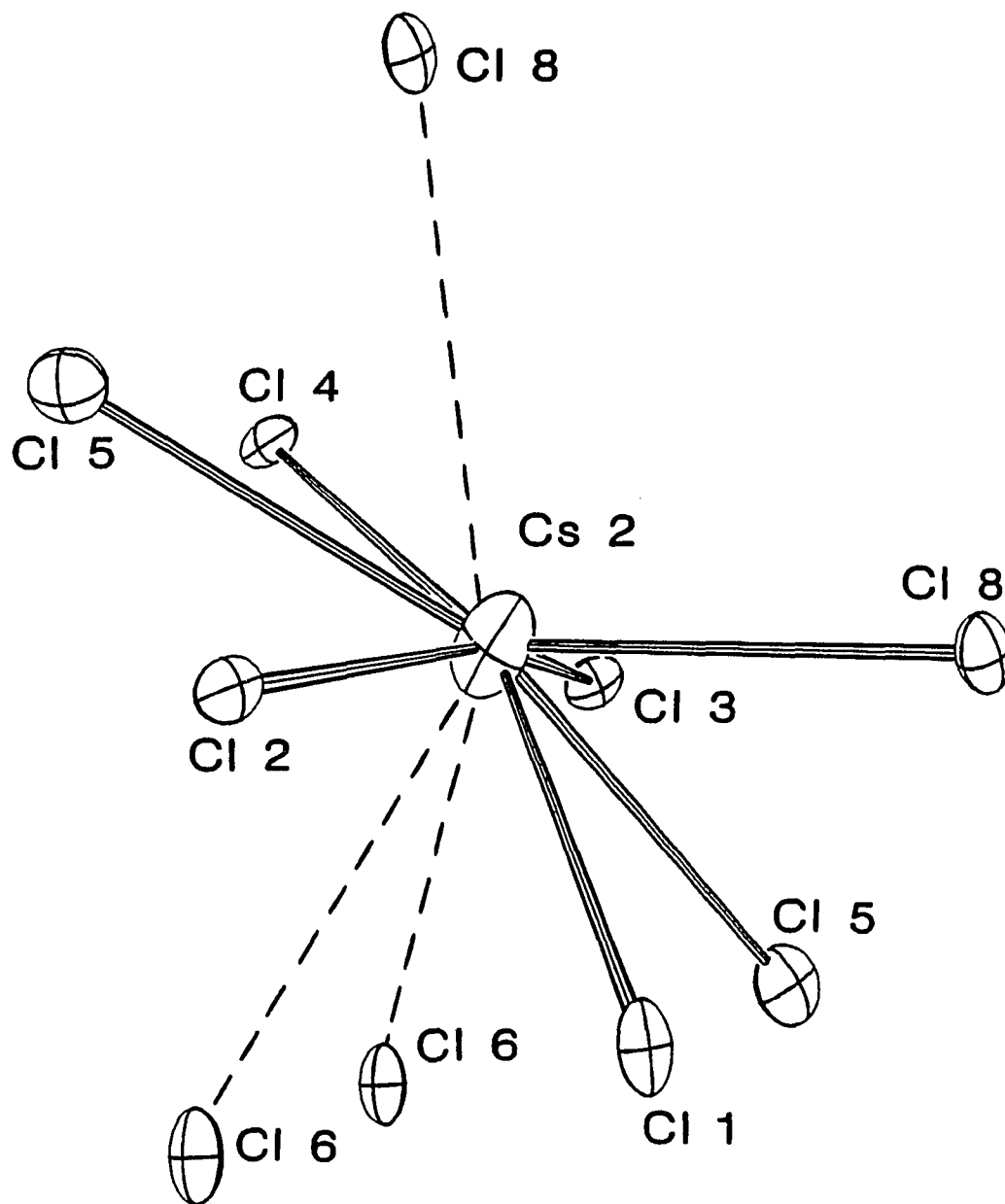


Figure 39. The Cs2 site in $\text{Cs}_{3.0}\text{Zr}_6\text{Cl}_{16}\text{C}$. The site has no crystallographically imposed symmetry and shows a remarkable similarity to the Cs1 site (Figure 38). Dashed lines indicate distances over 3.90 Å. Cl5 atoms are unshared terminal chlorine atoms. Ellipsoids are drawn at 50% probability

both of the latter are somewhat elongated in the direction perpendicular to the 'Cl₆ ring' (~2:1).

The Cs_{3.0}Zr₆Cl₁₆C structure and, hence, the Na_{3.9}Zr₆Cl₁₆Be structure show an unmistakable similarity to the structure of K₃Zr₆Cl₁₅Be. The puckered square net-like sheets of Zr₆Cl₁₂Z clusters in K₃Zr₆Cl₁₅Be are clearly evident lying perpendicular to \vec{a} in Figure 26. The linear Cl^{a-a} bridges between cluster layers have disappeared in Cs_{3.0}Zr₆Cl₁₆C as a result of the addition of one chlorine atom to each cluster in K₃Zr₆Cl₁₅Be. The cluster layers have been translated half a unit cell in the \vec{b} and \vec{c} directions (K₃Zr₆Cl₁₅Be cell) with respect to one another to make room for the additional chlorine atoms and have also opened up slightly, reducing the cluster tilt. The $(\vec{b}+\vec{c})/2$ translation of the cluster layers with respect to one another may also be thought of as a reflection of every other layer through a mirror plane lying in the cluster layer. The end result in either case is the same, i.e., every cluster layer is puckered in the same direction at the same time. The relationship between the cation sites in the structures is considerably more distant because of the layer translation.

The layer-like structures of Na_{3.9}Zr₆Cl₁₆Be and Cs_{3.0}Zr₆Cl₁₆C offer an opportunity to pursue an intercalation/ion-exchange chemistry similar to the more common layered MX₂ compounds.¹⁴³ The flexibility of the cluster sheets through rotation and bending of the Zr-Cl^{a-a}-Zr bonds should allow many differently sized and shaped monoatomic and polyatomic cations to be accommodated. Oxidation and reduction of the

Zr_6Cl_{12} clusters under mild conditions may also be possible. Two initial ion-exchange reactions with $Na_{3.9}Zr_6Cl_{16}Be$ in $KAlCl_4$ and $CsAlCl_4$ at 300°C and 400°C, respectively, appear encouraging as reactions occurred in both cases. Unfortunately, the flexibility of cluster sheets which makes them attractive host materials, also makes indexing and interpretation of the powder diffraction patterns difficult because of the large intensity and line position changes associated with the puckering of the cluster sheets. Thus far, neither ion-exchange product has been characterized.

$Na_{3.9}Zr_6Cl_{16}Be$ also shows hints of what maybe an interesting solution chemistry. $Na_{3.9}Zr_6Cl_{16}Be$, when placed in acetone dissolves to give a dark red-violet solution which becomes colorless in air within minutes with the formation of a white precipitate. Further study will be required to determine if the chemistry can be controlled or is of interest.

M_6X_{18}

The terminus of the family of stoichiometries derived from the M_6X_{12} cluster, namely $[M_6X_{12}^i]X_6^a$, has been known in the niobium chlorides for some time.³ $K_4Nb_6Cl_{18}$ and a variety of other $Nb_6Cl_{18}^{n-}$ ($n = 2,3,4$) salts prepared from it have all been shown by single crystal X-ray diffraction studies to contain isolated $Nb_6Cl_{18}^{n-}$ clusters.^{2,3,33} The studies also showed systematic increases in the Nb-Nb distances occur with one- and two-electron cluster oxidations.¹⁴⁴ Recently, the synthesis and structure of $K_4Nb_6Br_{18}$ was also reported.¹³⁷ The significance of these compounds beyond their position at the end of the M_6X_{12} to M_6X_{18}

cluster series, particularly $K_4Nb_6Cl_{18}$ which is the only one prepared at high temperatures, is that they provide a facile route to $Nb_6Cl_{18}^{n-}$ clusters in solution, and to a cluster chemistry inaccessible in the solid state. Reversible cluster oxidation in solution and cluster insertion together with exhaustive oxidation in clay systems to form pillared clays are two examples of the chemistry now accessible.^{145,146}

The successful expansion of the interstitially stabilized zirconium chlorides into the M_6X_{18} compounds with $Rb_5Zr_6Cl_{18}B$ and more recently, $Li_6Zr_6Cl_{18}H^{73}$ should open the way for the rapid development of a potentially rich area of cluster solution chemistry.

Synthesis

$Rb_5Zr_6Cl_{18}B$ was initially obtained as the major product in the reaction of Zr powder, $ZrCl_4$, $RbCl$ and amorphous B powder at $850^\circ C$ in ratios to give the composition $Rb_4Zr_6Cl_{15}B$. The reaction was air quenched after 13 days. The composition used, was dictated by previous experience in systems with carbon interstitial atoms. Reactions loaded to prepare $M^I_3Zr_6Cl_{15}C$, $M^I = Na, K, \text{ and } Rb$, had given products with powder diffraction patterns similar to that of $K_4Nb_6Cl_{18}$.³ Electronically an $M^I_4Zr_6Cl_{18}C$ composition seemed entirely plausible, simply a combination of the known cluster $Zr_6Cl_{14}C$ and M^ICl . Unfortunately, all the crystals examined were apparently twinned and structurally intractable. Attempts to index the X-ray powder patterns also failed to provide a satisfactory solution. The Rb-B combination, although failing to solve the problem with the carbides, provided a compound with an entirely new powder diffraction pattern and for which the composition and structure

were determined by single crystal X-ray diffraction. $\text{Rb}_5\text{Zr}_6\text{Cl}_{18}\text{B}$ is most efficiently prepared by the reaction of Zr powder, ZrCl_4 , RbCl and amorphous B powder in a $\text{Rb}_5\text{Zr}_6\text{Cl}_{17}\text{B}$ composition. The slightly reducing conditions, as noted for $\text{Cs}_3\text{Zr}_6\text{Cl}_{16}\text{Z}$ ($\text{Z} = \text{B}, \text{C}$), appear to facilitate formation of the desired material. A stoichiometric reaction for $\text{Rb}_5\text{Zr}_6\text{Cl}_{18}\text{B}$ yielded an unidentified compound and Rb_2ZrCl_6 . Stoichiometric reactions with NaCl or KCl instead of RbCl produced yet another structurally uncharacterized compound in the former case, and $\text{K}_2\text{Zr}_6\text{Cl}_{15}\text{B}$ and K_2ZrCl_6 in the latter case.

Crystallography

Two octants of single crystal X-ray diffraction data were collected on a dark-red, rectangular prism of $\text{Rb}_5\text{Zr}_6\text{Cl}_{18}\text{B}$ using ω -scans and monochromatic $\text{Mo K}\alpha$ radiation. The orthorhombic unit, calculated by indexing twelve tuned reflections initially found by film methods,¹²⁶ was consistent with Polaroid axial photographs taken on the diffractometer both in terms of axial lengths and Laue symmetry. Details of the diffraction study are summarized in Table 35.

The space group Pmna was chosen on the basis of the observed systematic extinctions and an assumed centricity which was supported by a Wilson plot. The structural solution to the phase problem was obtained by direct methods. Two randomly oriented, octahedral Zr_6 units were included as input to the normalization routine. The positions of the two most intense peaks in a Fourier map calculated using the phase solution obtained with the program MULTAN-80⁹⁵ were assigned to zirconium atoms and used as a starting point for further calculations. Successive cycles

Table 35. Summary of crystallographic data for $\text{Rb}_5\text{Zr}_6\text{Cl}_{18}\text{B}$

Space Group	Pmna
Z	2
a, Å ^a	10.914(4)
b	9.078(4)
c	17.769(5)
V, Å ³	1760(1)
Crystal dimen., mm	0.18x0.21x0.37
Radiation	Mo K α , graphite monochromator
2 θ (max), deg.	55.0
Scan Mode	ω
Reflections	
octants	hk \bar{l} ; $\bar{h}k\bar{l}$
measured refl.	4528
observed refl.	2750
independent refl.	1437
R(ave), %	1.5
μ , cm ⁻¹	97.2
Transm. coeff. range	0.74 – 1.00
Secondary ext. coeff.	1.9(3) x 10 ⁻⁶
R, %	2.5
R(w), %	2.7

^aGuinier powder diffraction data.

of least-squares refinement and Fourier map calculations were used to locate the remaining atoms in the structure. The boron interstitial atom, located last on a difference map as an approximately 5-electron residual in the cluster center, was added to the model following isotropic refinement of all other atoms in the structure. Electron density maps of the structure showed large streaks of positive density corresponding to 4-5 electrons at the peak running through the cell parallel to the \tilde{a} and \tilde{c} axes, apparently a consequence of termination effects in the Fourier series. Difference maps of the structure were unaffected. The Rb3 atom, positioned at a site of $2/m$ symmetry at $(0,1/2,1/2)$, exhibited an extremely long cigar-like thermal ellipsoid in the approximately $[011]$ direction. Principal axial ratios of 1.5:14.7:1 were observed. The symmetry at the Rb3 site was accordingly reduced to m by allowing the Rb3 atom to move from the inversion center, within the plane perpendicular to \tilde{a} . Refinement of the split Rb3 site proceeded smoothly to give two-inversion related Rb3 sites separated by 1.08 Å. Occupancies of the two sites were constrained to be equal. Anisotropic refinement of the Rb3 atom in the new position gave a still elongated, but more reasonable thermal ellipsoid, with principal axial ratios of 1.9:6.0:1. The Rb3 atom appears to be disordered over the two symmetry-related positions. Superstructure reflections were not observed in any of the axial photographs taken on the diffractometer or in powder diffraction patterns of the compound. Attempts to reduce the space group symmetry to the acentric group $Pmn2_1$ or $Pm2a$ (the latter requires the origin be moved to $(1/4,0,1/4)$) failed to provide a more satisfactory fit

of the data than the disordered Pmna model. Refinements in the acentric space groups required formerly inversion-related atoms to be varied in alternate cycles to prevent excessive shifts associated with coupling of inversion-related parameters. Thermal parameters for Rb3 in Pmn2₁ and Pm2a were 1.5-3.0 times larger in the direction of elongation than those in the split Rb3, Pmna refinement. Further reductions in space group symmetry, namely to monoclinic groups, appears to be unwarranted on the basis of the acentric orthorhombic refinements, the satisfactory data averaging in Pmna, the axial photographs and the otherwise very satisfactory refinement of the disordered Pmna model.

Application of a secondary extinction correction and a reweighting of the data in ten overlapping groups based on $|F_{obs}|$ gave final R and R_w values of 2.5 and 2.7%, respectively. Refinement of the structure with the Rb3 atom constrained to the inversion center gave R and R_w values of 3.0 and 3.7%, respectively. Final positional and thermal parameters for the disordered model are given in Table 36. Observed and calculated structure factor amplitudes are available in Appendix N.

Structure and discussion

The structure of $Rb_5Zr_6Cl_{18}B$ is composed of isolated $[Zr_6Cl_{12}^iB]Cl_6^a$ clusters in a sea of rubidium cations. The clusters, when viewed down the \vec{c} axis as in Figure 40, are arranged in close-packed layers with the pseudo- $\bar{3}$ axis of each cluster oriented perpendicular to the cluster layers. The cluster layers stack directly on top of one another in an ...AA... fashion along the \vec{b} axis to give, what can be thought of as, columns of stacked $Zr_6Cl_{18}B$ clusters. The

Table 36. Positional and thermal parameters for $\text{Rb}_5\text{Zr}_6\text{Cl}_{18}\text{B}$

Atom	x	y	z	B_{11}
Zr1	0	0.14059 (7)	0.10858(3)	1.69(2)
Zr2	0.35076(3)	0.15361(5)	0.54965(2)	1.44(1)
C11	0.1679(1)	0	1/2	1.45(5)
C12	0.33388(9)	0.0127(1)	0.67368(6)	2.26(4)
C13	0.3327(1)	0.3202(1)	0.43381(6)	2.75(5)
C14	0	0.6679(2)	0.11266(9)	2.14(6)
C15	0.3251(1)	0.6825(1)	0.11011(7)	2.26(4)
C16	0	0.2834(2)	0.24198(9)	3.40(7)
Rb1 ^a	0	0.04118(9)	0.66387(4)	3.05(3)
Rb2 ^b	1/4	0.47501(9)	1/4	3.80(4)
Rb3 ^c	0	0.4551(3)	0.4801(2)	4.87(9)
B ^d	0	0	0	1.5(2)

^aOccupancy refined to 0.997(3).

^bOccupancy refined to 0.991(4).

^cOccupancy refined to 0.504(4).

^dOccupancy refined to 1.05(4).

B_{22}	B_{33}	B_{12}	B_{13}	B_{23}
2.25(2)	1.35(2)	0	0	-0.26(2)
2.16(2)	1.54(1)	0.15(1)	0.07(1)	-0.09(1)
3.37(7)	2.34(6)	0	0	-0.55(5)
3.75(5)	1.48(4)	0.52(4)	0.50(3)	0.30(4)
2.71(5)	2.46(4)	0.82(4)	0.23(3)	0.63(3)
2.70(7)	3.11(7)	0	0	1.07(6)
2.91(5)	3.28(5)	0.53(4)	-0.53(4)	0.42(4)
3.25(7)	2.33(6)	0	0	-0.89(6)
4.14(4)	2.67(3)	0	0	0.86(3)
4.17(4)	3.71(4)	0	0.43(3)	0
9.7(3)	8.3(3)	0	0	6.4(2)

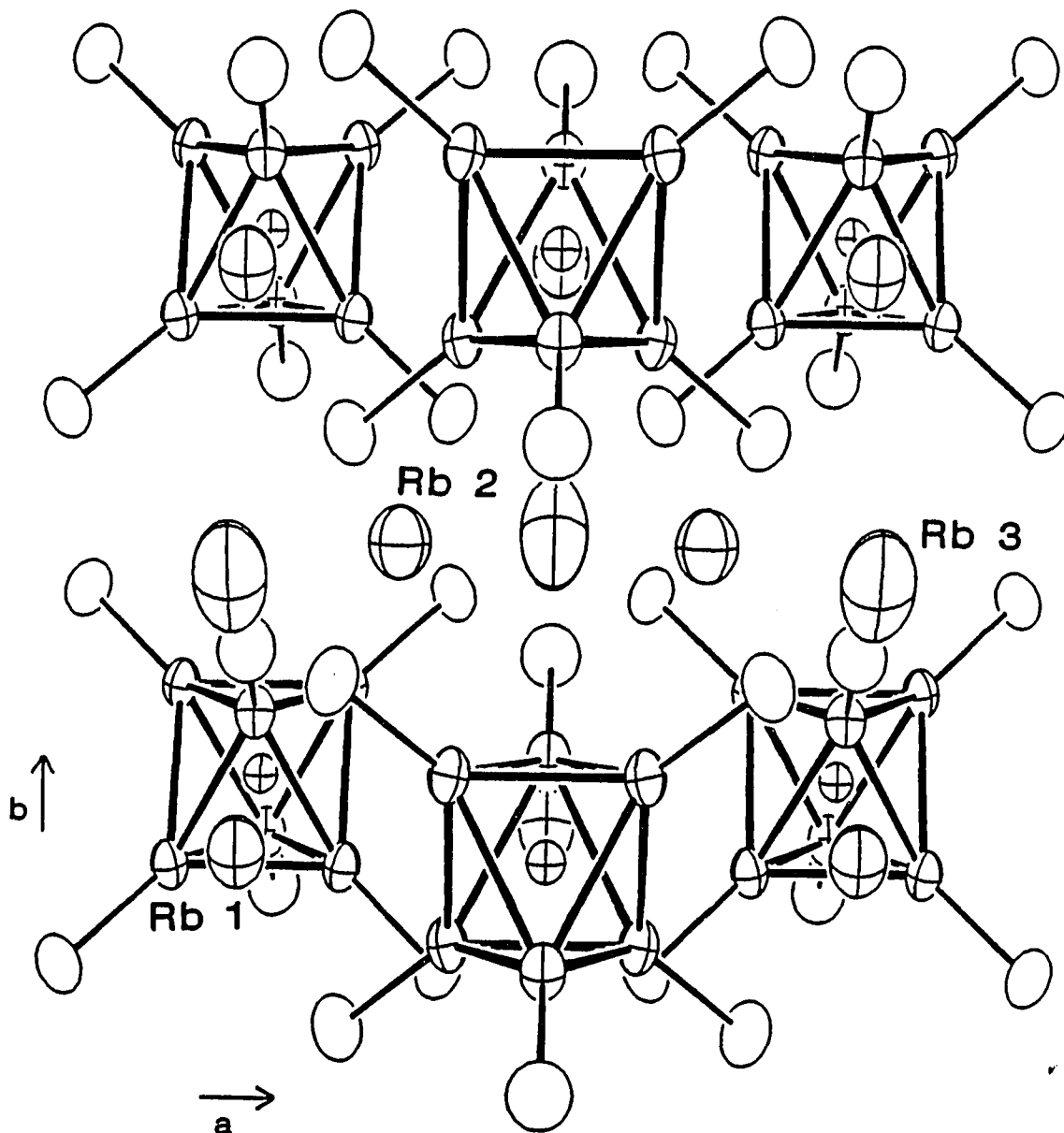


Figure 40. An approximately $[001]$ view of the three-dimensional structure of $\text{Rb}_5\text{Zr}_6\text{Cl}_{18}\text{B}$ with Cl^- atoms omitted for clarity. Small crossed ellipsoids inside the trigonal antiprismatic Zr_6 clusters are B atoms. Rb2 and Rb3 lie between cluster layers while Rb1 resides within the cluster layers (90% ellipsoids)

rubidium cations are distributed around the cluster columns, both within and between the cluster layers. A projection of the cluster columns down \vec{b} is shown in Figure 41.

The individual $Zr_6Cl_{18}B$ clusters have crystallographically imposed $2/m (C_{2h})$ symmetry, the mirror plane being perpendicular to \vec{a} . The Zr_6B cluster is mildly elongated along the pseudo- $\vec{3}$ axis. The Zr-Zr distances normal to the $\vec{3}$ axis (intralayer) are within 2σ of 3.254 Å, while the interlayer distances are 3.299(1) and 3.300(1) Å, which give the metal cluster an experimentally observed D_{3d} symmetry. The Zr-B distances are consistent with a boron crystal radius of 1.46 Å. The Zr-Cl distances are typical for zirconium chloride clusters with Zr-Clⁱ distances averaging 2.56 Å and longer Zr-Cl^a distances of 2.702(2) and 2.655(1) Å. Interatomic distances are compiled in Table 37.

The rubidium atoms occupy three crystallographically distinct sites within the cluster array. Rb1 occupies a nine-coordinate site situated between clusters within the cluster layer. The site is bounded by a ring of six chlorine atoms ~ 0.4 Å below the Rb plane ($y = 0.04$), two terminal chlorine atoms above (Cl5^a) and one below (Cl6^a) as shown in Figure 42. The Rb-Cl distances range from 3.294(2) - 3.657(2) Å and average 3.450 Å. The summation of the crystal radii for chlorine and nine-coordinate rubidium is 3.44 Å.¹²⁷

Rb2 resides in a six-coordinate site approximately midway between cluster layers. The chlorine polyhedron around the site, shown in Figure 43, approximates a trigonal antiprism. The rubidium atom lies slightly closer to the rectangular face of the prism made up solely of terminal

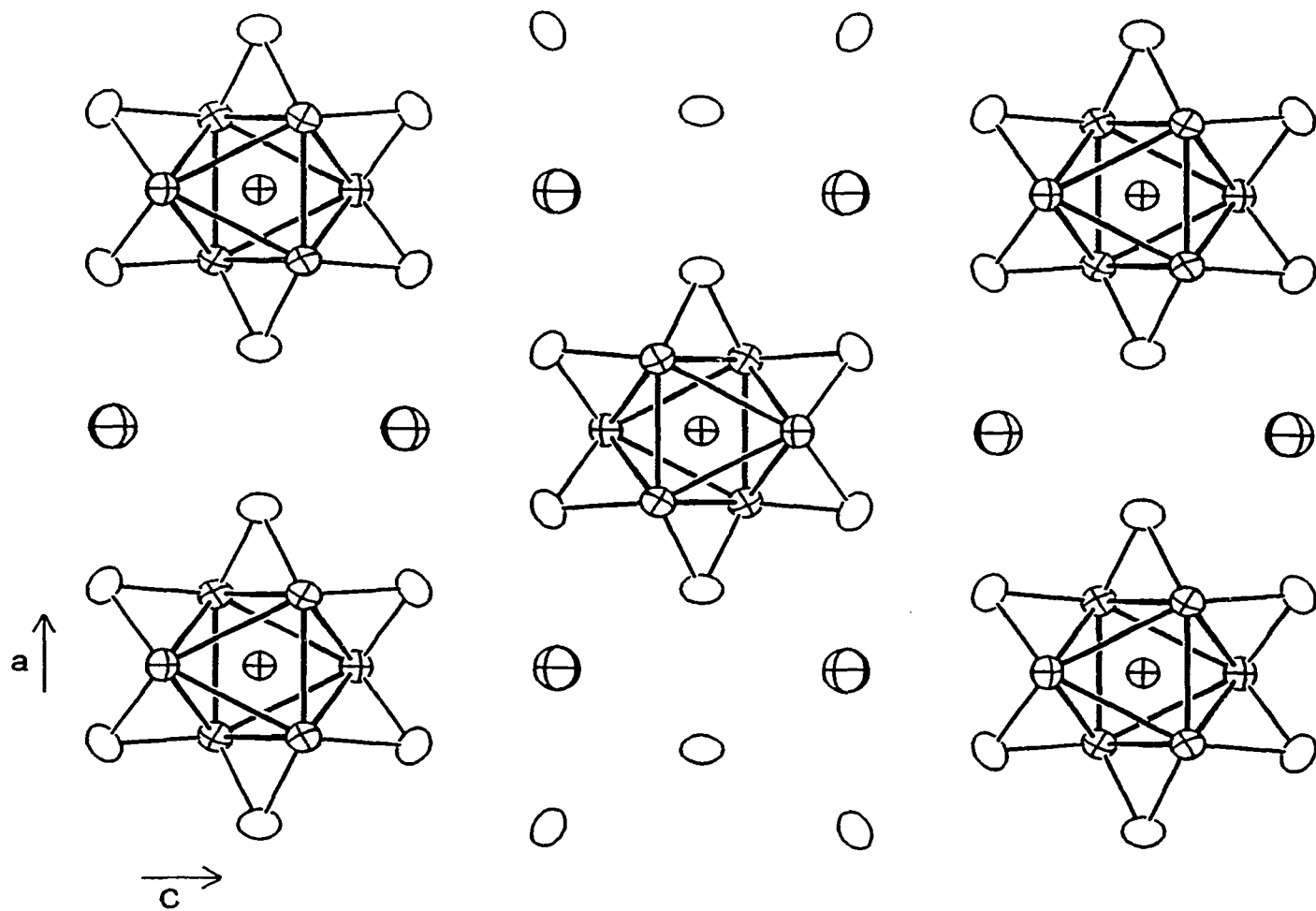


Figure 41. A [010] projection on $y = 0$ of the cluster columns in $\text{Rb}_5\text{Zr}_6\text{Cl}_{18}\text{B}$. The six Cl^{i} and six Cl^{a} atoms above and below each Zr_6B cluster have been omitted for clarity. Crossed ellipses between clusters are Rb^{i} atoms (50% ellipsoids)

Table 37. Interatomic distances in $\text{Rb}_5\text{Zr}_6\text{Cl}_{18}\text{B}$ (Å)

Zr-Zr			Zr-Cl^a		
Zr1-Zr2	(x4) ^a	3.2515(9)	Zr1-Cl6	(x2)	2.702(2)
Zr1-Zr2	(x4)	3.299(1)	Zr2-Cl5	(x4)	2.655(1)
Zr2-Zr2	(x2)	3.258(1)	Rb-Cl		
Zr2-Zr2	(x2)	3.300(1)	Rb1-Cl5	(x2)	3.294(2)
\bar{d}		3.277	Rb1-Cl6	(x1)	3.388(2)
Zr-B			Rb1-Cl2	(x2)	3.418(1)
Zr1-B	(x2)	2.3133(8)	Rb1-Cl1	(x2)	3.461(1)
Zr2-B	(x4)	2.3186(7)	Rb1-Cl2	(x2)	3.657(2)
\bar{d}		2.3168	Rb2-Cl5	(x2)	3.225(1)
Zr-Clⁱ			Rb2-Cl6	(x2)	3.239(1)
Zr1-Cl3	(x4)	2.561(1)	Rb2-Cl3	(x2)	3.668(1)
Zr1-Cl2	(x4)	2.562(1)	Rb3-Cl5	(x2)	3.237(3)
Zr2-Cl2	(x4)	2.555(1)	Rb3-Cl5	(x2)	3.247(3)
Zr2-Cl4	(x4)	2.555(1)	Rb3-Cl3	(x2)	3.920(2)
Zr2-Cl3	(x4)	2.562(1)	Rb3-Cl3	(x1)	1.079(6)
Zr2-Cl1	(x4)	2.589(1)	Rb3-Cl6	(x2)	4.509

^aNumber of times the distance occurs per cluster or cation.

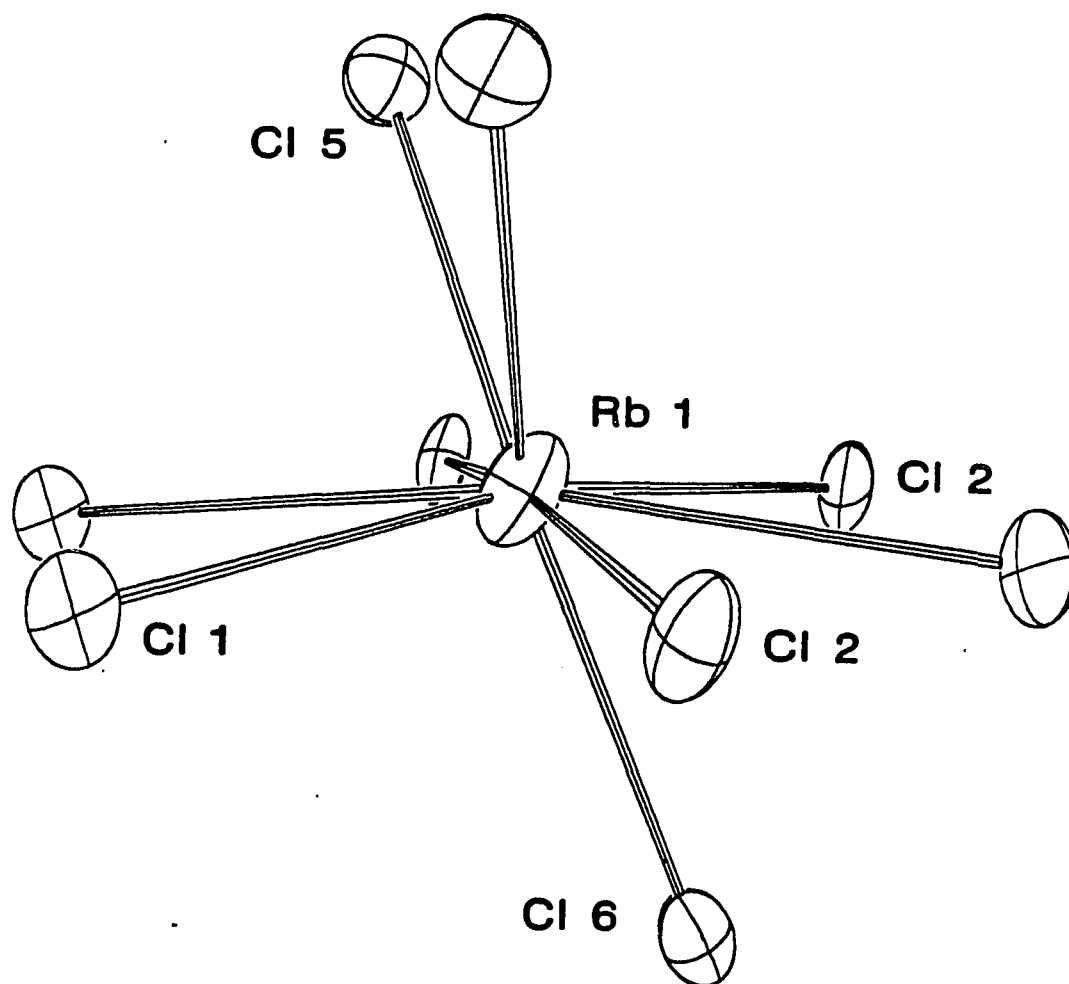


Figure 42. The nine-coordinate Rb1 site in $\text{Rb}_5\text{Zr}_6\text{Cl}_{18}\text{B}$. The Rb1 position lies about 0.3 Å above the least-squares plane formed by the six Cl1 and Cl2 atoms shown. The Cl5 and Cl6 atoms above and below the plane occupy terminal positions on the cluster. A crystallographic mirror plane lies approximately in the page (50% ellipsoids)

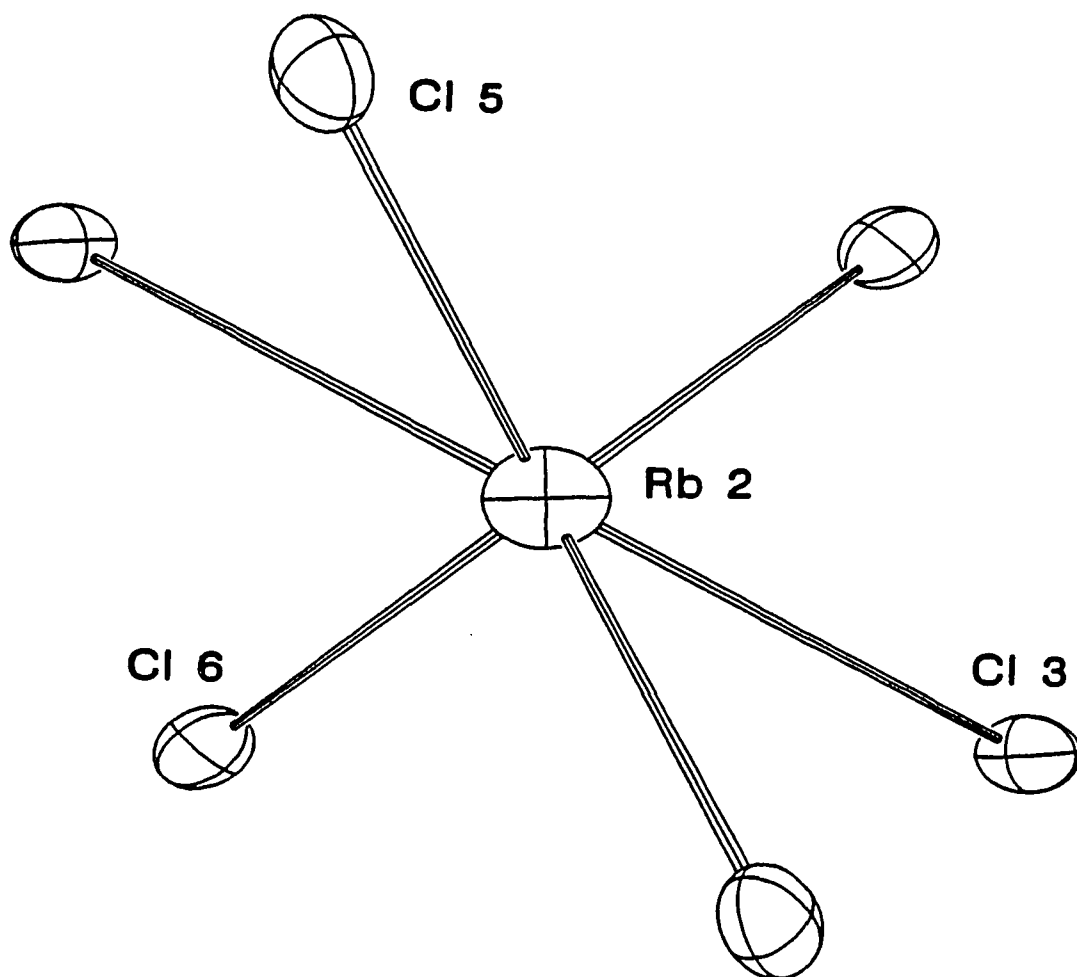


Figure 43. The Rb2 site in $\text{Rb}_5\text{Zr}_6\text{Cl}_{18}\text{B}$ viewed along the two-fold axis. Cl5 and Cl6 are terminal chlorine atoms on the cluster. All ellipsoids are drawn at 50% probability

chlorine atoms (C15, C16). The rubidium to terminal chlorine distances average 3.232 Å, while the other two distances (to C13) are 3.668(1) Å. Both the Rb1 and Rb2 positions refined to full occupancy.

The Rb3 site also lies approximately midway between cluster layers. The site, illustrated in Figure 44, actually consists of two preferred rubidium positions situated 0.54 Å from the cavity center. Rb3 is disordered over the two positions, randomly occupying one or the other position. Occupation of both positions within a single cavity is, of course, precluded by the very short Rb3-Rb3 contact that would result (1.08 Å). Displacement of the rubidium atom from the inversion center in the middle of the cavity effectively lengthens what would apparently be four short Rb3-C15^a distances in the eight-coordinate site and shortens two of the four long Rb3-C13 distances. In the new six-coordinate position, the Rb3-C15^a distances have increased from 3.196 Å to 3.237 and 3.247 Å and two Rb3-C13 distances have shortened to 3.920 Å from 4.151 Å. The average Rb3-Cl distance is 3.468 Å in the six-coordinate site.

The eclipsed stacking of clusters in $\text{Rb}_5\text{Zr}_6\text{Cl}_{18}\text{B}$ appears to be the most favorable cluster arrangement for providing five appropriately sized cation sites per cluster, while maximizing the number of rubidium to terminal chlorine contacts. The columnar stacking provides an average of 3.6 terminal chlorine contacts for each rubidium cation, three for Rb1 (x2) and four each for Rb2 (x2) and Rb(3) (x1). In contrast, the $\text{K}_4\text{Nb}_6\text{Cl}_{18}$ structure,³ which only has four cation sites per cluster and hence cannot be used for $\text{Rb}_5\text{Zr}_6\text{Cl}_{18}\text{B}$, only provides three terminal chlorine contacts per cation. The nearly close-packed clusters in

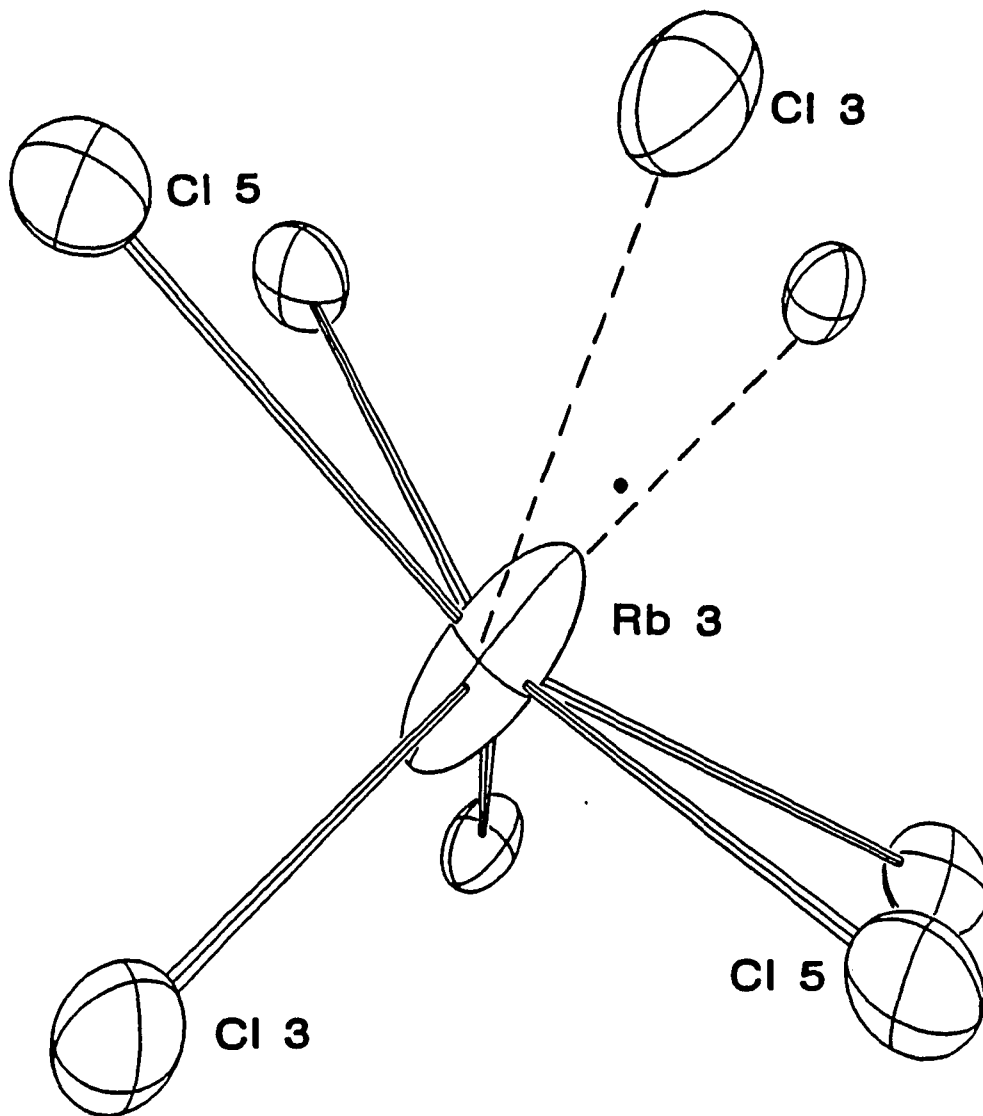


Figure 44. The Rb3 cavity in $\text{Rb}_5\text{Zr}_6\text{Cl}_{18}\text{B}$ shown with one Rb3 position occupied. The inversion-related Rb3 position is indicated by the small filled circle. A mirror plane lies approximately in the page and an inversion center lies midway between the Rb3 positions. Distances between the Rb3 atom shown and surrounding Cl atoms over 4.0 Å are marked by the dashed lines (50% ellipsoids)

$\text{Li}_6\text{Zr}_6\text{Cl}_{18}\text{H}^{73}$ provide six cation sites per cluster, but also provide only three terminal chlorine contacts per cation.

The structure of $\text{Rb}_5\text{Zr}_6\text{Cl}_{18}\text{B}$ may also be viewed as a composition of close-packed chlorine layers stacked in the \vec{b} direction with an ordered arrangement of zirconium atoms in octahedral holes between the layers. Layer A, at $y = 0$, runs through the center of the cluster layer and is made-up of a close-packed array of twelve chlorine, two boron and four rubidium(1) atoms per cell. A projection of the layer is shown in Figure 45.

The second layer at $y \approx 1/3$ and designated B', is a pseudo-close-packed layer similar in nature to the B' layer in $\text{K}_2\text{Zr}_6\text{Cl}_{15}\text{B}$. The layer, projected in Figure 26, is made-up of zones of six close-packed chlorine atoms separated by narrow gaps. In this case, as was the situation in $\text{K}_2\text{Zr}_6\text{Cl}_{15}\text{B}$, the triangular zones correspond to regions of B and C type packing, i.e., half the zones belong to what would be a B layer and half to what would be a C layer in a cubic close-packed system. The narrow gaps are necessary to maintain minimal Cl-Cl distances.

The third layer, B'' at $y \approx 2/3$, is related to B' by an inversion center at $(1/2, 1/2, 1/2)$, or as a consequence of the mirror plane and a translation of $(\vec{a} + \vec{c})/2$.

The chlorine layer stacking in $\text{Rb}_5\text{Zr}_6\text{Cl}_{18}\text{B}$ is then ...AB'B''... with zirconium atoms occupying all the trigonal antiprismatic sites between the A and B' and A and B'' layers. Rubidium cations are found both in the A layer and between the B' and B'' layers. A projection of the sites between the B' and B'' layers is shown in Figure 47. Interestingly, a

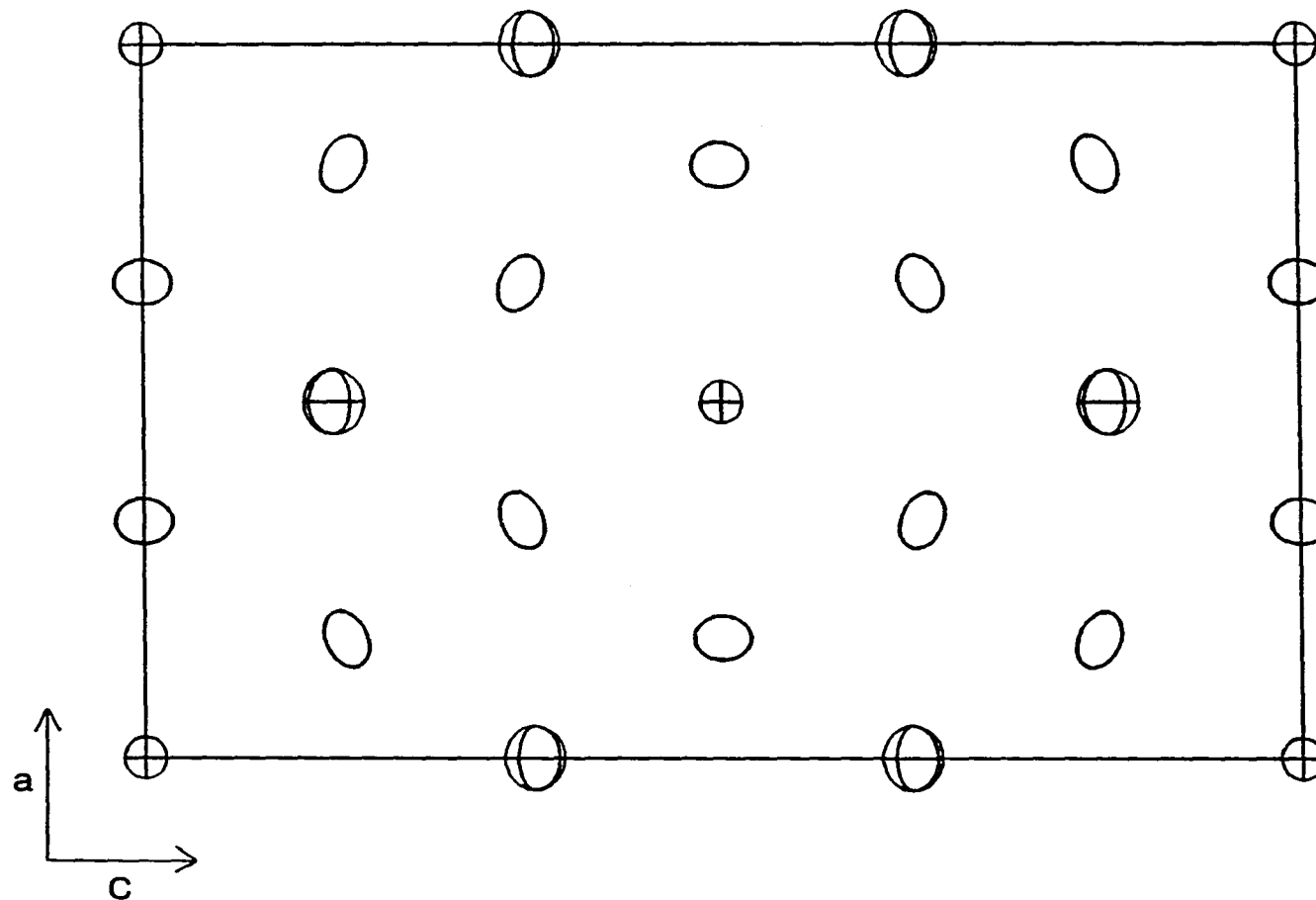


Figure 45. A [010] projection on $y = 0$ of the close-packed layer of atoms in $\text{Rb}_5\text{Zr}_6\text{Cl}_{18}\text{B}$ designated A. The large and small crossed ellipses represent Rb1 and B atoms, respectively. The open ellipses denote Cl^{i} atoms

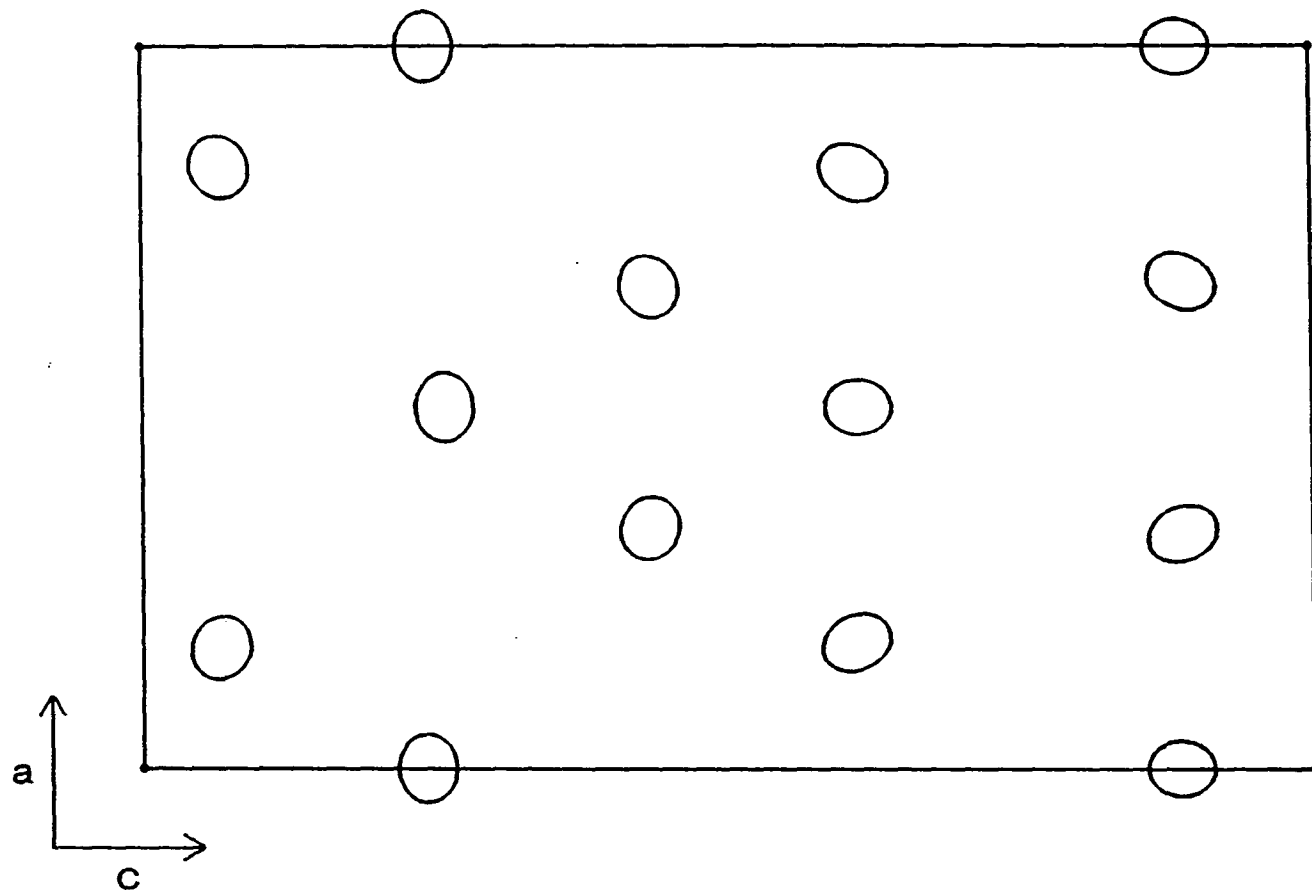


Figure 46. A [010] projection on $y = 1/3$ of the layer of chlorine atoms $\text{Rb}_5\text{Zr}_6\text{Cl}_{18}\text{B}$ denoted B' . The triangular zone of close-packed chlorine atoms in the center of the figure is related to others by two-fold axes normal to the projection plane at $(x = \pm 1/4, z = \pm 1/4)$. Terminal chlorine atoms occupy the vertices of the triangular zones

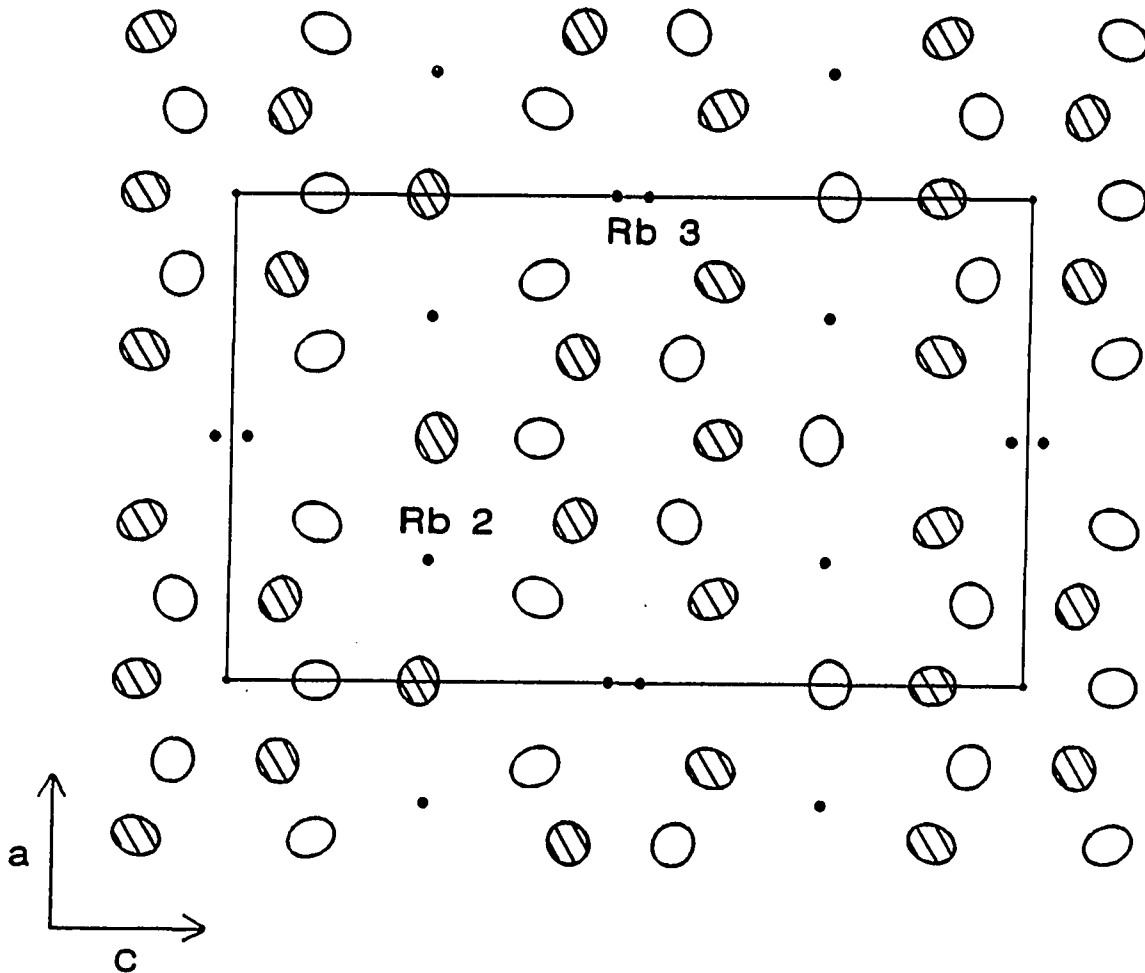


Figure 47. A [010] projection of the cation sites between the B' (open ellipses, $y = 1/3$) and B'' (cross-hatched ellipses, $y = 2/3$) layers in $\text{Rb}_5\text{Zr}_6\text{Cl}_{18}\text{B}$. $\text{Rb}2$ atoms occupy the sites filled with a single small solid ellipse and $\text{Rb}3$ atoms occupy the cavities with pairs of solid ellipses. Note the unoccupied trigonal antiprismatic sites bounded only by Cl^{I} atoms at the corner and center of the cell projection

fourth cation position, a small octahedral hole between clusters in \vec{b} , i.e., within the cluster columns, also exists, but is unoccupied. Distances from the center of the small octahedral site to the neighboring chlorine atoms are 2.727 (x4) and 2.516 (x2) Å.

Structurally, $\text{Rb}_5\text{Zr}_6\text{Cl}_{18}\text{B}$ can easily be derived from the $\text{Cs}_3\text{Zr}_6\text{Cl}_{16}\text{C}$ structure (M_6X_{16} section). The conversion requires an oxidation of two chlorine atoms per cluster of $\text{Cs}_3\text{Zr}_6\text{Cl}_{16}\text{C}$ which opens the remaining $\text{Cl}^{\text{a-a}}$ bridges and yet retains the spatial arrangement and orientation of the clusters within the layer. The cluster tilt is increased to $\sim 55^\circ$ to line-up the pseudo- $\bar{3}$ axes of the clusters perpendicular to the layer, and the 130.8° angle which staggers the cluster layers, has been straightened up to 90° to give an eclipsed stacking of clusters.

The structure of $\text{K}_4\text{Nb}_6\text{Cl}_{18}^3$ also shows a close relationship to the structure of $\text{Rb}_5\text{Zr}_6\text{Cl}_{18}\text{B}$. Like $\text{Rb}_5\text{Zr}_6\text{Cl}_{18}\text{B}$, $\text{K}_4\text{Nb}_6\text{Cl}_{18}$ is built-up of close-packed cluster layers, in this case, coincident with the [001] plane. Stacking of the cluster layers is staggered even though the repeat unit contains only one cluster layer, because of the pseudo-translation provided by the 115° monoclinic angle. In $\text{Rb}_5\text{Zr}_6\text{Cl}_{18}\text{B}$, as was noted, the clusters stack directly on top of one another. The other significant structural difference between the two structure types is in the relative orientation of the clusters with respect to one another within the layer. In $\text{K}_4\text{Nb}_6\text{Cl}_{18}$, the orientation of every cluster within a layer is identical, i.e., all clusters are related by translational symmetry elements of the space group. In contrast, the cluster centered on the [010] face of $\text{Rb}_5\text{Zr}_6\text{Cl}_{18}\text{B}$ is oriented differently than those on

the cell corners. In other words, one-half of the clusters in $\text{Rb}_5\text{Zr}_6\text{Cl}_{18}\text{B}$ are related simply by translational symmetry elements of the cell, while the other half also require a reflection or rotation.

The most recent addition to the M_6X_{18} family is $\text{Li}_6\text{Zr}_6\text{Cl}_{18}\text{H}$.⁷³ The structure is composed of cubic close-packed layers of $\text{Zr}_6\text{Cl}_{18}\text{H}^{6-}$ clusters arranged in the same fashion as the clusters in $\text{Zr}_6\text{Cl}_{12}\text{H}$. Lithium cations occupy six symmetry-related octahedral sites between clusters, while leaving a seventh octahedral site which is located directly above and below each cluster, completely unoccupied.

The proposed solution chemistry for isolated $\text{Zr}_6\text{Cl}_{18}\text{Zn}^{n-}$ clusters has recently gotten underway.¹⁴⁷ The initial work with $\text{Rb}_5\text{Zr}_6\text{Cl}_{18}\text{B}$ appears promising, but further work is needed to verify the integrity of the cluster after dissolution.

Bonding

To gain a better understanding of the role of the interstitial atom in the bonding and stabilization of $\text{Zr}_6\text{Cl}_{18}\text{Zn}^{n-}$ clusters, extended-Hückel molecular orbital calculations were carried out for a series of isolated clusters. The clearest approach to understanding the role of the interstitial atom is to examine the electronic structure of the unoccupied cluster first, and then to observe the effects as an atom is added at the cluster center.

Several authors have previously examined the bonding in isolated $\text{M}_6\text{X}_{12}^{n+}$ clusters,^{30-32,36} much of the work having been done on $\text{Nb}_6\text{Cl}_{12}^{n+}$. In general, except for the most recent work,³⁶ the results, although predicting the right number of metal-metal bonding orbitals, are

in error because of the failure to include terminal halogen atoms in the calculations. The importance of the terminal atoms in correctly establishing the symmetries and energy ordering of the metal-metal bonding levels in the cluster are discussed in detail by Smith and Corbett.³⁶ The effects of the interstitial atom on cluster bonding have also been examined by several authors with results consistent with those presented here.^{36,40,148}

Although virtually all of the $Zr_6Cl_{12}Z$ clusters found in the structures studied are distorted from O_h symmetry, all calculations were done on clusters with octahedral symmetry for the sake of simplicity. The energy level splittings associated with the observed cluster distortions are all quite small (<0.2 eV) and do not change the ordering of the cluster orbitals. The major effect of the distortions is simply to remove the orbital degeneracies imposed by O_h symmetry.

Molecular geometries and parameters used to describe the atomic orbital energies and spatial characteristics are given in Appendix A.

$Zr_6Cl_{18}^{4-}$

The one-electron molecular orbital energies for an unoccupied $Zr_6Cl_{18}^{4-}$ cluster are shown on the left side of Figure 48. At low energies, off the bottom of the figure, centered -30.5 eV, are a block of 18 chlorine 3s orbitals. Above them, between -16.0 and -14.5 eV, are the 54 molecular orbitals associated with Zr-Cl bonding and the chlorine 3p lone pairs. Considerable mixing between the Zr-Cl bonding orbitals and chlorine lone pairs prevents separation of the two groups. The next

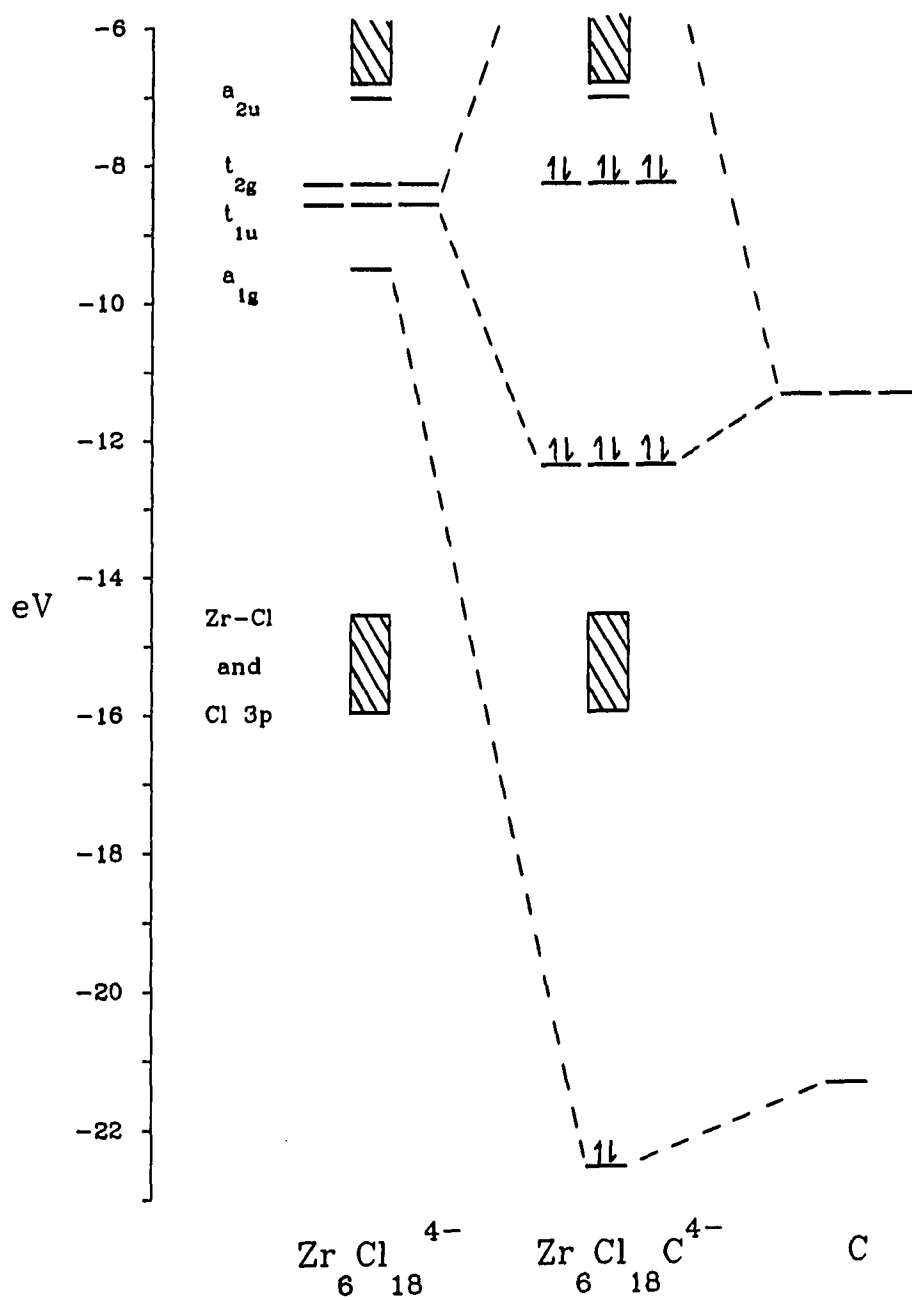


Figure 48. Molecular orbital diagrams from extended-Hückel calculations. Left: Hypothetical $Zr_6Cl_{18}^{4-}$ cluster (O_h); Right: Atomic C; Center: Carbon-centered $Zr_6Cl_{18}^{4-}$ cluster (O_h)

eight orbitals, which will also be referred to as cluster bonding orbitals, are responsible for the metal-metal bonding in the cluster. In octahedral symmetry, the orbitals break down into four irreducible representations, a_{1g} , t_{1u} , t_{2g} and a_{2u} in order of increasing energy. Above the metal-metal bonding orbitals lie sets of metal-metal and metal-chlorine antibonding levels. A sizable gap of 1.4 eV is calculated between the seventh (t_{2g}) and eighth (a_{2u}) cluster orbitals. The size of the gap is at least partially a consequence of the Zr-Clⁱ antibonding component of the a_{2u} orbital. From an electron counting standpoint, the 72 orbitals below the metal-metal bonding levels, can be considered to be all of the chlorine valence levels. Hence, the number of electrons for metal-metal bonding is simply the number of metal valence electrons minus the number needed to fill the chlorine valence orbitals. Thus, for the cluster in question, $Zr_6Cl_{18}^{4-}$, one has $6(4) - 18(1) + 4 = 10$ cluster electrons which gives the cluster an $a_{1g}^2 t_{1u}^6 t_{2g}^2$ electronic configuration. It is clear that the cluster can contain at least 4 more electrons and needs 6 more to fill all of the metal-metal bonding states.

$Zr_6Cl_{18}C^{4-}$

The role of the interstitial atom in stabilizing the $Zr_6Cl_{18}^{4-}$ cluster is depicted in the remainder of Figure 48 which shows the energy level changes associated with the inclusion of a carbon atom at the center of the $Zr_6Cl_{18}^{4-}$ cluster. Two things should initially be noticed: 1) there is a strong interaction between the interstitial carbon orbitals

and the symmetry equivalent cluster orbitals, and 2) the number of cluster bonding orbitals does not change, only their energies.

The molecular orbital diagram for the centered cluster, $Zr_6Cl_{18}C^{4-}$ is much the same as that of the unoccupied $Zr_6Cl_{18}^{4-}$ cluster of the same dimensions. The chlorine 3s and 3p levels, as well as the Zr-Cl bonding orbitals, remain essentially unchanged. Two significant changes, however, occur in the metal-metal bonding region. Interaction of the carbon 2s orbital with the lowest energy Zr-Zr bonding orbital (both with a_{1g} symmetry) creates a low lying a_{1g} orbital at -22.6 eV, primarily carbon in character, although a small zirconium contribution is discernible, and a very high lying antibonding counterpart. In a similar fashion, a t_{1u} set of Zr-C bonding orbitals is formed at -12.4 eV and a higher energy antibonding set by the interaction of the carbon 2p orbitals with the cluster bonding orbitals of t_{1u} symmetry. The remaining metal-metal bonding levels are unaffected by inclusion of the interstitial atom, which leaves the total number of cluster bonding orbitals unchanged at eight. Stabilization of the cluster by the interstitial atom, therefore, results from the formation of strong Zr-interstitial bonds and by the addition of the interstitial atom's valence electrons to the cluster bonding manifold. For electron counting purposes, the interstitial atom's valence electrons are counted as being 'donated' to the cluster because no change in the number of cluster bonding orbitals has occurred. Hence, for $Zr_6Cl_{18}C^{4-}$ there are $6(4) - 18(1) + 4 + 4 = 14$ cluster bonding electrons, which gives the cluster an $a_{1g}^2 t_{1u}^6 t_{2g}^6$ electronic configuration. Although, the interstitial atom's valence electrons are

viewed as 'donated' to the cluster, a charge transfer from the interstitial atom to the metal cluster is definitely not implied. Rather the bonding is largely covalent, with the four new bonding orbitals in the carbide example having somewhat more carbon character, so that the charge on carbon is calculated to be about -1.8. Although the extent of charge transfer is probably exaggerated, it is certainly correct in sign. XPS carbon 1s core data also support the charge transfer to carbon with sizable shifts to lower binding energies from the adventitious carbon reference (285.0 eV) in both $Zr_6Cl_{14}C$ (282.0 eV) and the related condensed cluster compound Zr_2Cl_2C (282.8 eV).^{60,74}

The ubiquity of 14-electron zirconium chloride clusters and their ease of formation compared to 15- and 16-electron examples, appears anomalous in light of the calculations which clearly suggest a 16-electron/8 metal-metal bonding orbital system. The calculations are supported by the sizable number of 15- and 16-electron clusters that are known for the zirconium iodides and the niobium and tantalum halides,²⁻⁶ as well as by the changes in metal-metal distances in 14-, 15- and 16-electron clusters.¹⁴⁵ Two factors appear to be responsible for the 14-electron preference shown by interstitially stabilized zirconium chloride clusters. First, compared with the zirconium iodide clusters, the magnitude of the $Zr-X^i$ antibonding contribution in the zirconium chlorides to the a_{2u} orbital which contains the 15th and 16th electrons is larger. The difference, reflected in the $t_{2g}-a_{2u}$ gap and the percent X^i character of the a_{2u} orbital, 1.4 eV and 10.3% and 1.3 eV and 8.0% for the $Zr_6Cl_{18}^{4-}$ and $Zr_6I_{18}^{4-}$, respectively, is a direct consequence of

the matrix effect and the resultingly poorer overlap of the zirconium 4d orbitals with the X^i 5p levels than the analogous overlap in the chlorides. A measure of the matrix effect and, hence, the overlap, is the X^i-Zr-X^i angle formed across trans-corners of the square of X^i atoms around each zirconium atom. The angle indicates the extent to which the zirconium atoms have 'pulled in' from the square faces of the octahedron formed by the X^i atoms of the cluster. The smaller the angle, the larger the matrix effect and the poorer the overlap. The angle ranges from 156.3 to 163.1 in the zirconium iodide carbide clusters³⁶ and from 166.8 to 170.8 in the zirconium chloride carbides. One of the implications is that 15- and 16-electron clusters should be more easily formed in systems with small interstitial atoms which allow shorter metal-metal bonds and produce a larger matrix effect. Indeed, $KZr_6Cl_{15}N$ ($KZr_6Cl_{15}C$ -type) represents the first example prepared under this reasoning. Undoubtedly, more will follow.

The second factor and clearly the most important where the niobium and tantalum halides are concerned, is the strength of the zirconium-interstitial bonding. The stabilizing influence of the interstitial atom is particularly evident in the number of $M_6X_{12}Z$ clusters which have been prepared with fewer than 14-cluster bonding electrons, the fewest found in any unoccupied M_6X_{12} cluster. At least 6 examples of interstitially stabilized zirconium halide clusters with 11-13 cluster bonding electrons are known.¹⁴⁹ In contrast, all of the unoccupied niobium and tantalum halide clusters, which are held together entirely by comparatively weak metal-metal bonding, contain at least 15-cluster electrons if prepared by

solid state routes at high temperatures.³⁻⁶ All of the 14-electron Group V halide clusters are formed by oxidation of 15- and 16-electron clusters in solution near room temperature, and are most likely unstable at higher temperatures. Indeed, higher temperature reactions in 14-electron niobium halide systems, i.e., those with a Nb:X ratio of 6:16, preferentially form trimers, namely Nb_3X_8 ,^{150,151} over Nb_6X_{12} clusters. Clearly, efforts to prepare empty zirconium halide clusters should focus on stoichiometries which provide at least 15 cluster-bonding electrons.

Although the strength of the metal-interstitial bonding is a major factor in stabilizing the metal framework of a centered cluster, significant amounts of metal-metal bonding also exist and are important in cluster formation and stability, particularly in the compounds with less electronegative interstitial elements. In 14-electron centered clusters, a maximum of 8 cluster-bonding electrons are involved in metal-interstitial bonding which leaves 6 electrons exclusively for metal-metal bonding (t_{2g} set). A convenient method of accessing the differences in metal-metal bonding between centered and empty clusters and between clusters with different interstitial atoms is found in the metal-metal overlap populations of the occupied cluster orbitals. For instance, by comparing the metal-metal overlap populations of the hypothetical 14-electron cluster $\text{Zr}_6\text{Cl}_{18}^{4-}$ and $\text{Zr}_6\text{Cl}_{18}\text{C}^{4-}$, one finds that the centered cluster has only 35% of the metal-metal bonding of the empty cluster. Approximately 80% of the Zr-Zr bonding in the centered cluster comes from the 6 electrons in the t_{2g} set, while the remaining 20% is residual

metal-metal bonding in the a_{1g} and t_{1u} Zr-C bonding sets. The a_{1g} and t_{1u} orbitals retain approximately 6 and 12.5% of their original Zr-Zr bonding character, respectively, after carbon inclusion. The energy of the interstitial atom's valence orbitals strongly affect the percentage of interstitial character present in the newly formed a_{1g} and t_{1u} orbitals and, hence, the degree of metal-metal bonding retained. Beryllium, with valence orbital ionization energies of -10.0 and -6.0 eV for the 2s and 2p orbitals, respectively, compared to values of -21.4 and -11.4 eV for carbon, gives a centered cluster which retains more than 60% of the Zr-Zr bonding present in an unoccupied isoelectronic cluster. The a_{1g} and t_{1u} orbitals, respectively, retain 26 and 56.5% of the Zr-Zr bonding character of the equivalent orbitals in the unoccupied cluster. The smaller Be contribution to the a_{1g} and t_{1u} orbitals gives the interstitial beryllium atom a calculated charge of -0.2. Overlap populations for $Zr_6Cl_{18}^{8-}$, $Zr_6Cl_{18}C^{4-}$ and $Zr_6Cl_{18}Be^{6-}$ clusters with identical geometries and dimensions are given in Table 38.

Additional Observations

The systematic chemistry observed for centered zirconium chloride clusters appears to be controlled by two principal factors: 1) the stability of 14-electron clusters and 2) the efficient packing of these clusters with the appropriate chlorine atom bridges and number of cations. These two factors have been combined and manipulated in this work to prepare over 35 examples of centered zirconium halide clusters in twelve different structure types plus several variations thereon. A

Table 38. Calculated Zr-Zr overlap populations for $Zr_6Cl_{18}Z^{n-}$

<u>∑ Zr-Zr overlap populations</u>			
Orbital	$Zr_6Cl_{18}^{8-}$	$Zr_6Cl_{18}C^{4-}$	$Zr_6Cl_{18}Be^{6-}$
a_{1g}	0.994	0.058	0.262
t_{1u} (x3)	0.562	0.070	0.317
t_{2g} (x3)	<u>0.347</u>	<u>0.347</u>	<u>0.347</u>
Total	3.721	1.309	2.254
<u>% Zr-Zr bonding retained^a</u>			
a_{1g}	100	6	26
t_{1u}	100	12.5	56.5
t_{2g}	<u>100</u>	<u>100</u>	<u>100</u>
Total	100	35	61

$${}^a\% \text{ Zr-Zr bonding retained} = \frac{\sum \text{Zr-Zr overlap pop of } Zr_6Cl_{18}Z^{n-}}{\sum \text{Zr-Zr overlap pop of } Zr_6Cl_{18}^{8-}} \times 100\%.$$

summary of the compounds, structure types and connectivities is given in Table 39.

The first factor, the so-called '14-electron rule', has been responsible for much of the stoichiometric diversity observed. The entire series $[\text{Zr}_6\text{Cl}_{12}\text{Z}]\text{Cl}_n$, where n ranges from 0 to 3, was generated simply by changes in Z and, hence, the number of electrons available from the interstitial atom. Additional stoichiometries became accessible by the addition of cations. In a limited sense, it has become possible to predict and even control the stoichiometry of a reaction product by the combination of interstitial atoms and cations present in the reaction.

The second factor, which is responsible for the structural diversity within a group of compounds having the same metal to chlorine stoichiometry, is considerably less well-understood. The consequences of this factor, however, are impressively shown by the group of $\text{M}_x\text{Zr}_6\text{Cl}_{15}\text{Z}$ compounds which exhibit four distinct structural frameworks and at least three additional variations thereon. Within the M_6X_{15} section, the general principles that govern the preferred formation of one M_6X_{15} structure type over another under a given set of conditions are noted, however, in general, the subtle ionic, covalent and repulsive interactions that determine the formation of a particular structure are difficult to recognize and to assess, particularly a priori.

Some generalities, noted after the fact and based on the variety of systems studied, can be made, however. First, the $[\text{Zr}_6\text{Cl}_{12}\text{Z}]$ unit is an integral feature in all of the reduced zirconium halide systems studied that contain a small amount of a potential interstitial element, Z . In

Table 39. Summary of interstitially stabilized zirconium clusters prepared

Structure ^a type	New isostructural compounds	Cluster connectivity ^b	Space group
$Zr_6I_{12}C$	$Zr_6Cl_{12}H$ $Zr_6Cl_{12}Be$ $Zr_6Br_{12}B$	$[Zr_6Cl_6^i Cl_{6/2}^{i-a}] Cl_{6/2}^{a-i}$	$\bar{R}3$ hexagonal
$K_2ZrCl_6 \cdot Zr_6Cl_{12}H$	$K_2Zr_7Cl_{18}H$ $Cs_2Zr_7Cl_{18}Be$	$[Zr_6Cl_{12}^i] Cl_6^a$	$\bar{R}3$ hexagonal
$KZr_6Cl_{13}Be$	$(K,Rb)Zr_6Cl_{13}Be$ $Zr_6Cl_{13}B$ $Zr_6Br_{13}B$	$[Zr_6Cl_{10}^i Cl_{2/2}^{i-i}] Cl_{6/3}^{a-a}$	Pnnm orthorhombic
Nb_6Cl_{14}	$Zr_6Cl_{14}C$ $Zr_6Cl_{14}B$ $(Li-Cs,Tl)Zr_6Cl_{14}B$ $Zr_6Br_{14}C$ $CsZr_6Br_{14}C$ $Zr_6Br_{14}Fe$	$[Zr_6Cl_{10}^i Cl_{2/2}^{i-a}] Cl_{2/2}^{a-i} Cl_{4/2}^{a-a}$	Cmca orthorhombic
Ta_6Cl_{15}	$Zr_6Cl_{15}N$ $Na_0.5Zr_6Cl_{15}C$ $Na_2Zr_6Cl_{15}B$	$[Zr_6Cl_{12}^i] Cl_{6/2}^{a-a}$	Ia3d cubic (tetragonal distortion)

$\text{CsNb}_6\text{Cl}_{15}$	$(\text{Cs}, \text{Rb})\text{Zr}_6\text{Cl}_{15}\text{C}$ $\text{KZr}_6\text{Cl}_{15}\text{C}$ $(\text{CsK}, \text{CsRb}, \text{Rb}_2)\text{Zr}_6\text{Cl}_{15}\text{B}$ $\text{KZr}_6\text{Cl}_{15}\text{N}$ $\text{CsZr}_6\text{Br}_{15}\text{Fe}$	$[\text{Zr}_6\text{Cl}_{12}^i]\text{Cl}^{a-a}_{6/2}$	Pmma orthorhombic
$\text{K}_2\text{Zr}_6\text{Cl}_{15}\text{B}$	$\text{K}_2\text{Zr}_6\text{Cl}_{15}\text{B}$ $\text{K}_2\text{Zr}_6\text{Cl}_{15}\text{Be}$	$[\text{Zr}_6\text{Cl}_{12}^i]\text{Cl}^{a-a}_{6/2}$	Cccm orthorhombic
$\text{K}_3\text{Zr}_6\text{Cl}_{15}\text{Be}$	$(\text{K}_3, \text{Rb}_3)\text{Zr}_6\text{Cl}_{15}\text{Be}$	$[\text{Zr}_6\text{Cl}_{12}^i]\text{Cl}^{a-a}_{6/2}$	C2/c monoclinic
$\text{Cs}_3\text{Zr}_6\text{Cl}_{16}\text{C}$	$\text{Cs}_3\text{Zr}_6\text{Cl}_{16}\text{C}$ $\text{Cs}_{3+}\text{Zr}_6\text{Cl}_{16}\text{B}$ $\text{Cs}_{4-}\text{Zr}_6\text{Cl}_{16}\text{Be}$	$[\text{Zr}_6\text{Cl}_{12}^i]\text{Cl}^{a-a}_{4/2}\text{Cl}^a_2$	$\text{P2}_1/\text{n}$ monoclinic
$\text{Na}_4\text{Zr}_6\text{Cl}_{16}\text{Be}$	$\text{Na}_4\text{Zr}_6\text{Cl}_{16}\text{Be}$	$[\text{Zr}_6\text{Cl}_{12}^i]\text{Cl}^{a-a}_{4/2}\text{Cl}^a_2$	Pccn orthorhombic
$\text{Rb}_5\text{Zr}_6\text{Cl}_{18}\text{B}$	$\text{Rb}_5\text{Zr}_6\text{Cl}_{18}\text{B}$	$[\text{Zr}_6\text{Cl}_{12}^i]\text{Cl}^a_6$	Pmna orthorhombic
$\text{Li}_6\text{Zr}_6\text{Cl}_{18}\text{H}$	$\text{Li}_6\text{Zr}_6\text{Cl}_{18}\text{H}^{\text{C}}$	$[\text{Zr}_6\text{Cl}_{12}^i]\text{Cl}^a_6$	$\text{R}\bar{3}$ hexagonal

^aSee Table 2 for references.

^bReference 1.

^cReference 73.

other words, no compounds containing Zr, Cl and Z (Z = Be, B, C, N or H) which could not be viewed as constructed of $Zr_6Cl_{12}Z$ clusters have been observed. The strength of the Zr-Z bond is apparently responsible. In addition, as noted in the Introduction, the terminal positions of each $Zr_6Cl_{12}Z$ cluster are invariably occupied by additional chlorine atoms in some fashion, whether it be with isolated chlorine atoms or those shared with other clusters.

Secondly, many of the structures are built-up of close-packed or pseudo-close-packed layers of atoms. The structures of $Zr_6Cl_{12}Be$, $M^I_2Zr_7Cl_{18}H$, $KZr_6Cl_{13}Be$, $Zr_6Cl_{14}C$, $K_2Zr_6Cl_{15}B$, $Rb_5Zr_6Cl_{18}B$ and $Li_6Zr_6Cl_{18}H$ can all be considered 'close-packed'. Many of the rare-earth and early transition metal halide systems that contain condensed cluster units also fit into this category.⁵⁶ The packing efficiency in close-packed structures is, of course, well-recognized. The structures which are not close-packed appear to be forced to adopt other arrangements to maintain both discrete $M_6X_{12}Z$ cluster units and to accommodate the necessary number of cations. Evidence of this is seen in both the M_6X_{15} and M_6X_{16} compounds.

Clear and largely predictable trends in the zirconium to interstitial (Z) distances and, hence, the average cluster dimensions are observed. As expected on the basis of covalent radii, Zr-Be distances are longer than Zr-B distances which are longer than Zr-C and Zr-N distances. The trend, which appears linear at least from Be to C, is plotted in Figure 49 and suggests that the cluster dimensions, i.e., the Zr-Zr distances, are determined almost exclusively by the Zr-Z contact.

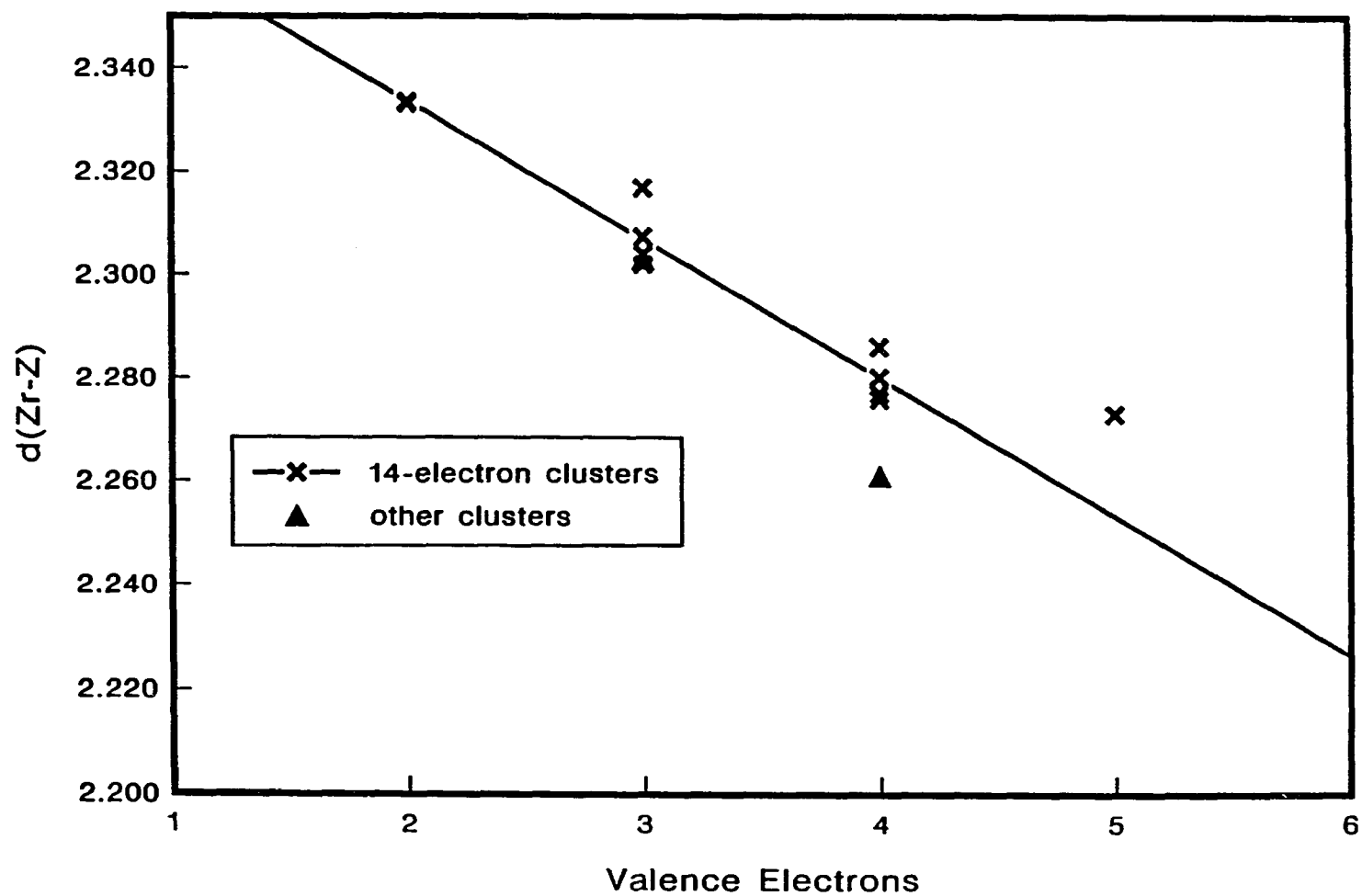


Figure 49. The average Zr-interstitial (Z) distance in structurally characterized $Zr_6Cl_{12}Z$ clusters plotted as a function of the number of interstitial valence electrons. The line was calculated by a least-squares fit of the 14-electron cluster data excluding $Zr_6Cl_{15}N$

Notable exceptions are seen in $K_2Zr_7Cl_{18}H$ and $Li_6Zr_6Cl_{18}H$ where the Zr-H distance is longer than expected and in $Cs_3Zr_6Cl_{16}C$ where the addition of a 15th electron reduces the Zr-C and Zr-Zr distances over the 14-electron examples plotted. The two hydride examples give a valuable baseline for Zr-Zr distances in 13-electron clusters ($\sim 3.196 \text{ \AA}$), as the distances in these examples are determined largely by metal-metal interactions rather than metal-interstitial contacts. The baseline for 14-electron clusters is expected to be at least 0.027 \AA shorter than in these hydrides based on the shortening of the Zr-Zr distances in $Cs_3Zr_6Cl_{16}C$ over the average distance in 14-electron carbide clusters.

Finally, all of the centered clusters prepared with the rare-earth and early transition metals other than $Nb_6I_{11}H$ and $CsNb_6I_{11}H$, are of the M_6X_{12} -type. Whether this is simply a result of the centered cluster dimensions being large enough to accommodate twelve edge-bridging X atoms around it or an inherent instability of centered M_6X_8 -type clusters because of the short interstitial to X^i atom distance is not known.

FUTURE WORK

The interstitially stabilized zirconium halide clusters studied in the course of this work are part of what has developed into an extensive class of compounds. The primary focus of this research has been the preparation and structural characterization of compounds containing $Zr_6Cl_{12}Z$ clusters with new stoichiometries and structure types. The results obtained using a relatively limited number of different interstitial elements have been nothing less than impressive. Further research along these lines is bound to result in even more new and interesting compounds. The following are suggested as potentially fruitful avenues of investigation.

Considerable effort has been expended on the preparation of new materials, but little time has been devoted to the characterization of these materials by methods other than single crystal X-ray diffraction. Other measurements of possible interest are outlined below. The odd electron clusters, $Zr_6Cl_{12}H$, $Zr_6Cl_{14}B$ and $Cs_3Zr_6Cl_{16}C$ should probably have their magnetic susceptibilities measured. The heat capacity of $Zr_6Cl_{12}H$ will likely show an anomaly when the hydrogen motion within the cluster freezes out. Although all of the cluster phases prepared are very likely to be semiconductors, conductivity measurements should be made on a couple of compounds to confirm this notion. If single crystals can be prepared of the related and highly anisotropic, condensed cluster compounds Zr_2Cl_2Z , ($Z = B, C, N$),⁶⁰ conductivity measurements would be interesting. Ionic conductivities of $MZr_6Cl_{13}Be$ and $M_xZr_6Cl_{16}Z$ compounds with one- and two-dimensional structures for cation motion,

respectively, might also be enlightening. The use of Raman or infrared spectroscopy may provide useful information on the strengths of zirconium to interstitial bonds. The vibrational stretching frequencies of the M-Z bonds are expected to lie above the lattice vibrational modes. Several centered organometallic clusters of the late transition metals show M-Z stretching frequencies in the range of 550 – 1090 cm^{-1} .^{70,152-154} Observation of a characteristic M-Z band may also provide evidence of centered metal clusters in structurally uncharacterized systems.

Several phases prepared in the course of this investigation remain unidentified. Reactions with the initial compositions $\text{LiZr}_6\text{Cl}_{15}\text{C}$, $\text{M}^{\text{I}}_3\text{Zr}_6\text{Cl}_{15}\text{C}$ ($\text{M}^{\text{I}} = \text{Na, K, Rb}$), $\text{Na}_4\text{Zr}_6\text{Cl}_{15}\text{B}$, $\text{BaZr}_6\text{Cl}_{15}\text{B}$, $\text{Cs}_3\text{Zr}_6\text{Cl}_{16}\text{C}$ and $\text{Cs}_3\text{Zr}_6\text{Cl}_{16}\text{B}$ yielded unknown products. Structural characterization of these phases will likely uncover new combinations of connectivities and possibly the first example of the elusive M_6X_{17} stoichiometry. Several of these will require preparation of single crystals, others will simply require data collection and a solution to the phase problem.

The preparation of zirconium halide clusters with multivalent cations combined with interstitial atoms has already shown some signs of success. $\text{KLaZr}_6\text{Cl}_{18}\text{C}^{63}$ ($\text{K}_2\text{Zr}_7\text{Cl}_{18}$ H-type) and an unknown compound with Ba and B have already been prepared. Not only does the potential exist for the synthesis of additional centered clusters with multivalent cation in the chlorine lattice, but the preparation of empty zirconium halide clusters may be possible. Two specific routes to empty clusters are possible, namely, outright preparation of the empty cluster by an appropriate combination of reactants or the preparation of a hydrogen-centered

cluster followed by dehydrogenation. The first route, as noted in the Bonding section, will probably require compositions which provide 15-16 cluster-bonding electrons. Possible target compounds and their electron counts include $\text{ScZr}_6\text{Cl}_{12}$ (15), $\text{Ba}_3\text{Zr}_6\text{Cl}_{15}$ (15), $\text{La}_2\text{Zr}_6\text{Cl}_{15}$ (15) and $\text{Sr}_4\text{Zr}_6\text{Cl}_{16}$ (16). The second route can be conveniently illustrated with the first target compound above. The formation of the $\text{Zr}_6\text{Cl}_{12}$ cluster may be facilitated by the presence of hydrogen to give the 16-electron cluster $\text{ScZr}_6\text{Cl}_{12}\text{H}$. Removal of the hydrogen by moderate heating in vacuum to give the empty cluster would complete the synthesis. An alternative approach to this latter route is to attempt reductive cation exchange, multivalent for monovalent, with subsequent or simultaneous hydrogen removal. For example, cations in the recently prepared compound $\text{Li}_6\text{Zr}_6\text{Cl}_{18}\text{H}^{73}$ might be exchanged for higher valent Mg^{2+} cations in a molten salt under reducing conditions to give a 15- or 16-electron cluster which could then be dehydrogenated under vacuum. Alternatively, the dehydrogenation could be attempted while the cluster was still in the molten salt with concurrent cation exchange and hydrogen removal. Interstitial extraction will of course probably be limited to those clusters containing hydrogen.

The preparation of zirconium chloride and bromide clusters with heavier interstitial elements including transition metals should be attempted. Some success in these systems has already been noted.^{63,155} Further work with the zirconium chloride and bromide systems may afford structure types not presently observed in the heavy interstitial zirconium iodide and rare earth metal halide systems.⁶²

Application of the systematic chemistry learned from this work with centered zirconium chloride clusters to other similar systems, most notably the titanium and hafnium halides, should provide further examples of centered clusters. The zirconium bromide interstitial systems, from the limited amount of work that has been done, appears to have a cluster chemistry intermediate to that observed in the chloride and iodide systems, exhibiting both a variety of structure types and cluster electron counts.

The inclusion of interstitial atoms to stabilize clusters need not be limited to halide clusters. Several known metal sulfides suggest more opportunities may be available there. The double-metal layers in $\text{Hf}_2\text{S}^{156}$ suggest an interstitial derivative chemistry similar to that seen for ZrCl with B, C, N^{60,132} and O⁵² may be possible. $\text{Ag}_2\text{F}^{157}$ may also hold some interesting possibilities. The known compound, $\text{Ta}_2\text{S}_2\text{C}^{158}$ suggests compounds with B, N and O replacing C may also be possible. In addition, chains of condensed clusters with 10-13 electrons per M_4X_6 unit such as $\text{Ta}_4\text{S}_6\text{B}$ and $\text{KNb}_4\text{S}_6\text{B}$, should not be overlooked. The electron count range encompasses the known M_4X_6 chains for scandium, $\text{Sc}_4\text{Cl}_6\text{B}$, $\text{Sc}_4\text{Cl}_6\text{N}^{40}$ and $\text{Sc}_5\text{Cl}_8\text{C}^{41}$ and the related molybdenum analogue $\text{NaMo}_4\text{O}_6^{34}$. High temperatures ($>1000^\circ\text{C}$) will probably be necessary to prepare these metal-rich sulfides.

Finally, the potential of solution and molten salt chemistry of interstitially stabilized zirconium halide clusters has barely been scratched in the present work. Opportunities for ligand exchange, cation exchange and cluster oxidation or reduction clearly exist in both media.

Once in solution, the clusters should be susceptible to many of the reactions organometallic clusters undergo,⁶⁷⁻⁷¹ possibly including even cluster condensation.¹⁵⁹⁻¹⁶¹ Intercalation of several materials including $Zr_6Cl_{13}B$ and $Zr_2Cl_2Z^{60}$ may be possible using n-butyl lithium or recently described intercalation reagents.¹⁶²

REFERENCES

1. Schäfer, H.; Schnering, H.-G. Angew Chem. 1964, 76, 833.
2. Wells, A. F. "Structural Inorganic Chemistry"; 5th ed.; Clarendon Press: Oxford, 1984; pp. 432-437.
3. Simon, A.; von Schnering, H.-G.; Schäfer, H. Z. Anorg. Allg. Chem. 1968, 361, 235.
4. Bauer, D.; von Schnering, H.-G. Z. Anorg. Allg. Chem. 1968, 361, 259.
5. Schäfer, H.; Schnering, H.-G.; Niehues, K.-J.; Nieder-Vahrenholz, H.G. J. Less-Common Met. 1965, 9, 95.
6. Simon, A.; von Schnering, H.-G.; Wöhrle, H.; Schäfer, H. Z. Anorg. Allg. Chem. 1965, 339, 155.
7. Corbett, J. D. Pure and Applied Chem. 1984, 56, 1527.
8. Corbett, J. D. Adv. Chem. Ser. 1980, 186, 329.
9. Simon, A. Angew. Chem., Int. Ed., Engl. 1981, 20, 1.
10. Poeppelmeier, K. R.; Corbett, J. D. J. Am. Chem. Soc. 1978, 100, 5039.
11. Mattausch, H.J.; Eger, R.; Simon, A. Rev. Chim. Miner. 1980, 17, 516.
12. Berroth, K.; Simon, A. J. Less-Common Met. 1981, 76, 41.
13. Berroth K.; Mattausch, H.J.; Simon, A. Z. Naturforsch. B 1980, 35, 626.
14. Corbett, J. D.; Daake, R. L.; Poeppelmeier, K. R.; Guthrie, D. H. J. Am. Chem. Soc. 1978, 100, 652.
15. Guthrie, D. H.; Corbett, J. D. Inorg. Chem. 1982, 21, 3290.
16. Berroth, K., Ph.D. Dissertation, University of Stuttgart, FRG, 1980.
17. Corbett, J. D.; Poeppelmeier, K. R.; Daake, R. L. Z. Anorg. Allg. Chem. 1982, 491, 51.
18. Lokken, D. A.; Corbett, J. D. Inorg. Chem. 1973, 12, 556.

19. Simon, A.; Holzer, N.; Mattausch, H. Z. Anorg. Allg. Chem. 1979, 456, 207.
20. Poeppelmeier, K. R.; Corbett, J. D. Inorg. Chem. 1977, 16, 1107.
21. Adolphson, D. G.; Corbett, J. D. Inorg. Chem. 1976, 15, 1820.
22. Corbett, J. D. Acc. Chem. Res. 1981, 14, 239.
23. Imoto, H.; Corbett, J. D.; Cisar, A. Inorg. Chem. 1981, 20, 145.
24. Mattausch, H.; Hendricks, J. B.; Eger, R.; Corbett, J. D.; Simon, A. Inorg. Chem. 1980, 19, 2128.
25. Poeppelmeier, K. R.; Corbett, J. D. Inorg. Chem. 1977, 16, 294.
26. Araujo, R.; Corbett, J. D. Inorg. Chem. 1981, 20, 3082.
27. Mattausch, H.; Simon, A. Holzer, N.; Eger, R. Z. Anorg. Allg. Chem. 1980, 466, 7.
28. Troyanov, S. I. Vestn. Mosk. Univ., Ser. 2: Khim. 1973, 28, 369.
29. Daake, R. L.; Corbett, J. D. Inorg. Chem. 1977, 16, 2029.
30. Cotton, F. A.; Haas, T. E. Inorg. Chem. 1964, 3, 10.
31. Robbins, D. J.; Thomson, A. J. J. Chem. Soc., Dalton Trans. 1972, 2350.
32. Bursten, B. E.; Cotton, F. A.; Stanley, G. G. Israel J. of Chem. 1980, 19, 132.
33. Hughes, B. G.; Meyer, J. L.; Fleming, P. B.; McCarley, R. E. Inorg. Chem. 1970, 9, 1343.
34. Torardi, C. C.; McCarley, R. E. J. Am. Chem. Soc. 1979, 101, 3963.
35. Ford, J. E.; Corbett, J. D.; Hwu, S.-J. Inorg. Chem. 1983, 22, 2789.
36. Smith, J. D.; Corbett, J. D. J. Am. Chem. Soc. 1985, 107, 5704.
37. Smith, J. D.; Corbett, J. D. J. Am. Chem. Soc. 1986, 108, 1927.
38. Hwu, S.-J.; Corbett, J. D.; Poeppelmeier, K. R. J. Solid State Chem. 1985, 57, 43.

39. Simon, A. J. Solid State Chem. 1985, 57, 2.
40. Hwu, S.-J.; Corbett, J. D. J. Solid State Chem. 1986, 64, 331.
41. Hwu, S.-J.; Dudis, D. S.; Corbett, J. D. Inorg. Chem. 1987, 26, 469.
42. Meyer, G.; Hwu, S.-J.; Wijeyesekera, S.; Corbett, J. D. Inorg. Chem. 1986, 25, 4811.
43. Hartman, H.; Ebert, F.; Bretschneider, O. Z. Anorg. Allg. Chem. 1931, 198, 116.
44. Ehrlich, P.; Gentsch, L. Naturwissenschaften 1953, 40, 460.
45. Filonenko, N. E.; Kudryavtsev, V. I. Doklady Akad. Nauk SSSR 1953, 88, 891.
46. Hagg, G.; Schonberg, N. Acta Crystallogr. 1954, 7, 351.
47. Ehrlich, P.; Alt, B.; Gentsch, L. Z. Anorg. Allg. Chem. 1956, 283, 58.
48. Kudielka, H.; Rohde, H. Z. Kristallogr. 1960, 114, 447.
49. Ti_2S has since been prepared. Owens, J. P.; Conard, B. R.; Fränzen, H. F. Acta Crystallogr. 1967, 23, 77.
50. Simon, A. Z. Anorg. Allg. Chem. 1967, 355, 311.
51. Imoto, H.; Corbett, J. D. Inorg. Chem. 1980, 19, 1241.
52. Seaverson, L. M.; Corbett, J. D. Inorg. Chem. 1983, 22, 2789.
53. Bateman, L. R.; Blount, J. F.; Dahl, L. F. J. Am. Chem. Soc. 1966, 88, 1082.
54. Simon, A.; von Schnering, H.-G.; Schäfer, H.; Z. Anorg. Allg. Chem. 1967, 355, 295.
55. Simon, A. Warkentin, E.; Masse, R. Angew. Chem., Int. Ed., Engl. 1981, 20, 1013.
56. Warkentin, E.; Masse, R.; Simon, A. Z. Anorg. Allg. Chem. 1982, 491, 323.
57. Simon, A. Ann. Chim. Fr. 1982, 7, 539.

58. Warkentin, E.; Simon, A. Rev. Chim. Miner. 1983, 20, 488.
59. Ziebarth, R. P.; Corbett, J. D. J. Am. Chem. Soc. 1985, 107, 4571.
60. Hwu, S.-J.; Ziebarth, R. P.; Winbush, S. v.; Ford, J. E.; Corbett, J. D. Inorg. Chem. 1986, 25, 283.
61. Rosenthal, G.; Corbett, J. D., Iowa State University, Ames, IA, unpublished research, 1985.
62. Hughbanks, T.; Rosenthal, G.; Corbett, J. D. J. Am. Chem. Soc. 1986, 108, 8289.
63. Zhang, J.; Corbett, J. D., Iowa State University, Ames, IA, unpublished research, 1986.
64. Smith, J. D.; Corbett, J. D. J. Am. Chem. Soc. 1984, 106, 4618.
65. Smith, J. D., Ph.D. Dissertation, Iowa State University, Ames, IA, 1984.
66. Albano, V. G.; Martinengo, S. Nachr. Chem. Tech. Lab. 1980, 9, 654.
67. Heaton, B. T. "Organometallic Chemistry"; Vol. 11; Burlington House: London, 1982; Chapter 9.
68. Bradley, J. S. "Adv. in Organometallic Chemistry"; Vol. 22; Academic Press, Inc.: New York, 1983; p. 1.
69. Heaton, B. T. "Organometallic Chemistry"; Vol. 12; Burlington House: London, 1983; Chapter 9.
70. Soloveichik, G. L.; Bulychev, B. M.; Semenenko, K. N. Soviet J. Coord. Chem. 1983, 9, 891.
71. Gladfelter, W. L. "Adv. Organometallic Chem"; Vol. 24; Academic Press, Inc.: New York, 1985; p. 41.
72. Imoto, H.; Simon, A., Max-Planck-Institut für Festkörperforschung, Stuttgart, FRG, unpublished research, 1980.
73. Ziebarth, R. P.; Zhang, J.; Corbett, J. D. Iowa State University, Ames, IA, unpublished research, 1986.
74. Ziebarth, R. P.; Hwu, S.-J.; Corbett, J. D. J. Am. Chem. Soc. 1986, 108, 2594.

75. Holmberg, B.; Dagerhamn, T. Acta Chem. Scand. 1961, 15, 919.
76. Juza, R. v.; Heners, J. Z. Anorg. Allg. Chem. 1964, 332, 159.
77. "The Merck Index", 8th Ed., Merck and Co., Inc.: Rahway, NJ; 1968; p. 143.
78. Corbett, J. D. and coworkers, Iowa State University, Ames, IA, unpublished research.
79. Corbett, J. D. Inorg. Syn. 1983, 22, 15.
80. Miller, A. E.; Daane, A. H.; Haberman, C. E.; Beaudry, B. J. Rev. Sci. Inst. 1963, 34, 644.
81. Schafer, H. "Chemical Transport Reactions"; Academic Press Inc.: New York, 1964; Chapter 2.
82. Holland, L. "The Properties of Glass Surfaces"; Chapman and Hall: London, 1966; Chapter 4.
83. Daake, R. L.; Corbett, J. D. Inorg. Chem. 1978, 17, 1192.
84. Imoto, H., Ames Laboratory, Iowa State University, Ames, IA, unpublished research, 1978.
85. Takusagawa, F., Ames Laboratory, Iowa State University, Ames, IA, unpublished research, 1981.
86. Clark, C. M.; Smith, D. K.; Johnson, G. J. "A Fortran IV Program for Calculating X-Ray Powder Diffraction Patterns - Version 5"; Department of Geosciences, Pennsylvania State University: University Park, PA, 1973.
87. Ziebarth, R. P., Department of Chemistry, Iowa State University, Ames, IA, unpublished research, 1984.
88. Powder Diffraction File, JCPDS International Centre for Diffraction Data, 1601 Park Lane, Swathmore, PA, 1982.
89. Similar to the instrument described by Schroeder, D. R.; Jacobson, R. A. Inorg. Chem. 1973, 12, 210.
90. Jacobson, R. A., Ames Laboratory, Iowa State University, Ames, IA, unpublished research, 1982.

91. Karcher, B. A., Ph.D. Dissertation, Iowa State University, Ames, IA, 1981.
92. Rogers, J.; Jacobson, R. A., United States AEC Report IS-2155, Iowa State University, Ames, IA, 1967.
93. Helland, B., Ames Laboratory, Iowa State University, Ames, IA, unpublished research, 1981.
94. Hubbard, C. R.; Jacobson, R. A. J. Applied Crystallogr. 1970, 3, 549.
95. Main, P.; Fiske, S. J.; Hull, S. E.; Lessinger, L.; Germain, G.; Declerq, J. P.; Woolfson, M. M.; "MULTAN 80. A System of Computer Programs for the Automatic Solution of Crystal Structures from X-Ray Diffraction Data", Department of Physics, University of York Printing Unit, York, England, 1980.
96. Richardson, J. W., Jr.; Kim, S.; Jacobson, R. A., Ames Laboratory Report IS-4902, USDOE, Iowa State University, Ames, IA, 1986.
97. Lapp, R. L.; Jacobson, R. A., United States AEC Report IS-4708, Iowa State University, Ames, IA, 1979.
98. "International Tables for X-Ray Crystallography", Vol. III; Kynoch Press: Birmingham, England, 1968.
99. Coppens, P.; Hamilton, W. C. Acta Crystallogr., Section A 1970, A26, 71.
100. Jacobson, R. A., Ames Laboratory, Iowa State University, Ames, IA, unpublished research, 1980.
101. Powell, D. R.; Jacobson, R. A., United States AEC Report IS-4737, Iowa State University, Ames, IA, 1980
102. Johnson, C. K. "ORTEP: A Fortran Thermal-Ellipsoid Plot Program for Crystal Structure Illustrations", ORNL Report 3794, Oak Ridge National Laboratory, Oak Ridge, TN, 1970.
103. Cheung, T. T. P.; Worthington, L. E.; Murphy, P. D.; Gerstein, B. C. J. Magn. Reson. 1980, 41, 158.
104. Chu, P. J.; Ziebarth, R. P.; Flanagan, L. C.; Corbett, J. D.; Gerstein, B. C. J. Am. Chem. Soc., submitted.
105. Hoffmann, R. J. Chem. Phys. 1963, 39, 1397.

106. Miller, G.; Burdett, J., University of Chicago, Chicago, IL, private communication, 1984.
107. Hughbanks, T.; Hoffmann, R. J. Am. Chem. Soc. 1983, 105, 1150.
108. Basch, H.; Gray, H. B. Theor. Chim. Acta (Berl.) 1966, 4, 367.
109. Cisar, A., Ph.D. Dissertation, Iowa State University, Ames, IA, 1978.
110. Cisar, A.; Corbett, J. D.; Daake, R. L. Inorg. Chem. 1979, 18, 836.
111. Fry, C. G.; Smith, J. D.; Gerstein, B. C.; Corbett, J. D. Inorg. Chem. 1986, 25, 117.
112. Wijeyesekera, S. D.; Corbett, J. D. Iowa State University, Ames, IA, unpublished research, 1984.
113. Wijeyesekera, S. D.; Corbett, J. D. Inorg. Chem. 1986, 25, 4709.
114. Corbett, J. D.; Marek, H. S. Inorg. Chem. 1983, 22, 3194.
115. Dudis, D. S.; Corbett, J. D.; Hwu, S.-J. Inorg. Chem. 1986, 25, 3434.
116. Gerstein, B. C.; Dybowski, C. R. "Transient Techniques in NMR of Solids"; Academic Press: New York, 1985; Chapter 3.
117. Gerstein, B. C.; Dybowski, C. R. "Transient Techniques in NMR of Solids"; Academic Press: New York, 1985; Chapter 6.
118. Rhim, W.-K.; Elleman, D. D.; Vaughan, R. W. J. Chem. Phys. 1973, 58, 1772.
119. Gerstein, B. C. Phil. Trans. Royal Soc., London 1981, A299, 521.
120. Gerstein, B. C.; Dybowski, C. R. "Transient Techniques in NMR of Solids"; Academic Press: New York, 1985; Chapter 5.
121. McLauchlan, K. A. "Magnetic Resonance"; Clarendon Press: Oxford, England, 1972; Chapter 4.
122. Carrington, A.; McLachlan, A. "Introduction to Magnetic Resonance"; Harper & Row: New York, 1967; Chapter 13.

123. Carrington, A.; McLachlan, A. "Introduction to Magnetic Resonance"; Harper & Row: New York, 1967; Chapter 6.
124. Carrington, A.; McLachlan, A. "Introduction to Magnetic Resonance"; Harper & Row: New York, 1967; Chapter 2.
125. Pearson, W. B. "The Crystal Chemistry and Physics of Metals and Alloys", Wiley-Interscience: New York, 1972.
126. Jacobson, R. A. J. Applied Crystallogr. 1976, 9, 115.
127. Shannon, R. D. Acta Crystallogr., Sec. A 1976, A32, 751.
128. Dudis, D. S.; Corbett, J. D. Inorg. Chem. 1987, accepted.
129. McCarley, R. E. Am. Chem. Soc., Symp. Ser. 1983, 211, 273.
130. Corbett, J. D.; McCarley, R. E. "Crystal Chemistry and Properties of Materials with Quasi-One-Dimensional Structures", Rouxel, J. (ed.); D. Riedel Publishing Co.: Dordrecht, Holland, 1986; p. 179-204.
131. Bodenstein, M.; Winkelband, P. Angew. Chem. 1924, 37, 439.
132. Ziebarth, R. P.; Corbett, J. D. Iowa State University, Ames, IA, unpublished research, 1983.
133. Imoto, H.; Corbett, J. D. Iowa State University, Ames, IA, unpublished research, 1978.
134. Ziebarth, R. P.; Corbett, J. D. J. Am. Chem. Soc. 1987, accepted.
135. Wells, A. F. "Structural Inorganic Chemistry"; 5th ed.; Clarendon Press: Oxford, 1984; p. 1283.
136. Biltz, W. "Raumchemie der festen Stoffe", L. Voss: Leipzig, Germany, 1935.
137. Ueno, F.; Simon, A. Acta Crystallogr., Sec. C 1985, C41, 308.
138. Schäfer, H.; von Schnering, H.-G.; Tillack, J.; Kuhnen, F.; Wöhrle, H.; Baumann, H. Z. Anorg. Allg. Chem. 1967, 353, 281.
139. Leduc, L.; Perrin, A.; Sergent, M. Comptes Rendus des Seances de L'Academie des Sciences, Series 2 1983, 296, 961.
140. Perrin, C.; Sergent, M. J. Less-Common Met. 1986, 123, 117.

141. C-centered orthorhombic cell, space group = Cmc₂ or Cmc₂; a = 18.518, b = 31.022, c = 18.406 Å.
142. Hughbanks, T.; Dudis, D. S.; Corbett, J. D., Iowa State University, Ames, IA, unpublished research, 1986.
143. Rouxel, J. "Intercalated Layered Materials" Levy, F. (ed.); D. Riedel Publishing Co., Dordrecht, Holland, 1979; p. 201-250.
144. Koknat, F. W.; McCarley, R. E. Inorg. Chem. 1974, 13, 295.
145. Schäfer, H.; Plantz, H.; Baumann, H. Z. Anorg. Allg. Chem. 1973, 401, 63.
146. Christiano, S. P.; Wang, J.; Pinnavaia, T. J. Inorg. Chem. 1985, 24, 1222.
147. Rogel, F.; Corbett, J. D., Iowa State University, Ames, IA, unpublished research, 1986.
148. Lauher, J. W. J. Am. Chem. Soc. 1978, 100, 5305.
149. Zr^I K, ⁶⁴Zr X₆ H (X = Cl, Br), M^I₂Zr₇Cl₁₈H, Zr₆Cl₁₄B, K₂Zr₆Cl₁₅Be and ¹²Li₆Zr₆Cl₁₈H.⁷³
150. von Schnering, H.-G.; Wöhrle, H.; Schäfer, H. Naturwissenschaften 1961, 48, 159.
151. Simon, A.; von Schnering, H.-G. J. Less-Common Met. 1966, 11, 31.
152. Oxtan, I. A.; Kettle, S. F. A.; Jackson, P. F.; Johnson, B. F. G.; Lewis, J. J. Chem. Soc., Chem. Commun. 1979, 687.
153. Bor, G.; Stanghellini, P. L. J. Chem. Soc., Chem. Commun. 1979, 886.
154. Stanghellini, P. L.; Longoni, G. J. Chem. Soc., Dalton Trans. 1987, 685.
155. Hughbanks, T.; Corbett, J. D. Iowa State University, Ames, IA, unpublished research, 1987.
156. Franzen, H. F.; Graham, J. Z. Kristallogr. 1966, 123, 133.
157. Argay, Gy.; Naray-Szabó, Acta Chim., Acad. Sci. Hung. 1966, 49, 329.

158. Beckman, O.; Boller, H.; Nowotny, H. Monatshefte Chem. 1970, 101, 945.
159. Drake, S. R.; Hendrick, K.; Johnson, B. F. G.; Lewis, J.; McPartlin, M.; Morris, J. J. Chem. Soc., Chem. Commun. 1986, 929.
160. Adams, R. D.; Babin, J. E. Inorg. Chem. 1987, 26, 980.
161. Mednikov, E. G.; Eremenko, N. K.; Slovokhotov, Y. L.; Struchkov, Y. T. J. Chem. Soc., Chem. Commun. 1987, 218.
162. Kanatzidis, M. G.; Marks, T. J. Inorg. Chem. 1987, 26, 783.

ACKNOWLEDGEMENTS

The author wishes to thank Professor John D. Corbett for his support, encouragement, enthusiasm and constructive criticism during the course of this work.

Thanks are due to Professor R. A. Jacobson and members of his group for assistance with and use of the diffractometers and crystallographic programs, and to B. Beaudry and coworkers for use of the metal-working facilities. Use of the equipment and facilities of the Ames Laboratory, DOE is gratefully acknowledged.

The solid state NMR results were made possible by the excellent work of P. J. Chu. P. J. Chu and B. C. Gerstein are also thanked for their useful discussions of the NMR results.

S. Wijeyesekera is kindly thanked for his help with and knowledgeable advice concerning the extended-Hückel calculations. The friends and coworkers of the author are warmly remembered for their help, suggestions and patience.

The author wishes to express his sincere appreciation for the recognition and support of the Proctor and Gamble and Gilman Fellowships during this research.

Finally, special thanks are extended to my parents and family for their love, support and encouragement.

"Composition is, for the most part, an effort of slow diligence and steady perseverance to which the mind is dragged by necessity or resolution."

Samuel Johnson

APPENDIX A. ATOMIC ORBITAL PARAMETERS AND CLUSTER GEOMETRIES
USED IN EXTENDED-HÜCKEL CALCULATIONS

ATOMIC ORBITAL PARAMETERS USED IN EXTENDED-HÜCKEL CALCULATIONS

	orbital	H_{ij} (eV)	ζ_1^a	c_1^b	ζ_2^a	c_2^b
Zr	5s	-7.71	1.82			
	5p	-4.88	1.78			
	4d	-8.04	3.84	0.6213	1.505	0.5798
Cl	3s	-30.00	2.36			
	3p	-15.00	2.04			
C	2s	-21.4	1.625			
	2p	-11.4	1.625			
Be	2s	-10.0	0.975			
	2p	- 6.0	0.975			
Nb	5s	- 8.24	1.89			
	5p	- 5.24	1.85			
	4d	- 9.72	4.08	0.6404	1.637	0.5519

^aSlater-type orbital exponents.

^bCoefficients used in the double-zeta expansion.

CLUSTER GEOMETRIES USED IN EXTENDED-HÜCKEL CALCULATIONS

CLUSTER	ATOM	x	y	z
$Zr_6Cl_{18}^{4-}$	Zr	0	0	2.2840
	Zr	1.6150	1.6150	
	Cl	0	0	4.8840
	Cl	3.4535	3.4535	0
	Cl	3.5625	0	0
	Cl	1.7812	1.7812	2.5191
$Zr_6Cl_{18}Zn^{n-}$	Zr	0	0	2.2840
	Zr	1.6150	1.6150	
	Cl	0	0	4.8840
	Cl	3.4535	3.4535	0
	Cl	3.5625	0	0
	Cl	1.7812	1.7812	2.5191
	Z	0	0	0

APPENDIX B. OBSERVED AND CALCULATED STRUCTURE FACTOR AMPLITUDES
FOR $\text{KZr}_6\text{Cl}_{13}\text{Be}$

H = 0				H = 1				H = 2				H = 3			
K	L	Fo	Fc	K	L	Fo	Fc	K	L	Fo	Fc	K	L	Fo	Fc
0	0	2	154	0	0	1	80	7	7	1	32	1	1	8	43
0	0	4	436	0	0	3	70	7	7	2	134	2	0	0	35
0	0	6	14	0	0	5	153	7	7	3	19	2	1	1	80
0	0	8	182	0	0	7	87	7	7	4	61	2	2	2	247
1	1	1	135	0	0	9	105	7	7	5	61	2	3	3	207
1	1	3	54	1	1	0	211	7	7	6	61	2	4	4	17
1	1	5	183	1	1	1	61	7	7	7	30	2	5	5	46
1	1	7	98	1	1	2	76	7	7	8	49	2	6	6	135
1	1	9	114	1	1	3	97	7	7	9	49	2	7	7	177
2	2	0	34	1	1	4	129	8	8	0	107	2	8	8	135
2	2	2	103	1	1	7	76	8	8	1	39	2	9	9	177
2	2	6	29	1	1	8	24	8	8	2	68	2	9	9	38
2	2	8	40	2	2	0	65	8	8	3	16	3	0	0	213
3	3	1	105	2	2	1	64	8	8	4	16	3	1	1	18
3	3	3	92	2	2	2	42	8	8	5	16	3	1	1	5
3	3	5	75	2	2	3	90	9	9	0	25	3	2	2	253
3	3	7	61	2	2	4	13	9	9	1	70	3	4	4	107
3	3	9	39	2	2	6	16	9	9	2	25	3	6	6	91
4	4	0	106	2	2	7	60	9	9	3	24	3	8	8	18
4	4	2	21	2	2	8	30	9	9	4	24	4	0	0	159
4	4	4	65	3	3	0	84	9	9	5	100	4	0	0	159
4	4	6	56	3	3	1	13	9	9	7	16	4	1	1	107
5	5	1	31	3	3	2	77	10	10	0	61	4	2	2	12
5	5	3	114	3	3	3	88	10	10	1	49	4	3	3	29
5	5	5	129	3	3	4	57	10	10	2	30	4	4	4	105
5	5	7	120	3	3	5	52	10	10	3	30	4	5	5	156
5	5	9	90	3	3	6	42	10	10	4	36	4	7	7	61
6	6	0	147	3	3	7	79	10	10	6	50	4	8	8	62
6	6	2	415	3	3	8	21	10	10	7	78	4	9	9	98
6	6	4	67	3	3	9	30	11	11	0	90	5	0	0	167
6	6	6	230	4	4	0	26	11	11	1	45	5	1	1	13
6	6	8	37	4	4	1	120	11	11	2	116	5	2	2	24
7	7	1	40	4	4	2	58	11	11	3	54	5	4	4	112
7	7	3	138	4	4	3	47	11	11	4	55	5	5	5	27
7	7	5	49	4	4	4	27	11	11	5	32	5	6	6	43
7	7	7	127	4	4	5	107	11	11	6	43	5	8	8	36
8	8	0	54	4	4	8	53	12	12	0	111	6	0	0	63
8	8	2	51	4	4	9	59	12	12	1	119	6	1	1	50
8	8	4	35	4	4	1	120	12	12	2	19	6	3	3	60
8	8	6	47	4	4	2	58	12	12	3	43	6	4	4	45
8	8	8	138	4	4	3	47	12	12	4	97	6	5	5	28
9	9	1	32	4	4	4	27	12	12	5	62	6	6	6	28
9	9	3	33	4	4	5	107	12	12	6	24	6	7	7	39
9	9	5	28	4	4	8	53	12	12	7	23	6	8	8	16
9	9	7	25	4	4	9	59	13	13	0	68	7	0	0	108
10	10	0	52	4	4	1	120	13	13	1	19	7	1	1	16
10	10	2	52	5	5	0	149	13	13	2	55	7	2	2	62
10	10	4	33	5	5	1	89	13	13	3	40	7	2	2	62
11	11	0	210	5	5	2	148	14	14	0	39	7	4	4	65
11	11	2	100	5	5	3	56	14	14	1	16	7	5	5	17
11	11	4	169	5	5	4	75	14	14	2	76	7	5	5	14
12	12	0	24	5	5	5	79	14	14	3	21	8	0	0	179
12	12	2	27	5	5	6	47	14	14	4	21	8	1	1	109
12	12	4	44	5	5	7	26	15	15	0	21	8	2	2	22
12	12	6	48	5	5	8	21	15	15	1	25	8	2	2	25
13	13	1	44	5	5	9	43					8	4	4	148
13	13	3	33	6	6	0	18					8	5	5	162
13	13	5	79	6	6	1	12					8	7	7	45
14	14	0	42	6	6	2	115					8	8	8	89
14	14	2	24	6	6	3	101					9	0	0	215
14	14	4	46	6	6	4	18					9	2	2	73
14	14	6	30	6	6	5	80					9	3	3	12
				6	6	6	66					9	4	4	151
				6	6	7	110					10	1	1	14
				6	6	8	20					10	2	2	23
				7	7	0	16					10	3	3	56
												10	4	4	67
												10	5	5	67
												10	6	6	22
												10	6	6	22

7	1	24	26	3	2	31	30	H = 8		8	5	54	52	6	1	15	16			
7	2	59	59	3	3	95	95	K	L	Fo	Fc	8	6	15	19	6	2	42	44	
7	3	27	27	3	5	70	69	0	0	355	356	9	0	58	58	6	3	71	69	
7	4	109	106	3	6	14	15	0	2	53	56	9	1	30	32	6	4	22	22	
7	5	54	53	3	7	98	96	0	4	261	261	9	2	27	31	6	5	73	73	
7	6	14	7	4	0	67	65	0	8	109	109	9	3	31	34	6	6	33	32	
7	7	44	44	4	1	78	77	1	0	133	131	9	4	35	34	7	0	15	17	
8	0	161	161	4	2	77	77	1	1	74	74	9	5	25	26	7	2	89	89	
8	1	74	75	4	3	62	60	1	2	60	61	10	2	45	46	7	6	37	36	
8	2	49	40	4	4	25	24	1	3	16	20	10	3	40	40	8	0	28	26	
8	4	128	128	4	5	62	61	1	4	93	94	10	4	28	27	8	2	19	20	
8	5	116	113	4	7	36	36	1	5	113	112	10	5	33	30	8	3	18	15	
8	6	37	19	4	8	33	33	1	6	20	22	11	0	53	52	8	4	26	20	
8	7	29	32	5	0	75	73	1	7	47	51	11	2	55	52	8	6	20	21	
9	0	108	106	5	1	60	61	1	8	36	38	11	3	67	62	9	1	40	41	
9	2	29	31	5	2	39	31	2	0	29	30	11	4	40	40	9	2	51	51	
9	4	65	63	5	3	17	18	2	2	63	64	12	0	149	140	9	3	31	32	
9	6	21	20	5	4	47	47	2	3	54	55	12	2	56	56	9	5	40	38	
10	0	42	45	5	5	73	73	2	5	49	50	13	0	53	54	10	1	24	23	
10	1	24	26	6	1	23	22	2	6	26	26	13	1	26	32	10	2	55	53	
10	2	60	61	6	2	85	87	2	7	63	63					10	3	72	67	
10	3	26	28	6	3	59	61	2	8	20	20					10	4	31	6	
10	4	30	29	6	5	19	10	3	0	70	70	H = 9				11	0	107	101	
10	5	65	60	6	6	53	53	3	1	78	78	K	L	Fo	Fc	11	1	32	35	
10	6	28	29	6	7	60	60	3	2	67	70	0	3	56	56	11	2	83	78	
11	1	17	19	7	0	17	19	3	3	73	71	0	5	106	106	11	3	28	30	
11	2	84	76	7	1	27	28	3	4	32	36	0	7	73	73	12	0	50	49	
11	4	17	16	7	2	84	83	3	5	62	64	1	0	142	140	12	2	23	27	
11	5	38	37	7	3	37	37	3	7	54	52	1	1	27	28					
12	0	40	39	7	4	26	26	4	0	81	80	1	2	33	35	H = 10				
12	1	53	54	7	5	71	67	4	1	26	28	1	3	22	23	K	L	Fo	Fc	
12	2	19	22	7	6	51	51	4	3	32	34	1	4	91	90	0	0	71	70	
12	3	27	27	7	7	49	50	4	4	54	51	1	5	23	25	0	2	77	77	
12	4	23	25	8	0	115	113	4	5	65	65	1	6	23	23	0	4	31	34	
13	0	87	85	8	1	12	10	4	6	36	35	2	0	41	40	0	6	20	23	
13	2	69	67	8	2	56	55	4	7	47	49	2	1	18	19	1	2	37	39	
13	3	28	30	8	3	20	2	5	0	75	74	2	3	49	49	1	3	42	42	
14	0	23	23	8	4	71	67	5	2	95	95	2	4	37	37	1	4	15	15	
14	2	85	83	8	7	16	7	5	3	71	70	2	7	40	42	1	5	37	39	
				9	0	25	28	5	4	49	52	3	0	83	81	1	7	50	51	
				9	1	67	68	5	5	72	71	3	1	19	18	2	0	29	30	
	H = 7			9	2	24	23	5	6	53	54	3	2	55	55	2	1	50	49	
	K	L	Fo	Fc	9	4	15	21	5	7	77	77	3	3	20	25	2	2	48	48
0	1	61	61	9	5	106	106	6	0	73	70	3	4	62	63	2	3	112	112	
0	5	83	85	10	0	79	79	6	2	254	257	3	6	43	41	2	4	14	16	
1	0	84	85	10	1	52	52	6	4	31	29	4	0	40	42	2	6	42	47	
1	1	20	21	10	1	19	18	6	6	131	143	4	1	59	59	2	7	97	104	
1	2	26	26	10	2	57	53	7	0	47	46	4	2	30	30	3	0	124	122	
1	3	78	80	10	3	53	49	7	1	30	31	4	4	37	39	3	2	162	162	
1	4	60	60	10	4	41	38	7	2	91	92	4	5	77	78	3	4	74	77	
1	5	26	27	10	5	15	17	7	3	87	88	4	6	21	24	3	6	77	77	
1	7	72	74	10	6	27	31	7	4	32	27	5	0	83	80	4	0	24	11	
1	8	22	23	11	1	67	63	7	5	21	23	5	1	43	44	4	1	61	60	
2	0	84	83	11	2	42	44	7	6	47	49	5	2	123	124	4	2	42	41	
2	1	48	47	11	3	108	105	7	7	73	83	5	3	46	44	4	4	20	20	
2	2	96	96	12	0	89	84	8	0	32	32	5	4	34	35	4	5	91	92	
2	3	53	52	12	4	54	53	8	1	22	23	5	5	31	30	5	0	63	61	
2	4	30	33	13	0	16	19	8	2	46	46	5	6	50	48	5	1	25	27	
2	5	24	23	13	1	28	31	8	3	21	23	5	7	33	35	5	2	19	18	
2	7	35	36	13	2	28	29	8	4	21	20	6	0	26	27	5	3	21	26	

APPENDIX C. OBSERVED AND CALCULATED STRUCTURE FACTOR AMPLITUDES
FOR $Zr_6Cl_{14}C$

APPENDIX D. OBSERVED AND CALCULATED STRUCTURE FACTOR AMPLITUDES
FOR $Zr_6Cl_{14}B$

H = 0	K L FO FC	10 5 72 71	9 8 76 79	12 7 42 37	2 3 449 390	H = 5	K L FO FC	H = 6	K L FO FC
0 6 148 147	10 7 85 87	9 9 56 55	14 0 43 34	2 4 247 210	2 4 247 210	0 4 1 88 82	0 4 1 88 82	0 4 1 88 82	0 4 1 88 82
0 8 418 429	10 8 71 77	9 10 73 74	14 4 68 54	2 5 266 237	2 5 266 237	1 2 212 187	1 2 212 187	1 2 212 187	1 2 212 187
0 10 99 103	10 10 59 61	9 12 40 41	16 0 40 35	2 6 228 208	2 6 228 208	1 3 91 84	1 3 91 84	1 3 91 84	1 3 91 84
0 14 125 130	10 11 92 92	11 2 43 37	16 0 40 35	2 7 93 84	2 7 93 84	1 4 51 43	1 4 51 43	1 4 51 43	1 4 51 43
2 0 79 79	12 1 70 63	13 1 107 95	16 0 40 35	2 8 73 67	2 8 73 67	1 5 86 72	1 5 86 72	1 5 86 72	1 5 86 72
2 1 56 62	12 4 50 47	13 3 41 42	16 0 40 35	2 9 56 58	2 9 56 58	1 6 109 95	1 6 109 95	1 6 109 95	1 6 109 95
2 2 45 48	12 6 38 39	13 5 101 92	16 0 40 35	2 10 58 54	2 10 58 54	1 7 53 47	1 7 53 47	1 7 53 47	1 7 53 47
2 3 43 49	12 7 51 45	13 7 50 49	16 0 40 35	2 11 229 225	2 11 229 225	1 8 72 70	1 8 72 70	1 8 72 70	1 8 72 70
2 4 137 141	12 8 158 160	13 9 85 80	16 0 40 35	2 12 91 90	2 12 91 90	1 9 75 70	1 9 75 70	1 9 75 70	1 9 75 70
2 5 51 56	12 9 61 59	13 10 115 115	16 0 40 35	2 13 46 46	2 13 46 46	1 10 115 110	1 10 115 110	1 10 115 110	1 10 115 110
2 6 56 53	14 0 134 115	15 5 50 46	16 0 40 35	2 14 122 122	2 14 122 122	1 11 46 41	1 11 46 41	1 11 46 41	1 11 46 41
2 7 39 38	14 4 130 112	15 5 50 46	16 0 40 35	2 15 89 87	2 15 89 87	1 12 59 62	1 12 59 62	1 12 59 62	1 12 59 62
2 8 55 59	14 6 66 65	15 5 50 46	16 0 40 35	2 16 83 82	2 16 83 82	1 13 55 51	1 13 55 51	1 13 55 51	1 13 55 51
2 9 36 41	16 2 91 82	15 5 50 46	16 0 40 35	2 17 38 43	2 17 38 43	1 14 93 97	1 14 93 97	1 14 93 97	1 14 93 97
2 11 44 46	16 3 51 42	15 5 50 46	16 0 40 35	2 18 78 82	2 18 78 82	2 212 209	2 212 209	2 212 209	2 212 209
2 12 60 62	16 3 51 42	15 5 50 46	16 0 40 35	2 19 80 82	2 19 80 82	3 3 70 65	3 3 70 65	3 3 70 65	3 3 70 65
2 13 40 45	16 3 51 42	15 5 50 46	16 0 40 35	2 20 82 82	2 20 82 82	3 4 29 26	3 4 29 26	3 4 29 26	3 4 29 26
4 0 127 131	16 3 51 42	15 5 50 46	16 0 40 35	2 21 158 158	2 21 158 158	3 5 145 133	3 5 145 133	3 5 145 133	3 5 145 133
4 1 41 39	16 3 51 42	15 5 50 46	16 0 40 35	2 22 49 45	2 22 49 45	3 6 182 168	3 6 182 168	3 6 182 168	3 6 182 168
4 2 244 249	16 3 51 42	15 5 50 46	16 0 40 35	2 23 81 84	2 23 81 84	3 7 41 35	3 7 41 35	3 7 41 35	3 7 41 35
4 3 342 362	16 3 51 42	15 5 50 46	16 0 40 35	2 24 49 45	2 24 49 45	3 8 93 87	3 8 93 87	3 8 93 87	3 8 93 87
4 4 141 144	16 3 51 42	15 5 50 46	16 0 40 35	2 25 82 82	2 25 82 82	3 9 69 67	3 9 69 67	3 9 69 67	3 9 69 67
4 5 234 230	16 3 51 42	15 5 50 46	16 0 40 35	2 26 82 82	2 26 82 82	3 10 107 104	3 10 107 104	3 10 107 104	3 10 107 104
4 6 240 240	16 3 51 42	15 5 50 46	16 0 40 35	2 27 82 82	2 27 82 82	3 11 79 83	3 11 79 83	3 11 79 83	3 11 79 83
4 7 105 104	16 3 51 42	15 5 50 46	16 0 40 35	2 28 43 43	2 28 43 43	3 12 47 43	3 12 47 43	3 12 47 43	3 12 47 43
4 8 65 62	16 3 51 42	15 5 50 46	16 0 40 35	2 29 82 82	2 29 82 82	3 13 79 83	3 13 79 83	3 13 79 83	3 13 79 83
4 9 34 35	16 3 51 42	15 5 50 46	16 0 40 35	2 30 36 36	2 30 36 36	3 14 70 72	3 14 70 72	3 14 70 72	3 14 70 72
4 10 65 64	16 3 51 42	15 5 50 46	16 0 40 35	2 31 76 78	2 31 76 78	3 15 68 71	3 15 68 71	3 15 68 71	3 15 68 71
4 11 206 211	16 3 51 42	15 5 50 46	16 0 40 35	2 32 32 32	2 32 32 32	3 16 30 36	3 16 30 36	3 16 30 36	3 16 30 36
4 12 51 47	16 3 51 42	15 5 50 46	16 0 40 35	2 33 48 50	2 33 48 50	3 17 52 58	3 17 52 58	3 17 52 58	3 17 52 58
4 13 57 56	16 3 51 42	15 5 50 46	16 0 40 35	2 34 39 41	2 34 39 41	3 18 82 87	3 18 82 87	3 18 82 87	3 18 82 87
4 14 126 133	16 3 51 42	15 5 50 46	16 0 40 35	2 35 82 82	2 35 82 82	3 19 35 38	3 19 35 38	3 19 35 38	3 19 35 38
6 0 138 141	16 3 51 42	15 5 50 46	16 0 40 35	2 36 36 36	2 36 36 36	3 20 58 64	3 20 58 64	3 20 58 64	3 20 58 64
6 1 81 83	16 3 51 42	15 5 50 46	16 0 40 35	2 37 82 82	2 37 82 82	3 21 41 41	3 21 41 41	3 21 41 41	3 21 41 41
6 2 35 34	16 3 51 42	15 5 50 46	16 0 40 35	2 38 43 43	2 38 43 43	3 22 57 55	3 22 57 55	3 22 57 55	3 22 57 55
6 3 116 122	16 3 51 42	15 5 50 46	16 0 40 35	2 39 62 62	2 39 62 62	3 23 45 40	3 23 45 40	3 23 45 40	3 23 45 40
6 4 46 53	16 3 51 42	15 5 50 46	16 0 40 35	2 40 72 73	2 40 72 73	3 24 55 63	3 24 55 63	3 24 55 63	3 24 55 63
6 5 59 61	16 3 51 42	15 5 50 46	16 0 40 35	2 41 62 62	2 41 62 62	3 25 55 63	3 25 55 63	3 25 55 63	3 25 55 63
6 7 93 96	16 3 51 42	15 5 50 46	16 0 40 35	2 42 43 43	2 42 43 43	3 26 55 63	3 26 55 63	3 26 55 63	3 26 55 63
6 8 99 104	16 3 51 42	15 5 50 46	16 0 40 35	2 43 35 35	2 43 35 35	3 27 55 63	3 27 55 63	3 27 55 63	3 27 55 63
6 11 79 80	16 3 51 42	15 5 50 46	16 0 40 35	2 44 71 72	2 44 71 72	3 28 55 63	3 28 55 63	3 28 55 63	3 28 55 63
8 0 57 49	16 3 51 42	15 5 50 46	16 0 40 35	2 45 62 58	2 45 62 58	3 29 55 63	3 29 55 63	3 29 55 63	3 29 55 63
8 2 108 107	16 3 51 42	15 5 50 46	16 0 40 35	2 46 52 52	2 46 52 52	3 30 55 63	3 30 55 63	3 30 55 63	3 30 55 63
8 3 235 241	16 3 51 42	15 5 50 46	16 0 40 35	2 47 82 82	2 47 82 82	3 31 55 63	3 31 55 63	3 31 55 63	3 31 55 63
8 4 176 173	16 3 51 42	15 5 50 46	16 0 40 35	2 48 35 38	2 48 35 38	3 32 55 63	3 32 55 63	3 32 55 63	3 32 55 63
8 5 151 153	16 3 51 42	15 5 50 46	16 0 40 35	2 49 58 58	2 49 58 58	3 33 55 63	3 33 55 63	3 33 55 63	3 33 55 63
8 6 114 117	16 3 51 42	15 5 50 46	16 0 40 35	2 50 45 45	2 50 45 45	3 34 55 63	3 34 55 63	3 34 55 63	3 34 55 63
8 8 42 41	16 3 51 42	15 5 50 46	16 0 40 35	2 51 64 61	2 51 64 61	3 35 55 63	3 35 55 63	3 35 55 63	3 35 55 63
8 9 56 64	16 3 51 42	15 5 50 46	16 0 40 35	2 52 45 45	2 52 45 45	3 36 55 63	3 36 55 63	3 36 55 63	3 36 55 63
8 10 37 39	16 3 51 42	15 5 50 46	16 0 40 35	2 53 45 45	2 53 45 45	3 37 55 63	3 37 55 63	3 37 55 63	3 37 55 63
8 11 151 160	16 3 51 42	15 5 50 46	16 0 40 35	2 54 45 45	2 54 45 45	3 38 55 63	3 38 55 63	3 38 55 63	3 38 55 63
8 12 93 96	16 3 51 42	15 5 50 46	16 0 40 35	2 55 45 45	2 55 45 45	3 39 55 63	3 39 55 63	3 39 55 63	3 39 55 63
10 0 136 130	16 3 51 42	15 5 50 46	16 0 40 35	2 56 45 45	2 56 45 45	3 40 55 63	3 40 55 63	3 40 55 63	3 40 55 63
10 1 76 76	16 3 51 42	15 5 50 46	16 0 40 35	2 57 45 45	2 57 45 45	3 41 55 63	3 41 55 63	3 41 55 63	3 41 55 63
10 2 40 36	16 3 51 42	15 5 50 46	16 0 40 35	2 58 45 45	2 58 45 45	3 42 55 63	3 42 55 63	3 42 55 63	3 42 55 63
10 3 114 112	16 3 51 42	15 5 50 46	16 0 40 35	2 59 45 45	2 59 45 45	3 43 55 63	3 43 55 63	3 43 55 63	3 43 55 63
10 4 62 58	16 3 51 42	15 5 50 46	16 0 40 35	2 60 45 45	2 60 45 45	3 44 55 63	3 44 55 63	3 44 55 63	3 44 55 63
				2 61 45 45	2 61 45 45	3 45 55 63	3 45 55 63	3 45 55 63	3 45 55 63
				2 62 45 45	2 62 45 45	3 46 55 63	3 46 55 63	3 46 55 63	3 46 55 63
				2 63 45 45	2 63 45 45	3 47 55 63	3 47 55 63	3 47 55 63	3 47 55 63
				2 64 45 45	2 64 45 45	3 48 55 63	3 48 55 63	3 48 55 63	3 48 55 63
				2 65 45 45	2 65 45 45	3 49 55 63	3 49 55 63	3 49 55 63	3 49 55 63
				2 66 45 45	2 66 45 45	3 50 55 63	3 50 55 63	3 50 55 63	3 50 55 63
				2 67 45 45	2 67 45 45	3 51 55 63	3 51 55 63	3 51 55 63	3 51 55 63
				2 68 45 45	2 68 45 45	3 52 55 63	3 52 55 63	3 52 55 63	3 52 55 63
				2 69 45 45	2 69 45 45	3 53 55 63	3 53 55 63	3 53 55 63	3 53 55 63
				2 70 45 45	2 70 45 45	3 54 55 63	3 54 55 63	3 54 55 63	3 54 55 63
				2 71 45 45	2 71 45 45	3 55 55 63	3 55 55 63	3 55 55 63	3 55 55 63
				2 72 45 45	2 72 45 45	3 56 55 63	3 56 55 63	3 56 55 63	3 56 55 63
				2 73 45 45	2 73 45 45	3 57 55 63	3 57 55 63	3 57 55 63	3 57 55 63
				2 74 45 45	2 74 45 45	3 58 55 63	3 58 55 63	3 58 55 63	3 58 55 63
				2 75 45 45	2 75 45 45	3 59 55 63	3 59 55 63	3 59 55 63	3 59 55 63
				2 76 45 45	2 76 45 45	3 60 55 63	3 60 55 63	3 60 55 63	3 60 55 63
				2 77 45 45	2 77 45 45	3 61 55 63	3 61 55 63	3 61 55 63	3 61 55 63
				2 78 45 45	2 78 45 45	3 62 55 63	3 62 55 63	3 62 55 63	3 62 55 63
				2 79 45 45	2 79 45 45	3 63 55 63	3 63 55 63	3 63 55 63	3 63 55 63
				2 80 45 45	2 80 45 45	3 64 55 63	3 64 55 63	3 64 55 63	3 64 55 63
				2 81 45 45	2 81 45 45	3 65 55 63	3 65 55 63	3 65 55 63	3 65 55 63
				2 82 45 45	2 82 45 45	3			

										H = 18												
										K	L	FO	FC									
										0	0	103	113									
5	8	66	62	10	5	45	54	0	10	58	55	2	3	228	217	11	2	113	119			
5	10	84	81	10	7	58	68	0	12	93	93	2	4	128	118	H = 14						
5	12	59	60	10	8	57	65	2	4	65	56	2	5	156	141	K	L	FO	FC			
9	1	35	32	12	0	189	183	4	0	104	106	2	6	149	138	0	0	63	62			
9	2	87	86	12	1	54	49	4	1	73	80	2	7	50	43	0	0	62	62			
9	3	40	42	12	4	42	46	4	2	45	40	2	8	44	33	0	8	94	104			
9	5	68	75	14	4	102	92	4	3	106	104	2	9	55	50	2	1	76	84			
9	6	59	72	14	4	98	99	4	4	49	44	2	10	51	46	2	3	106	106			
9	8	49	54	H = 9				K				L	FO	FC								
9	10	38	40	1	1	159	154	4	8	73	67	4	1	37	41	2	4	41	45			
13	1	72	67	1	3	114	102	4	10	70	65	4	3	45	47	2	7	109	107			
13	5	55	H = 8				K				L	FO	FC									
K				L	FO	FC	H = 11				K				L	FO	FC					
0	0	568	534	1	7	81	74	6	1	51	51	6	10	38	34	4	0	80	76			
0	6	121	109	1	8	51	41	6	3	57	58	6	0	292	297	4	1	39	33			
0	8	378	339	1	9	137	123	6	7	59	61	6	6	62	62	4	3	41	40			
0	10	85	82	3	13	121	122	6	8	45	42	6	10	41	48	4	5	40	37			
2	0	40	45	3	1	37	33	6	11	42	45	8	0	76	79	6	0	90	100			
2	1	34	34	3	2	137	128	8	0	65	65	8	4	83	96	6	4	113	123			
2	2	36	28	3	6	130	120	8	1	46	51	8	6	49	50	6	6	61	58			
2	4	99	93	3	8	54	48	8	3	67	73	8	8	59	59	6	8	65	63			
2	5	33	35	3	10	78	75	8	8	53	55	10	2	97	101	8	0	63	62			
2	6	40	37	3	11	40	40	10	0	79	83	10	3	93	94	8	0	63	62			
2	8	45	41	5	1	64	64	10	1	38	39	10	5	63	73	10	0	38	42			
2	12	47	48	5	2	196	200	10	3	42	41	12	6	103	116	10	1	39	36			
4	0	88	86	5	3	57	57	10	4	41	45	12	1	54	48	10	3	53	52			
4	1	35	30	5	4	46	43	10	7	45	46	12	3	76	76	H = 15						
4	2	169	165	5	5	84	78	10	8	42	51	K				L	FO	FC				
4	3	272	252	5	6	131	124	12	0	41	37	K				L	FO	FC				
4	4	119	107	5	8	82	81	12	4	41	44	K				L	FO	FC				
4	5	189	169	5	9	65	60	H = 11				K				L	FO	FC				
4	6	209	190	5	10	141	136	K				L	FO	FC								
4	7	81	74	5	12	72	73	K				L	FO	FC								
4	8	51	48	7	1	50	53	K				L	FO	FC								
4	10	61	57	7	3	43	46	K				L	FO	FC								
4	11	175	172	7	9	55	54	K				L	FO	FC								
4	12	40	40	7	11	44	39	K				L	FO	FC								
4	13	50	46	9	1	44	39	K				L	FO	FC								
6	0	81	91	9	2	127	135	K				L	FO	FC								
6	1	54	60	9	3	55	58	K				L	FO	FC								
6	3	81	91	9	5	86	99	K				L	FO	FC								
6	5	46	46	9	6	98	109	K				L	FO	FC								
6	7	76	74	9	8	72	78	K				L	FO	FC								
6	8	75	76	9	9	51	60	K				L	FO	FC								
6	11	64	66	9	10	78	79	K				L	FO	FC								
8	2	82	88	11	2	53	53	K				L	FO	FC								
8	3	179	192	11	6	47	50	K				L	FO	FC								
8	4	125	132	13	1	90	88	K				L	FO	FC								
8	5	111	125	13	3	51	47	K				L	FO	FC								
8	6	84	87	13	5	99	96	K				L	FO	FC								
8	9	54	57	H = 10				K				L	FO	FC								
8	10	40	38	K				L	FO	FC												
8	11	132	137	K				L	FO	FC												
10	0	106	106	0	0	144	147	K				L	FO	FC								
10	1	57	57	0	4	195	164	K				L	FO	FC								
10	3	81	86	0	6	98	85	K				L	FO	FC								
10	4	39	45	0	8	91	84	K				L	FO	FC								

APPENDIX E. OBSERVED AND CALCULATED STRUCTURE FACTOR AMPLITUDES
FOR $Zr_6Cl_{15}N$

L = 0				6 3 186 184	21 4 105 89	19 19 133 142	23 6 135 140
H	K	Fo	Fc	7 2 86 46	21 8 156 155	20 2 122 86	23 10 112 39
2	2	906	897	7 4 170 173	21 14 235 235	20 6 103 84	24 13 124 123
4	0	190	174	7 6 349 342	21 16 128 118	20 8 103 77	25 4 166 143
4	4	364	347	8 3 92 79	22 1 196 192	20 16 153 149	25 8 152 111
6	2	333	361	8 5 150 150	22 3 239 239	21 3 112 89	26 3 187 188
6	4	123	103	8 7 195 198	22 5 300 312	21 5 114 80	
8	0	570	593	9 2 265 265	22 7 107 77	21 15 145 123	L = 4
8	2	203	190	9 4 276 278	23 6 136 131	21 17 139 132	H K Fo Fc
8	4	129	128	9 6 155 158	23 8 121 119	22 14 120 103	4 4 459 420
8	6	292	291	9 8 358 353	23 10 123 85	23 9 110 77	6 6 416 406
8	8	543	540	10 1 170 146	24 5 124 79	23 11 118 84	7 5 458 466
10	2	318	320	10 3 180 187	25 2 171 179	23 13 113 67	9 5 235 239
10	4	228	228	10 5 96 96	25 6 119 83	24 8 142 132	9 7 263 264
10	6	191	194	10 7 400 394	27 4 148 121	24 12 210 214	10 8 97 63
10	8	145	145	10 9 141 156		25 11 163 170	11 5 146 151
10	10	235	228	11 2 81 72	L = 2	26 6 156 138	11 9 261 264
12	0	211	203	11 4 320 323	H K Fo Fc	27 3 179 181	12 4 320 308
12	2	94	76	11 6 194 193	3 3 163 160		12 6 113 111
12	4	238	243	11 10 206 211	4 2 187 180	L = 3	12 8 182 199
12	12	319	320	12 3 373 378	5 3 216 218	H K Fo Fc	13 5 161 175
14	4	263	261	12 5 250 256	5 5 583 556	6 3 471 442	13 9 239 237
14	6	116	137	12 7 89 80	7 3 92 96	6 5 471 461	13 11 298 294
14	8	163	162	12 9 273 282	7 5 268 261	7 4 645 639	14 6 201 193
14	14	251	250	12 11 168 158	7 7 593 575	8 5 339 330	14 14 162 166
16	6	357	359	13 4 341 349	8 2 346 358	9 4 232 233	15 5 194 192
16	8	231	233	13 6 109 118	8 6 247 258	9 8 96 86	15 11 107 105
16	10	332	334	13 8 182 203	9 3 243 260	10 3 376 362	15 13 236 241
16	14	130	129	13 10 200 200	9 5 102 98	10 7 166 165	16 4 215 213
16	16	135	138	14 1 148 154	9 9 432 431	10 9 262 260	16 12 108 99
18	6	237	238	14 3 187 186	10 6 291 290	11 4 116 90	17 5 106 106
18	8	200	194	14 7 132 141	10 8 273 266	11 6 248 241	17 11 274 277
18	10	170	167	15 2 255 255	11 3 482 472	11 8 174 179	17 15 127 97
18	12	282	279	15 4 286 278	11 5 157 142	12 5 97 97	18 6 98 97
18	14	121	93	15 6 306 305	11 7 158 152	12 9 127 136	18 8 195 193
18	16	153	152	15 12 106 95	11 11 172 168	13 4 247 254	18 16 122 105
18	18	176	189	15 14 137 128	12 2 275 273	13 6 207 222	19 7 115 82
20	0	397	389	16 3 96 74	12 4 100 99	13 8 108 117	19 13 120 128
20	2	125	120	16 5 125 126	12 8 109 121	13 12 102 83	19 15 164 174
20	4	137	150	16 7 121 120	12 10 198 203	14 5 123 136	19 17 125 82
20	6	156	150	16 9 191 200	13 5 345 348	14 7 113 97	20 6 132 145
20	8	126	108	16 11 193 204	14 4 289 279	14 11 178 188	20 14 129 135
20	16	137	153	16 13 125 123	14 6 116 109	15 4 323 329	20 16 107 56
22	2	137	131	17 2 103 64	14 8 123 130	15 10 143 161	21 15 111 104
22	4	157	159	17 4 193 196	14 10 186 200	15 12 251 258	21 17 273 275
22	12	129	115	17 6 115 115	15 3 201 200	16 9 126 140	22 6 114 97
22	14	144	136	17 8 245 250	15 5 280 279	17 6 128 124	22 8 149 156
22	16	121	107	17 12 216 220	15 13 145 111	17 10 360 355	23 7 108 92
24	4	128	133	17 14 156 150	16 4 166 168	18 7 132 134	23 13 126 86
24	6	171	161	18 9 215 225	16 10 167 190	18 17 228 228	24 12 149 116
24	8	150	158	18 11 152 165	16 12 292 286	19 6 126 119	25 9 121 107
26	2	157	167	19 6 198 201	16 14 116 100	19 8 132 121	
26	4	147	119	19 8 150 154	17 3 229 232	19 10 106 91	L = 5
				19 10 208 210	17 5 141 153	19 16 169 161	H K Fo Fc
				19 18 116 54	18 6 336 328	20 9 167 162	6 5 370 387
				20 3 332 343	18 8 177 182	21 12 130 101	7 6 195 190
				20 5 343 332	18 10 157 151	21 14 131 134	8 7 131 128
				20 7 125 106	18 14 220 226	22 3 233 234	9 6 95 84
				20 11 125 118	19 7 140 130	22 5 105 77	10 5 112 105
				20 17 120 121	19 17 129 126	22 7 144 157	10 7 130 129
L = 1							
H	K	Fo	Fc				
2	1	56	47				
3	2	166	151				
5	4	317	320				
6	1	90	76				

10 9 100 87	17 11 121 108	18 12 178 178	17 15 143 136
11 8 221 224	17 13 173 168	18 16 132 142	18 14 133 127
12 9 110 120	17 17 122 136	19 15 124 130	18 16 128 105
13 6 133 141	18 10 253 253	20 8 116 90	21 13 124 100
13 10 253 255	18 12 114 76	20 14 180 170	
13 12 164 154	18 14 138 128	21 9 137 79	L = 13
14 7 98 48	19 7 268 276	21 11 121 105	H K Fo Fc
14 9 289 296	19 11 140 135	21 13 143 136	16 15 107 91
14 13 110 79	20 6 134 94	24 10 116 107	17 14 114 103
15 6 123 113	20 8 169 171		18 13 239 238
15 8 143 142	20 12 110 93	L = 9	
15 10 225 233	23 9 113 101	H K Fo Fc	L = 14
16 11 234 240	24 8 144 145	10 9 433 434	H K Fo Fc
16 15 124 59		12 11 126 133	15 15 220 216
17 6 107 94	L = 7	13 12 222 234	16 14 208 197
17 10 263 273	H K Fo Fc	14 11 119 105	
17 12 140 128	9 8 348 348	15 14 141 126	
17 14 111 65	10 7 174 174	16 11 128 99	
17 16 111 81	10 9 95 70	17 10 148 150	
18 5 98 96	11 10 340 356	17 14 170 168	
18 11 116 79	13 8 225 237	18 9 157 160	
18 15 138 139	13 10 127 100	19 10 105 88	
19 8 283 295	13 12 165 181	19 12 139 139	
19 12 186 171	14 7 124 127	19 16 162 158	
19 14 121 111	14 9 102 107	20 15 164 172	
20 7 218 217	14 13 185 189	21 14 112 71	
21 6 103 73	15 8 116 117	22 9 141 132	
21 8 143 142	15 10 115 109	22 13 120 103	
22 5 236 243	15 14 211 212	23 10 130 92	
22 9 186 179	16 9 175 171		
22 13 143 124	16 11 104 54	L = 10	
23 8 128 134	17 8 185 179	H K Fo Fc	
23 10 188 179	17 12 137 140	11 11 108 85	
24 7 170 173	17 16 139 124	12 10 140 128	
24 9 125 117	18 11 144 146	13 13 176 183	
24 11 144 116	19 10 226 234	14 12 122 123	
25 8 145 154	19 18 132 134	17 11 117 100	
	20 13 139 117	18 14 121 122	
L = 6	21 8 123 108	19 11 145 146	
H K Fo Fc	21 10 213 212	21 13 199 206	
7 7 134 148	21 14 134 91		
9 9 190 181	22 7 185 179	L = 11	
11 7 93 68	23 8 249 259	H K Fo Fc	
11 9 120 108		14 13 123 89	
11 11 413 417	L = 8	17 14 149 157	
12 6 167 168	H K Fo Fc	17 16 122 108	
12 8 109 115	8 8 222 222	18 11 124 98	
13 9 187 188	11 9 145 144	19 12 125 131	
13 11 189 194	12 8 258 270	19 14 183 177	
13 13 173 174	12 10 105 92	20 13 116 67	
14 8 164 170	12 12 324 332	20 15 175 176	
14 10 182 181	13 9 208 207	21 12 159 164	
14 12 253 258	13 11 351 357		
15 7 183 187	14 12 109 102	L = 12	
15 9 247 248	14 14 238 236	H K Fo Fc	
15 15 165 183	15 13 123 105	12 12 148 119	
16 6 248 242	16 8 115 100	14 14 137 135	
16 10 101 78	16 10 169 167	15 13 105 75	
16 12 250 243	16 12 168 169	16 12 192 195	
16 14 226 222	18 10 110 70	16 16 149 147	

APPENDIX F. OBSERVED AND CALCULATED STRUCTURE FACTOR AMPLITUDES

FOR $\text{Na}_{0.5}\text{Zr}_6\text{Cl}_{15}\text{C}$

1	59	65	7	2	514	509	12	6	76	75	14	7	59	62	16	14	35	40	
2	59	148	7	6	164	162	12	8	217	209	15	6	191	192	17	3	262	253	
3	191	194	8	5	119	118	13	3	100	104	16	7	106	105	17	5	201	193	
4	46	47	9	4	236	237	13	5	36	40	16	7	124	124	17	9	122	120	
5	88	90	10	5	131	133	13	7	205	202	17	2	40	49	18	2	109	107	
6	244	250	11	4	116	117	14	2	116	117	17	6	39	43	18	4	46	46	
7	217	216	12	7	128	128	14	6	160	158	18	7	33	37	18	6	195	188	
8	250	248	13	6	131	132	15	5	132	129	18	9	132	127	18	12	34	38	
9	283	279	14	5	61	62	16	4	131	131	19	2	32	38	19	3	74	74	
10	27	31	15	3	41	44	17	3	96	95	19	6	49	53	19	5	39	42	
11	67	72	16	2	46	45	18	2	28	32	19	8	50	50	19	7	188	180	
12	324	320	17	1	42	42	19	1	62	61	20	3	114	114	19	9	60	64	
13	162	165	18	6	61	59	20	7	120	119	21	4	56	63	19	15	28	25	
14	97	88	19	3	64	64	21	4	132	132	21	8	58	63	20	4	59	60	
15	24	27	20	2	87	85	22	3	138	134	22	3	33	38	20	8	49	54	
16	52	38	21	1	68	70	23	2	68	70	22	5	126	125	20	10	63	65	
17	393	384	22	4	40	43	24	1	92	92	22	9	176	175	20	10	63	65	
18	184	184	23	5	156	155	25	5	224	216	23	6	57	64	21	3	53	58	
19	211	212	24	4	24	24	26	2	70	71	24	3	70	73	21	7	134	130	
20	57	56	25	3	28	34	27	1	112	111	24	5	75	75	22	6	31	32	
21	42	44	26	2	55	55	28	0	40	42	25	2	37	43	22	12	33	35	
22	49	51	27	1	45	46	29	8	70	69	25	4	48	53	23	5	126	122	
23	241	240	28	3	88	90	30	2	75	80	25	8	53	58	23	9	61	66	
24	208	206	29	4	45	46	31	4	64	68	25	8	53	58	24	4	42	46	
25	31	30	30	19	4	189	181	23	5	69	69	10	0	245	250	24	8	56	60
26	72	76	31	6	59	63	32	7	162	156	10	4	43	52	10	4	43	52	
27	489	485	32	4	159	157	33	2	94	93	10	8	32	38	11	2	138	140	
28	432	425	33	2	59	59	34	2	24	24	11	3	59	59	11	6	340	330	
29	327	333	34	6	80	82	35	6	80	82	11	7	288	279	11	10	47	49	
30	623	36	35	3	87	88	36	3	68	73	12	2	143	142	12	7	30	29	
31	240	234	36	2	111	109	37	7	146	142	12	6	35	37	12	9	128	125	
32	421	418	37	4	47	58	38	5	88	93	12	8	78	81	13	2	54	58	
33	78	78	38	2	49	49	39	2	26	26	13	5	207	201	13	6	163	159	
34	293	285	39	3	42	48	40	2	57	66	13	7	88	89	13	8	288	276	
35	95	93	40	5	127	126	41	3	68	73	14	4	40	40	14	3	152	150	
36	212	214	41	6	42	48	42	6	68	73	14	4	40	40	14	3	152	150	
37	23	26	42	5	22	22	43	2	68	73	15	0	245	250	15	4	106	107	
38	51	55	43	2	201	197	44	2	42	46	15	0	245	250	15	4	106	107	
39	114	110	44	2	49	54	45	4	46	54	16	0	245	250	15	4	106	107	
40	84	83	45	3	458	493	46	1	200	209	16	0	245	250	15	4	106	107	
41	117	118	46	0	175	174	47	1	145	144	17	0	245	250	15	4	106	107	
42	128	129	47	2	305	303	48	1	145	144	17	0	245	250	15	4	106	107	
43	89	89	48	3	184	84	49	2	375	369	18	2	288	279	11	10	47	49	
44	293	291	49	4	0	119	50	6	139	141	18	8	78	81	13	2	54	58	
45	126	126	50	5	151	151	51	10	62	63	19	10	95	85	13	4	250	244	
46	107	110	51	6	281	238	52	6	229	226	19	10	95	85	13	4	250	244	
47	26	29	52	7	167	168	53	7	58	59	20	13	7	88	14	3	152	150	
48	76	75	53	8	0	513	507	11	2	57	63	14	2	144	141	14	9	79	80
49	230	227	54	8	8	8	54	11	4	204	202	14	4	35	39	15	4	106	107
50	177	176	55	8	8	160	165	11	6	79	80	14	6	123	120	15	10	69	68
51	31	31	56	9	3	66	67	11	8	128	126	14	8	132	120	15	10	69	68
52	114	114	57	9	260	254	58	9	3	105	104	15	3	98	97	16	9	80	79
53	114	114	58	10	246	247	59	10	5	84	86	15	5	174	172	17	2	46	50
54	91	93	59	10	2	29	37	13	2	55	57	15	7	38	45	17	4	195	189
55	7	7	60	10	6	69	69	13	2	170	170	15	9	58	55	17	4	195	189
56	75	75	61	11	3	186	147	13	6	136	135	16	2	132	128	17	10	57	60
57	81	81	62	11	5	167	164	13	8	174	172	16	4	64	68	18	5	55	58
58	146	146	63	12	2	104	107	13	18	30	23	16	6	54	54	18	7	109	108
59	320	320	64	12	4	161	158	14	5	221	216	16	8	122	120	19	2	77	78
60	320	320	65	12	4	161	158	14	5	221	216	16	8	122	120	19	2	77	78

19 8	100	100	20 2	44	55	2 0	61	66	67	16 11	66	67	H = 17	K L	FO	FC	H = 21	K L	FO	FC			
19 10	70	69	21 3	61	62	4 0	193	192	17 4	60	66	2 1	53	55	55	55	55	55	55	55	55		
20 1	80	82	21 5	41	41	5 1	51	53	17 12	91	91	4 1	183	181	8 1	115	116	10 1	32	39			
21 4	53	55	21 7	31	31	6 0	93	95	18 1	49	49	6 1	170	166	8 1	75							
21 8	62	63	21 11	84	88	7 1	92	92	18 5	56	55	8 1	170	166	17 6	71	75						
22 5	64	67	22 2	37	44	8 0	105	106	18 5	81	86	17 6	71	75	17 14	99	95	H = 22	K L	FO	FC		
22 11	43	52	23 1	44	53	10 0	56	54	18 7	34	42	17 14	99	95	18 3	154	149	1 1	151	146			
23 9	61	65	23 5	61	65	12 0	67	72	18 15	115	117	18 3	154	149	18 11	47	51	2 0	110	108			
24 5	47	55	23 9	61	65	14 0	197	190	19 4	96	93	19 6	36	37	19 2	73	73	3 1	174	170			
25 2	71	76	24 4	50	57	14 8	209	193	19 8	73	76	19 8	73	76	19 4	43	46	4 0	98	99			
25 4	61	65	24 6	37	42	14 12	78	76	20 9	108	106	20 1	76	76	5 1	228	223	5 1	70	73			
25 5	4	61	25 3	86	86	15 1	99	100	20 11	105	105	20 9	77	77	7 1	70	73	7 1	37	42			
H = 12	K L	FO	FC	H = 13	K L	FO	FC	H = 14	K L	FO	FC	H = 15	K L	FO	FC	H = 16	K L	FO	FC	H = 17	K L	FO	FC
0 0	168	175	2 0	56	54	15 3	42	48	21 2	75	74	21 4	49	50	21 4	148	147	12 0	55	58			
3 1	315	316	4 1	273	269	15 5	66	70	21 4	49	50	21 4	49	50	21 6	77	79	14 0	77	83			
4 0	178	177	6 1	82	85	15 7	118	119	21 8	49	54	21 6	77	79	14 0	77	79	16 0	55	59			
5 1	203	202	8 1	147	145	16 2	77	77	21 10	55	61	21 10	55	61	21 10	55	61	21 10	55	61			
6 0	42	45	13 2	55	55	16 6	166	161	23 4	63	67	23 4	63	67	23 4	63	67	23 4	63	67			
7 1	74	77	10 1	147	145	16 2	77	77	23 4	63	67	23 4	63	67	23 4	63	67	23 4	63	67			
8 0	42	45	13 2	55	55	16 6	166	161	23 4	63	67	23 4	63	67	23 4	63	67	23 4	63	67			
9 1	233	232	13 6	180	172	16 8	145	140	23 4	63	67	23 4	63	67	23 4	63	67	23 4	63	67			
10 0	30	38	13 10	133	132	16 14	170	163	23 4	63	67	23 4	63	67	23 4	63	67	23 4	63	67			
11 1	138	138	14 3	158	158	17 1	107	107	23 4	63	67	23 4	63	67	23 4	63	67	23 4	63	67			
12 4	242	242	14 7	135	134	17 3	73	78	23 4	63	67	23 4	63	67	23 4	63	67	23 4	63	67			
12 8	239	230	14 11	54	58	17 5	36	36	23 4	63	67	23 4	63	67	23 4	63	67	23 4	63	67			
13 1	50	52	15 2	75	74	17 9	101	100	23 4	63	67	23 4	63	67	23 4	63	67	23 4	63	67			
13 3	75	74	15 6	32	34	17 11	112	108	23 4	63	67	23 4	63	67	23 4	63	67	23 4	63	67			
13 5	111	110	15 12	40	39	18 2	159	154	23 4	63	67	23 4	63	67	23 4	63	67	23 4	63	67			
13 7	134	131	16 1	90	91	18 10	87	87	23 4	63	67	23 4	63	67	23 4	63	67	23 4	63	67			
13 9	165	160	16 9	44	50	18 12	93	93	23 4	63	67	23 4	63	67	23 4	63	67	23 4	63	67			
14 2	65	64	17 2	45	48	19 5	56	57	23 4	63	67	23 4	63	67	23 4	63	67	23 4	63	67			
14 4	34	43	17 6	122	121	19 7	34	44	23 4	63	67	23 4	63	67	23 4	63	67	23 4	63	67			
14 6	195	192	17 8	43	45	19 9	43	46	23 4	63	67	23 4	63	67	23 4	63	67	23 4	63	67			
14 8	82	81	17 12	45	47	19 11	112	110	23 4	63	67	23 4	63	67	23 4	63	67	23 4	63	67			
14 10	112	111	18 5	42	49	20 2	36	29	23 4	63	67	23 4	63	67	23 4	63	67	23 4	63	67			
15 1	171	175	18 13	149	142	20 4	72	74	23 4	63	67	23 4	63	67	23 4	63	67	23 4	63	67			
15 3	210	202	19 4	99	100	20 8	106	109	23 4	63	67	23 4	63	67	23 4	63	67	23 4	63	67			
15 9	34	37	19 8	42	48	21 1	134	130	23 4	63	67	23 4	63	67	23 4	63	67	23 4	63	67			
16 2	207	199	19 12	41	47	21 3	79	82	23 4	63	67	23 4	63	67	23 4	63	67	23 4	63	67			
16 4	66	72	20 7	73	73	21 9	39	43	23 4	63	67	23 4	63	67	23 4	63	67	23 4	63	67			
16 6	164	161	21 4	38	39	21 11	65	60	23 4	63	67	23 4	63	67	23 4	63	67	23 4	63	67			
16 8	132	127	21 6	37	45	22 2	47	53	23 4	63	67	23 4	63	67	23 4	63	67	23 4	63	67			
16 10	33	32	21 8	65	74	23 1	86	83	23 4	63	67	23 4	63	67	23 4	63	67	23 4	63	67			
16 12	113	109	21 10	125	123	23 1	86	83	23 4	63	67	23 4	63	67	23 4	63	67	23 4	63	67			
17 1	172	166	21 12	67	64	23 1	86	83	23 4	63	67	23 4	63	67	23 4	63	67	23 4	63	67			
17 3	58	63	22 5	60	62	23 1	86	83	23 4	63	67	23 4	63	67	23 4	63	67	23 4	63	67			
17 5	118	117	22 9	65	68	23 1	86	83	23 4	63	67	23 4	63	67	23 4	63	67	23 4	63	67			
17 7	116	112	22 11	37	48	23 1	86	83	23 4	63	67	23 4	63	67	23 4	63	67	23 4	63	67			
17 9	47	50	23 4	43	49	23 1	86	83	23 4	63	67	23 4	63	67	23 4	63	67	23 4	63	67			
18 6	62	65	23 8	57	60	23 1	86	83	23 4	63	67	23 4	63	67	23 4	63	67	23 4	63	67			
18 8	121	120	24 1	43	46	23 1	86	83	23 4	63	67	23 4	63	67	23 4	63	67	23 4	63	67			
19 3	96	96	24 3	58	58	23 1	86	83	23 4	63	67	23 4	63	67	23 4	63	67	23 4	63	67			
19 5	122	120	24 5	44	48	23 1	86	83	23 4	63	67	23 4	63	67	23 4	63	67	23 4	63	67			
19 7	43	48	24 7	45	54	23 1	86	83	23 4	63	67	23 4	63	67	23 4	63	67	23 4	63	67			
19 9	44	50	24 9	44	54	23 1	86	83	23 4	63	67	23 4	63	67	23 4	63	67	23 4	63	67			
19 11	77	78	24 11	129	127	23 1	86	83	23 4	63	67	23 4	63	67	23 4	63	67	23 4	63	67			
H = 18	K L	FO	FC	H = 19	K L	FO	FC	H = 20	K L	FO	FC	H = 21	K L	FO	FC	H = 22	K L	FO	FC	H = 23	K L	FO	FC
2 0	54	53	4 0	54	58	6 0	157	155	8 1	89	90	8 1	89	90	8 1	89	90	8 1	89	90			
6 0	157	155	8 1	89	90	8 1	89	90	8 1	89	90	8 1	89	90	8 1	89	90	8 1	89	90			
8 0	148	146	10 1	47	53	9 1	163	160	10 1	47	53	9 1	163	160	10 1	47	53	9 1	163	160			
H = 24	K L	FO	FC	H = 25	K L	FO	FC	H = 26	K L	FO	FC	H = 27	K L										

APPENDIX G. OBSERVED AND CALCULATED STRUCTURE FACTOR AMPLITUDES
FOR $\text{KZr}_6\text{Cl}_{15}\text{C}$

5	2	31	31	14	24	26	14	4	14	15	20	1	40	39	1	17	91	86	5	12	308	304	9	12	28	28	
5	3	65	64	10	78	76	14	5	92	12	20	2	30	29	2	0	120	120	5	13	20	22	9	13	50	52	
5	4	147	148	10	144	146	14	6	17	14	20	3	39	40	2	1	218	223	5	14	100	98	9	14	44	45	
5	5	48	48	10	24	22	14	7	24	35	20	4	77	78	2	2	16	17	5	16	20	19	9	15	28	31	
5	6	28	28	10	3	115	116	4	152	132	20	6	59	59	2	4	72	72	6	3	80	81	10	0	390	398	
5	7	27	25	10	69	69	14	8	74	75	20	6	58	57	2	4	72	72	6	3	80	81	10	1	116	115	
5	8	65	63	10	159	159	14	10	52	52	20	7	22	24	2	6	20	20	6	5	87	86	10	3	55	55	
5	9	19	19	10	41	41	14	12	14	16	20	8	68	70	2	6	20	20	6	5	87	86	10	4	84	87	
5	10	41	41	10	72	72	14	14	30	29	20	9	32	35	2	8	119	117	6	6	51	48	10	5	40	39	
5	11	76	77	10	8	55	56	15	0	107	104	21	1	17	2	8	77	76	6	6	70	70	10	6	29	31	
5	12	19	20	20	9	122	121	15	1	80	79	21	2	25	25	2	9	178	171	6	10	24	24	10	7	76	77
5	13	30	34	10	11	19	22	15	2	67	65	21	3	27	27	2	10	31	31	6	12	32	35	10	8	289	289
6	0	128	131	10	12	27	28	15	3	21	23	4	15	16	2	12	36	36	6	12	276	272	10	9	91	90	
6	1	263	271	10	13	108	106	15	5	27	27	5	16	14	2	13	47	48	6	13	48	48	10	11	43	43	
6	2	38	39	10	13	108	106	15	6	55	56	6	20	19	2	14	47	47	6	14	47	47	10	12	38	39	
6	3	160	163	11	0	159	158	15	7	78	74	22	0	17	19	2	15	23	26	6	15	16	19	10	14	25	30
6	4	103	103	11	1	81	80	15	8	79	80	22	1	75	71	2	16	35	37	6	16	15	17	10	15	30	32
6	5	198	199	11	2	67	67	15	9	49	50	22	3	76	73	2	17	87	84	7	0	53	53	11	0	502	513
6	6	120	119	11	3	90	89	15	10	46	47	22	4	22	22	3	0	185	192	7	1	35	33	11	2	114	113
6	7	82	81	11	4	52	51	15	13	20	21	23	1	19	21	3	1	109	111	7	2	23	24	11	3	37	37
6	8	232	229	11	5	102	101	16	0	62	60	23	2	26	28	3	2	125	127	7	3	230	231	11	4	71	71
6	9	48	47	11	6	54	55	16	1	166	162	3	3	76	77	3	3	76	77	7	4	94	93	11	5	41	41
6	10	46	46	11	7	69	69	16	2	53	51	4	4	72	71	3	4	72	71	7	5	250	249	11	6	38	37
6	11	46	53	11	8	118	118	16	3	102	102	5	5	85	83	3	5	85	83	7	6	45	44	11	8	385	382
6	12	52	53	11	9	52	53	16	4	167	168	6	6	15	16	3	6	82	80	7	7	42	41	11	10	121	122
6	13	117	116	11	9	52	53	16	5	151	149	7	7	18	16	3	7	48	46	7	8	43	44	11	11	16	19
6	14	23	24	11	10	49	48	16	6	55	55	8	8	15	14	3	8	129	127	7	9	62	61	11	12	23	26
7	0	140	145	11	11	41	41	16	6	55	55	9	9	14	15	3	8	129	127	7	9	62	61	11	12	23	26
7	1	168	169	11	12	28	30	16	7	74	75	10	10	14	15	3	9	96	95	7	11	102	101	11	13	23	25
7	2	116	117	11	13	28	30	16	8	47	45	0	0	482	544	3	10	101	99	7	12	47	48	12	0	87	87
7	3	87	87	11	14	26	30	16	9	153	153	0	1	147	149	3	11	23	25	7	13	147	146	12	1	203	201
7	4	33	34	11	15	38	40	16	10	16	10	0	2	149	150	3	12	37	39	7	14	32	33	12	2	22	22
7	5	65	66	12	0	227	224	16	12	45	47	0	3	70	67	3	13	43	44	7	15	66	64	12	3	44	45
7	6	71	70	12	2	47	47	17	0	69	68	0	4	92	92	3	14	30	31	7	16	26	28	12	4	28	27
7	7	54	53	12	3	59	60	17	3	61	60	0	5	60	59	3	16	33	32	8	1	23	25	12	5	82	82
7	8	105	104	12	4	240	240	17	4	119	117	0	6	24	25	3	17	48	48	8	2	87	87	12	6	13	15
7	9	51	51	12	5	68	67	17	5	52	52	0	7	133	133	4	0	12	11	8	3	46	47	12	7	143	145
7	10	92	91	12	6	121	119	17	7	15	15	0	8	384	380	4	1	79	79	8	4	42	43	12	8	62	63
7	11	58	59	12	8	159	160	17	8	50	52	0	9	160	160	4	2	21	24	8	5	41	41	12	9	146	146
7	12	18	20	12	10	23	27	17	11	39	41	0	10	188	160	4	3	288	303	8	6	79	78	12	10	18	19
7	13	26	30	12	11	27	26	18	0	273	261	0	11	30	30	4	4	68	69	8	7	31	31	12	12	18	17
7	14	24	24	12	12	118	120	18	2	35	36	0	12	35	35	4	5	293	291	8	8	15	4	12	13	58	60
7	15	26	28	12	13	42	44	18	3	16	16	0	13	30	29	4	6	17	17	8	10	53	54	13	0	25	27
7	16	50	51	13	0	101	97	18	4	78	77	0	14	32	31	4	9	77	75	8	11	23	27	13	1	119	118
8	0	214	216	13	1	54	52	18	5	34	32	0	15	77	74	4	10	13	16	8	12	19	22	13	2	26	28
8	1	59	60	13	2	13	16	18	6	26	29	0	16	172	163	4	11	156	151	8	13	17	18	13	3	27	27
8	2	88	87	13	3	48	48	18	6	197	196	1	0	372	393	4	12	37	34	8	14	43	45	13	4	16	20
8	3	83	82	13	4	118	120	18	10	70	72	1	1	266	273	4	13	157	153	8	15	20	23	13	5	61	60
8	4	56	56	13	5	38	37	19	0	56	54	1	4	82	81	4	15	28	28	9	0	86	85	13	6	36	36
8	5	42	42	13	6	13	13	19	1	74	72	1	5	46	47	5	0	124	127	9	1	195	194	13	7	75	76
8	6	144	143	13	7	42	42	19	2	35	34	1	6	27	26	5	1	12	13	9	2	13	15	13	8	17	19
8	7	39	41	13	8	70	71	19	3	17	18	1	7	179	178	5	2	51	54	9	3	22	23	13	9	94	94
8	8	68	67	13	9	30	33	19	4	22	22	1	8	255	250	5	3	68	69	9	4	69	68	13	13	44	46
8	9	13	15	13	11	33	33	19	5	17	17	1	9	195	187	5	4	544	556	9	5	68	69	13	14	28	26
8	10	36	38	13	12	67	68	19	6	23	23	1	11	42	42	5	5	54	52	9	6	49	49	14	0	108	105
8	11	18	16	13	13	15	17	19	7	61	62	1	12	43	42	5	6	122	120	9	7	114	114	14	1	27	28
8	12	57	57	14	0	217	213	19	8	41	42	1	13	35	36	5	8	80	79	9	8	61	61	14	2	38	38
9	2	20	20	14	1	81	80	19	9	47	50	1	14	20	22	5	9	14	13	9	9	158	155	14	3	62	60
9	3	24	24	14	2	32	31	19	10	23	22	1	15	67	67	5	10	18	18	9	10	14	14	14	4	52	52
9	4	62	63	14	3	62	63	20	0	97	92	1	16	105	101	5	11	39	42	9	11	26	26	14	5	86	86

L =

K =

H =

F =

P =

C =

L =

H =

F =

P =

C =

L =

H =

F =

P =

C =

L =

14	8	77	79	21	6	15	17	3	15	64	72	8	9	31	30	13	5	36	36	20	4	50	50	3	12	25	25	
14	9	29	33	22	0	212	198	3	16	74	60	8	10	56	54	13	6	20	21	20	5	45	46	3	14	23	25	
14	10	50	52	22	2	22	23	4	0	232	235	8	13	21	23	13	8	96	95	21	0	35	34	4	0	293	297	
14	11	36	37	22	4	1	149	152	4	1	149	152	8	14	46	47	13	10	57	57	21	1	77	74	4	1	261	262
14	12	59	62	4	2	41	41	4	2	41	41	9	1	116	113	13	11	36	37	21	3	31	29	4	2	10	30	
14	13	18	16	4	3	50	49	9	1	17	18	13	12	103	104	10	4	105	102	21	4	105	102	4	3	11	12	
14	14	20	21	4	4	26	28	9	2	45	46	14	0	34	34	14	2	21	21	5	54	54	4	4	5	36	37	
14	15	23	23	4	5	43	44	9	3	81	81	14	2	21	21	14	3	21	21	5	54	54	4	4	5	36	37	
14	16	151	149	3	7	120	115	4	7	120	115	9	5	110	110	14	4	42	42	2	0	6	6	4	7	166	160	
14	17	154	158	0	-9	102	100	9	5	110	110	14	4	42	42	14	4	42	42	2	0	6	6	4	7	166	160	
14	18	19	22	0	0	120	120	4	10	45	45	9	6	36	36	14	5	37	36	4	18	18	4	8	216	212		
14	19	37	37	0	1	150	152	4	11	36	35	9	7	16	16	14	6	27	29	18	3	16	16	4	9	220	214	
14	20	17	12	0	2	112	113	4	12	18	18	9	8	81	80	14	7	18	16	-18	-3	16	20	4	10	27	26	
14	21	80	82	0	3	25	25	4	13	22	24	9	9	35	36	14	8	30	31	-12	-2	18	20	4	11	60	57	
14	22	64	66	0	4	31	32	4	15	22	24	9	10	89	88	14	11	24	26	-11	-9	14	14	4	12	21	21	
14	23	62	64	0	4	31	32	4	15	22	24	9	10	89	88	14	11	24	26	-4	-6	13	15	4	13	31	32	
14	24	62	59	0	5	51	48	4	16	71	71	9	12	35	34	15	0	31	30	-3	-3	20	17	4	15	52	51	
14	25	158	158	0	-9	102	100	9	5	110	110	14	4	42	42	14	4	42	42	-1	-1	14	15	5	0	24	23	
14	26	19	22	0	0	120	120	4	10	45	45	9	6	36	36	14	5	37	36	0	-9	15	13	5	2	38	40	
14	27	37	37	0	1	150	152	4	11	36	35	9	7	16	16	14	6	27	29	0	0	177	178	5	3	32	33	
14	28	17	12	0	2	112	113	4	12	18	18	9	8	81	80	14	7	18	16	0	1	25	24	5	4	70	70	
14	29	80	82	0	3	25	25	4	13	22	24	9	9	35	36	14	8	30	31	0	3	14	17	5	7	17	17	
14	30	64	66	0	4	31	32	4	15	22	24	9	10	89	88	14	11	24	26	0	0	146	146	5	5	25	26	
14	31	62	64	0	4	31	32	4	15	22	24	9	10	89	88	14	11	24	26	0	3	14	17	5	7	17	17	
14	32	62	59	0	5	51	48	4	16	71	71	9	12	35	34	15	0	31	30	0	5	17	14	5	11	20	24	
14	33	34	33	0	6	95	94	5	0	192	194	9	13	78	78	15	0	31	30	0	7	26	25	2	12	34	36	
14	34	71	72	0	7	71	69	5	1	150	150	9	14	54	54	15	0	31	30	0	8	118	110	6	1	32	34	
14	35	241	238	0	8	93	91	5	3	227	226	9	15	28	31	15	4	129	128	0	0	177	178	5	3	32	33	
14	36	43	44	0	10	72	70	5	4	68	67	10	1	68	67	15	6	58	60	0	2	146	146	5	5	25	26	
14	37	36	40	0	11	37	36	5	5	270	267	10	2	55	54	15	7	23	24	0	3	14	17	5	7	17	17	
14	38	61	61	0	15	51	49	5	7	33	32	10	3	48	48	15	8	29	31	0	4	20	6	5	10	51	51	
14	39	61	61	0	15	51	49	5	7	33	32	10	3	48	48	15	8	29	31	0	4	20	6	5	10	51	51	
14	40	61	61	0	15	51	49	5	7	33	32	10	3	48	48	15	8	29	31	0	4	20	6	5	10	51	51	
14	41	61	61	0	15	51	49	5	7	33	32	10	3	48	48	15	8	29	31	0	4	20	6	5	10	51	51	
14	42	61	61	0	15	51	49	5	7	33	32	10	3	48	48	15	8	29	31	0	4	20	6	5	10	51	51	
14	43	61	61	0	15	51	49	5	7	33	32	10	3	48	48	15	8	29	31	0	4	20	6	5	10	51	51	
14	44	61	61	0	15	51	49	5	7	33	32	10	3	48	48	15	8	29	31	0	4	20	6	5	10	51	51	
14	45	61	61	0	15	51	49	5	7	33	32	10	3	48	48	15	8	29	31	0	4	20	6	5	10	51	51	
14	46	61	61	0	15	51	49	5	7	33	32	10	3	48	48	15	8	29	31	0	4	20	6	5	10	51	51	
14	47	61	61	0	15	51	49	5	7	33	32	10	3	48	48	15	8	29	31	0	4	20	6	5	10	51	51	
14	48	61	61	0	15	51	49	5	7	33	32	10	3	48	48	15	8	29	31	0	4	20	6	5	10	51	51	
14	49	61	61	0	15	51	49	5	7	33	32	10	3	48	48	15	8	29	31	0	4	20	6	5	10	51	51	
14	50	61	61	0	15	51	49	5	7	33	32	10	3	48	48	15	8	29	31	0	4	20	6	5	10	51	51	
14	51	61	61	0	15	51	49	5	7	33	32	10	3	48	48	15	8	29	31	0	4	20	6	5	10	51	51	
14	52	61	61	0	15	51	49	5	7	33	32	10	3	48	48	15	8	29	31	0	4	20	6	5	10	51	51	
14	53	61	61	0	15	51	49	5	7	33	32	10	3	48	48	15	8	29	31	0	4	20	6	5	10	51	51	
14	54	61	61	0	15	51	49	5	7	33	32	10	3	48	48	15	8	29	31	0	4	20	6	5	10	51	51	
14	55	61	61	0	15	51	49	5	7	33	32	10	3	48	48	15	8	29	31	0	4	20	6	5	10	51	51	
14	56	61	61	0	15	51	49	5	7	33	32	10	3	48	48	15	8	29	31	0	4	20	6	5	10	51	51	
14	57	61	61	0	15	51	49	5	7	33	32	10	3	48	48	15	8	29	31	0	4	20	6	5	10	51	51	
14	58	61	61	0	15	51	49	5	7	33	32	10	3	48	48	15	8	29	31	0	4	20	6	5	10	51	51	
14	59	61	61	0	15	51	49	5	7	33	32	10	3	48	48	15	8	29	31	0	4	20	6	5	10	51	51	
14	60	61	61	0	15	51	49	5	7	33	32	10	3	48	48	15	8	29	31	0	4	20	6	5	10	51	51	
14	61	61	61	0	15	51	49	5	7	33	32	10	3	48	48	15	8	29	31	0	4	20	6	5	10	51	51	
14	62	61	61	0	15	51	49	5	7	33	32	10	3	48	48	15	8	29	31	0	4	20	6	5	10	51	51	
14	63	61	61	0	15	51	49	5	7	33	32	10	3	48	48	15	8	29	31	0	4	20	6	5	10	51	51	
14	64	61	61	0	15	51	49	5	7	33	32	10	3	48	48	15	8	29	31	0	4	20	6	5	10	51	51	
14	65	61	61	0	15	51	49	5	7	33	32	10	3	48	48	15	8	29	31	0	4	20	6	5	10	51	51	
14	66	61	61	0	15	51	49	5	7	33	32	10	3	48	48	15	8	29	31	0	4	20	6	5	10	51	51	
14	67	61	61	0	15	51	49	5	7	33	32	10	3	48	48	15	8	29	31	0	4	20	6	5	10	51	51	
14	68	61	61	0	15	51	49	5	7	33	32	10	3	48	48	15	8	29	31	0	4	20	6	5	10	51	51	
14	69	61	61	0	15	51	49	5	7	33	32	10	3	48	48	15	8	29	31	0	4	20	6	5	10	51	51	
14	70	61	61	0	15	51	49	5	7	33	32	10	3	48	48	15	8	29	31	0	4	20	6	5	10	51	51	
14	71	61	61	0	15	51	49	5	7	33	32	10	3	48	48	15	8	29</										

11	7	31	33	1	7	20	22	7	9	22	23	16	1	49	49	6	5	25	25	1	4	175	169	0	5	22	26
11	8	325	318	1	8	69	68	7	11	24	25	16	3	86	83	6	9	36	39	1	6	92	113	1	0	80	78
11	10	102	101	1	10	69	65	8	10	53	53	16	3	86	83	6	10	89	88	1	6	92	113	1	0	79	77
11	11	23	20	1	11	20	22	8	1	19	23	16	3	86	83	6	10	89	88	1	6	92	113	1	0	79	77
12	0	19	17	1	12	70	68	8	3	52	52	16	3	86	83	6	10	89	88	1	6	92	113	1	0	79	77
12	1	13	14	2	0	88	87	8	4	19	22	16	3	86	83	6	10	89	88	1	6	92	113	1	0	79	77
12	4	35	33	2	2	69	67	8	5	56	56	16	3	86	83	6	10	89	88	1	6	92	113	1	0	79	77
13	0	36	37	2	3	86	85	8	6	23	24	16	3	86	83	6	10	89	88	1	6	92	113	1	0	79	77
13	1	96	95	2	4	131	150	8	7	24	24	16	3	86	83	6	10	89	88	1	6	92	113	1	0	79	77
13	4	23	26	2	5	88	87	8	8	36	37	16	3	86	83	6	10	89	88	1	6	92	113	1	0	79	77
13	5	29	31	2	7	19	18	8	11	29	31	16	3	86	83	6	10	89	88	1	6	92	113	1	0	79	77
13	7	55	56	2	8	63	63	9	0	87	85	16	3	86	83	6	10	89	88	1	6	92	113	1	0	79	77
13	8	25	28	2	10	95	91	9	1	26	27	16	3	86	83	6	10	89	88	1	6	92	113	1	0	79	77
13	9	82	82	2	11	54	51	9	2	27	30	16	3	86	83	6	10	89	88	1	6	92	113	1	0	79	77
14	0	36	35	2	12	79	77	9	3	41	43	16	3	86	83	6	10	89	88	1	6	92	113	1	0	79	77
14	1	16	22	3	0	31	30	9	5	42	42	16	3	86	83	6	10	89	88	1	6	92	113	1	0	79	77
14	3	37	38	3	1	65	65	9	8	62	64	16	3	86	83	6	10	89	88	1	6	92	113	1	0	79	77
14	4	52	51	3	2	30	36	9	9	21	24	16	3	86	83	6	10	89	88	1	6	92	113	1	0	79	77
14	5	29	28	3	3	69	69	9	10	31	33	16	3	86	83	6	10	89	88	1	6	92	113	1	0	79	77
14	8	26	27	3	4	32	32	10	0	72	72	16	3	86	83	6	10	89	88	1	6	92	113	1	0	79	77
14	9	17	21	3	5	51	51	10	1	65	65	16	3	86	83	6	10	89	88	1	6	92	113	1	0	79	77
15	0	38	37	3	7	45	46	10	2	43	43	16	3	86	83	6	10	89	88	1	6	92	113	1	0	79	77
15	3	127	123	3	8	18	23	10	3	30	31	16	3	86	83	6	10	89	88	1	6	92	113	1	0	79	77
15	4	114	112	3	9	61	59	10	4	26	28	16	3	86	83	6	10	89	88	1	6	92	113	1	0	79	77
15	5	134	131	3	10	38	39	10	6	18	20	16	3	86	83	6	10	89	88	1	6	92	113	1	0	79	77
15	7	24	27	3	11	58	57	10	7	31	33	16	3	86	83	6	10	89	88	1	6	92	113	1	0	79	77
15	8	24	28	3	12	19	20	10	8	35	37	16	3	86	83	6	10	89	88	1	6	92	113	1	0	79	77
16	2	20	21	4	0	15	18	10	9	60	62	16	3	86	83	6	10	89	88	1	6	92	113	1	0	79	77
16	7	16	16	4	1	55	55	10	10	44	46	16	3	86	83	6	10	89	88	1	6	92	113	1	0	79	77
17	0	57	56	4	3	22	24	11	1	112	111	16	3	86	83	6	10	89	88	1	6	92	113	1	0	79	77
17	1	45	44	4	5	19	23	11	4	56	57	16	3	86	83	6	10	89	88	1	6	92	113	1	0	79	77
17	2	18	17	4	6	58	58	11	5	21	22	16	3	86	83	6	10	89	88	1	6	92	113	1	0	79	77
17	3	52	51	4	7	39	39	11	6	25	28	16	3	86	83	6	10	89	88	1	6	92	113	1	0	79	77
17	4	188	186	4	9	47	47	11	7	80	81	16	3	86	83	6	10	89	88	1	6	92	113	1	0	79	77
17	5	57	56	4	10	33	34	11	9	92	93	16	3	86	83	6	10	89	88	1	6	92	113	1	0	79	77
				5	0	106	106	12	0	125	122	16	3	86	83	6	10	89	88	1	6	92	113	1	0	79	77
				5	1	39	40	12	2	31	33	16	3	86	83	6	10	89	88	1	6	92	113	1	0	79	77
				5	3	96	96	12	4	36	38	16	3	86	83	6	10	89	88	1	6	92	113	1	0	79	77
				5	5	101	102	12	6	17	21	16	3	86	83	6	10	89	88	1	6	92	113	1	0	79	77
				5	8	83	84	12	7	23	28	16	3	86	83	6	10	89	88	1	6	92	113	1	0	79	77
				5	9	49	51	12	8	92	93	16	3	86	83	6	10	89	88	1	6	92	113	1	0	79	77
				5	11	54	54	13	0	21	22	16	3	86	83	6	10	89	88	1	6	92	113	1	0	79	77
				6	1	181	177	6	1	17	18	16	3	86	83	6	10	89	88	1	6	92	113	1	0	79	77
				6	2	35	35	13	2	20	22	16	3	86	83	6	10	89	88	1	6	92	113	1	0	79	77
				6	3	77	77	13	7	27	31	16	3	86	83	6	10	89	88	1	6	92	113	1	0	79	77
				6	4	83	82	13	8	15	17	16	3	86	83	6	10	89	88	1	6	92	113	1	0	79	77
				6	5	101	101	14	0	61	60	16	3	86	83	6	10	89	88	1	6	92	113	1	0	79	77
				6	6	57	58	14	1	110	107	16	3	86	83	6	10	89	88	1	6	92	113	1	0	79	77
				6	7	27	27	14	2	21	23	16	3	86	83	6	10	89	88	1	6	92	113	1	0	79	77
				6	9	176	169	6	7	27	27	16	3	86	83	6	10	89	88	1	6	92	113	1	0	79	77
				6	12	114	107	6	9	39	39	16	3	86	83	6	10	89	88	1	6	92	113	1	0	79	77
				1	0	90	90	6	11	27	26	16	3	86	83	6	10	89	88	1	6	92	113	1	0	79	77
				1	1	21	24	7	1	17	19	16	3	86	83	6	10	89	88	1	6	92	113	1	0	79	77
				1	2	61	60	7	2	51	50	16	3	86	83	6	10	89	88	1	6	92	113	1	0	79	77
				1	3	59	57	7	3	43	42	16	3	86	83	6	10	89	88	1	6	92	113	1	0	79	77
				1	4	104	103	7	4	139	138	16	3	86	83	6	10	89	88	1	6	92	113	1	0	79	77
				1	5	21	20	7	5	39	40	16	3	86	83	6	10	89	88	1	6	92	113	1	0	79	77
				1	6	27	26	7	6	68	69	16	3	86	83	6	10	89	88	1	6	92	113	1	0	79	77

L=9
H K PO FC
-14 -4 15 19
-8 -2 14 12
-7 -10 15 18
-4 -11 18 19
0 0 45 46
0 1 181 177
0 3 57 59
0 4 172 169
0 5 106 104
0 7 93 89
0 8 39 40
0 9 176 169
0 12 114 107
1 0 90 90
1 1 21 24
1 2 61 60
1 3 59 57
1 4 104 103
1 5 21 20
1 6 27 26

L=10
H K PO FC
-7 -7 14 19
-5 -8 48 52
0 0 121 118
0 1 67 67
0 3 37 36
0 5 42 42
0 7 53 52
0 8 93 93
0 9 94 93
1 0 22 27
1 1 22 27
1 2 65 65
1 3 104 102
1 4 68 67

L=11
H K PO FC
-7 -7 14 19
-5 -8 48 52
0 0 121 118
0 1 67 67
0 3 37 36
0 5 42 42
0 7 53 52
0 8 93 93
0 9 94 93
1 0 22 27
1 1 22 27
1 2 65 65
1 3 104 102
1 4 68 67

L=12
H K PO FC
12 12
H K PO FC
0 0 294 279
0 2 35 38
0 3 25 28
0 4 68 67

APPENDIX H. OBSERVED AND CALCULATED STRUCTURE FACTOR AMPLITUDES
FOR $\text{CsKZr}_6\text{Cl}_{15}\text{B}$

L = 0				L = 1									
H	K	FO	FC	H	K	FO	FC						
0 1	20	21	8 0 298 313	18 3	178 175	2 2	124 119	6 3	180 181	9 16	65 64	14 4	35 31
0 2	368	346	8 1 64 62	18 5	197 196	2 4	33 33	6 4	150 149	10 0	200 206	14 7	55 52
0 4	41	42	8 2 197 204	18 9	96 95	2 6	35 31	6 5	207 207	10 1	57 58	14 8	58 53
0 6	145	143	8 4 321 316	18 10	33 22	2 7	24 18	6 6	45 45	10 2	96 100	14 9	95 94
0 8	1054	1077	8 6 180 181	18 11	94 95	2 8	173 173	6 7	78 77	10 3	148 150	14 10	56 52
0 9	28	25	8 7 30 39	20 0	150 149	2 9	38 28	6 8	133 136	10 4	197 203	15 0	79 76
0 10	313	306	8 8 223 222	20 1	136 130	2 10	115 116	6 9	135 136	10 5	160 160	15 1	52 53
0 16	514	512	8 9 45 48	20 4	110 103	2 11	30 19	6 10	49 10	10 6	68 63	15 3	35 39
0 17	56	20	8 10 126 124	20 5	35 34	2 12	33 24	6 11	70 67	10 7	147 150	15 4	94 95
0 18	193	190	8 12 177 180	20 6	54 50	2 16	72 72	6 12	71 73	10 8	62 59	15 5	44 44
2 0	74	75	8 14 101 100	20 7	73 72	2 18	72 69	6 13	131 130	10 9	81 80	15 7	45 47
2 1	319	319	8 16 118 113	20 8	123 120	3 0	142 148	6 14	35 32	10 10	70 71	15 8	55 55
2 2	95	90	10 0 526 544	20 9	136 135	3 1	68 70	6 16	74 73	10 11	126 130	15 9	47 43
2 3	258	254	10 1 237 239	22 0	340 337	3 2	79 78	6 17	74 74	10 12	95 100	15 10	48 45
2 4	125	124	10 2 70 70	22 2	102 101	3 3	47 48	7 0	495 514	10 13	73 72	15 11	35 22
2 5	332	324	10 3 80 78	22 3	60 59	3 4	82 76	7 1	147 147	11 0	202 208	15 12	56 58
2 6	122	118	10 4 53 52	22 5	70 68	3 5	83 83	7 2	39 40	11 1	99 101	15 13	33 31
2 7	168	165	10 5 90 90	22 6	53 50	3 6	128 126	7 3	69 70	11 2	69 69	15 14	38 28
2 8	49	45	10 6 194 192	24 0	71 68	3 7	76 73	7 4	277 280	11 3	147 148	16 0	55 56
2 9	215	213	10 7 389 387	24 1	58 56	3 8	76 75	7 5	77 75	11 4	80 80	16 1	113 113
2 11	42	46	10 8 157 157			3 13	65 61	7 6	56 60	11 5	216 220	16 3	103 104
2 12	62	61	10 9 99 97			3 14	92 91	7 7	108 109	11 6	69 65	16 4	48 44
2 13	195	195	10 10 51 49			3 15	46 46	7 8	343 341	11 8	158 159	16 5	124 123
2 14	85	84	10 11 38 43			4 0	100 102	7 9	87 89	11 9	119 118	16 7	51 47
2 15	54	49	10 12 105 107	0 0	173 166	4 1	251 253	7 10	95 97	11 10	42 42	16 8	43 46
2 16	39	26	10 13 38 43	0 1	289 269	4 2	134 132	7 11	30 16	11 11	32 25	16 9	115 114
2 17	111	110	10 14 181 182	0 2	75 66	4 3	179 178	7 12	144 144	11 12	51 51	16 11	43 49
4 0	141	139	12 0 403 419	0 3	244 235	4 4	151 150	7 13	43 39	11 13	164 167	16 12	40 32
4 1	27	25	12 1 260 259	0 4	151 150	4 5	181 178	7 14	81 79	11 14	43 41	16 13	89 88
4 2	56	53	12 2 31 30	0 5	309 295	4 6	174 172	7 15	55 56	11 15	42 35	17 0	56 55
4 3	407	407	12 3 97 96	0 6	60 59	4 7	173 172	7 16	147 147	11 16	91 88	17 1	107 106
4 4	586	586	12 4 169 166	0 7	137 132	4 8	102 101	7 17	43 41	12 0	110 109	17 3	51 50
4 5	452	447	12 5 310 311	0 8	102 101	4 9	158 160	8 0	243 248	12 1	57 59	17 4	96 96
4 7	70	71	12 6 215 216	0 9	189 186	4 10	32 30	8 1	31 30	12 2	100 100	17 5	56 55
4 8	95	92	12 7 48 48	0 10	34 33	4 11	88 90	8 2	41 42	12 3	145 149	17 6	47 40
4 9	69	66	12 8 79 80	0 11	44 44	4 12	82 81	8 4	174 175	12 4	54 55	17 7	62 58
4 10	51	53	12 9 65 59	0 12	174 175	4 13	99 102	8 5	31 15	12 5	162 163	17 8	38 39
4 11	166	166	12 10 261 262	0 13	174 175	4 14	125 124	8 6	30 24	12 6	38 35	17 9	102 101
4 12	279	281	14 0 178 178	0 14	37 36	4 15	76 75	8 8	171 170	12 7	43 42	17 10	38 35
4 13	272	272	14 1 178 178	0 15	44 39	4 16	76 75	8 9	32 28	12 8	76 79	17 11	34 24
4 15	94	96	14 2 153 158	0 16	55 54	5 0	104 105	8 10	42 39	12 9	53 48	17 12	62 62
4 16	41	36	14 3 94 93	0 17	104 102	5 1	249 255	8 12	97 96	12 10	110 111	18 1	78 78
4 17	41	41	14 4 31 31	1 0	228 221	5 2	49 51	8 16	90 85	12 11	76 75	18 2	38 33
6 0	87	90	14 5 114 113	1 1	122 120	5 3	85 87	9 0	204 207	12 12	113 110	18 3	50 50
6 1	259	267	14 6 95 99	1 2	22 19	5 4	210 206	9 1	149 151	12 13	36 18	18 4	129 128
6 2	121	120	14 7 104 105	1 3	74 72	5 5	160 160	9 2	33 32	13 0	36 36	18 5	51 49
6 3	143	140	14 8 196 197	1 4	158 154	5 6	45 48	9 3	119 120	13 1	26 26	18 6	76 72
6 4	750	780	14 9 155 155	1 5	100 95	5 7	110 105	9 4	292 293	13 2	38 40	18 7	65 67
6 5	91	94	14 10 148 146	1 6	67 63	5 8	71 67	9 5	135 137	13 3	202 203	18 8	63 62
6 6	201	202	14 11 35 37	1 7	64 63	5 9	224 224	9 6	36 40	13 4	202 203	18 9	63 62
6 7	149	148	14 12 75 78	1 8	140 139	5 10	40 31	9 7	91 92	13 5	31 28	18 11	43 34
6 8	61	58	14 13 84 81	1 9	84 81	5 11	116 115	9 8	145 147	13 6	45 45	18 12	83 80
6 9	180	182	14 14 42 33	1 10	72 71	5 12	116 115	9 9	108 111	13 7	71 72	19 0	69 68
6 11	89	82	16 0 97 96	1 11	70 70	5 13	119 117	9 10	69 72	13 8	36 29	19 1	41 40
6 12	411	419	16 1 69 70	1 12	54 56	5 14	41 27	9 11	49 50	13 9	117 117	19 2	36 36
6 13	37	30	16 2 658 666	1 13	70 70	5 15	34 6	9 12	147 148	13 10	65 65	19 3	35 38
6 14	165	164	16 3 36 33	1 14	72 72	5 16	38 36	9 13	90 89	13 11	34 24	19 4	34 16
			16 4 134 131	1 15	63 62	5 17	126 125	9 14	60 60	14 0	75 74	19 5	53 54
			16 5 36 33	1 16	63 62	5 18	59 57	9 15	34 24	14 1	92 94	19 6	45 45
			16 6 65 63	1 17	43 42	6 0	263 263			14 2	35 38	19 7	39 33
			16 7 36 33	1 18	59 57	6 1	176 175						

2	13	83	81	8	5	46	46	13	4	211	223	0	7	282	282	5	9	71	71	10	13	57	59	20	1	41	44
2	14	40	41	6	6	34	39	13	5	63	66	0	6	60	59	5	10	91	96	10	14	59	59	20	3	54	56
3	0	343	332	8	7	32	18	13	8	108	110	0	8	95	96	5	11	46	49	11	0	106	107	20	4	158	161
3	1	204	194	8	8	59	61	13	10	78	75	0	11	34	30	6	12	43	47	11	5	65	55	20	5	64	65
3	2	33	27	8	12	35	25	13	11	58	61	0	13	49	46	6	0	105	103	11	6	55	51	20	5	64	65
3	3	145	144	8	13	37	38	13	12	129	131	0	14	233	237	6	2	138	136	11	8	80	80	80	80		
3	4	221	227	8	14	36	30	13	13	37	33	0	15	39	40	6	4	81	81	11	13	57	55				
3	5	137	142	9	0	113	116	14	4	44	49	0	16	39	24	6	6	52	52	12	1	166	169				
3	10	35	39	9	2	75	75	14	6	36	28	1	2	32	66	6	7	36	35	12	1	152	158				
3	15	74	73	9	3	101	103	14	9	33	21	1	2	72	66	6	8	36	35	12	1	152	158				
3	16	96	98	9	4	100	101	15	2	36	33	1	2	37	37	6	9	35	35	12	4	139	142				
4	0	299	295	9	5	128	132	15	4	119	121	1	5	74	77	6	10	142	142	12	6	40	38				
4	1	192	187	9	8	82	87	15	6	76	66	1	6	100	96	6	15	44	38	12	9	75	75				
4	2	102	100	9	10	110	114	15	12	81	80	1	7	30	32	7	1	99	98	12	11	70	68				
4	3	43	37	9	11	39	42	16	0	51	59	1	8	34	33	7	2	79	76	12	11	70	68				
4	4	108	109	9	12	42	44	16	3	34	32	1	8	69	71	7	3	46	48	12	13	153	157				
4	5	31	19	9	13	96	99	16	6	34	7	1	14	79	78	7	4	38	33	13	2	66	68				
4	6	70	72	9	14	53	50	16	8	52	50	1	15	40	37	7	5	77	77	13	3	68	68				
4	7	128	132	9	15	42	37	16	11	40	32	2	2	239	237	7	6	46	48	13	4	99	103				
4	8	208	216	10	0	38	36	17	0	56	55	2	2	102	99	7	7	49	47	13	5	80	85				
4	9	132	139	10	1	80	79	17	1	36	15	2	2	92	86	7	8	101	104	13	6	73	77				
4	10	72	76	10	2	71	76	17	3	77	80	2	3	128	121	7	9	101	104	13	6	73	77				
4	11	39	39	10	3	95	95	17	4	119	119	2	4	32	32	7	10	69	70	13	10	34	38				
4	12	67	65	10	4	40	41	17	5	93	97	2	5	190	190	8	13	59	70	13	11	36	38				
4	14	35	31	10	5	100	100	17	6	37	37	2	6	42	39	8	0	128	129	13	12	66	67				
4	15	62	61	10	6	58	57	17	7	34	28	2	7	37	33	8	2	150	154	14	0	32	33				
4	16	110	112	10	7	50	50	17	9	48	48	2	8	175	177	8	4	79	82	14	2	84	87				
5	0	162	164	10	9	59	70	18	0	99	98	2	9	97	98	8	5	98	96	14	3	35	30				
5	1	222	224	10	10	69	61	18	1	105	106	2	10	67	84	8	6	129	133	14	5	50	51				
5	2	240	239	10	11	54	51	18	2	48	48	2	13	45	153	8	7	33	26	14	7	38	31				
5	3	283	289	10	13	67	66	18	3	35	31	3	0	47	37	8	8	100	103	14	7	38	31				
5	4	60	65	10	13	39	27	18	7	72	73	3	2	77	69	8	10	113	115	14	10	40	31				
5	5	119	125	11	0	34	25	18	8	77	78	3	3	41	44	8	11	47	54	14	12	138	138				
5	9	135	142	11	1	243	248	18	9	95	95	3	4	52	49	8	12	54	58	15	0	40	36				
5	11	93	95	11	2	34	30	19	0	57	61	3	5	34	30	8	13	65	66	15	2	36	34				
5	12	42	43	11	3	86	92	19	1	40	30	3	6	60	61	8	14	80	80	15	8	39	30				
5	13	192	198	11	4	91	91	19	3	105	110	3	8	32	28	9	0	111	112	15	10	44	40				
5	14	36	26	11	5	154	159	19	4	172	174	3	10	46	48	9	2	69	70	16	1	35	29				
5	15	51	53	11	6	40	43	19	5	120	122	3	11	38	40	9	3	54	54	16	2	99	103				
5	16	72	71	11	7	149	153	19	8	50	51	3	12	35	31	9	4	33	33	16	4	91	93				
6	1	54	51	11	9	217	223	20	3	48	47	3	14	38	40	9	5	64	67	16	7	34	31				
6	5	28	25	11	12	65	64	20	4	95	96	4	0	318	308	9	6	59	64	16	10	139	143				
6	7	34	27	11	13	126	127	20	5	52	50	4	1	240	230	9	7	34	27	17	0	53	57				
6	9	43	42	11	14	36	32	20	6	38	27	4	2	45	42	9	8	67	60	17	1	65	65				
6	13	36	20	12	0	67	70	21	0	61	56	4	3	36	33	9	10	53	52	17	2	61	63				
6	14	36	24	12	2	56	55	21	1	80	81	4	4	58	54	9	11	39	24	17	4	33	33				
7	0	198	202	12	3	98	100	21	2	39	34	4	5	80	77	9	12	32	24	17	8	45	46				
7	1	32	31	12	4	192	196	21	3	16	19	4	6	34	34	9	13	55	53	17	9	75	76				
7	4	150	152	12	5	102	104	21	4	104	101	4	7	139	143	10	14	39	40	18	0	48	38				
7	6	128	130	12	6	57	55	21	5	50	49	4	8	221	229	10	15	49	53	18	1	194	197				
7	7	34	29	12	8	55	53	22	0	42	37	4	9	190	200	10	16	101	101	18	4	79	80				
7	8	135	137	12	10	37	32	22	0	42	37	4	11	37	28	10	17	83	83	18	4	104	104				
7	10	65	71	12	11	58	59	22	0	42	37	4	12	34	29	10	18	29	24	18	5	55	54				
7	12	90	90	12	12	123	124	22	0	42	37	4	13	34	29	10	19	31	32	18	7	117	117				
7	14	142	144	12	13	68	69	0	0	152	150	4	15	49	58	10	20	29	24	18	8	26	29				
8	0	84	86	12	14	43	35	0	1	60	58	5	1	52	54	10	21	62	62	19	0	54	54				
8	2	41	41	13	0	138	143	0	2	185	178	5	2	80	78	10	22	62	62	19	1	52	43				
8	3	38	37	13	2	49	46	0	3	67	65	5	3	47	47	10	23	66	71	19	2	35	30				
8	4	51	49	13	3	79	81	0	5	73	71	5	4	88	87	10	24	69	70	19	3	38	35				

L=7

L=6

H K F O P C

8	0	107	104	3	5	70	67
8	2	49	52	3	7	55	52
8	3	52	48	3	8	89	88
8	4	63	62	4	0	143	142
8	5	53	51	4	1	52	50
8	6	38	38	4	2	91	93
8	8	85	86	4	4	49	48
9	0	47	49	4	4	71	72
9	1	48	42	4	8	116	116
9	3	55	54	5	1	165	160
9	4	78	78	5	4	53	48
9	5	67	66	5	5	71	69
9	6	37	34	5	7	99	103
9	8	38	38	6	0	123	125
10	0	64	64	6	1	128	124
10	3	40	30	6	2	39	32
10	4	65	63	6	4	89	89
10	5	46	43	6	7	84	81
10	6	71	72	7	0	235	236
10	8	50	49	7	2	54	48
11	3	47	41	7	3	49	34
11	5	62	63	7	4	58	61
11	6	44	39	7	5	46	40
11	7	37	31	8	1	79	79
12	1	55	53	8	2	38	37
12	3	67	69	8	3	57	56
12	5	117	114	8	5	50	47
12	6	41	35	9	0	70	68
13	0	36	36	9	1	56	57
14	0	70	70	9	4	168	167
14	2	45	47	10	0	39	34
				10	2	43	36
				10	3	68	65
				10	4	105	108
				11	0	50	48
				11	3	128	130

L = 11				L = 12			
H	K	FO	FC	H	K	FO	FC
0	1	45	42	0	0	186	185
0	3	119	117	0	1	101	101
0	4	110	112	0	5	41	28
0	5	132	134	1	0	147	148
0	6	45	45	1	1	106	110
0	7	47	42	1	3	48	46
0	8	159	160	2	0	77	72
1	0	52	51	2	1	51	46
1	1	39	28	2	5	43	44
1	2	43	34	3	3	74	75
1	3	73	71	3	5	82	80
1	4	132	132	4	2	45	40
1	5	76	74	4	3	51	41
1	6	61	57	5	0	83	84
1	7	35	16	5	3	77	81
1	8	47	38	5	4	206	202
2	2	47	50	7	0	47	34
2	3	67	64	7	1	43	37
2	4	109	108				
2	5	78	75				
2	6	51	51				
3	0	112	111				
3	1	45	44				
3	3	56	55				

APPENDIX I. SELECTED REFLECTIONS FROM CALCULATED AND OBSERVED
POWDER DIFFRACTION PATTERNS OF $\text{CsZr}_6\text{Cl}_{15}\text{C}$

SELECTED REFLECTIONS FROM CALCULATED AND OBSERVED POWDER DIFFRACTION PATTERNS OF $\text{CsZr}_6\text{Cl}_{15}\text{Ca}^a$

2 θ (calc)	hk ℓ	Calc. Intensity		I(obs)
		$\text{CsNb}_6\text{Cl}_{15}$ -type	$\text{KZr}_6\text{Cl}_{15}$ C-type	
2.16	0 0 1	16	18	10
9.55	2 0 0	1	8	-
10.33	1 0 1	100	4	100
11.15	0 1 1	52	77	60
11.47	2 1 0	87	100	80
12.13	1 1 1	37	24	40
12.70	0 2 0	81	1	70
13.25	2 0 1	82	1	85
21.23	0 3 1	20	3	20
21.40	2 3 0	22	1	20
21.72	2 1 2	25	1	20
22.22	4 1 1	42	3	35
24.26	3 1 2	11	2	15
26.55	5 1 1	21	7	20
26.70	3 2 2	7	17	5
27.07	1 3 2	31	9	20
27.19	4 3 0	32	14	30
29.64	6 1 0	14	1	20
31.67	0 4 2	13	1	15
32.15	4 4 0	33	15	30

^aListed are only those lines out to $2\theta = 32.5^\circ$ that exhibit the greatest intensity differences for the two structure types.

APPENDIX J. OBSERVED AND CALCULATED STRUCTURE FACTOR AMPLITUDES
FOR $K_2Zr_6Cl_{15}B$

H = 0			14 -4	118	120	7-11	75	74	0 0	41	37	12 -9	140	143
K L	Fo	Fc	14 -2	49	52	7-10	65	65	2-15	58	55	12 -7	87	89
0-18	92	89	14 0	73	74	7 -9	104	101	2-14	32	32	12 -5	82	84
0-16	258	263	16-10	54	54	7 -8	82	84	2-13	161	164	12 -4	99	96
0-12	39	38	16 -8	231	235	7 -7	45	44	2-12	120	116	12 -3	50	48
0-10	133	136	16 -4	44	47	7 -6	35	33	2-11	99	101	12 -2	30	31
0 -8	552	587	16 -2	40	40	7 -5	156	156	2 -9	24	25	12 -1	152	155
0 -6	39	40	16 0	285	295	7 -3	149	149	2 -7	45	45	12 6	35	30
0 -4	86	93	18 -8	77	71	7 -2	69	68	2 -6	38	35	14-13	116	115
0 -2	147	146	18 -4	36	30	7 -1	114	115	2 -5	263	267	14-12	41	44
2-18	54	53	18 -2	37	39	7 0	117	121	2 -4	274	256	14-11	62	62
2-16	73	72	18 0	86	87	9-15	44	41	2 -3	246	243	14 -9	38	43
2-14	75	75	20 -4	72	73	9-13	102	100	2 -2	18	18	14 -6	26	22
2-12	65	64	20 -2	34	28	9-11	73	72	4-17	91	86	14 -5	147	153
2-10	61	64				9-10	32	32	4-16	48	48	14 -4	71	69
2 -8	152	157	H = 1			9 -9	52	52	4-13	140	141	14 -3	128	128
2 -6	65	63	K L	Fo	Fc	9 -5	152	153	4-12	35	33	14 -1	30	30
2 -4	135	139	1-17	81	80	9 -4	27	19	4-11	47	48	16-11	36	37
2 -2	18	18	1-15	56	54	9 -3	140	141	4-10	29	28	16 -7	30	17
2 0	249	256	1-14	45	48	9 -2	29	30	4 -9	148	151	16 -5	62	63
4-16	35	37	1-13	75	78	9 -1	40	38	4 -8	93	89	16 -3	62	59
4-14	83	83	1-12	26	26	9 8	26	14	4 -7	69	66	18 -5	66	65
4-12	79	77	1 -9	153	157	11-10	74	75	4 -6	34	32	18 -4	75	77
4-10	93	93	1 -7	136	136	11 -9	64	63	4 -5	211	216	18 -3	52	55
4 -8	55	56	1 -6	67	67	11 -4	32	35	4 -4	70	61	20 -3	77	77
4 -6	136	134	1 -5	126	123	11 -2	63	62	4 -3	171	170	20 0	65	68
4 -4	120	122	1 -4	48	56	11 -1	50	51	4 -2	46	41	20 1	34	22
4 -2	154	154	1 -3	85	79	11 0	27	22	4 -1	174	173			
4 0	67	68	1 -2	57	53	13-14	46	46	4 0	160	147	H = 3		
6-16	54	52	1 -1	235	235	13-13	33	33	6-17	120	120	K L	Fo	Fc
6-12	85	85	1 0	18	19	13-10	29	27	6-16	63	62	1-17	72	73
6-10	88	91	3-15	43	44	13 -9	62	59	6-15	54	54	1-14	60	59
6 -8	120	123	3-14	84	86	13 -8	87	88	6-13	35	37	1-13	30	27
6 -4	157	157	3-13	75	72	13 -7	79	78	6-11	40	42	1-12	107	110
6 -2	74	71	3 -9	31	31	13 -6	36	38	6-10	34	34	1-11	25	25
6 0	178	183	3 -8	70	68	13 -5	34	34	6 -9	203	210	1-10	25	26
6 14	26	25	3 -7	77	74	13 -1	84	84	6 -8	132	128	1 -9	122	124
8-14	93	91	3 -6	102	104	13 0	116	120	6 -7	153	155	1 -7	57	58
8-12	310	320	3 -5	91	95	15-12	58	57	6 -5	42	40	1 -6	82	83
8 -8	55	58	3 -4	23	4	15 -9	69	71	6 -2	32	29	1 -5	26	27
8 -6	102	106	3 -3	46	52	15 -7	62	62	6 -1	255	262	1 -4	202	197
8 -4	526	566	3 -2	54	53	15 -6	50	50	6 0	222	203	1 -2	71	70
8 -2	59	59	3 -1	95	88	15 -5	75	75	8 -9	46	48	1 -1	138	142
8 0	86	87	3 0	127	126	15 -4	89	91	8 -8	42	37	1 0	28	26
10-14	77	74	5-17	50	48	15 -3	61	58	8 -7	42	42	3-17	36	34
10-12	89	89	5-14	34	32	15 -2	40	37	8 -4	30	26	3-14	93	89
10-10	43	46	5-13	45	47	15 -1	84	85	8 -1	58	60	3-13	44	45
10 -8	55	56	5-12	62	61	17 -9	72	76	8 0	63	60	3-12	215	219
10 -6	65	67	5-11	78	79	17 -7	62	58	10-15	38	38	3-11	72	70
10 -4	145	146	5-10	83	84	17 -4	43	42	10-11	40	43	3 -9	66	66
10 0	76	85	5 -9	68	71	17 -1	85	85	10-10	28	27	3 -8	50	47
12-14	39	37	5 -5	104	99	19 -6	43	39	10 -9	136	136	3 -7	44	44
12-10	80	77	5 -4	143	143	19 -5	36	34	10 -8	124	121	3 -6	110	109
12 -8	99	98	5 -3	133	128	19 -1	37	34	10 -7	99	100	3 -5	96	93
12 -6	63	66	5 -2	65	65				10 -3	30	26	3 -4	407	422
12 -2	86	88	5 -1	58	63	H = 2			10 -1	156	157	3 -3	121	114
12 0	118	121	5 0	30	9	K L	Fo	Fc	10 0	163	163	3 -2	70	67
14-12	72	74	7-17	59	59	0-12	28	25	12-13	70	68	3 -1	104	97
14 -8	60	59	7-16	42	37	0 -8	22	16	12-12	66	67	3 0	68	70
14 -6	73	77	7-13	98	95	0 -4	76	70	12-10	26	21	5-17	28	27

5-16	138	136	17 -9	79	77	10-12	107	109	5-12	32	29	19	1	31	36		
5-15	60	60	17 -7	43	45	10 -8	97	99	5-10	47	47						
5-14	28	27	17 -5	32	37	10 -6	74	76	5 -9	122	117		H =	6			
5-13	29	28	17 -4	46	44	10 -4	183	190	5 -8	200	195		K	L	Fo	Fc	
5-12	43	43	17 -1	75	76	10 -2	37	39	5 -7	136	135		0-16	60	61		
5-10	85	86	17 3	30	24	10 0	134	132	5 -4	55	53		0-10	68	67		
5 -9	67	68	19 -6	50	50	12-12	30	25	5 -2	29	27		0 -8	108	110		
5 -8	288	286	19 -4	130	131	12-10	43	43	5 -1	167	168		0 -6	38	40		
5 -7	102	99	19 -3	31	24	12 -8	72	71	5 0	280	276		0 -4	38	35		
5 -5	56	51	19 -1	38	37	12 -6	34	34	5 5	22	15		0 -2	69	69		
5 -4	79	81	19 2	38	37	12 -4	36	36	5 6	24	14		0 0	146	148		
5 -3	51	45				12 -2	49	49	7-15	27	24		2-15	47	46		
5 -2	66	66	H =	4		12 0	92	90	7-13	111	115		2-13	96	100		
5 -1	121	118	K	L	Fo	Fc	14-12	37	39	7-11	29	23		2-12	126	125	
5 0	414	427	0-14	26	26	14 -8	35	34	7-10	43	40		2-11	66	66		
7-16	75	78	0-12	49	51	14 -6	34	31	7 -9	36	36		2 -9	26	31		
7-13	57	60	0-10	186	187	14 -5	30	22	7 -8	79	78		2 -8	43	43		
7-10	84	84	0 -8	27	13	14 -4	63	64	7 -5	143	146		2 -7	25	29		
7 -9	29	24	0 -6	39	38	14 0	35	31	7 -3	101	102		2 -5	154	154		
7 -8	141	143	0 -4	138	135	16-10	90	91	7 -2	38	37		2 -4	222	217		
7 -6	46	48	0 -2	168	168	16 -4	61	62	7 -1	25	22		2 -3	137	139		
7 -5	73	77	0 0	102	58	16 -2	64	65	7 0	104	101		2 0	51	52		
7 -3	39	41	2-16	36	40	18 -4	65	65	9-13	155	155		2 6	29	20		
7 -2	87	89	2-14	32	32	18 -2	50	48	9-11	74	74		4-16	65	67		
7 0	193	190	2-12	91	92	18 -1	28	15	9 -9	38	40		4-13	109	109		
9-13	94	95	2-10	70	70	18 0	160	153	9 -8	63	63		4-12	68	70		
9-11	34	31	2 -8	112	114				9 -5	207	207		4-11	28	28		
9-10	33	31	2 -5	31	33	H =	5		9 -3	166	170		4 -9	110	113		
9 -9	41	42	2 -4	183	181	K	L	Fo	Fc	9 0	80	79		4 -8	115	114	
9 -8	93	94	2 -3	32	36	1-17	123	125	9 1	28	27		4 -7	40	42		
9 -5	125	128	2 -2	44	42	1-13	36	34	9 15	31	24		4 -6	27	25		
9 -3	95	97	2 0	172	174	1-12	64	65	11-13	37	37		4 -5	151	151		
9 -2	35	32	2 13	28	20	1-11	26	28	11-12	32	23		4 -4	109	107		
9 -1	36	35	4-16	46	43	1 -9	199	205	11-10	47	46		4 -3	106	109		
9 0	120	121	4-14	44	42	1 -7	123	122	11 -9	87	87		4 -2	26	27		
11-13	45	44	4-12	73	75	1 -6	33	33	11 -8	155	155		4 -1	114	113		
11-10	82	83	4-10	50	49	1 -5	30	34	11 -7	82	83		4 0	154	149		
11 -9	43	45	4 -8	85	84	1 -4	112	109	11 -5	52	52		6-15	30	34		
11 -8	212	215	4 -6	78	75	1 -2	27	24	11 -4	39	40		6-13	40	39		
11 -7	54	55	4 -4	136	134	1 -1	231	236	11 -3	39	41		6-11	34	32		
11 -6	35	36	4 -3	19	14	1 0	31	31	11 -2	37	36		6 -9	129	128		
11 -5	63	62	4 -2	82	84	1 14	25	26	11 -1	109	109		6 -8	139	139		
11 -4	30	27	4 0	123	121	1 15	27	25	11 0	205	200		6 -7	92	95		
11 -3	51	51	6-16	45	47	3-14	54	51	13-12	88	88		6 -5	45	44		
11 -2	78	77	6-14	40	39	3-13	91	91	13-11	82	80		6 -4	33	31		
11 -1	64	65	6-10	43	41	3-12	152	154	13 -8	33	28		6 -1	146	150		
11 0	280	281	6 -9	27	29	3-11	95	97	13 -5	96	95		6 0	193	188		
13-13	32	30	6 -8	106	107	3 -9	46	43	13 -4	141	142		8-14	52	51		
13-12	128	131	6 -7	28	30	3 -8	46	45	13 -3	105	106		8-12	76	75		
13-11	57	60	6 -4	39	40	3 -6	54	55	13 0	30	37		8-10	28	22		
13-10	30	30	6 -1	38	37	3 -5	155	153	13 10	29	27		8 -9	46	46		
13 -8	52	54	6 0	157	151	3 -4	283	280	15 -9	55	57		8 -8	26	25		
13 -6	40	39	6 6	27	26	3 -3	163	162	15 -5	34	27		8 -7	39	38		
13 -5	59	61	8-14	139	140	3 -2	23	20	15 -4	55	58		8 -6	65	63		
13 -4	207	210	8 -8	73	72	3 -1	57	56	15 -1	44	42		8 -4	114	114		
13 -3	73	76	8 -6	153	152	3 0	62	63	17 -7	86	85		8 -2	48	49		
13 0	68	70	8 -4	23	5	3 7	29	21	17 -5	29	30		8 -1	54	54		
15 -6	64	64	8 -2	82	80	5-16	96	93	17 -4	39	39		8 0	36	36		
15 -4	109	108	8 0	114	112	5-15	74	78	17 -1	132	129		10-12	35	37		
15 -2	45	45	10-14	69	71	5-14	28	28	19 -3	47	45		10-11	32	34		

10 -8	53	57	H = 12		4 -1	39	36
10 -7	57	56	K L	Fo Fc	4 0	78	79
10 -4	46	45	0-10	87 92	6 0	96	101
10 -1	95	93	0 -4	58 60			
10 0	70	70	0 -2	57 58			
12 -8	44	40	2-10	42 43			
12 -7	66	63	2 -8	48 48			
12 -6	44	46	2 -5	43 43			
12 -5	60	61	2 -4	86 86			
12 -4	47	48	2 -3	46 44			
12 -3	38	37	2 -2	29 25			
12 -2	48	51	2 0	67 66			
12 -1	104	103	4 -8	34 30			
12 0	53	49	4 -7	27 7			
14 -5	108	104	4 -4	47 47			
14 -3	88	83	4 -2	28 22			
14 1	30	24	4 0	38 38			
			6 -9	44 43			
			6 -8	56 58			
			6 -7	44 40			
			6 -1	52 50			
			6 0	72 74			
			8 -6	71 69			
			8 0	60 56			
			10 -4	91 92			
			10 -3	32 27			
			10 0	74 73			
			12 -1	30 26			
			12 0	36 37			
			H = 13				
			K L	Fo Fc			
			1 -7	76 78			
			1 -5	32 32			
			1 -1	131 133			
			3 -8	32 32			
			3 -5	93 93			
			3 -4	64 69			
			3 -3	87 91			
			3 0	42 40			
			3 1	30 23			
			5 -7	80 81			
			5 -4	29 23			
			5 -1	95 96			
			5 0	66 63			
			7 -5	98 99			
			7 -3	66 69			
			7 -1	32 27			
			9 -3	109 110			
			9 -1	30 23			
			H = 14				
			K L	Fo Fc			
			0 -2	57 55			
			0 0	95 97			
			2 -5	35 28			
			2 -4	100 109			
			2 0	51 51			
			4 -4	75 67			
			4 -3	34 32			

APPENDIX K. OBSERVED AND CALCULATED STRUCTURE FACTOR AMPLITUDES
FOR $K_3Zr_6Cl_{15}Be$

K = 0				K = 1				K = 2				K = 3			
H	L	Fo	Fc	H	L	Fo	Fc	H	L	Fo	Fc	H	L	Fo	Fc
0 2	156	150	8-16	114	112	16 -2	43	39	3-16	74	72	5 14	29	26	
0 4	104	105	8-14	41	43	16 0	233	228	3-15	25	24	5 15	19	25	
0 6	24	23	8-12	20	25	16 2	152	153	3-14	25	21	5 16	30	25	
0 8	255	253	8-10	38	39	16 4	50	47	3-13	114	116	5 17	87	88	
0 10	67	65	8 -4	394	403	16 6	46	46	3-11	44	44	7-17	61	56	
0 12	72	70	8 -2	141	145	16 8	95	94	3-10	43	44	7-16	122	122	
0 14	55	54	8 0	59	60	16 10	80	80	3 -9	29	27	7-15	45	45	
2-16	20	15	8 4	436	449	18-10	49	49	3 -8	28	26	7-13	60	58	
2-14	42	42	8 6	146	146	18 -8	93	91	3 -7	45	42	7-12	27	28	
2-12	46	44	8 8	63	64	18 -6	41	38	3 -6	86	88	7-10	67	67	
2-10	66	67	8 12	59	62	18 -4	14	12	3 -5	103	104	7 -9	56	57	
2 -8	256	260	8 14	41	41	18 -2	17	20	3 -4	102	95	7 -8	211	210	
2 -6	92	91	8 16	79	81	18 0	75	73	3 -2	57	58	7 -7	79	80	
2 -4	171	170	10-16	17	7	18 2	70	71	3 -1	28	30	7 -6	47	47	
2 -2	73	72	10-14	33	33	18 4	33	34	3 0	117	113	7 -5	29	31	
2 0	207	205	10-12	83	82	18 8	38	36	3 1	44	41	7 -4	114	115	
2 2	34	31	10-10	24	19	20 -6	15	9	3 2	44	44	7 -3	115	117	
2 4	102	100	10 -6	49	50	20 -4	74	72	3 3	41	42	7 -2	31	31	
2 6	26	23	10 -4	187	189	20 -2	19	17	3 4	123	124	7 -1	114	111	
2 8	60	57	10 -2	18	16	20 2	25	18	3 5	39	39	7 0	115	118	
2 10	61	61	10 0	108	107	20 4	51	52	3 6	110	110	7 1	140	141	
2 12	32	36	10 2	19	10				3 7	88	85	7 2	89	89	
2 14	26	33	10 4	81	80				3 9	91	89	7 3	106	108	
2 16	17	4	10 6	73	76				3 10	20	16	7 4	150	151	
2 18	85	84	10 8	22	24				3 11	51	48	7 5	240	244	
4-18	25	4	10 12	19	25				3 12	109	108	7 6	56	57	
4-16	21	25	10 14	31	30				3 13	43	43	7 8	38	37	
4-14	164	164	10 16	19	16				3 14	53	53	7 9	89	90	
4-12	18	13	12-14	44	46				3 15	25	21	7 11	52	54	
4 -8	61	60	12-12	108	109				3 16	16	14	7 12	154	155	
4 -6	149	149	12 -8	58	57				3 17	77	76	7 13	81	79	
4 -4	66	69	12 -4	23	23				5-17	22	12	7 14	84	81	
4 -2	175	178	12 -2	51	51				5-16	23	23	7 16	17	19	
4 0	148	149	12 0	143	143				5-15	32	32	9-16	41	39	
4 2	200	207	12 2	107	107				5-13	122	124	9-15	31	30	
4 4	102	102	12 4	24	25				5-12	18	12	9-14	35	29	
4 6	81	78	12 6	45	46				5-11	23	22	9-13	24	22	
4 8	44	44	12 8	21	11				5-10	42	44	9-12	137	140	
4 10	149	149	12 10	14	11				5 -9	20	23	9-11	126	126	
4 12	22	29	12 12	26	23				5 -8	144	145	9 -9	40	39	
4 14	15	0	12 14	102	101				5 -7	15	9	9 -8	43	41	
4 16	24	18	14-14	21	6				5 -5	201	200	9 -7	16	11	
6-16	85	87	14-12	36	35				5 -4	97	98	9 -6	21	16	
6-14	75	75	14-10	31	32				5 -3	142	139	9 -5	125	128	
6-12	127	129	14 -8	160	163				5 -2	54	55	9 -4	139	141	
6-10	39	39	14 -6	61	61				5 -1	70	70	9 -3	253	261	
6 -8	49	50	14 -4	74	74				5 0	17	5	9 -2	70	70	
6 -6	40	39	14 -2	43	44				5 1	53	50	9 -1	21	19	
6 -4	40	39	14 0	22	24				5 2	37	37	9 0	31	32	
6 -2	23	20	14 2	15	1				5 3	73	70	9 1	42	41	
6 0	165	163	14 4	121	123				5 4	99	98	9 2	21	24	
6 2	142	144	14 6	150	152				5 5	36	35	9 3	55	53	
6 4	200	200	14 8	77	83				5 6	16	5	9 4	67	69	
6 6	123	124	14 10	44	45				5 7	88	85	9 5	103	106	
6 8	123	124	14 12	83	82				5 8	30	29	9 6	22	21	
6 10	123	124	16-12	45	45				5 9	148	149	9 7	34	35	
6 12	107	107	16-10	33	35				5 10	35	35	9 8	93	94	
6 14	31	29	16 -8	58	58				5 11	56	59	9 9	83	83	
6 16	59	55	16 -6	56	58				5 12	69	71	9 10	104	101	
			16 -4	38	37				5 13	58	57	9 11	31	34	

9	12	20	26	15-12	118	118	K = 2		4 -7	26	24	8-11	29	28
9	13	22	28	15-11	46	46	H L	Fo Fc	4 -6	50	48	8-10	34	35
9	14	56	55	15-10	38	37	0 1	44 42	4 -5	154	155	8 -9	141	143
9	16	85	84	15 -9	30	30	0 2	17 18	4 -4	31	30	8 -8	20	22
11-16	22	12	15	15 -8	58	58	0 3	79 77	4 -3	186	189	8 -7	118	116
11-14	54	54	15	15 -7	20	18	0 4	52 51	4 -2	25	23	8 -6	68	71
11-13	31	32	15	15 -6	18	13	0 5	104 101	4 -1	161	159	8 -5	48	47
11-12	69	69	15	15 -4	112	114	0 6	29 29	4 0	71	65	8 -4	27	26
11-11	37	34	15	15 -3	18	21	0 7	48 47	4 1	144	142	8 -3	15	11
11-10	51	50	15	15 -2	79	80	0 8	31 33	4 2	153	151	8 -2	21	20
11 -9	88	93	15	15 -1	24	19	0 9	109 108	4 3	111	110	8 -1	54	54
11 -8	31	32	15	15 0	19	17	0 10	46 46	4 5	191	187	8 0	40	39
11 -7	33	35	15	15 1	102	102	0 11	16 8	4 6	18	15	8 1	80	82
11 -6	27	32	15	15 2	22	15	0 12	57 57	4 7	33	32	8 2	15	11
11 -5	25	26	15	15 3	38	36	0 13	142 141	4 8	15	16	8 3	25	25
11 -4	21	21	15	15 4	74	71	0 14	18 12	4 9	86	85	8 5	75	76
11 -3	40	39	15	15 5	96	97	0 16	59 56	4 10	57	57	8 6	41	43
11 -2	67	69	15	15 6	39	38	0 17	71 69	4 11	22	18	8 7	29	28
11 -1	23	27	15	15 7	23	12	0 18	20 15	4 12	34	32	8 8	27	25
11 0	15	11	15	15 8	105	105	2-18	37 32	4 13	26	21	8 9	85	85
11 1	20	9	15	15 9	113	110	2-17	96 95	4 14	17	20	8 11	25	24
11 2	62	63	15	15 10	55	57	2-16	121 119	4 16	35	36	8 12	47	48
11 3	17	11	15	15 12	17	18	2-15	79 80	4 17	36	32	8 13	98	99
11 4	14	3	17	17-11	18	7	2-13	18 25	6-17	48	45	8 14	20	18
11 5	18	14	17	17-10	27	17	2-12	41 43	6-16	16	4	8 15	55	54
11 7	55	56	17	17 -8	90	90	2-11	46 45	6-15	38	40	8 16	35	34
11 8	108	110	17	17 -7	106	111	2-10	21 16	6-14	22	23	10-16	25	25
11 10	82	84	17	17 -6	35	35	2 -9	96 97	6-12	20	12	10-14	41	43
11 11	20	3	17	17 -5	16	14	2 -8	81 81	6-10	34	32	10-13	85	87
11 12	25	15	17	17 -4	51	52	2 -7	117 118	6 -9	234	237	10-12	79	80
11 13	16	9	17	17 -3	16	5	2 -6	58 57	6 -8	170	169	10-11	89	89
11 14	18	15	17	17 -2	32	33	2 -5	130 130	6 -7	110	113	10-10	59	56
11 15	48	48	17	17 -1	55	50	2 -3	215 211	6 -6	16	13	10 -9	17	10
13-14	24	14	17	17 0	17	6	2 -2	54 54	6 -5	42	46	10 -8	34	33
13-13	24	23	17	17 1	111	109	2 -1	15 15	6 -4	20	18	10 -7	26	25
13-12	44	42	17	17 2	25	22	2 0	33 34	6 -3	64	63	10 -5	69	71
13-11	24	21	17	17 4	20	20	2 2	53 53	6 -2	30	29	10 -4	21	19
13-10	22	6	17	17 6	30	30	2 3	131 130	6 -1	290	292	10 -3	54	55
13 -9	111	113	17	17 7	22	21	2 4	387 373	6 0	208	200	10 -2	61	62
13 -8	36	38	17	17 8	26	27	2 5	392 381	6 1	206	206	10 -1	80	72
13 -7	88	90	17	17 9	56	55	2 6	56 55	6 2	66	64	10 0	86	87
13 -5	37	35	17	17 10	44	46	2 7	17 15	6 3	45	46	10 1	178	183
13 -4	66	66	19	19 -8	25	27	2 8	15 15	6 4	63	61	10 2	64	66
13 -3	31	30	19	19 -7	32	30	2 9	55 56	6 5	20	19	10 3	35	37
13 -2	18	1	19	19 -6	43	43	2 10	68 68	6 6	26	27	10 4	41	38
13 -1	110	109	19	19 -5	37	34	2 11	48 49	6 7	80	81	10 5	43	40
13 0	112	111	19	19 -4	17	17	2 12	69 65	6 8	54	55	10 6	40	38
13 1	55	53	19	19 -3	20	14	2 13	166 165	6 9	69	68	10 7	27	28
13 2	18	19	19	19 -2	16	14	2 15	49 48	6 10	25	24	10 8	124	126
13 3	53	53	19	19 -1	26	27	2 17	20 11	6 11	86	87	10 9	197	198
13 4	18	18	19	19 0	23	6	4-17	60 61	6 12	117	116	10 10	24	26
13 5	23	23	19	19 1	63	60	4-16	16 9	6 13	80	81	10 11	57	57
13 6	16	12	19	19 2	21	22	4-15	28 17	6 15	57	58	10 13	40	42
13 7	67	69	19	19 3	17	1	4-14	41 39	6 16	24	24	10 14	27	24
13 8	17	9	19	19 4	48	46	4-13	20 16	6 17	36	34	10 15	23	17
13 9	30	32	19	19 6	46	44	4-12	62 65	8-17	82	82	12-15	18	2
13 10	17	15	19	19 7	17	8	4-11	21 8	8-16	24	9	12-13	71	70
13 11	41	39	21	21 -3	78	75	4-10	18 9	8-15	41	33	12-12	37	37
13 13	99	100	21	21 -2	23	26	4 -9	25 22	8-13	60	60	12-11	29	33
15-13	24	22	21	21 -1	40	39	4 -8	18 8	8-12	72	74	12-10	26	22

12 -9	61	63	16	2	23	17	1	9	56	59	5	6	50	50	9	6	46	46
12 -8	41	43	16	3	37	37	1	10	47	47	5	7	143	143	9	7	56	55
12 -7	63	64	16	4	14	1	1	11	22	14	5	8	167	169	9	8	43	44
12 -6	16	11	16	5	35	33	1	12	52	52	5	9	111	112	9	9	39	42
12 -5	22	10	16	6	15	14	1	13	55	54	5	13	21	19	9	10	87	86
12 -4	62	64	16	7	28	25	1	14	79	78	5	14	47	49	9	11	24	20
12 -3	28	27	16	9	58	61	1	15	16	14	5	15	19	12	9	12	40	39
12 -2	23	27	16	10	23	27	1	16	29	24	5	17	57	59	9	13	35	38
12 -1	112	108	16	11	60	59	3	17	18	21	7	17	75	73	9	14	45	44
12 0	37	37	18	10	20	18	3	16	38	41	7	16	38	40	9	15	23	8
12 1	184	186	18	9	51	50	3	15	47	45	7	15	23	27	11	14	72	69
12 2	32	31	18	7	46	49	3	13	86	88	7	14	19	17	11	13	59	60
12 3	22	17	18	6	34	33	3	12	21	21	7	13	16	15	11	12	64	66
12 4	39	43	18	5	22	16	3	11	59	62	7	12	24	21	11	11	22	16
12 5	86	85	18	2	20	22	3	10	105	106	7	11	24	22	11	10	22	20
12 6	38	37	18	1	36	32	3	9	117	118	7	10	81	81	11	9	34	33
12 7	47	48	18	1	14	3	3	8	24	27	7	9	23	22	11	8	64	64
12 8	44	44	18	2	33	28	3	7	63	63	7	8	148	148	11	7	124	125
12 9	106	107	18	3	15	8	3	6	29	28	7	7	21	22	11	6	135	135
12 10	17	9	18	4	59	58	3	5	64	64	7	5	61	61	11	5	91	90
12 11	41	42	18	5	93	94	3	4	323	319	7	4	17	17	11	4	46	46
12 12	18	20	18	6	55	56	3	3	332	335	7	3	35	34	11	3	62	61
12 13	18	14	18	7	43	38	3	2	203	199	7	2	64	65	11	2	18	12
12 14	36	39	18	8	21	21	3	0	69	68	7	1	17	9	11	1	31	18
14 -13	59	60	20	6	23	7	3	1	33	32	7	0	199	193	11	0	196	199
14 -12	38	36	20	5	55	55	3	2	27	27	7	1	17	5	11	1	153	154
14 -11	41	46	20	3	83	82	3	3	51	49	7	2	73	73	11	2	169	173
14 -9	26	26	20	2	17	13	3	4	285	282	7	3	84	82	11	3	26	26
14 -8	21	21	20	0	37	39	3	5	34	33	7	4	18	15	11	4	66	67
14 -7	45	43	20	1	23	26	3	6	112	113	7	5	21	16	11	5	18	17
14 -6	24	24	20	2	17	1	3	7	70	69	7	6	24	26	11	7	56	56
14 -5	147	149	20	3	44	45	3	8	100	101	7	7	29	25	11	8	107	108
14 -4	109	114	20	4	42	44	3	9	69	68	7	8	33	34	11	9	45	46
14 -3	134	134					3	10	28	29	7	9	64	63	11	10	87	88
14 -2	35	35					3	12	65	64	7	11	22	22	11	11	36	32
14 -1	21	15					3	13	56	55	7	12	15	5	11	12	36	34
14 0	28	27					3	14	24	26	7	13	26	27	11	13	82	82
14 1	56	55					3	15	41	41	7	14	77	77	11	14	36	38
14 3	71	71					3	16	35	34	7	15	52	51	13	13	35	35
14 4	13	7					3	17	95	95	7	16	32	28	13	12	16	13
14 5	118	121					5	17	52	47	9	16	55	54	13	11	22	21
14 6	38	37					5	15	28	20	9	15	56	55	13	10	19	3
14 7	42	42					5	14	30	32	9	14	48	50	13	9	60	59
14 8	16	3					5	13	110	110	9	13	46	42	13	8	37	39
14 9	22	21					5	11	120	123	9	12	20	5	13	7	88	90
14 10	33	30					5	9	34	33	9	11	20	10	13	6	22	21
14 11	24	26					5	8	102	102	9	10	19	17	13	4	119	121
14 12	26	22					5	7	15	6	9	8	69	68	13	3	20	19
16 -11	77	75					5	6	18	14	9	7	48	50	13	2	34	32
16 -10	17	21					5	5	22	20	9	6	42	41	13	1	19	16
16 -9	19	18					5	4	109	111	9	5	50	49	13	0	61	64
16 -8	17	19					5	3	31	31	9	4	37	34	13	1	15	6
16 -7	19	22					5	2	60	59	9	3	41	41	13	2	31	32
16 -6	37	37					5	1	187	188	9	2	15	5	13	3	121	123
16 -5	72	74					5	0	383	377	9	1	20	21	13	4	178	177
16 -4	50	51					5	1	107	107	9	0	69	69	13	5	107	107
16 -3	120	121					5	2	57	57	9	1	62	65	13	6	47	45
16 -2	32	31					5	3	14	10	9	2	87	88	13	7	19	7
16 0	32	27					5	4	53	53	9	3	110	111	13	8	46	45
16 1	16	16					5	5	50	48	9	5	123	125	13	10	27	19

13	11	23	16	0	3	88	87	4	-2	72	73	8	-4	70	70	12	1	17	16
13	12	42	40	0	4	25	24	4	-1	14	9	8	-3	43	44	12	2	29	32
13	13	76	75	0	5	67	66	4	0	25	25	8	-2	23	24	12	3	16	16
15-13	54	54	0	6	73	71	4	1	12	7	8	-1	70	68	12	4	88	88	
15-12	64	63	0	7	28	27	4	2	41	42	8	0	80	78	12	5	19	10	
15	-8	18	0	8	123	121	4	3	43	42	8	1	54	53	12	6	99	99	
15	-7	39	39	0	9	21	16	4	4	16	14	8	2	14	10	12	7	52	51
15	-6	36	35	0	10	142	141	4	6	59	58	8	3	42	45	12	8	24	2
15	-5	24	16	0	11	25	23	4	7	131	130	8	4	60	59	12	9	32	34
15	-4	127	129	0	12	38	38	4	8	318	319	8	5	14	13	12	10	16	9
15	-3	19	6	0	13	44	42	4	9	87	87	8	6	131	132	12	11	77	78
15	-2	48	48	0	14	52	53	4	10	153	156	8	7	54	53	12	12	148	149
15	-1	42	42	0	15	18	3	4	11	49	52	8	8	25	28	12	13	25	21
15	0	19	16	0	16	47	47	4	12	29	29	8	9	18	9	14-13	15	1	
15	2	16	4	0	17	23	23	4	13	26	22	8	10	25	26	14-12	34	31	
15	4	72	71	2	-17	27	25	4	14	25	29	8	11	20	24	14-11	60	60	
15	5	48	51	2	-16	43	44	4	15	93	91	8	12	80	82	14-10	32	31	
15	6	45	46	2	-15	22	12	4	16	145	145	8	13	26	30	14-9	15	5	
15	8	14	7	2	-14	21	17	4	17	21	20	8	14	77	77	14-8	45	44	
15	11	28	32	2	-12	87	87	6	-17	26	27	8	15	23	26	14-6	19	24	
17-11	60	59	2	-11	82	85	6	-16	27	14	10-15	19	13	14	-3	43	42		
17-10	15	5	2	-10	81	80	6	-15	48	44	10-14	61	63	14	-2	32	34		
17	-9	49	46	2	-9	33	31	6	-14	51	54	10-13	38	36	14	0	38	38	
17	-8	15	11	2	-8	90	90	6	-13	20	12	10-12	78	80	14	1	16	8	
17	-7	21	14	2	-6	16	11	6	-12	79	76	10	-9	31	36	14	2	28	25
17	-6	22	22	2	-5	74	71	6	-11	23	22	10	-8	121	123	14	3	39	35
17	-4	40	38	2	-4	183	182	6	-10	28	30	10	-7	75	75	14	4	79	79
17	-3	24	26	2	-3	121	120	6	-9	17	17	10	-6	38	43	14	6	62	61
17	-2	21	18	2	-2	102	99	6	-8	54	58	10	-5	66	67	14	7	20	6
17	-1	49	46	2	-1	54	52	6	-7	82	82	10	-4	186	188	14	8	21	13
17	0	14	2	2	0	167	166	6	-6	16	15	10	-3	21	5	14	9	15	8
17	1	62	61	2	1	41	44	6	-5	27	26	10	-2	106	108	14	10	35	34
17	2	36	34	2	2	64	63	6	-4	17	14	10	-1	65	63	14	11	44	44
17	3	56	56	2	3	13	5	6	-3	26	25	10	0	78	77	14	12	50	48
17	5	58	55	2	4	65	63	6	-2	26	29	10	1	36	35	16-11	31	33	
17	6	43	42	2	5	40	40	6	-1	46	46	10	2	29	17	16-10	24	26	
17	7	29	28	2	6	22	23	6	0	133	133	10	3	71	73	16-9	18	2	
17	8	25	19	2	7	33	30	6	1	26	24	10	4	118	120	16-8	24	24	
17	9	59	61	2	8	17	13	6	2	20	18	10	5	30	28	16-7	21	5	
19	-8	69	68	2	10	34	34	6	4	64	62	10	6	73	74	16-5	23	17	
19	-7	50	52	2	11	57	57	6	6	78	79	10	7	19	22	16-3	16	8	
19	-6	20	16	2	12	65	66	6	7	107	108	10	8	42	41	16-2	37	35	
19	-5	19	21	2	13	48	49	6	8	138	141	10	9	36	35	16-1	31	29	
19	-4	54	52	2	14	56	58	6	9	19	16	10	10	58	56	16	0	31	30
19	-3	77	80	2	15	49	51	6	10	90	89	10	12	18	9	16	2	21	18
19	-2	92	95	2	16	80	82	6	13	16	9	10	14	19	9	16	3	32	35
19	-1	21	11	2	17	19	22	6	14	71	72	12-14	33	26	16	4	29	31	
19	0	19	19	4	-16	28	21	6	15	49	47	12-13	33	31	16	6	21	19	
19	1	37	34	4	-14	87	85	6	16	26	23	12-12	61	62	16	7	14	15	
19	2	16	7	4	-13	78	80	8	-16	44	43	12-10	35	36	16	8	61	60	
19	3	34	36	4	-12	255	255	8	-15	25	25	12-9	84	85	16	9	23	18	
19	4	73	76	4	-11	125	125	8	-14	23	23	12-8	207	209	16	10	82	83	
19	5	15	4	4	-10	48	50	8	-13	26	25	12-7	56	58	18	-9	39	39	
19	6	101	98	4	-9	22	22	8	-12	47	45	12-6	103	104	18	-8	90	91	
				4	-8	59	60	8	-10	39	40	12-5	64	64	18	-7	18	10	
	K	4		4	-7	51	53	8	-9	28	32	12-4	54	55	18	-6	49	50	
H	L	Fo	Fc	4	-6	113	114	8	-8	43	44	12-3	32	33	18	-5	43	42	
0	0	34	26	4	-5	103	102	8	-7	19	16	12-2	21	21	18	-4	59	58	
0	1	115	111	4	-4	282	285	8	-6	126	128	12-1	21	15	18	-3	16	17	
0	2	84	85	4	-3	86	85	8	-5	38	37	12	0	73	71	18	-1	65	64

4 -6	82	83	8 -2	122	124	12 6	59	57	1 -8	120	119	5 -3	127	127
4 -5	111	109	8 -1	55	55	12 7	22	22	1 -6	22	16	5 -2	18	19
4 -4	64	63	8 0	14	3	12 8	39	36	1 -5	33	31	5 -1	52	51
4 -3	26	26	8 1	44	46	12 9	97	94	1 -4	30	30	5 0	66	66
4 -2	66	66	8 2	37	39	12 10	32	32	1 -3	25	23	5 2	31	26
4 -1	26	13	8 3	76	77	12 11	29	32	1 -2	162	162	5 3	64	66
4 0	30	29	8 4	69	69	14-11	54	54	1 -1	73	74	5 4	32	32
4 1	135	137	8 5	75	75	14-10	75	76	1 0	21	22	5 5	14	12
4 2	92	93	8 6	23	24	14 -6	40	42	1 1	98	99	5 6	15	13
4 3	108	109	8 7	29	29	14 -4	45	47	1 2	37	41	5 8	44	48
4 4	54	53	8 8	40	38	14 -3	113	114	1 3	19	6	5 9	59	59
4 5	105	103	8 9	14	6	14 -2	128	128	1 4	109	109	5 10	26	26
4 6	48	49	8 10	56	57	14 -1	37	37	1 5	51	52	5 11	34	33
4 7	32	34	8 11	13	13	14 0	25	24	1 6	91	90	5 13	27	29
4 8	31	34	8 12	70	71	14 1	41	42	1 7	85	85	5 14	73	72
4 9	57	57	8 13	104	106	14 2	45	45	1 8	31	33	5 15	17	7
4 10	26	31	8 14	29	25	14 3	20	24	1 9	69	69	7-15	72	70
4 12	16	9	10-14	36	34	14 5	63	62	1 10	51	51	7-14	97	98
4 13	25	24	10-13	136	136	14 6	23	18	1 11	133	131	7-12	28	29
4 14	30	31	10-12	17	6	14 7	30	37	1 12	102	104	7-11	75	76
4 15	19	6	10-11	72	71	14 8	14	7	1 14	69	68	7-10	72	71
4 16	23	19	10-10	29	28	14 9	20	19	1 15	48	53	7 -9	52	52
6-15	41	41	10 -9	21	20	14 10	14	8	1 16	26	20	7 -8	110	111
6-14	50	45	10 -7	24	20	16-10	39	40	3-16	58	59	7 -7	80	81
6-12	22	23	10 -6	17	8	16 -9	30	29	3-15	40	42	7 -6	59	59
6-11	51	52	10 -5	44	42	16 -8	22	3	3-14	20	5	7 -5	116	116
6-10	63	64	10 -4	59	57	16 -7	29	28	3-13	23	20	7 -4	46	46
6 -9	49	49	10 -3	62	63	16 -6	74	75	3-12	55	52	7 -3	50	50
6 -8	85	85	10 -2	34	32	16 -5	92	89	3-10	39	39	7 -2	125	125
6 -7	190	195	10 -1	144	142	16 -4	52	51	3 -9	20	12	7 -1	90	90
6 -6	167	167	10 0	57	58	16 -3	68	71	3 -8	38	39	7 0	115	114
6 -4	15	8	10 1	47	47	16 -1	35	38	3 -6	21	17	7 1	49	49
6 -3	21	13	10 3	15	12	16 0	28	23	3 -5	58	59	7 3	47	48
6 -2	36	37	10 4	53	55	16 1	14	9	3 -4	110	109	7 4	15	16
6 0	91	90	10 5	44	43	16 2	49	50	3 -3	24	18	7 5	125	123
6 1	203	203	10 6	71	73	16 3	32	31	3 -2	29	30	7 6	193	198
6 2	65	65	10 7	149	150	16 4	25	8	3 -1	33	32	7 7	39	38
6 3	68	69	10 8	110	110	16 5	32	31	3 1	47	46	7 8	51	52
6 4	45	45	10 9	76	79	16 7	61	59	3 3	14	20	7 9	25	27
6 5	22	20	10 10	33	33	16 8	56	59	3 4	130	130	7 10	15	16
6 6	50	53	10 11	48	47	18 -7	69	68	3 5	69	71	7 11	71	72
6 7	53	55	10 12	65	67	18 -6	38	35	3 6	90	91	7 12	71	71
6 9	38	36	10 13	19	19	18 -5	18	7	3 7	92	94	7 13	33	36
6 11	23	20	12-13	25	16	18 -1	17	15	3 9	33	34	7 14	94	98
6 12	21	16	12-12	24	20	18 0	40	38	3 10	22	19	9-14	32	32
6 13	135	135	12-11	50	50	18 2	17	7	3 11	65	66	9-13	57	57
6 14	37	40	12 -9	39	39	18 3	80	77	3 12	94	95	9-12	101	101
6 15	52	50	12 -8	32	28	18 4	52	51	3 14	60	60	9-11	50	51
8-15	44	42	12 -7	44	41	18 5	49	47	3 15	19	12	9-10	16	12
8-14	52	51	12 -6	14	8				5-14	30	25	9 -9	50	50
8-13	71	70	12 -5	17	4				5-13	21	14	9 -8	38	37
8-11	22	14	12 -4	39	38				5-12	42	41	9 -7	36	36
8-10	84	86	12 -3	42	42	1-16	80	76	5-11	28	28	9 -6	95	94
8 -9	99	99	12 -2	81	82	1-15	60	60	5-10	62	61	9 -5	146	149
8 -8	18	19	12 -1	71	72	1-14	19	15	5 -9	36	35	9 -4	101	103
8 -7	94	96	12 0	23	26	1-13	30	30	5 -8	92	92	9 -3	75	77
8 -6	18	12	12 1	85	85	1-12	17	12	5 -7	52	54	9 -2	61	60
8 -5	42	40	12 2	53	54	1-11	52	48	5 -6	57	58	9 -1	24	24
8 -4	58	58	12 3	56	56	1-10	151	152	5 -5	29	30	9 2	42	41
8 -3	55	55	12 5	51	53	1 -9	135	134	5 -4	56	58	9 3	23	25

9 4	21	17	15 1	15	14	2 13	24	15	8 -9	41	42	12 7	17	7
9 5	65	65	15 2	100	100	2 14	35	32	8 -7	16	6	12 9	22	22
9 6	38	36	15 3	39	41	2 15	22	6	8 -6	65	66	14-10	47	46
9 7	79	78	15 4	90	93	4-15	61	62	8 -5	108	109	14 -9	53	53
9 8	79	80	15 5	31	29	4-14	51	52	8 -4	120	121	14 -8	69	70
9 10	52	54	15 6	28	32	4-13	57	58	8 -3	109	111	14 -7	20	21
9 11	57	60	15 7	18	16	4-12	70	69	8 -2	114	114	14 -6	84	82
9 12	21	15	15 8	21	12	4-11	28	30	8 -1	132	131	14 -5	22	18
9 13	20	7	15 9	51	51	4-10	22	22	8 0	22	22	14 -4	38	33
11-13	33	31	17 -5	35	35	4 -7	47	45	8 1	35	35	14 -3	32	33
11-12	62	64	17 -4	46	46	4 -5	59	60	8 2	89	92	14 -2	20	17
11-11	23	18	17 -3	21	21	4 -4	84	84	8 3	172	173	14 -1	20	5
11 -9	45	44	17 -1	64	62	4 -3	40	39	8 4	146	149	14 0	16	15
11 -8	68	69	17 0	38	39	4 -2	135	134	8 5	80	78	14 1	36	36
11 -7	16	16	17 1	58	57	4 0	91	89	8 6	94	95	14 2	34	30
11 -6	16	2	17 2	44	45	4 1	38	38	8 7	81	84	14 3	91	90
11 -4	36	35	17 4	18	5	4 2	40	42	8 8	18	12	14 4	96	97
11 -3	51	49	17 6	19	8	4 3	21	24	8 9	22	18	14 5	41	46
11 0	102	102				4 4	37	38	8 10	23	13	14 6	32	32
11 2	38	41				4 5	25	26	8 11	36	36	14 7	78	78
11 3	40	38				4 6	44	44	8 12	42	42	14 8	17	19
11 4	30	30				4 7	18	8	8 13	17	12	16 -7	21	16
11 7	40	40				4 8	63	64	10-13	37	38	16 -6	28	23
11 8	88	90				4 9	82	81	10-12	45	43	16 -5	69	70
11 9	19	21				4 10	17	12	10-11	30	29	16 -3	20	13
11 10	99	98				4 11	55	55	10-10	23	19	16 -2	37	39
11 11	35	31				4 12	19	17	10 -7	40	42	16 -1	95	92
11 12	29	25				4 13	16	10	10 -6	41	46	16 0	89	88
13-12	26	23				4 14	28	25	10 -5	79	79	16 1	36	31
13-11	37	36				6-14	37	35	10 -4	65	65	16 2	83	84
13-10	48	46				6-13	20	21	10 -3	40	43	16 3	99	102
13 -8	48	49				6-12	71	71	10 -2	47	46	16 4	18	13
13 -7	54	55				6-11	26	28	10 -1	19	2	16 6	13	6
13 -5	53	55				6-10	56	55	10 0	28	27			
13 -4	21	21				6 -9	19	7	10 1	75	74			
13 -3	17	15				6 -8	16	6	10 2	46	46			
13 -2	36	35				6 -7	50	50	10 3	75	75			
13 -1	25	20				6 -6	37	39	10 4	46	48			
13 0	60	62				6 -5	18	11	10 5	14	3			
13 1	60	60				6 -3	52	53	10 6	37	36			
13 2	54	54				6 -2	73	73	10 8	21	23			
13 3	24	23				6 -1	97	94	10 9	35	31			
13 4	16	9				6 0	77	76	10 11	20	22			
13 5	24	19				6 1	58	58	12-11	40	39			
13 6	24	24				6 3	88	88	12-10	17	20			
13 7	17	16				6 4	47	45	12 -9	36	36			
13 8	35	36				6 5	94	97	12 -8	59	60			
13 9	18	14				6 7	101	98	12 -7	67	67			
13 10	16	19				6 8	84	85	12 -6	24	20			
15-10	80	78				6 9	29	33	12 -5	19	18			
15 -9	47	46				6 10	27	28	12 -4	14	7			
15 -8	27	26				6 11	87	88	12 -3	18	15			
15 -7	45	46				6 12	26	28	12 -2	15	8			
15 -6	43	46				6 13	41	41	12 0	50	49			
15 -5	68	68				6 14	18	15	12 1	52	53			
15 -4	102	103				8-14	37	30	12 2	95	96			
15 -3	21	14				8-13	20	19	12 3	35	34			
15 -2	43	42				8-12	24	29	12 4	51	53			
15 -1	62	63				8-11	15	5	12 5	26	24			
15 0	40	39				8-10	16	16	12 6	15	3			

1 13	73	73	7 -4	13	5	13 1	37	32	4-12	43	45	8 10	62	62
1 14	88	88	7 -3	78	79	13 2	43	42	4-10	26	25	8 11	24	23
3-14	92	90	7 -2	78	80	13 3	31	34	4 -9	27	30	10-10	44	44
3-13	56	56	7 0	35	32	13 5	52	51	4 -8	23	25	10 -9	51	51
3-12	46	46	7 1	38	40	13 6	22	14	4 -7	65	65	10 -6	20	2
3-11	61	59	7 2	121	119	13 7	42	38	4 -6	92	92	10 -4	26	25
3-10	56	60	7 3	58	57	13 8	39	41	4 -5	52	54	10 -3	50	50
3 -8	36	36	7 4	78	79	15 -7	28	36	4 -4	46	49	10 -2	22	21
3 -7	29	29	7 5	65	65	15 -6	16	9	4 -3	60	61	10 -1	37	36
3 -6	43	40	7 6	62	64	15 -5	48	44	4 -2	109	111	10 0	17	20
3 -5	44	44	7 8	41	41	15 -4	42	43	4 -1	48	52	10 1	69	67
3 -4	19	17	7 10	98	100	15 -3	18	21	4 0	49	49	10 2	102	102
3 -3	56	57	7 11	78	78	15 -2	22	17	4 2	142	145	10 3	45	45
3 -2	68	68	7 12	66	67	15 -1	20	21	4 3	14	3	10 4	62	63
3 -1	20	15	9-11	82	85	15 0	39	39	4 4	83	83	10 6	14	8
3 0	18	7	9-10	105	105	15 1	29	27	4 5	53	54	10 7	17	11
3 1	20	10	9 -9	51	50	15 2	53	53	4 6	69	68	10 9	87	85
3 2	25	25	9 -8	28	30	15 3	17	5	4 7	14	15	12 -9	45	45
3 3	48	46	9 -7	19	9	15 5	44	44	4 9	17	7	12 -8	34	34
3 4	21	22	9 -6	47	49	15 6	84	80	4 10	84	84	12 -7	24	22
3 5	21	21	9 -5	51	52				4 11	40	40	12 -6	24	24
3 6	81	81	9 -3	105	105				4 12	38	35	12 -5	23	19
3 7	21	26	9 -2	114	114				6-12	25	10	12 -4	15	6
3 9	62	61	9 -1	62	63				6-11	37	37	12 -3	47	48
3 10	25	25	9 0	16	12				6-10	69	69	12 -2	72	74
3 11	61	63	9 1	28	24				6 -9	126	127	12 -1	82	80
3 12	33	31	9 2	56	59				6 -8	28	31	12 0	87	85
3 13	25	27	9 3	66	67				6 -7	19	13	12 1	55	57
3 14	42	41	9 4	35	35				6 -6	37	40	12 2	62	66
5-14	44	52	9 5	58	57				6 -5	37	35	12 3	25	23
5-13	83	82	9 7	25	27				6 -3	32	36	12 4	16	11
5-12	38	41	9 8	18	15				6 -2	146	146	12 6	92	93
5-11	43	44	9 9	44	42				6 -1	125	127	12 7	15	10
5-10	82	81	9 10	56	57				6 0	15	4	12 8	64	63
5 -9	26	28	9 11	98	98				6 1	63	63	14 -6	71	70
5 -7	75	73	11-11	23	12				6 2	91	92	14 -5	93	94
5 -6	86	85	11-10	72	74				6 3	59	59	14 -3	47	50
5 -5	94	95	11 -9	30	26				6 4	37	35	14 -2	58	58
5 -3	54	53	11 -8	25	29				6 5	16	14	14 0	31	29
5 -2	23	21	11 -7	60	59				6 6	15	10	14 2	42	42
5 -1	34	34	11 -6	75	72				6 9	44	47	14 3	33	33
5 0	46	44	11 -4	20	6				6 10	16	6	14 4	14	14
5 1	41	41	11 -3	22	14				6 11	94	95	14 5	45	47
5 2	56	57	11 -2	28	26				6 12	28	26			
5 3	25	26	11 1	16	15				8-11	18	12			
5 4	21	12	11 2	21	5				8-10	94	94			
5 5	19	17	11 3	22	20				8 -9	41	40	H L	Fo	Fc
5 6	96	96	11 4	18	15				8 -8	20	17	1-12	20	16
5 7	83	80	11 6	25	22				8 -7	53	54	1-11	57	57
5 8	43	42	11 7	32	34				8 -6	39	42	1 -9	17	6
5 9	89	90	11 10	52	54				8 -5	47	50	1 -8	28	20
5 10	68	68	13 -9	79	77				8 -4	27	29	1 -5	25	22
5 11	36	36	13 -8	21	17				8 -2	33	32	1 -4	34	36
5 12	71	71	13 -7	65	63				8 0	27	25	1 -3	45	51
7-13	28	29	13 -6	58	57				8 1	26	29	1 -2	41	41
7-11	62	58	13 -4	47	48				8 1	26	29	1 -1	20	19
7-10	61	62	13 -3	47	47				8 3	51	52	1 0	24	20
7 -9	79	82	13 -2	85	87				8 4	41	45	1 1	55	55
7 -8	63	65	13 -1	71	70				8 6	18	16	1 2	57	57
7 -6	28	26	13 0	28	31				8 8	25	24	1 3	66	66
									8 9	28	35	1 4	48	47

1	5	29	27	7	2	57	56	2	-6	50	51	8	3	22	16	5	3	106	105
1	6	67	69	7	3	22	18	2	-5	19	13	8	4	49	45	5	4	31	34
1	7	60	59	7	4	47	47	2	-4	23	20	8	5	25	13	5	5	15	9
1	11	76	75	7	7	33	34	2	-3	112	111	8	6	49	46	5	6	44	45
1	12	59	57	7	8	46	42	2	-2	15	4	8	7	62	62	7	-6	58	58
3	-12	42	45	9	-7	16	20	2	-1	54	56	10	-6	22	23	7	-5	18	15
3	-11	17	10	9	-6	18	3	2	0	37	39	10	-5	93	93	7	-3	38	36
3	-10	101	101	9	-3	17	6	2	1	16	14	10	-4	55	56	7	-2	39	43
3	-8	23	21	9	-2	24	26	2	2	28	29	10	-3	31	31	7	-1	22	24
3	-7	42	39	9	-1	15	8	2	3	26	27	10	-1	59	57	7	0	30	31
3	-6	16	14	9	0	15	6	2	4	18	15	10	0	25	27	7	1	26	27
3	-5	26	25	9	1	21	19	2	5	70	70	10	1	60	62	7	2	60	63
3	-4	50	51	9	2	65	65	2	6	32	33	10	2	18	17	7	4	25	22
3	-3	73	76	9	3	33	34	2	7	19	20	10	3	60	60	7	5	36	36
3	-2	148	150	9	5	34	36	2	9	51	52	10	4	16	15	7	6	68	66
3	-1	116	113	9	6	21	1	2	10	53	53	12	-3	21	23	9	-3	56	55
3	0	33	30	9	7	57	58	4	-10	57	58	12	-1	26	27	9	-2	76	75
3	1	89	87	9	9	17	8	4	-9	60	61	12	0	17	18	9	-1	27	18
3	2	45	48	11	-7	21	10	4	-8	33	31	12	1	30	30	9	1	61	65
3	3	114	115	11	-6	129	131	4	-7	84	83	12	2	36	34	9	2	83	84
3	4	77	79	11	-5	29	29	4	-6	47	46					9	3	62	63
3	5	36	34	11	-4	43	42	4	-5	64	64								
3	6	19	20	11	-3	44	41	4	-4	36	36	H	L	Fo	Fc				
3	7	76	77	11	-2	37	37	4	-3	60	61	1	-8	31	35	H	L	Fo	Fc
3	8	18	4	11	-1	51	52	4	-2	55	52	1	-7	46	50	0	0	46	45
3	9	21	23	11	0	39	40	4	-1	24	10	1	-6	43	41	0	1	19	13
3	10	35	38	11	1	23	23	4	0	25	21	1	-5	15	3	0	2	16	7
3	11	32	32	11	2	92	90	4	1	17	12	1	-4	40	40	0	3	28	30
5	-11	38	37	11	3	92	93	4	3	38	37	1	-3	52	50	0	4	45	46
5	-10	48	45	11	4	20	22	4	4	27	26	1	-2	96	97	0	5	46	47
5	-9	35	34	11	5	47	50	4	6	83	82	1	-1	69	66	2	-5	68	65
5	-8	55	58	11	6	37	36	4	7	77	75	1	0	15	8	2	-4	32	29
5	-7	69	70	11	7	98	95	4	8	39	41	1	1	31	32	2	-3	32	25
5	-6	18	18	13	-5	51	51	4	9	46	46	1	2	109	109	2	-2	25	20
5	-5	71	72	13	-4	37	41	6	-9	35	37	1	3	40	39	2	-1	23	23
5	-4	19	11	13	-3	54	54	6	-8	24	13	1	4	18	12	2	1	62	61
5	-3	64	63	13	-2	17	14	6	-7	38	35	1	5	37	36	2	2	85	84
5	-2	62	62	13	-1	76	76	6	-6	49	52	1	6	47	49	2	3	57	59
5	-1	100	101	13	0	16	10	6	-5	41	40	1	7	19	20	2	4	16	4
5	0	76	77	13	1	34	29	6	-4	18	9	1	8	28	25	4	-5	18	15
5	1	59	57	13	2	39	40	6	-3	22	12	3	-8	34	34	4	-3	19	5
5	2	28	25	13	3	104	103	6	-2	57	57	3	-7	25	25	4	-2	18	6
5	3	77	78	13	4	47	46	6	-1	60	62	3	-6	114	113	4	-1	22	16
5	4	54	54					6	0	18	15	3	-5	44	42	4	0	18	1
5	5	94	92					6	2	22	22	3	-4	13	1	4	1	20	1
5	6	75	77	H	L	Fo	Fc	6	3	31	30	3	-2	65	62	4	2	98	96
5	7	59	59	0	0	67	67	6	4	36	32	3	-1	21	13	4	3	16	5
5	8	16	15	0	1	20	16	6	5	25	28	3	1	85	83	4	4	31	33
7	-10	35	37	0	2	28	6	6	6	25	18	3	2	57	54	6	-3	17	13
7	-9	30	31	0	3	38	35	6	7	104	101	3	3	64	64	6	-2	19	12
7	-8	74	78	0	4	28	26	6	8	17	1	3	6	17	15	6	-1	19	23
7	-7	72	72	0	5	17	7	6	9	31	29	3	7	20	13	6	0	22	17
7	-6	45	45	0	6	24	25	8	-8	30	29	5	-7	42	41	6	1	52	49
7	-5	30	31	0	7	14	13	8	-6	59	57	5	-6	22	13	6	2	41	40
7	-4	21	20	0	8	43	42	8	-5	16	6	5	-5	61	61				
7	-3	25	23	0	10	81	82	8	-4	56	60	5	-2	23	22				
7	-2	44	45	2	-10	19	9	8	-3	32	33	5	-1	29	27				
7	-1	53	53	2	-9	52	52	8	-2	35	34	5	0	18	17				
7	0	62	61	2	-8	36	34	8	-1	28	26	5	1	50	49				
7	1	26	23	2	-7	35	32	8	2	36	30	5	2	91	90				

APPENDIX L. OBSERVED AND CALCULATED STRUCTURE FACTOR AMPLITUDES
FOR $\text{Na}_{3.9}\text{Zr}_6\text{Cl}_{16}\text{Be}$

H = 0		7 -6	45	44	2-13	247	251	7-11	104	103	15 -7	158	165	
K L Fo Fc		8-16	82	79	2-12	83	77	7-10	169	175	15 -1	92	79	
0-18	75	73	8-14	135	135	2-11	72	75	7 -9	139	147	16 -7	59	18
0-16	105	103	8-12	59	60	2 -9	184	183	7 -8	240	239	17 -7	85	88
0-10	234	231	8 -8	70	74	2 -7	105	104	7 -7	67	65	17 -5	85	90
0 -8	718	720	8 -6	177	176	2 -5	158	158	7 -6	104	100	18 -3	138	131
0 -6	82	82	8 -4	123	130	2 -4	108	109	7 -5	48	37	18 -1	103	106
0 -4	246	245	8 0	230	234	2 -3	43	39	7 -2	197	200			
0 -2	309	307	8 10	57	63	2 -1	43	39	7 -1	181	182	H = 2		
1-18	70	61	9 -6	190	193	2 8	45	45	7 0	464	457	K L Fo Fc		
1-16	153	151	9 -2	119	123	2 15	52	57	8 -9	120	124	0-18	69	65
1-14	70	62	9 8	49	52	3-15	79	82	8 -7	160	158	0-14	154	156
1-12	135	140	9 14	57	53	3-14	80	82	8 -6	152	148	0-12	102	99
1 -8	407	411	10-12	129	131	3-13	107	106	8 -2	144	146	0 -8	77	73
1 -6	50	52	10 -6	127	134	3-12	105	104	8 -1	281	288	0 -6	374	372
1 -4	149	147	10 -4	277	281	3-10	67	72	9-14	127	136	0 -4	109	115
1 -2	43	42	10 -2	92	99	3 -9	108	105	9-13	96	96	0 -2	142	141
1 10	56	53	11-14	75	76	3 -6	180	176	9 -9	83	73	0 0	384	376
2-16	197	203	11-12	103	97	3 -5	340	333	9 -8	148	145	1-18	92	91
2-14	123	129	11 -4	58	60	3 -4	435	435	9 -7	127	121	1-14	119	119
2-12	206	209	11 -2	124	126	3 -3	224	219	9 -6	163	165	1-10	88	88
2-10	100	99	12-12	145	143	3 -2	166	164	9 -5	158	160	1 -8	177	181
2 -8	300	300	12-10	169	170	3 -1	175	176	9 -3	74	69	1 -6	52	54
2 -6	185	189	12 -6	64	58	3 0	45	40	9 -2	92	93	1 -4	55	56
2 -4	134	130	12 -4	90	90	3 11	48	49	9 -1	176	174	1 -3	41	34
2 -2	257	255	12 8	61	51	4-13	66	68	9 0	189	193	1 -2	36	36
2 0	297	301	13-10	114	116	4 -5	203	204	9 12	58	56	1 -1	52	48
3-16	120	119	13 -2	122	121	4 -4	41	43	10-13	105	106	2-16	63	58
3-14	92	98	14-10	76	84	4 -3	263	259	10-12	63	58	2-14	82	75
3-12	293	288	14 -8	154	166	4 -2	149	145	10 -8	56	47	2-13	73	68
3-10	147	150	14 -2	116	119	4 -1	48	48	10 -7	169	171	2-10	99	102
3 -8	172	176	14 0	208	209	5-16	70	84	10 -3	131	131	2 -6	207	207
3 -6	126	127	15 -6	160	160	5-14	53	42	10 -1	79	82	2 -5	45	42
3 -4	357	348	15 -2	111	112	5-13	86	89	10 4	56	46	2 -4	156	157
3 -2	56	57	16 -8	128	132	5-12	132	144	11-14	84	81	2 -2	237	236
4-14	93	98	16 -6	72	71	5-11	166	167	11-12	63	76	2 0	120	114
4-12	182	179	16 -4	72	62	5-10	208	210	11-11	177	182	3-15	58	47
4-10	62	65	16 -2	53	48	5 -9	151	153	11 -6	110	110	3-14	124	125
4 -8	111	111	16 0	98	98	5 -8	80	77	11 -4	148	152	3-12	115	116
4 -6	189	187	17 -6	116	113	5 -7	50	42	11 -3	106	108	3-10	162	170
4 -4	893	885	17 -2	54	43	5 -6	96	99	11 -2	69	66	3 -8	48	40
4 0	284	291	18 -4	107	108	5 -5	224	228	11 1	56	52	3 -6	64	68
5-12	157	156	18 -2	74	77	5 -4	289	289	11 9	47	28	3 -4	184	181
5-10	115	117				5 -3	380	375	12-13	71	68	3 -3	44	50
5 -8	62	61	H = 1			5 -2	279	280	12-11	65	53	3 -1	42	41
5 -6	87	85	K L Fo Fc			5 -1	152	155	12-10	54	57	4-11	137	136
5 -4	189	189	0-10	46	51	5 0	60	54	12 -6	59	56	4-10	207	208
5 -2	213	212	0 -8	84	76	6-17	173	166	12 -5	123	121	4 -9	59	50
5 16	67	71	0 -2	52	50	6-16	65	69	12 -3	140	135	4 -8	112	111
6-12	158	156	1-15	76	79	6-13	94	95	12 -2	104	98	4 -5	125	130
6-10	55	49	1-13	96	93	6-12	93	93	13-11	77	73	4 -4	276	272
6 -8	82	87	1-12	52	56	6-11	115	117	13-10	60	59	4 -3	182	181
6 -4	119	123	1 -9	204	209	6 -9	184	184	13 -9	144	143	4 -2	192	190
6 -2	74	71	1 -7	264	271	6 -8	134	136	13 -1	134	138	4 -1	80	72
6 0	291	295	1 -6	134	135	6 -7	73	73	13 2	51	20	4 0	148	154
7-16	120	118	1 -5	253	252	6 -5	62	59	14-11	94	97	4 7	46	46
7-14	137	131	1 -3	204	204	6 -4	100	101	14 -7	106	113	4 17	60	21
7-12	60	58	1 -2	76	71	6 -3	115	112	14 -5	52	43	5-17	74	75
7-10	147	149	1 -1	385	381	7-16	89	81	14 -3	168	165	5-12	106	107
7 -8	234	230	2-17	152	150	7-15	68	66	14 -1	125	121	5-11	57	56

5 -7	49	45	11 -5	87	98	2 -8	126	135	9 -9	128	123	16 -1	112	114
5 -4	123	125	11 -4	94	92	2 -5	64	65	9 -8	66	69	17 -5	76	65
5 -2	84	86	11 -3	115	123	2 -4	136	134	9 -7	143	143	17 -3	81	81
5 -1	69	69	11 -1	86	81	2 -3	46	44	9 -5	194	197	17 -1	124	121
6-17	96	85	11 8	57	51	2 15	76	66	9 -3	116	119	18 -1	87	89
6-16	57	31	11 10	52	47	3-17	67	74	9 -2	81	85			
6-12	94	93	12-11	123	120	3-13	57	65	9 -1	196	198			
6-11	97	90	12 -7	56	53	3-11	146	154	9 0	139	143	H = 4		
6 -9	203	205	12 -6	156	163	3-10	49	46	9 6	48	40	K L	Fo	Fc
6 -8	77	82	12 -5	103	105	3 -9	155	151	9 13	75	73	0-14	125	118
6 -6	47	50	12 -4	125	132	3 -7	66	66	10-15	80	67	0-12	127	135
6 -4	74	76	12 -3	177	176	3 -6	125	128	10-13	114	115	0-10	55	45
6 -3	79	81	12 -2	110	111	3 -5	101	98	10 -7	158	165	0 -8	172	175
6 -2	137	131	12 -1	70	73	3 -4	165	165	10 -6	121	118	0 -6	343	347
6 -1	164	164	13-10	165	168	3 -3	165	165	10 -3	132	132	0 -4	346	351
6 0	210	213	13 -6	139	145	3 -2	42	40	10 -2	78	71	0 -2	237	230
7-16	73	76	13 -2	256	260	3 -1	185	188	10 -1	144	143	0 0	377	364
7-14	137	141	13 -1	52	51	3 0	113	108	11-13	109	102	1-14	84	87
7-10	107	111	13 11	56	30	3 16	57	50	11-11	89	90	1-13	85	86
7 -9	55	56	14-10	143	147	4-14	81	67	11 -8	72	73	1-12	86	87
7 -8	187	186	14 -9	85	87	4-13	67	61	11 -7	168	161	1-10	75	84
7 -6	96	97	14 -4	109	107	4-12	92	95	11 -5	174	169	1 -8	89	85
7 -3	58	64	14 -2	54	57	4-11	55	46	11 -4	52	44	1 -3	47	29
7 -2	56	60	14 -1	68	72	4 -5	85	81	11 -2	48	33	1 4	42	44
7 -1	149	148	14 0	64	59	4 -4	139	141	11 -1	65	60	2-14	63	71
7 15	77	65	15 -8	64	61	4 -3	142	142	11 0	116	114	2-12	58	50
8-15	117	111	15 -6	58	53	4 -1	62	59	12-13	79	89	2-10	122	125
8-14	79	75	15 -1	72	72	4 6	52	44	12-12	71	63	2 -9	150	150
8-10	70	68	16 -2	166	161	4 10	64	67	12-10	63	64	2 -8	53	46
8 -9	141	146	17 -6	185	182	5-17	91	98	12 -9	77	69	2 -7	179	178
8 -8	120	123	17 -2	171	167	5 -9	286	292	12 -5	196	195	2 -6	120	122
8 -7	262	268	18 -3	66	47	5 -7	148	147	12 -4	58	51	2 -5	92	94
8 -6	52	58	18 -1	69	67	5 -5	50	56	12 -3	183	181	2 -4	228	226
8 -4	127	126				5 -4	120	117	12 -1	81	87	2 -2	199	193
8 -3	66	68	H = 3			5 -1	317	315	12 2	73	56	2 -1	226	230
8 -2	83	82	K L	Fo	Fc	5 8	52	40	12 7	56	43	2 0	97	92
8 -1	246	249	0-14	108	108	6-14	58	52	13-11	103	103	2 3	52	53
8 0	296	296	0-10	94	87	6-13	79	83	13-10	65	58	3-16	77	77
9-13	62	67	0 -8	142	143	6-12	74	80	13 -7	59	62	3-15	70	55
9 -8	87	95	0 -6	51	60	6-11	79	75	13 -6	76	76	3-14	99	93
9 -6	190	197	0 -4	85	84	6 -9	120	125	13 -5	200	202	3-13	83	79
9 -3	87	89	0 -2	71	71	6 -8	76	77	13 -4	66	50	3-12	167	164
9 -2	165	166	1-16	67	59	6 -3	125	125	13 -3	209	214	3-11	68	64
9 5	58	46	1-15	56	55	6 10	59	50	13 -2	72	71	3-10	86	85
9 12	61	52	1-13	192	193	7-15	106	106	14-11	97	99	3 -9	100	102
9 14	62	61	1-11	60	58	7-11	63	65	14-10	87	93	3 -8	123	128
10-15	94	90	1 -7	94	92	7 -7	171	170	14 -7	120	108	3 -7	76	72
10-14	111	116	1 -6	91	89	7 -5	103	104	14 -5	78	72	3 -6	67	68
10-13	157	157	1 -5	267	271	7 -4	67	60	14 -3	161	164	3 -4	141	144
10 -8	117	121	1 -4	56	52	7 -3	54	51	14 -2	107	108	3 -3	102	105
10 -7	133	134	1 -3	165	169	7 -2	58	59	14 -1	122	120	3 -1	67	65
10 -6	67	64	1 -2	58	53	7 0	171	177	15 -9	165	165	4-17	72	68
10 -5	261	262	1 -1	90	90	7 1	43	31	15 -5	74	71	4-15	62	66
10 -4	112	122	1 0	178	178	7 12	52	41	15 -3	167	159	4-13	60	67
10 -3	104	113	2-17	119	111	8-10	59	39	15 -1	124	123	4-12	67	73
10 -1	86	92	2-16	56	42	8 -9	142	142	15 2	55	57	4-10	176	175
10 0	159	161	2-13	130	130	8 -8	140	141	16 -7	69	63	4 -9	103	111
11-12	121	119	2-12	65	60	8 -7	124	132	16 -6	111	108	4 -8	145	146
11 -7	60	54	2-11	87	89	8 -1	220	217	16 -5	73	69	4 -7	60	53
11 -6	76	78	2 -9	78	83	8 13	66	66	16 -2	60	65	4 -6	57	40
												4 -5	227	223

4 -4	319	324	10-11	139	138	1-11	57	58	5 -4	412	420	11 13	61	52
4 -3	183	180	10 -9	64	62	1-10	87	86	5 -3	255	254	12 -3	53	45
4 -2	191	189	10 -8	174	168	1 -9	234	236	5 -2	147	149	12 -2	99	101
4 0	230	232	10 -7	150	157	1 -8	222	223	5 -1	194	192	12 10	70	71
4 11	56	56	10 -6	65	70	1 -7	318	321	5 0	110	118	13-11	98	86
5-17	83	80	10 -4	155	150	1 -5	66	67	6-14	64	62	13 -9	101	95
5 -7	53	49	10 -3	97	100	1 -4	146	150	6-13	74	75	13 -8	80	82
5 -6	65	65	10 -1	214	215	1 -3	61	64	6-12	61	50	13 -6	53	38
5 -5	77	78	10 0	229	230	1 -2	61	60	6-11	77	82	13 -3	54	53
5 -3	123	117	10 ,2	69	58	1 -1	497	493	6-10	135	133	13 -2	64	59
5 -2	177	171	10 13	68	63	1 0	680	681	6 -9	127	129	13 -1	92	89
5 9	53	55	11-12	63	75	2-17	113	123	6 -8	93	91	13 0	111	109
5 15	55	58	11 -8	79	75	2-13	176	177	6 -6	65	64	14 -7	66	62
6-15	96	95	11 -7	78	78	2-12	76	67	6 -3	146	144	14 -6	57	69
6-13	68	59	11 -6	53	42	2-11	66	71	6 -2	77	83	14 -5	72	71
6-12	144	143	11 -5	50	27	2-10	65	59	6 1	42	19	14 -3	111	109
6-11	142	151	11 -4	61	56	2 -9	173	176	7-16	86	90	15 -7	97	89
6 -8	126	124	11 -3	128	124	2 -8	85	92	7-15	66	59	15 -2	81	71
6 -7	111	109	11 -2	63	59	2 -7	137	139	7-14	98	94	15 1	67	57
6 -5	209	211	11 9	50	40	2 -6	72	71	7-12	149	147	16 -6	132	129
6 -4	311	309	12-10	74	73	2 -5	189	189	7-11	85	89	16 -2	73	73
6 -3	315	314	12 -9	99	100	2 -4	90	91	7-10	61	50	17 2	62	46
6 -2	48	45	12 -7	71	66	2 -2	48	37	7 -7	66	63			
6 0	300	289	12 -6	121	126	2 1	57	42	7 -6	171	176	H =	6	
7-16	109	106	12 -5	86	85	2 3	44	32	7 -5	53	54	K L	Fo	Fc
7-14	96	91	12 -4	69	64	3-16	112	115	7 -4	225	222	0-16	162	162
7-13	58	46	12 -1	85	81	3-15	104	99	7 -2	63	61	0-14	64	66
7-12	105	100	12 0	52	58	3-14	68	50	7 0	135	135	0-12	75	81
7-11	97	97	13-10	112	112	3-13	91	98	8 -9	117	123	0-10	111	111
7 -9	75	75	13 -6	106	110	3-12	61	59	8 -8	122	122	0 -8	376	384
7 -8	157	159	13 -5	70	63	3-11	77	84	8 -7	81	84	0 -6	123	126
7 -7	124	122	13 -2	168	167	3-10	137	135	8 -6	59	64	0 -4	88	89
7 -5	115	112	14 -8	76	73	3 -8	247	246	8 -1	117	117	0 -2	145	146
7 -4	104	103	14 -7	97	101	3 -7	79	83	8 12	53	55	0 0	532	528
7 -3	49	44	14 0	83	84	3 -6	59	49	9-13	96	88	1-17	96	95
7 -1	84	84	14 3	52	46	3 -5	251	248	9-12	85	84	1-16	65	55
8-14	81	89	14 4	67	51	3 -4	281	280	9-10	66	67	1-13	159	160
8-13	130	127	15 -7	63	63	3 -3	270	273	9 -9	89	90	1-12	124	124
8-11	97	92	15 -3	60	70	3 -2	196	198	9 -8	79	75	1-11	82	76
8-10	165	166	15 -2	60	52	3 0	381	381	9 -6	65	61	1 -9	100	107
8 -9	158	160	15 -1	84	82	4-16	94	96	9 -5	177	178	1 -8	60	59
8 -8	136	135	15 6	62	48	4-14	64	62	9 -4	146	146	1 -7	71	72
8 -7	77	78	16 -2	68	65	4-13	86	85	9 -3	107	112	1 -6	47	45
8 -6	67	78	16 7	55	34	4-12	202	203	9 -2	109	104	1 -5	108	106
8 -5	118	121	17 -5	63	56	4 -9	64	69	9 -1	62	67	1 -4	111	104
8 -4	62	59	17 -3	67	75	4 -8	118	127	9 0	161	157	1 -3	40	13
8 -3	83	83	17 -2	85	84	4 -5	122	127	10-14	68	65	2-16	79	80
8 -2	93	91				4 -4	225	227	10 -7	101	103	2-14	62	68
8 -1	223	226	H =	5		4 -3	114	115	10 -6	91	91	2-13	147	148
8 0	295	291	K L	Fo	Fc	4 -2	80	79	10 -3	56	60	2-12	113	110
8 15	64	45	0-16	135	141	4 -1	41	40	10 -1	147	148	2-11	80	81
9-13	77	73	0-14	70	66	5-14	111	110	10 4	50	35	2 -9	154	154
9 -9	73	80	0-12	138	142	5-13	82	88	10 13	67	67	2 -8	193	192
9 -6	176	186	0-10	62	66	5-12	79	73	11-11	121	120	2 -7	121	119
9 -2	188	187	0 -8	364	374	5-11	122	123	11-10	114	112	2 -6	120	119
9 -1	122	123	0 -4	153	150	5 -9	112	109	11 -8	71	76	2 -5	368	364
9 10	56	47	0 -2	67	61	5 -8	59	63	11 -6	56	49	2 -4	328	325
9 11	51	41	1-17	61	47	5 -7	68	79	11 -3	107	103	2 -3	299	294
9 14	68	46	1-15	110	117	5 -6	157	159	11 0	66	69	2 -2	104	112
10-12	70	72	1-12	74	76	5 -5	251	257	11 5	60	53	2 -1	210	210

2	0	313	310	9-13	86	89	1 -5	87	91	8 -6	85	82	2-12	83	80
2	10	54	63	9-12	77	81	1 -4	82	78	8 -2	131	132	2-10	101	97
3-14	59	54		9 -9	57	66	1 -1	56	58	8 -1	78	75	2 -9	67	65
3-13	82	83		9 -4	68	73	1 0	203	207	9-14	178	184	2 -7	53	49
3-11	55	58		9 -3	83	84	2-13	76	86	9 -8	133	128	2 -6	100	103
3-10	90	101		9 -2	77	78	2-12	67	69	9 -6	221	214	2 -5	134	142
3 -9	72	72		9 7	61	58	2-10	69	69	9 -5	55	39	2 -2	95	100
3 -8	84	82		10-13	81	81	2 -9	64	61	9 -4	73	72	2 0	66	64
3 -7	68	67		10-12	82	87	2 -5	87	87	9 -2	92	93	3-13	63	55
3 -6	64	66		10-11	133	131	2 -4	81	78	9 0	137	141	3-12	64	43
3 -5	60	63		10 -5	123	123	2 -2	50	38	10-10	70	68	3-10	56	47
3 -3	155	156		10 -1	78	81	2 8	52	42	10 -7	60	50	3 -9	52	58
3 -2	137	138		11-10	72	76	3-14	72	65	10 -6	132	132	3 -8	82	80
3 -1	56	53		11 -7	88	85	3-12	68	70	10 -5	107	112	3 -4	95	93
4-16	76	82		11 -5	75	76	3-11	73	72	10 -4	65	48	3 -3	58	54
4-14	64	48		11 -3	142	146	3 -9	60	69	10 -3	83	81	4-13	83	85
4-13	51	43		11 -2	51	43	3 -8	68	67	10 -2	110	108	4-11	94	94
4-12	179	180		11 -1	54	54	3 -6	151	150	11-12	109	106	4-10	106	101
4-11	154	151		12-12	99	101	3 -5	95	97	11 -6	172	169	4 -8	87	87
4 -6	73	75		12-11	75	55	3 -4	303	300	11 -4	234	236	4 -6	102	102
4 -5	92	90		12-10	63	68	3 -3	115	116	11 -2	142	140	4 -5	110	102
4 -4	329	328		12 -9	113	106	3 -1	85	81	11 0	52	40	4 -3	125	120
4 -3	263	265		12 -5	53	48	3 0	139	139	12-11	69	68	4 -2	145	147
4 -2	82	81		12 -4	110	109	4-14	96	100	12-10	72	70	4 -1	43	19
4 0	157	149		12 -3	60	63	4-12	112	110	12 -6	93	88	4 0	174	174
4 10	55	57		12 -2	88	94	4-11	106	108	12 -3	71	70	4 4	47	52
5-16	76	78		12 -1	73	73	4-10	74	70	12 -2	174	167	5-13	78	86
5-13	118	115		12 0	132	132	4 -7	54	50	12 1	55	51	5 -9	108	94
5-11	84	88		12 8	69	54	4 -5	49	46	13-10	157	156	5 -8	92	89
5 -9	114	117		13 -7	79	84	4 -4	135	131	13 -7	68	67	5 -5	51	46
5 -8	149	149		13 -6	79	77	4 -3	63	57	13 -4	74	69	5 15	56	51
5 -5	124	123		13 -3	71	60	4 -2	62	65	13 -2	66	68	6-11	71	68
5 -4	49	44		13 -2	58	59	5-12	108	106	13 -1	58	60	6 -9	199	197
5 2	49	37		13 -1	110	104	5-10	187	188	14 -5	56	59	6 -8	100	101
5 6	59	49		14-10	72	65	5 -5	72	73	14 -3	61	65	6 -7	59	58
5 7	56	48		14 -8	124	125	5 -4	55	46	14 -2	108	114	6 -6	86	83
6 -9	238	241		14 -7	89	96	5 -2	132	133	15 -7	78	74	6 -2	69	65
6 -8	66	70		14 -2	54	40	5 0	76	62	15 -2	57	62	6 -1	221	219
6 -5	87	89		14 0	122	125	5 8	59	58	15 1	60	49	6 10	70	64
6 -4	93	92		14 1	50	32	5 9	51	44	15 4	60	51	6 14	69	65
6 -3	59	60		14 4	69	57	6-14	67	57	16 -2	111	116	7-12	63	57
6 -1	251	254		14 5	65	38	6-13	65	40				7-11	58	50
6 0	202	200		15 -3	72	66	6-10	87	83	H =	8		7 -7	106	106
6 12	63	57		15 -2	81	78	6 -9	124	124	K L	Fo	Fc	7 -6	72	69
7-14	94	90		15 -1	62	57	6 -8	117	113	0-14	103	97	7 -3	86	86
7 -7	124	123		16 -6	101	101	6 -6	97	96	0-10	56	46	7 -1	113	115
7 -6	139	141		16 -4	83	82	6 -2	74	82	0 -6	105	104	8 -9	93	96
7 -3	107	105		16 -1	58	46	6 -1	147	144	0 -4	127	125	8 -7	191	190
7 -2	108	106		16 0	112	117	7-10	161	158	0 -2	149	144	8 -6	81	81
7 -1	204	204		17 -3	90	89	7 -8	242	243	0 0	53	50	8 -4	90	93
7 5	56	45		17 -2	78	75	7 -7	128	127	1-15	64	54	8 -2	65	66
7 10	67	56					7 -6	58	64	1-13	84	86	8 -1	157	155
8-15	74	73		H =	7		7 -4	69	70	1-12	55	57	8 0	48	39
8 -7	181	184		K L	Fo	Fc	7 -2	216	214	1-11	72	73	9-13	118	112
8 -5	61	62		0-14	120	118	7 -1	113	113	1 -9	54	42	9-10	55	30
8 -4	114	117		0-10	101	101	7 0	386	393	1 -8	85	82	9 -9	101	99
8 -3	73	77		0 -8	195	193	8-12	66	61	1 -5	46	37	9 -5	63	68
8 -1	124	122		1-14	62	57	8 -9	61	58	1 -4	83	78	9 -2	89	86
8 0	56	57		1-10	54	52	8 -8	106	105	2-14	75	75	9 1	51	52
8 13	61	50		1 -6	101	98	8 -7	111	114	2-13	93	92	9 4	54	54

10 -8	76	81	3-14	56	50	9 0	128	122	4 -9	140	139	1 -8	154	161
10 -6	68	65	3-13	85	80	10-10	77	77	4 -7	197	197	1 -7	115	113
10 -5	229	229	3-11	82	80	10 -9	68	70	4 -5	73	70	1 -5	187	183
10 -3	132	135	3-10	64	61	10 -7	71	74	4 -4	51	49	1 -4	267	262
10 -2	65	62	3 -9	126	129	10 -6	95	94	4 -3	89	88	1 -3	181	178
10 0	101	105	3 -8	129	125	10 -3	48	12	4 -1	221	215	1 -1	120	126
10 1	54	52	3 -6	75	80	10 -2	109	108	4 12	71	62	1 0	211	211
11-11	71	80	3 -5	147	142	10 -1	119	127	5-13	130	126	2-11	57	59
11 -7	134	137	3 -4	206	202	11-10	64	65	5-12	93	90	2-10	63	50
11 -5	98	105	3 -3	172	168	11 -8	132	139	5 -9	162	163	2 -5	63	52
11 -3	186	188	3 -1	69	80	11 -7	127	135	5 -5	79	76	2 -3	76	76
11 -1	133	138	3 0	199	198	11 -4	60	61	5 -4	78	70	2 -2	89	89
11 8	54	41	3 12	55	60	11 -2	70	62	5 -1	57	52	3-12	84	80
12-10	59	49	4-15	78	64	11 -1	126	126	6-13	147	148	3-11	116	115
12 -8	57	44	4-14	102	102	11 0	234	233	6-12	61	46	3 -9	97	101
12 -6	100	94	4-13	81	79	12 -8	81	88	6-11	92	90	3 -8	206	201
12 -5	59	52	4-12	95	95	12 -6	100	92	6 -8	55	50	3 -7	91	92
12 -3	142	140	4-10	73	71	12 -4	56	50	6 -7	72	77	3 -4	181	176
12 4	65	49	4 -9	59	52	12 -2	125	119	6 -5	313	315	3 -3	134	131
12 7	56	54	4 -8	119	123	13 -8	73	73	6 -4	171	169	3 -1	124	119
13 -9	78	65	4 -7	65	69	13 -6	81	80	6 -3	268	264	3 0	358	349
13 -6	90	86	4 -5	83	82	13 -5	110	104	6 -1	49	38	4-12	111	113
13 -5	69	66	4 -4	73	69	13 -3	66	65	7 -7	99	101	4-10	54	51
13 -2	70	68	5-10	60	54	14 -6	66	69	7 -3	103	103	4 -8	179	176
14 -6	97	97	5 -9	100	98	14 -5	64	59	7 -1	85	81	4 -4	62	65
14 -4	119	121	5 -7	118	116	14 -2	100	90	8-11	153	150	5-12	70	62
14 -2	157	164	5 -5	95	88	15 -3	68	86	8-10	57	49	5 -9	94	90
14 -1	78	87	5 -4	99	97	15 -1	65	54	8 -5	177	179	5 -6	93	93
15 -5	107	106	5 -2	52	57				8 -3	187	188	5 -4	124	125
15 -3	144	151	5 -1	191	187		H = 10		9 -8	55	54	5 -1	84	79
15 -1	153	146	5 0	49	49	K L	Fo	Fc	9 -4	48	13	5 0	125	117
16 0	57	49	5 6	48	44	0-10	87	81	9 -2	85	77	6-10	64	52
16 2	69	66	6-14	69	64	0 -2	70	71	10-11	126	124	6 -7	74	77
			6 -6	64	72	0 0	128	124	10 -9	119	125	6 -6	139	134
			6 -5	96	95	1-13	150	149	10 -8	64	58	6 -2	131	133
H = 9			6 -3	114	112	1-11	61	47	10 -1	119	121	6 -1	105	107
K L	Fo	Fc	6 -2	54	67	1 -9	139	138	10 0	89	83	7-12	91	92
0-14	131	133	7-12	108	103	1 -8	91	95	10 3	57	52	7 -7	68	66
0-12	112	116	7-11	100	92	1 -7	101	100	10 6	58	47	7 -6	65	60
0-10	99	100	7 -8	84	84	1 -6	51	44	11 -7	70	72	7 -4	240	240
0 -8	85	79	7 -6	74	76	1 -5	134	134	11 -6	62	54	7 -3	50	27
0 -6	53	56	7 -4	257	249	1 -2	61	63	11 -3	75	85	7 -2	52	48
0 -4	87	77	7 -3	137	141	2 -9	245	244	11 -1	85	82	7 0	51	52
0 -2	47	24	7 -1	85	85	2 -8	67	72	12 -7	77	72	7 9	58	49
0 13	114	112	7 0	188	188	2 -7	222	219	12 -1	102	95	8 -4	62	65
1-12	56	35	8-12	99	102	2 -5	186	183	13 -6	63	61	8 -2	74	70
1-11	115	112	8-11	84	81	2 -3	164	166	13 -3	63	61	8 8	66	55
1-10	65	60	8 -9	87	87	2 -2	87	80	13 1	60	57	9-10	97	99
1 -9	79	87	8 -8	115	115	2 -1	405	400	14 2	62	59	9 -7	53	51
1 -8	89	83	8 -6	64	52	2 0	164	171				9 -4	71	65
1 -7	118	115	8 -5	73	64	2 10	61	55				9 -2	60	54
1 -6	102	99	8 -4	92	85	3-13	75	73	H = 11			9 -1	59	67
1 -5	227	230	8 -2	79	72	3-11	79	85	K L	Fo	Fc	9 0	61	58
1 -4	120	117	9-12	94	92	3 -9	91	89	0-12	216	224	10 -3	80	91
1 -3	209	207	9-10	95	100	3 -8	58	53	0 -8	141	138	10 -2	85	77
1 -1	101	94	9 -9	136	142	3 -7	90	91	0 -6	64	56	11 -8	85	90
1 0	153	151	9 -8	54	50	3 -4	51	50	0 -4	147	146	11 -5	68	61
2-13	56	48	9 -4	65	56	3 -3	104	105	1-13	102	106	11 -2	77	78
2 -5	71	55	9 -2	64	57	3 -2	63	74	1-12	60	50	11 -1	58	46
2 -1	53	48	9 -1	143	136	4-13	62	52	1-11	104	104	11 0	153	152
2 9	54	34							1 -9	63	63			

12 -6	85	93	8 -9	71	73	11 2	75	68	7 -3	59	62	
12 -2	85	90	8 -6	92	95				8 -2	83	78	
13 -5	67	60	8 -1	77	85	H = 14						
13 -3	70	62	8 4	56	43	K L	Fo	Fc	H = 16			
H = 12			8 7	70	62	0-10	116	121	K L	Fo	Fc	
K L	Fo	Fc	9 -9	66	70	0 -2	104	100	0 -6	68	66	
0-12	73	74	9 -6	66	53	0 0	94	98	0 -4	258	264	
0 -8	69	71	9 -5	77	86	0 6	56	37	0 0	107	117	
0 -6	82	81	9 -2	73	77	0 8	63	62	1 -5	64	83	
0 -4	134	129	10 -7	69	56	1 -5	56	58	2 -1	129	141	
1-12	59	17	10 -5	66	76	2-10	84	82	4 -4	95	99	
1 -9	72	72	10 -3	74	64	2 -9	69	64	4 -1	89	99	
1 -8	65	65	10 0	69	87	2 -6	81	80	4 0	187	201	
1 -5	85	85	10 8	62	63	2 -5	146	148	4 3	57	44	
1 -2	49	36	11 -7	78	80	2 -4	68	67	5 -2	64	70	
2-12	80	73	11 -3	64	68	2 -3	85	88	5 -1	76	65	
2-10	56	50	11 -2	73	76	2 -2	107	113				
2 -9	88	87	11 -1	94	94	2 -1	57	45				
2 -6	59	36	12 -4	74	91	4 -6	85	92				
2 -5	184	179	12 -3	59	59	4 -5	141	145				
2 -4	169	174	12 2	54	46	4 -4	104	100				
2 -3	147	141	H = 13				4 -3	121	128			
2 -1	113	122	K L	Fo	Fc	5 -9	87	82				
2 0	71	68	0-10	83	79	5 -8	66	61				
3-12	71	60	0 -4	53	42	5 -3	61	58				
3-11	61	50	1 -4	79	83	6 -1	140	140				
3 -9	62	59	1 5	51	26	6 0	58	55				
3 -4	59	64	1 6	61	44	6 2	54	52				
3 3	67	61	1 10	57	40	6 6	59	59				
4-12	75	74	1 6	61	44	6 7	82	67				
4-10	109	105	3 -6	67	71	7 -3	54	56				
4 -8	87	93	3 -4	51	47	7 7	59	41				
4 -5	63	68	3 0	79	86	8 -4	76	79				
4 -4	50	36	3 8	63	45	8 -3	70	77				
4 -3	56	56	4 -8	78	80	8 -1	130	134				
4 -2	79	84	5-10	86	90	8 0	98	95				
4 0	126	129	5 -2	98	97	9 -5	58	53				
5 -9	107	110	5 0	122	136	10 3	62	48				
5 -8	56	64	5 4	57	46	H = 15						
5 -5	65	64	6-10	65	50	K L	Fo	Fc				
5 -2	70	64	6 -7	62	55	0 -4	66	68				
5 -1	87	86	6 -6	71	73	1 -7	103	105				
5 6	55	53	6 -2	74	70	1 -4	101	92				
5 7	55	42	6 -1	64	59	1 -1	181	188				
6 -9	96	102	7 -8	140	143	1 0	75	62				
6 -8	138	133	7 -6	65	72	1 8	61	65				
6 -7	88	85	7 -2	99	96	2 -7	64	67				
6 -6	69	48	7 0	141	148	2 -3	65	61				
6 -5	64	57	7 4	53	49	3 -8	155	159				
6 -4	51	16	8 -4	65	64	3 -5	141	141				
6 -2	63	60	9 -6	164	165	3 -4	71	68				
6 -1	158	158	9 -4	99	101	3 -3	136	137				
6 0	216	215	9 -2	120	117	3 0	243	247				
7 -8	60	59	9 -1	64	59	5 -6	79	82				
7 -7	78	79	9 0	93	98	5 -5	83	91				
7 -6	61	47	9 5	56	48	6 -2	66	53				
7 -3	76	79	10 -6	78	78	6 6	59	47				
7 -2	74	79	10 -3	83	90	7 -5	65	62				
8-10	69	62	10 -2	107	124	7 -4	198	208				
			11 -4	151	157							

APPENDIX M. OBSERVED AND CALCULATED STRUCTURE FACTOR AMPLITUDES
FOR $\text{Cs}_{3.0}\text{Zr}_6\text{Cl}_{16}\text{C}$

H - 0	6 4	126	119	14 3	106	107	3 -1	58	59	7-12	65	69			
K L Fo Fc	6 5	87	89	14 6	71	74	3 0	291	304	7-10	58	60			
0 4	203	168	6 6	182	175		3 1	71	64	7 -9	90	88			
0 6	136	148	6 7	137	136		3 3	130	134	7 -7	66	60			
0 8	137	129	6 9	77	78	H - 1	3 4	68	62	7 -5	51	36			
0 10	142	141	6 11	93	92	K L Fo Fc	3 6	105	113	7 -4	116	120			
0 12	55	44	6 12	56	43	0 -11	61	47	3 7	56	32	124	124		
1 2	54	56	6 13	107	109	0 -9	138	137	3 9	136	134	7 -1	62	55	
1 4	176	168	6 14	103	102	0 -7	168	162	3 11	55	44	7 0	65	69	
1 5	302	284	7 1	46	60	0 -5	191	176	3 13	66	56	7 2	56	51	
1 7	74	87	7 3	124	133	0 -3	197	183	4-14	57	35	7 4	78	79	
1 8	304	310	7 4	172	171	0 -1	151	180	4-12	76	82	7 6	63	54	
1 9	63	77	7 6	180	176	0 1	213	229	4-11	69	58	7 7	148	143	
1 10	88	87	7 7	211	207	0 3	389	368	4 -9	56	49	7 10	81	77	
1 11	105	111	7 8	59	51	0 5	134	122	4 -9	56	49	7 10	81	77	
2 2	170	196	7 9	57	43	0 7	55	44	4 -7	95	94	7 12	69	59	
2 3	220	215	7 10	98	99	1-15	76	72	4 -6	88	85	8-10	53	33	
2 5	106	106	7 11	78	80	1-14	61	51	4 -5	196	204	8 -8	139	136	
2 6	128	137	7 12	107	110	1-13	84	83	4 -4	123	125	8 -4	58	37	
2 8	98	88	8 0	53	45	1-12	60	48	4 -2	114	120	8 -2	135	136	
2 9	184	186	8 1	321	330	1 -9	88	84	4 -1	207	209	8 -1	107	115	
2 10	65	57	8 2	124	121	1 -8	75	71	4 0	77	77	8 1	77	81	
2 11	89	87	8 3	57	53	1 -6	58	65	4 1	52	41	8 2	174	176	
2 12	138	140	8 4	97	102	1 -5	96	95	4 2	78	76	8 3	59	60	
2 13	120	125	8 5	101	105	1 -4	216	230	4 4	122	123	8 7	56	44	
2 15	70	68	8 6	68	66	1 -2	237	225	4 5	131	138	8 8	65	75	
3 2	210	212	8 7	99	97	1 0	160	134	4 7	125	121	9-10	63	55	
3 3	370	389	8 11	95	97	1 2	41	29	4 9	68	71	9 -4	59	55	
3 4	258	258	8 13	58	52	1 4	109	123	4 12	59	48	9 -3	212	216	
3 6	55	59	9 1	62	71	1 5	82	81	5-13	67	61	9 -2	54	52	
3 7	159	167	9 2	171	177	1 6	105	112	5-11	74	68	9 0	68	40	
3 8	90	89	9 3	74	68	1 8	128	124	5-10	60	64	9 1	70	68	
3 9	106	101	9 4	100	98	1 9	59	59	5 -7	87	91	9 3	119	122	
3 11	82	85	9 5	60	37	1 11	60	50	5 -6	161	161	9 4	60	57	
3 12	108	112	9 6	94	96	1 13	85	92	5 -5	48	58	9 7	70	63	
3 14	113	118	9 7	54	51	2-14	81	84	5 -4	95	91	9 9	77	72	
4 0	155	132	9 8	66	49	2-10	135	136	5 -2	52	47	10-11	82	81	
4 1	228	226	9 9	92	95	2 -9	89	93	5 -1	121	123	10-10	62	61	
4 2	58	72	10 0	98	96	2 -8	111	106	5 0	177	190	10 -8	59	60	
4 3	355	358	10 1	117	117	2 -7	81	76	5 1	130	130	10 -7	81	79	
4 4	426	421	10 2	68	68	2 -5	47	56	5 2	70	65	10 -5	75	71	
4 5	191	192	10 7	81	83	2 -4	94	95	5 4	177	166	10 -2	66	62	
4 6	128	117	10 10	197	185	2 1	143	155	5 5	124	117	10 0	52	37	
4 7	125	128	11 1	93	102	2 3	117	110	5 10	82	77	10 2	108	116	
4 8	79	81	11 2	84	90	2 4	129	131	6-14	87	82	10 4	65	62	
4 9	91	95	11 4	59	53	2 5	55	64	6-11	93	84	10 5	83	86	
4 13	61	53	11 5	57	25	2 8	139	142	6 -8	62	59	10 7	61	56	
5 1	255	244	11 6	98	94	2 10	59	64	6 -6	144	142	10 11	63	57	
5 2	143	148	11 7	94	98	2 11	67	68	6 -5	62	64	11-10	64	55	
5 4	154	156	11 8	86	87	2 12	62	66	6 -3	69	63	11 -6	63	61	
5 5	192	203	11 9	66	68	3-14	56	42	6 -1	153	151	11 -5	82	84	
5 6	59	59	12 2	149	152	3-13	59	52	6 0	64	59	11 -1	63	56	
5 8	123	120	12 3	84	86	3-12	64	60	6 1	70	66	11 1	78	81	
5 9	59	53	12 4	71	72	3-10	57	53	6 2	52	55	11 2	66	58	
5 10	59	59	12 7	111	113	3 -9	131	134	6 3	96	90	11 6	57	55	
5 11	66	63	12 9	56	13	3 -8	88	87	6 5	78	82	11 10	62	68	
6 0	76	89	13 2	117	120	3 -7	45	46	6 6	89	89	12 -6	86	90	
6 1	45	43	13 4	60	42	3 -6	40	27	6 8	56	55	12 -4	58	53	
6 2	111	123	13 6	93	103	3 -5	104	98	6 9	59	52	12 -3	55	43	
6 3	91	88	13 8	61	57	3 -4	42	52	6 12	98	95	12 -2	59	54	
							3 -3	66	63	7-13	83	84	12 0	59	50

12	2	57	49	3	9	64	62	9	5	58	2	2	-7	220	213	5	0	295	305	
12	3	56	46	4-15	64	51		9	6	70	60	2	-6	102	104	5	1	44	37	
12	6	89	93	4-12	60	54		10-10		57	31	2	-5	42	22	5	3	100	96	
13	-7	101	106	4	-6	73	72	10	-7	71	75	2	-4	395	413	5	4	81	87	
13	-1	76	80	4	-5	130	132	10	-4	80	79	2	-3	529	501	5	5	73	64	
13	1	107	105	4	-4	128	139	10	2	61	55	2	-1	211	228	5	6	168	165	
13	5	69	67	4	-3	53	49	10	3	65	56	2	1	540	486	5	7	136	144	
14	-3	62	43	4	-2	133	126	10	4	66	74	2	2	434	410	5	8	158	169	
14	-2	75	77	4	0	58	50	10	5	73	71	2	3	48	26	5	10	88	98	
				4	2	85	90	10	7	73	70	2	4	106	101	5	13	64	71	
				4	3	112	110	11	-2	73	74	2	5	198	186	6	-9	70	59	
				4	4	48	38	11	-1	113	119	2	6	94	95	6	-8	156	164	
				4	8	67	57	11	0	59	68	2	9	86	89	6	-7	78	84	
				4	10	111	112	11	4	74	76	2	12	66	68	6	-5	82	87	
				5	11	59	59	12	-5	54	27	3-14	61	51		6	-4	114	118	
				5-10	110	115		12	-3	68	57	3-13	71	71		6	-3	169	157	
				5	-9	54	54	12	-2	60	57	3-12	67	76		6	-2	335	349	
				5	-7	74	77	12	0	74	75	3-11	102	100		6	-1	256	248	
				5	-5	55	54	13	4	64	57	3	-9	119	123	6	0	336	337	
				5	-4	49	49	14	0	65	58	3	-8	80	76	6	1	154	142	
				5	-3	74	83	15	0	60	44	3	-7	82	78	6	2	127	129	
				5	-2	46	52					3	-5	82	83	6	3	64	76	
				5	1	116	123					3	-3	352	358	6	5	94	105	
				5	2	136	135					3	-2	108	85	6	6	139	148	
				5	4	60	63					3	1	420	395	6	7	76	65	
				5	5	122	130					3	3	73	72	7	-13	70	65	
				5	7	57	57					3	5	101	102	7	-9	81	80	
				5	8	90	87					3	6	92	87	7	-8	52	66	
				6-11	78	74						3	7	131	134	7	-7	137	141	
				6	-9	52	37					3	9	99	100	7	-6	165	162	
				6	-6	86	85					3	10	85	95	7	-5	68	73	
				6	-5	52	56					4-13	115	115		7	-4	69	64	
				6	-3	171	172					4-11	168	165		7	-3	107	114	
				6	0	91	97					4-10	190	190		7	-2	66	71	
				6	1	100	103					4	-7	56	58	7	0	71	74	
				6	4	109	103					4	-6	86	90	7	1	65	63	
				6	9	101	104					4	-5	76	90	7	2	83	81	
				7	-8	79	84					4	-4	145	145	7	3	97	105	
				7	-6	55	46					4	-3	91	80	7	4	156	149	
				7	-5	57	63					4	-1	101	112	7	5	154	150	
				7	-1	182	179					4	1	114	99	7	6	77	88	
				7	0	69	79					4	2	115	115	7	7	72	77	
				7	2	103	100					4	3	47	56	7	11	63	66	
				7	4	73	71					4	4	54	60	8	-9	139	136	
				7	6	81	75					4	5	85	92	8	-8	87	87	
				7	7	89	86					4	6	76	84	8	-6	122	130	
				8-13	58	45						4	8	178	179	8	-2	127	132	
				8	-7	60	55					4	9	178	178	8	0	119	123	
				8	-6	59	50					4	11	120	125	8	2	86	89	
				8	-4	90	87					5-15	70	67		8	4	117	119	
				8	-3	67	65					5-12	97	95		8	5	54	40	
				8	2	113	114					5-11	55	46		8	6	64	74	
				8	4	85	81					5-10	165	163		8	7	137	139	
				8	5	73	73					5	-9	125	126		9-13	73	70	
				8	7	99	102					5	-8	150	143		9-11	109	106	
				9	-6	104	111					5	-7	58	56		9	-8	53	40
				9	-2	76	74					5	-6	89	96		9	-7	65	65
				9	0	81	86					5	-5	67	73		9	-6	126	133
				9	1	57	53					5	-3	73	70		9	-5	183	182
				9	2	61	63					5	-2	271	288		9	3	210	205

9 4	121	125	1 -7	67	63	4 0	59	52	9 -4	112	115	1 8	64	75
9 5	78	81	1 -5	87	82	4 1	44	44	9 -3	61	66	1 11	61	50
9 9	111	110	1 -4	170	175	4 2	91	95	9 2	109	108	2-12	75	71
9 11	78	82	1 -3	177	189	4 3	127	130	9 3	68	66	2 -9	58	58
10-11	68	69	1 -2	56	61	4 4	142	135	9 4	111	116	2 -7	114	124
10-10	100	92	1 -1	45	51	4 6	83	84	9 6	58	51	2 -6	44	47
10 -6	55	48	1 0	126	121	4 7	80	77	9 9	69	73	2 -5	69	69
10 -5	210	207	1 1	105	107	4 8	90	92	10-12	60	65	2 -4	160	163
10 -4	81	81	1 2	152	142	4 10	93	90	10-10	56	43	2 -3	71	72
10 -3	107	109	1 4	108	106	5-13	58	50	10 -9	75	73	2 0	158	150
10 -2	70	73	1 5	191	177	5-11	94	94	10 -7	55	45	2 1	55	46
10 0	65	64	1 7	73	74	5-10	83	83	10 -6	151	153	2 3	125	130
10 1	111	116	1 9	92	89	5 -9	62	60	10 -4	54	44	2 5	74	75
10 2	78	68	1 10	65	52	5 -7	184	193	10 -2	76	77	2 7	67	66
10 3	211	208	1 11	78	82	5 -6	51	52	10 0	60	49	2 8	93	91
10 8	102	101	1 13	73	66	5 -4	103	105	10 2	95	97	3-11	69	68
10 9	70	69	2-10	130	127	5 -3	62	69	10 4	104	104	3-10	68	63
11 -6	103	109	2 -9	110	109	5 -1	144	140	10 7	72	68	3 -9	62	64
11 -4	73	72	2 -8	69	71	5 0	72	75	10 8	65	65	3 -8	78	86
11 -2	127	123	2 -7	174	175	5 1	47	45	11 -7	65	63	3 -5	65	59
11 0	139	135	2 -5	161	161	5 3	124	128	11 -6	86	77	3 -2	205	205
11 1	61	45	2 -3	250	245	5 5	142	138	11 -5	94	97	3 1	108	103
11 2	86	96	2 -2	74	65	5 7	53	32	11 -3	77	82	3 6	76	69
11 4	95	96	2 -1	96	88	5 8	108	122	11 -2	57	48	3 7	61	62
12 -8	68	61	2 0	186	173	5 9	110	108	11 -1	158	165	4-10	58	56
12 -5	118	117	2 1	216	207	6-12	64	56	11 0	54	51	4 -9	123	123
12 -4	58	54	2 2	96	101	6-11	81	82	11 3	96	95	4 -1	72	65
12 -1	71	76	2 3	44	40	6-10	53	43	12-10	65	38	4 3	67	74
12 2	62	57	2 4	61	57	6 -9	91	92	12 -2	119	121	4 5	146	142
12 3	100	113	2 5	188	188	6 -6	144	145	12 0	71	69	4 6	74	77
12 6	71	67	2 7	64	72	6 -3	117	122	12 3	64	55	5 -7	57	59
13 -3	66	54	2 8	77	77	6 -2	201	207	12 5	63	44	5 -4	107	106
13 2	70	63	2 10	59	60	6 0	105	104	12 7	84	89	5 -3	107	108
14 -6	68	62	3-12	76	69	6 1	207	206	13 -2	66	59	5 -2	57	71
14 -3	59	30	3-11	61	46	6 4	155	150	14 -5	64	57	5 -1	114	115
14 -1	156	157	3-10	97	96	7-11	52	35	14 -2	78	76	5 0	140	131
14 4	74	75	3 -8	120	119	7-10	82	79	14 3	92	74	5 11	63	68
15 -2	81	75	3 -6	46	48	7 -9	98	98				6 -8	128	134
15 0	67	61	3 -5	153	152	7 -8	116	119	H = 5			6 -6	58	57
			3 -4	186	191	7 -7	72	78	K L Fo Fc			6 -5	103	103
			3 -2	150	147	7 -6	54	46	0-13	106	100	6 0	50	45
			3 -1	46	36	7 -4	158	156	0 -5	203	197	6 1	72	67
			3 0	213	209	7 -3	54	34	0 1	190	174	6 2	51	42
			3 1	88	78	7 -1	172	173	0 9	119	120	6 4	176	172
			3 2	176	169	7 0	68	68	1-12	93	89	6 6	52	38
			3 4	68	64	7 2	65	64	1-10	67	65	7 -6	114	122
			3 6	97	94	7 3	123	119	1 -9	51	44	7 -5	50	39
			3 7	85	89	7 6	156	159	1 -7	68	74	7 -4	54	45
			3 8	65	66	8 -9	128	132	1 -6	51	51	7 -3	75	80
			3 9	89	91	8 -6	92	91	1 -5	41	33	7 -1	86	88
			3 10	57	46	8 -5	71	76	1 -4	58	55	7 2	126	125
			4-15	67	69	8 -4	81	86	1 -3	86	87	8 -6	62	67
			4-13	77	81	8 1	155	153	1 -2	61	69	8 -5	60	62
			4-12	154	150	8 2	77	73	1 -1	63	66	8 -3	64	60
			4 -8	63	64	8 4	56	43	1 0	118	105	8 -1	80	82
			4 -6	73	69	8 7	82	91	1 1	57	51	8 2	59	61
			4 -5	93	95	8 11	100	107	1 2	125	118	9-11	91	86
			4 -3	108	110	9-13	63	40	1 3	73	68	9 -5	75	76
			4 -2	46	51	9-11	64	59	1 5	65	60	9 1	119	121
			4 -1	54	60	9-10	57	56	1 6	76	76	9 3	65	56

7 -5	116	121	0 4	111	111	7-12	56	53	3 7	69	65	0-10	95	99
7 -2	82	79	1-12	55	42	7 -4	86	85	3 8	69	68	0 -8	78	79
7 1	58	47	1-10	55	56	7 -3	89	86	4-13	75	71	0 -6	69	50
7 4	74	76	1 -9	51	42	7 -2	85	86	4-12	96	98	0 -2	140	145
7 5	153	156	1 -7	103	109	7 2	67	65	4-11	51	40	0 2	119	122
7 7	65	63	1 -5	76	75	7 5	59	52	4 -8	69	61	0 4	68	71
7 8	93	95	1 -3	151	148	7 6	67	60	4 -6	55	59	0 6	56	13
8-10	124	129	1 -2	67	69	8 -9	81	90	4 -3	90	93	1-10	96	101
8 -7	54	30	1 -1	54	60	8 -7	63	68	4 -1	59	55	1 -6	102	107
8 -6	72	72	1 1	58	70	8 -6	66	71	4 6	77	84	1 -5	61	69
8 -4	145	141	1 2	50	29	8 -1	67	57	4 7	100	100	1 -1	52	50
8 -3	75	74	1 3	58	62	8 0	82	80	5-12	71	67	1 0	89	100
8 -1	69	67	1 6	65	69	8 1	99	98	5-11	55	54	1 2	81	88
8 0	172	177	2-15	75	64	8 3	77	80	5-10	55	48	1 3	129	132
8 4	57	58	2-11	56	60	9-10	68	77	5 -8	82	94	1 7	79	81
8 5	55	33	2 -8	88	88	9 -4	92	93	5 -5	68	69	2-12	67	67
8 6	87	87	2 -7	60	54	9 -2	74	76	5 -4	87	92	2-11	70	80
8 7	62	27	2 -4	52	48	9 4	63	63	5 -2	119	129	2-10	56	48
9-12	80	70	2 1	62	64	10 -9	79	73	5 1	70	62	2 -9	101	108
9 -6	76	71	2 2	107	106	10 3	77	68	5 2	82	83	2 -7	112	117
9 -5	176	182	2 3	74	74	11 -4	58	47	5 4	84	83	2 -5	134	138
9 -2	76	56	2 5	72	68	11 0	58	45	5 5	87	92	2 -3	51	42
9 -1	120	125	2 6	59	55	12 -5	69	69	5 6	69	76	2 -2	72	72
9 1	92	84	3-11	75	77				6-10	100	96	2 -1	133	136
9 2	61	58	3 -7	95	97	H =	9		6 -6	68	68	2 0	59	50
9 4	55	48	3 -6	55	53	K L	Fo	Fc	6 -5	82	83	2 3	109	109
9 5	85	83	3 -5	50	47	0-15	66	61	6 -4	179	176	2 5	57	52
10-10	67	58	3 -1	69	69	0-13	57	40	6 -3	112	101	3-14	63	62
10 -9	82	85	3 0	56	59	0 -9	92	96	6 -2	161	161	3-12	74	71
10 -7	72	69	3 1	136	131	0 -7	136	141	6 -1	56	57	3-10	67	65
10 0	93	93	3 5	76	74	0 -3	99	106	6 0	74	84	3 -7	65	68
10 1	55	37	3 7	57	40	0 1	57	58	6 4	64	61	3 -6	123	136
10 2	58	50	4-12	60	56	0 3	109	100	7 -9	65	64	3 -4	73	77
10 3	83	88	4-11	84	78	0 5	64	66	7 -8	81	76	3 -2	130	128
10 4	63	53	4 -7	59	60	1-14	63	47	7 -5	60	56	3 -1	85	87
10 5	73	74	4 -6	115	110	1-12	57	56	7 2	59	56	3 0	109	114
11 -8	59	59	4 -5	105	108	1 -9	139	145	7 3	83	79	3 4	71	68
11 -7	64	54	4 -4	115	120	1 -8	82	89	7 4	74	83	3 5	62	60
11 -3	59	49	4 -2	111	112	1 -2	89	91	8-11	93	85	3 6	68	51
11 -2	59	53	4 -1	70	70	1 0	86	88	8 -8	76	76	3 7	70	63
11 -1	79	69	4 0	77	87	1 2	153	158	8 -4	65	52	4 -5	92	94
11 0	64	68	4 5	99	103	1 3	149	141	8 -2	52	37	4 -4	50	37
11 4	73	77	4 6	69	71	1 6	56	52	8 2	63	63	4 1	66	65
12 -8	69	69	5-13	70	67	1 8	73	71	8 5	100	95	4 2	78	84
12 -4	79	81	5-12	57	64	2 -9	123	118	9 -8	63	63	4 4	74	80
12 0	67	55	5-11	58	50	2 -8	61	66	9 -7	68	70	4 5	98	95
12 1	59	23	5 -6	63	63	2 -6	165	161	9 -4	61	52	4 6	90	92
13 -5	64	67	5 -5	72	74	2 -5	241	235	9 -1	64	54	5-13	76	76
13 -3	59	61	5 -3	118	118	2 -3	73	75	9 1	111	116	5-12	60	54
13 -1	75	88	5 -1	104	107	2 -1	227	215	9 2	60	48	5 -9	100	100
13 1	66	75	5 0	87	85	2 0	161	149	10 -7	110	108	5 -3	104	107
			5 1	51	43	2 2	62	62	10 -6	63	65	5 -2	62	69
			6-13	76	67	2 3	80	71	10 1	108	107	5 1	63	73
H =	8		6-12	67	56	3-13	63	65	11 -4	57	44	5 3	117	112
K L	Fo	Fc	6-11	60	48	3 -5	103	109	11 -2	63	63	5 6	85	79
0-12	54	43	6 -5	54	49	3 -4	94	87	11 0	72	74	6-11	80	70
0-10	109	110	6 -1	58	56	3 -1	178	169				6 -8	89	83
0 -8	168	173	6 1	56	46	3 2	53	47				6 -7	52	11
0 -4	73	71	6 4	73	74	3 3	84	83	H =	10		6 -5	84	89
0 -2	131	133	6 7	85	83	3 4	62	51	K L	Fo	Fc	6 -4	142	146
0 2	181	182							0-14	71	62			

6 -2	68	69	5 2	67	69	3 -4	73	71
6 -1	101	106	6-10	96	98	3 -1	111	118
6 2	101	103	6 -9	84	83	4 -9	90	97
7-12	65	64	6 -7	76	71	4 -8	62	62
7-11	78	73	6 -3	68	65	4 -5	72	73
7-10	76	83	6 1	64	68	4 -2	64	58
7 -9	77	78	6 2	110	111	5 -4	61	58
7 -7	53	42	6 3	62	48	6 -5	69	66
7 -6	96	93	7 -8	108	109	6 -4	68	58
7 -3	90	87	7 -7	58	58	6 -3	57	47
7 -2	65	70	7 -5	74	81			
7 1	97	100	7 -3	63	58	H = 14		
7 4	111	118	7 -1	61	59	K L Fo Fc		
8-11	76	77	7 0	80	84	0 -6	77	62
8 -8	63	66	8 0	92	94	0 -4	96	92
8 -7	74	72	9 -5	75	60	1 -5	97	94
8 -2	54	37						
8 -1	108	108	H = 12					
9 -6	68	60	K L Fo Fc					
9 0	88	90	0-12	76	76			
9 1	61	55	0 -8	89	92			
9 2	91	75	0 -4	238	225			
10 -8	131	123	0 0	58	62			
10 0	72	66	1 -8	58	59			
11 -3	104	110	1 -5	62	70			
			1 0	56	55			
			1 3	75	73			
H = 11			1 4	79	87			
K L Fo Fc			2-11	65	63			
0 -5	67	65	2 -6	65	69			
0 -3	69	67	2 -3	64	57			
0 -1	110	115	3 -7	71	81			
1-11	57	52	3 -1	120	128			
1 -9	62	52	3 2	62	65			
1 -7	59	64	4 -9	58	61			
1 -5	74	79	4 -8	122	122			
1 -4	97	99	4 -7	73	70			
1 -1	58	49	4 -5	69	70			
1 2	70	64	4 -4	74	67			
1 3	65	67	4 -3	68	73			
2-12	58	56	4 0	86	81			
2-11	62	36	4 1	59	63			
2-10	59	60	5 0	95	95			
2 -9	90	87	6-10	54	11			
2 -6	145	155	6 -7	69	80			
2 -2	136	139	7 -5	66	60			
2 1	86	91	8 -5	82	71			
2 4	62	58	8 -3	84	80			
3-12	62	54						
3-11	91	93	H = 13					
3 -7	95	99	K L Fo Fc					
3 -4	75	87	0 -9	57	68			
3 -1	133	128	0 -5	106	113			
3 3	70	67	0 -3	66	65			
4-12	79	64	0 -1	90	90			
4-11	85	80	1 -8	69	70			
4 3	124	119	1 -4	95	94			
4 4	70	80	2 -9	57	36			
5 -6	59	56	2 0	62	68			
5 -3	54	62	3 -7	62	47			
5 -2	110	108						

APPENDIX N. OBSERVED AND CALCULATED STRUCTURE FACTOR AMPLITUDES
FOR $\text{Rb}_5\text{Zr}_6\text{Cl}_{18}\text{B}$

H = 0				H = 1			
K	L	Fo	Fc	K	L	Fo	Fc
0	2	180	177	0	1	204	199
0	4	22	23	0	3	25	26
0	6	140	141	0	5	200	200
0	10	175	177	0	7	211	211
0	12	62	62	0	11	102	101
0	14	228	232	0	13	137	137
0	16	118	114	0	17	104	104
0	18	217	214	0	19	40	44
0	20	99	98	7	5	98	98
0	22	24	26	7	6	20	23
1	0	212	220	7	7	46	47
1	1	19	18	7	8	39	37
1	2	114	114	7	10	40	37
1	3	186	183	7	11	42	43
1	4	176	173	7	12	54	54
1	5	21	20	7	14	60	59
1	6	307	303	7	15	59	61
1	7	164	166	7	16	27	26
1	8	216	215	7	17	96	94
1	9	42	42	7	18	77	79
1	10	16	19	8	1	59	59
1	11	34	37	8	3	23	23
1	13	83	82	8	4	38	39
1	14	45	44	8	5	98	98
1	15	87	87	8	6	33	36
1	16	41	40	8	7	160	157
1	17	111	110	8	8	32	30
1	18	163	161	8	9	48	47
1	19	20	24	8	11	113	108
1	22	55	55	8	13	51	52
2	0	102	105	8	15	47	48
2	1	78	79	9	3	27	31
2	2	197	202	9	4	45	44
2	4	154	152	9	5	42	43
2	5	335	337	9	7	149	144
2	6	306	303	9	8	37	40
2	7	369	373	9	10	85	82
2	8	61	59	9	11	86	85
2	9	88	89	9	12	28	27
2	10	20	22	9	13	57	57
2	11	265	267	9	14	25	22
2	12	224	225	10	0	74	72
2	13	126	124	10	1	42	43
2	14	20	21	10	2	51	50
2	15	50	52	10	3	55	53
2	19	31	32	10	5	29	33
2	20	31	36	10	6	29	30
2	21	24	22	10	7	35	37
3	0	50	43	10	8	45	44
3	1	42	43	10	9	23	25
3	2	103	107	10	10	48	47
3	4	211	212	10	12	57	56
3	6	198	199	11	0	82	77
3	7	148	150	11	2	35	35
3	9	30	32	11	4	63	63
3	10	142	141	11	5	79	76
3	11	129	129	11	6	41	43
3	12	176	177	11	6	41	43

8 14	64	64	2 13	24	29	6 19	22	24	1 14	38	38	4 20	34	36
8 15	51	49	2 14	76	75	7 1	75	75	1 15	105	106	4 21	86	85
9 3	55	53	2 15	93	92	7 2	46	47	1 16	121	118	5 1	35	39
9 4	30	33	2 16	68	67	7 3	28	30	1 17	44	44	5 3	152	153
9 6	67	68	2 17	33	33	7 6	82	80	1 18	66	66	5 4	186	189
9 7	22	22	2 18	43	44	7 7	23	25	1 19	23	24	5 5	46	47
9 11	35	37	2 21	43	46	7 8	91	89	1 20	20	22	5 6	101	101
9 12	31	33	3 0	17	20	7 9	26	26	1 22	36	37	5 7	24	25
10 1	56	56	3 1	92	93	7 10	19	21	2 1	39	37	5 10	92	92
10 2	31	33	3 2	164	164	7 11	70	69	2 2	412	420	5 13	84	83
10 3	33	31	3 3	141	144	7 13	20	20	2 3	303	298	5 14	105	101
10 4	24	27	3 4	141	144	7 14	40	39	2 4	280	277	5 15	109	108
10 5	44	46	3 5	15	15	8 1	68	68	2 5	17	19	5 16	57	57
11 1	32	32	3 6	39	37	8 2	34	36	2 6	62	64	5 17	23	29
11 4	26	27	3 7	19	22	8 4	48	50	2 7	121	119	5 18	66	64
11 5	32	32	3 9	41	44	8 5	88	85	2 8	37	37	6 1	60	60
			3 10	207	208	8 6	58	58	2 9	18	22	6 2	19	21
			3 11	108	107	8 7	71	70	2 10	16	15	6 3	60	61
H - 2			3 12	31	31	8 8	23	20	2 11	88	88	6 4	96	97
K L Fo Fc			3 13	49	50	8 9	26	25	2 12	24	23	6 5	72	73
0 0	26	25	3 18	45	47	8 10	41	40	2 14	112	110	6 7	107	106
0 2	12	10	3 20	33	35	8 12	26	28	2 15	149	148	6 8	54	55
0 4	200	200	4 0	84	85	8 15	78	77	2 16	179	178	6 9	231	233
0 6	129	130	4 1	22	26	9 0	29	29	2 17	27	28	6 10	68	65
0 8	96	97	4 2	62	62	9 2	21	27	2 18	42	44	6 11	100	98
0 10	129	127	4 3	168	174	9 3	75	74	2 20	86	85	6 14	64	65
0 14	41	43	4 4	45	48	9 9	31	32	2 21	57	59	6 15	24	26
0 16	94	95	4 5	42	45	9 11	41	40	2 22	47	49	6 16	48	48
0 18	47	47	4 6	82	83	9 12	45	46	3 1	128	130	6 17	28	29
0 22	50	52	4 7	131	129	10 0	48	46	3 2	169	171	6 18	36	39
1 0	158	154	4 8	105	103	10 4	52	52	3 3	266	263	7 1	42	43
1 1	86	84	4 9	27	29	10 7	30	32	3 5	17	17	7 3	46	45
1 2	211	207	4 10	85	84	10 10	36	41	3 6	29	31	7 4	65	67
1 3	70	69	4 14	82	82	10 11	22	22	3 7	22	23	7 5	29	32
1 4	92	91	4 16	20	23	11 4	31	31	3 8	22	24	7 6	71	69
1 5	57	56	4 17	55	54	11 5	24	23	3 9	74	74	7 7	71	70
1 6	127	125	4 19	37	40				3 10	52	54	7 8	102	101
1 7	85	83	5 1	130	133				3 11	150	147	7 9	171	164
1 8	90	90	5 2	19	19	H - 3			3 13	83	82	7 10	44	45
1 9	42	44	5 3	49	49	K L Fo Fc			3 14	18	22	7 11	80	78
1 10	60	59	5 6	62	63	0 1	205	201	3 15	46	44	7 12	29	30
1 11	86	85	5 7	33	36	0 3	76	76	3 16	69	69	7 13	32	31
1 12	83	83	5 9	24	25	0 5	266	263	3 17	20	20	7 14	21	19
1 13	26	28	5 10	57	57	0 7	144	143	3 19	55	55	7 16	36	35
1 14	65	66	5 11	19	22	0 9	530	539	3 20	46	50	8 1	28	29
1 15	74	73	5 13	38	39	0 11	129	130	3 21	115	115	8 2	160	157
1 17	55	54	5 15	60	61	0 13	64	64	4 1	23	28	8 3	36	37
1 20	22	25	5 17	76	75	0 17	27	30	4 2	152	156	8 4	80	79
1 21	24	30	5 18	26	27	1 1	70	69	4 3	241	246	8 6	56	56
1 22	70	69	6 0	91	91	1 2	21	26	4 4	266	268	8 8	44	42
2 0	33	33	6 1	65	66	1 3	247	238	4 5	63	64	8 13	25	28
2 1	75	76	6 3	96	96	1 4	20	26	4 7	99	100	8 14	30	31
2 2	197	195	6 4	85	86	1 5	47	48	4 8	91	90	8 15	22	23
2 3	153	154	6 5	60	62	1 6	136	137	4 9	94	93	8 16	105	101
2 4	142	142	6 8	51	52	1 7	22	25	4 10	38	40	9 1	68	67
2 5	94	93	6 10	91	90	1 8	103	103	4 11	148	146	9 2	137	133
2 6	152	152	6 11	47	48	1 9	256	259	4 14	148	147	9 3	23	26
2 7	105	105	6 13	35	36	1 10	18	20	4 15	99	98	9 4	65	63
2 8	141	141	6 16	35	36	1 11	48	50	4 16	63	61	9 11	24	22
2 11	44	45	6 17	68	67	1 12	32	35	4 18	28	30	9 13	33	35
2 12	50	51				1 13	33	34						

10	1	50	51	2	20	35	35	6	10	101	97	1	11	17	19	6	7	23	22
10	3	52	51	2	21	47	46	6	12	39	40	1	13	84	83	6	8	90	89
10	4	54	55	3	2	91	91	6	13	52	52	1	16	58	57	6	10	37	37
10	5	42	41	3	3	66	65	6	15	61	60	1	20	34	34	6	12	24	25
10	9	57	55	3	5	95	93	6	16	23	23	2	1	94	92	6	13	22	24
10	11	57	58	3	6	61	62	6	17	47	48	2	2	103	101	6	14	29	28
11	3	45	43	3	7	25	27	6	18	25	28	2	5	33	33	6	15	24	26
11	4	52	53	3	8	159	159	7	0	62	63	2	6	66	66	6	16	29	33
11	5	40	42	3	9	17	19	7	2	41	44	2	7	32	33	7	1	34	37
11	6	35	34	3	10	158	157	7	3	23	28	2	10	28	30	7	2	43	45
				3	11	51	51	7	4	56	56	2	12	75	74	7	3	50	50
				3	12	105	104	7	5	89	89	2	13	49	51	7	5	26	28
				3	13	18	18	7	6	29	28	2	16	54	54	7	10	31	33
				3	14	23	27	7	8	86	85	2	18	25	28	7	11	24	24
				3	15	42	43	7	9	29	31	2	20	36	39	7	12	26	29
				3	16	34	35	7	10	79	79	3	1	42	42	7	15	32	36
				3	18	32	35	7	15	34	33	3	2	50	51	8	1	25	29
				3	20	36	38	7	16	22	25	3	3	75	75	8	2	51	53
				4	0	104	106	8	1	29	29	3	4	46	48	8	3	49	49
				4	1	130	133	8	3	119	118	3	5	70	69	8	6	25	29
				4	3	129	130	8	5	72	72	3	6	53	53	8	13	38	39
				4	4	170	172	8	6	62	61	3	7	54	54	9	2	26	24
				4	5	86	86	8	7	19	18	3	9	69	69	9	3	23	23
				4	6	42	42	8	8	30	33	3	10	23	26	9	6	33	32
				4	7	73	72	8	10	26	25	3	11	22	26	9	9	36	36
				4	8	56	56	8	11	31	30	3	12	17	17	9	12	21	18
				4	9	52	53	8	13	47	47	3	13	37	38	10	2	24	28
				4	10	208	205	8	15	82	81	3	15	48	49	10	5	36	37
				4	11	40	43	9	1	46	47	3	16	28	31	10	6	22	19
				4	14	22	21	9	2	55	56	3	19	57	57				
				4	15	61	62	9	3	43	44	3	20	26	29				
				4	16	28	29	9	5	62	61	4	1	88	87				
				4	17	52	52	9	12	70	67	4	2	57	57				
				4	18	23	22	10	1	25	27	4	5	57	56				
				4	19	18	11	10	2	35	35	4	6	39	37				
				4	20	50	52	10	4	58	56	4	7	46	46				
				5	0	101	100	10	5	43	41	4	8	48	49				
				5	1	43	45	10	6	20	18	4	9	69	71				
				5	2	53	55	10	8	47	46	4	10	31	32				
				5	3	170	175	10	9	25	29	4	11	27	28				
				5	4	66	66	10	10	67	67	4	12	29	32				
				5	6	23	27	11	3	45	45	4	13	22	24				
				5	7	94	95	11	4	41	38	4	14	35	36				
				5	8	72	71					4	18	19	16				
				5	12	26	28					4	19	53	54				
				5	13	47	48					5	1	33	34				
				5	14	57	57					5	2	33	35				
				5	15	59	59					5	4	85	87				
				5	16	42	43					5	6	21	23				
				5	17	131	125					5	8	62	61				
				6	0	72	72					5	10	49	50				
				6	1	144	143					5	11	30	30				
				6	2	100	100					5	12	55	56				
				6	3	38	38					5	14	29	30				
				6	4	53	54					6	1	34	35				
				6	5	50	53					6	2	35	38				
				6	6	21	20					6	3	33	35				
				6	7	35	36					6	4	57	58				
				6	8	144	143					6	5	28	29				
				6	9	71	71					6	6	36	36				

2 0	64	62	5 15	26	28	1 8	103	100	6 1	133	133	2 2	34	36		
2 3	25	27	6 0	211	218	1 11	44	43	6 5	41	41	2 3	45	46		
2 4	31	31	6 1	42	44	1 12	54	54	6 6	69	68	2 5	50	50		
2 5	161	161	6 2	134	133	1 13	96	94	6 7	62	63	2 7	86	84		
2 6	305	303	6 4	67	66	1 14	85	83	6 8	91	88	2 9	51	50		
2 7	282	277	6 5	87	84	1 16	21	27	6 9	70	67	2 10	32	34		
2 8	69	67	6 8	49	50	1 17	35	36	6 10	26	26	2 11	65	63		
2 9	21	26	6 9	36	36	1 18	31	35	6 11	52	54	2 12	33	37		
2 10	68	67	6 12	34	36	1 19	22	24	6 12	54	53	3 0	171	167		
2 11	167	165	6 13	59	59	2 1	127	127	6 13	75	73	3 2	60	61		
2 12	90	89	6 14	28	28	2 2	18	21	7 1	92	94	3 3	18	20		
2 13	107	105	6 15	24	27	2 3	20	22	7 4	39	39	3 5	30	33		
2 14	44	44	6 16	26	30	2 4	123	122	7 7	38	39	3 6	84	82		
2 16	54	53	7 0	185	183	2 6	199	195	7 9	39	40	3 7	42	41		
2 18	34	36	7 1	101	99	2 8	87	87	7 10	34	36	3 8	26	27		
2 20	50	52	7 2	48	48	2 9	27	28	7 11	39	39	3 10	18	11		
3 0	139	139	7 5	25	27	2 10	40	41	7 13	46	47	3 11	33	35		
3 1	81	79	7 6	35	37	2 11	47	46	7 14	36	39	3 14	51	52		
3 2	164	166	7 7	18	19	2 12	131	127	8 1	22	25	3 16	43	43		
3 3	67	66	7 9	40	42	2 14	87	86	8 3	26	27	3 18	44	45		
3 5	42	41	7 10	35	35	2 17	23	28	8 4	72	71	4 0	45	43		
3 6	39	39	7 13	42	43	2 19	41	42	8 6	106	104	4 1	48	47		
3 7	59	58	7 14	57	58	3 1	144	143	8 8	56	55	4 2	81	81		
3 8	69	68	7 15	67	65	3 2	27	28	8 10	25	25	4 4	74	74		
3 9	19	20	8 3	53	53	3 3	37	37	8 12	51	53	4 5	20	23		
3 11	130	126	8 5	19	21	3 4	53	53	9 1	23	24	4 8	23	26		
3 12	188	185	8 6	43	43	3 5	38	40	9 3	47	50	4 10	59	56		
3 15	20	19	8 7	155	150	3 6	73	73	9 4	32	33	4 11	25	24		
3 16	40	43	8 10	22	23	3 7	25	27	9 6	67	68	4 12	55	54		
3 20	63	63	8 11	49	51	3 9	73	72	9 7	23	24	4 13	39	39		
4 0	92	92	8 13	61	60	3 11	73	72	10 1	66	66	4 14	26	28		
4 1	28	31	9 1	29	29	3 12	20	26	10 2	22	21	5 0	25	29		
4 2	67	67	9 4	22	24	3 13	69	68	10 3	31	34	5 2	47	49		
4 3	34	35	9 5	63	62	3 15	36	38	10 4	22	25	5 3	37	38		
4 4	19	24	9 7	79	77	3 19	108	107				5 4	44	46		
4 5	218	221	9 8	24	29	4 1	172	172	H =	8		5 5	116	114		
4 6	197	200	9 10	54	52	4 2	62	63	K	L	Fo	Fc	5 7	27	31	
4 7	45	46	9 11	90	89	4 3	35	36	0 0	199	196		5 8	51	53	
4 9	24	29	10 0	46	47	4 4	64	62	0 2	44	44		5 9	41	39	
4 10	46	47	10 2	31	32	4 5	60	60	0 4	23	24		5 11	43	44	
4 11	115	113	10 5	48	48	4 6	124	123	0 6	58	59		5 12	33	36	
4 12	130	127	10 6	23	24	4 7	21	20	0 8	70	68		5 13	37	37	
4 13	101	100				4 8	92	90	0 10	71	69		5 14	28	30	
4 14	72	70	H =	7		4 10	30	30	0 14	98	96		6 0	26	28	
4 15	23	24	K	L	Fo	Fc	4 11	52	51	0 18	23	27		6 1	84	82
4 17	45	48	0 1	189	187		4 12	77	77	1 0	24	27		6 6	37	38
4 18	24	25	0 3	50	50		4 13	51	53	1 1	38	39		6 7	62	60
4 19	38	40	0 5	128	127		4 15	19	18	1 2	49	47		6 9	37	36
5 1	68	67	0 7	146	144		4 16	34	38	1 3	23	21		6 12	28	29
5 2	44	46	0 9	36	37		4 17	44	44	1 4	137	136		6 13	64	64
5 3	67	67	0 11	105	103		5 2	42	43	1 5	30	32		6 14	21	20
5 4	83	81	0 13	141	138		5 4	39	42	1 7	124	120		7 0	28	28
5 5	117	116	0 17	100	98		5 5	25	28	1 8	62	61		7 2	25	27
5 6	107	105	0 19	63	64		5 6	102	100	1 11	65	65		7 3	39	40
5 7	68	66	1 1	98	96		5 8	101	102	1 12	45	48		7 6	45	43
5 9	38	40	1 3	77	77		5 9	24	27	1 13	67	65		7 7	48	47
5 10	42	44	1 4	93	91		5 10	24	26	1 15	19	18		7 12	44	43
5 11	42	41	1 5	23	25		5 12	83	82	1 16	31	34		8 0	26	28
5 12	60	61	1 6	129	126		5 14	45	48	1 18	52	53		8 4	25	26
5 13	84	84	1 7	62	62		5 16	52	52	2 0	57	57		8 5	24	25

